Australian Government
Geoscience Australia

Geoscience Australia Survey 234, Post-Cruise Report:

Cross-shelf sediment transport in the Torres Strait — Gulf of Papua Region

RV *Franklin* Cruise 01/-02, January-February, 2002

P.T. Harris, A. Heap, V. Passlow, M. Hughes, R. Porter-Smith, R. J. Beaman, M. Hemer, J. Daniell, C. Buchanan, T. Watson, D. Collins, N. Bleakley, O. Anderson and A. King.

Record
2002/26

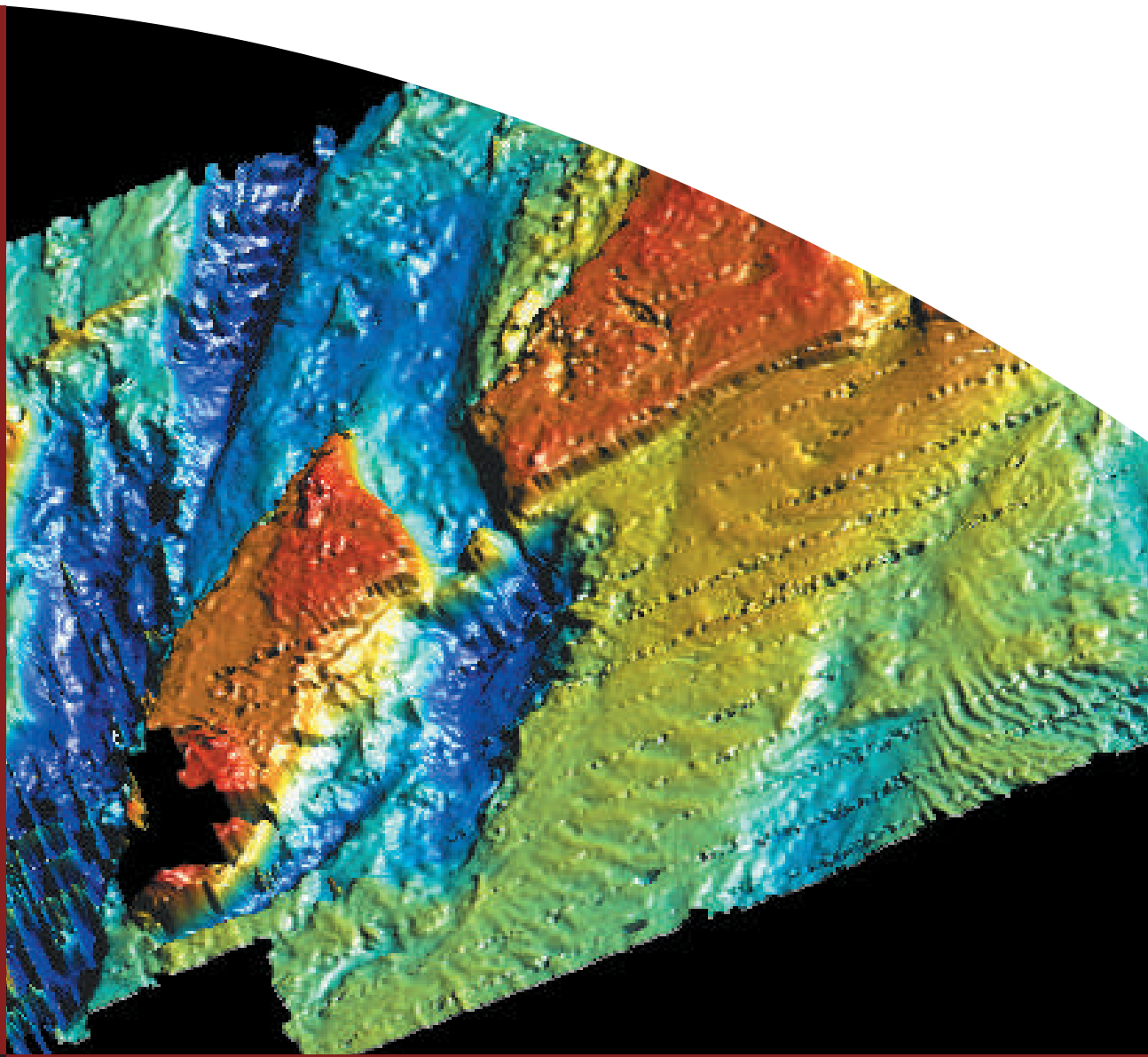

GEOSCIENCE AUSTRALIA SURVEY 234, POST-CRUISE REPORT:

Cross-Shelf Sediment Transport in the Torres Strait – Gulf of Papua Region

RV *Franklin* Cruise 01/02, January-February, 2002

GEOSCIENCE AUSTRALIA
RECORD 2002/26

by

Peter T. Harris[1], Andrew Heap[2], Vicki Passlow[3], Michael Hughes[4],
Rick Porter-Smith[1], Robin J. Beaman[5], Mark Hemer[6], James Daniell[3],
Cameron Buchanan[3], Tony Watson[3], Dylan Collins[3],
Nerida Bleakley[6], Ole Anderson[7] and Alix King[3]

1. Geoscience Australia and Antarctic CRC, University of Tasmania, GPO Box 252-80, Hobart TAS 7001
2. Geoscience Australia, c/o School of Geography and Environmental Studies, University of Tasmania, GPO Box 252- 80, Hobart TAS 7001
3. Geoscience Australia, Petroleum and Marine Division, GPO Box 378, Canberra, ACT 2601
4. School of Geosciences, University of Sydney, Sydney NSW 2006, Australia
5. School of Geography and Environmental Studies, University of Tasmania, GPO Box 252-80, Hobart TAS 7001
6. Antarctic CRC, University of Tasmania, GPO Box 252-80, Hobart TAS 7001
7. Kort & Matrikelstyrelsen, Geodetic Division, Rentemestervej 8, DK-2400 Copenhagen, Denmark

Geoscience Australia
Chief Executive Officer: Dr Neil Williams

ISSN 1039-0073
ISBN 0 642 46757 9

Bibliographic reference: Harris, P.T., Heap, A., Passlow, V., Hughes, M., Porter-Smith, R., Beaman, R.J., Hemer, M., Daniell, J., Buchanan, C., Watson, T., Collins, D., Bleakley, N., Anderson, O. & King, A. *Geoscience Australia Record 2002/26*.

Contents

LIST OF FIGURES

LIST OF TABLES

Executive Summary

The RV *Franklin* sailed from Brisbane on 17th January 2002 and returned to Cairns on 9th February 2002. The cruise discovered that a zone of strong tidal currents at the northern end of the Great Barrier Reef prevents the southward advance of sediment derived from Papua New Guinea's rivers that would otherwise bury the coral reefs. The Fly River, located in close proximity to the northern end of the Great Barrier Reef, discharges about 120 million tonnes/yr of sediment, equal to more than that all of Australia's rivers combined. This sediment does not penetrate as far south into the reef area as might be expected because, over glacial-interglacial cycles of sea level change, the southward-prograding deposits are eroded by tidal currents.

Deployment of an instrumented current meter and suspended sediment measurement frame on the seabed, directly offshore from the Fly River Delta in 30 m water depth, recorded a net sediment advection southwards towards the Torres Strait. Sediment transport was greatest following a northerly wind event, which caused high bottom stress and increased turbidity levels at the site.

Swath sonar mapping and underwater video equipment aboard the research vessel RV *Franklin*, was used to map a series of channels up to 220 m deep that extend for more than 80 km from eastern Torres Strait across the northern end of the Great Barrier Reef. It appears that there are two sorts of channels – those in the north are clearly relict fluvial channels, exhibiting lateral accretion surfaces and incised channels that intersect and truncate underlying strata. Over-deepened channels in the south, however, appear to have formed by tidal current scour. They exhibit closed bathymetric contours at both ends and are floored with well-sorted carbonate gravely sand. Oceanographic observations indicate that the channels provide a conduit onto the shelf for cool and saline (and nutrient-rich?) up-welled Coral Sea water. The deepest channels form isolated depressions, and possibly were the sites of lakes during the last ice age, when Torres Strait formed a land-bridge between Australia and Papua New Guinea. Preliminary tidal modelling indicates that the strongest tidal currents occur over the channels when sea level is about 40 m below its present position, suggesting the channels are Pleistocene or older in age and of relict origin.

Chapter 1. Introduction

On a global scale, surprisingly little sediment is transported across continental shelves to the shelf break under modern (high sea level) environmental conditions (Nittrouer and Wright, 1994). Rather, most terrigenous sediment is trapped in coastal environments (beaches, estuaries and embayments). Autochthonous shelf sediments that are mobilised by storm events tend to be transported short distances along isobath-parallel pathways (e.g. Gagan et al., 1990). Current energy drops off dramatically away from the shoreface on most wave-dominated shelves, and even on tide-dominated shelves the tidal current transport paths generally do not extend to the shelf break (e.g. Stride, 1982). The result is that cross-shelf sediment transport occurs mainly during sea level low stands, when rivers erode and transport material to the shelf break (Nittrouer and Wright, 1994). Exceptions to this pattern occur where large river systems have built deltas across the shelf to the shelf break (e.g. the Mississippi and Amazon Rivers), on some high-energy shelves and in some locations where the shelf width is very narrow (e.g. where the Sepic River empties directly into an ocean basin in northern Papua New Guinea).

In the Gulf of Papua, two separate processes appear to give rise to cross-shelf sediment transport in different locations. The first of these is the transport of fine-grained terrigenous muds delivered by the Fly, Aird and Puari Rivers to the inner shelf area of the Gulf (Fig. 1.1). This mud is thought to be advected eastwards by combined tidal currents, wind-driven currents and swell waves until it reaches the most narrow part of the shelf at around 146°E. The mud may then descend to the Coral Sea basin via the Moresby Canyon (Brunskill et al., 1995). Recent shelf current modeling work has demonstrated that these processes do indeed result in eastward advection of tracers introduced at specific locations (see also Brunskill et al., 2000). Cores and geophysical data collected by the RV *Franklin* during TROPICS cruises have formed the basis of detailed studies of this cross-shelf terrigenous sediment transport path.

The available evidence also identifies a second location of potential cross-shelf sediment transport path located adjacent to the northern end of the Great Barrier Reef. Numerical modeling predicts that this zone experiences elevated tidal current bottom stress (Hemer et al., in press), which corroborates sidescan sonar images of subtidal dunes comprised of coarse sand and gravel-sized sediments shown by Harris et al. (1996). Hence, energy is apparently available to mobilise and transport sediment grains, but whether the residual current regime results in any cross-shelf transport is not known. The key questions are: (1) Are modern oceanographic processes transporting calcareous and terrigenous sediments from NE Torres Strait to the outer shelf of the Gulf of Papua? (2) Do the sediments deposited at the receiving end-point of this transport path contain a record of variability through the Holocene? Through the late Quaternary?

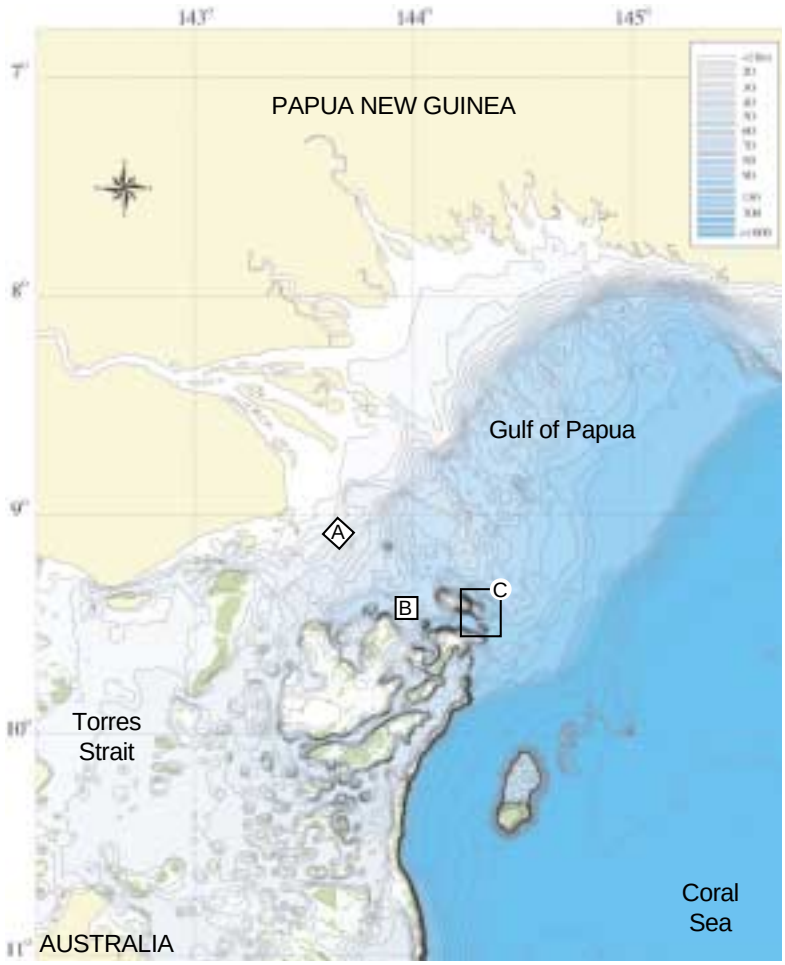

***Figure 1.1**. Location of the three study areas in the northern Great Barrier Reef region.*

The cruise aims were to verify and quantify modelling results predicting the occurrence of a potential sediment transport path across the northern end of the Great Barrier Reef and into the Gulf of Papua. The objectives were, therefore, to map the seabed bathymetry, bedforms and Holocene sediment deposits and to measure currents and near-bed suspended sediment concentrations in a transect across the shelf from northeastern Torres Strait (in the vicinity of the southern Fly River Delta) to the shelf break. Seabed photography and surface grab sampling provided information on seabed character, evidence of sediment mobility such as small-scale bedforms, as well as benthic habitats and communities. A second research goal was to establish linkages between benthic communities and sedimentary environments and facies.

The RV *Franklin* sailed from Brisbane on 17 January 2002 and returned to Cairns on 9 February 2002. A narrative of the cruise progress is given in Appendix A. Fine weather was experienced for the duration of the voyage (Fig. 1.2) and no days were lost due to bad weather or rough sea conditions. In this report, the methods used to collect and analyse the data are outlined and preliminary results are presented. This is followed by a brief discussion of some of the main findings of the cruise.

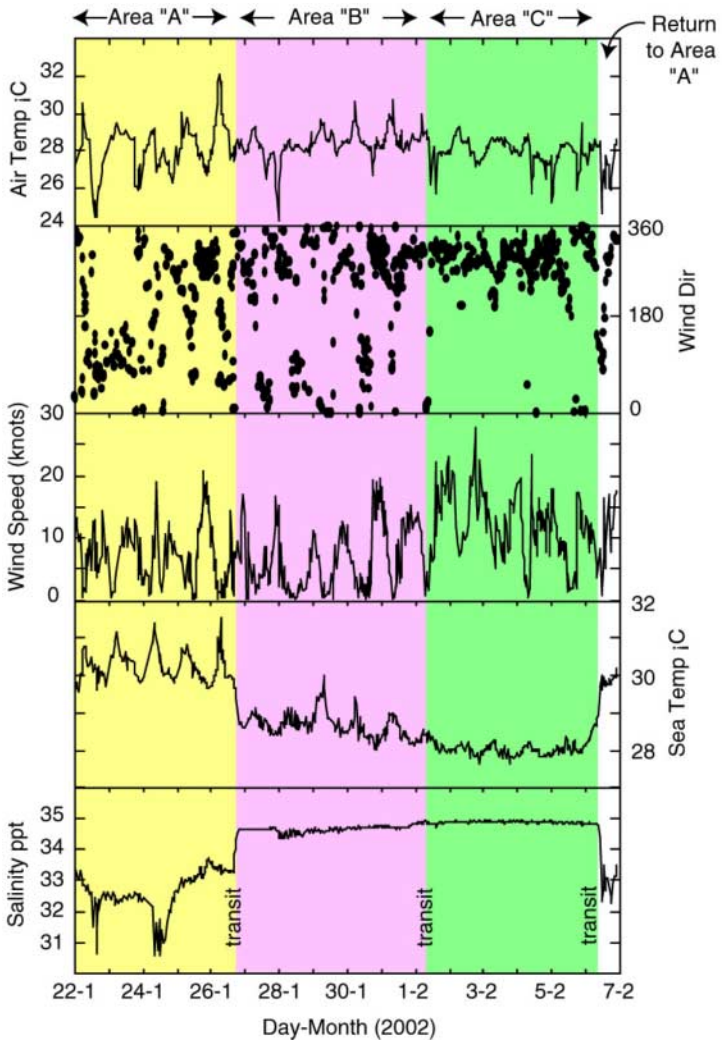

Figure 1.2. *Ship's log of air temperature, wind speed and direction, sea surface temperature and sea surface salinity during voyage FR01/02 (GA cruise 234). The colours indicate the times when surveys were carried out in areas A, B and C, (yellow, pink, and green, respectively). Hence, surface waters in Area A were warmer and fresher than Areas B and C. Winds were generally characterized by weak north-westerly monsoon winds. A diurnal pattern is evident in the wind record, with very weak variable winds (1-2 knots) occurring each afternoon, and 10 knots NW'erly winds occurring each night and early morning. A period of stronger winds from the NW was observed between 2-5 February, when mean exceeded 20 knots.*

Chapter 2. Methods

2.1 SWATH MAPPING SYSTEM

A Reson™ 240 kHz swath system (model no. 8101) was hired from James Cook University, School of Earth Sciences. The system recorded data using Reson 6042 Ver. 7.2 format software. The total amount of data recorded was 70 GB. An Applied Microsystems Ltd SV PLUS acoustic velocity profiler was used to measure the acoustic velocity range, which was from 1542 - 1546 m/s in the study area.

The transducer array was mounted on a 'trolley' through the moon pool about 30 cm below the hull. The moon pool is offset about 4 m from the vessel centre line. The motion sensor was mounted on the centre line. A hydraulic ram was used to pin the array against the aft wall of the moon pool with about 1 tonne of pressure so that the transducer array did not move during the survey.

Three areas were surveyed, designated Areas A, B and C (Fig. 1.1). Patch test lines were performed prior to the survey acquisition in each area. Our survey strategy was to maintain a consistent line spacing throughout the survey of each of the three areas. This gave the best coverage in the time available for the cruise, although it is recognised that some data would be missing in the more shallow areas. In Area B, where a line spacing of 250m was used, some data were missed in depths < 50m and in Area C, where a line spacing of 300m was used, some data were missed at depths less than about 60m.

2.1.1 Swath Data Processing

We encountered a range of problems in processing the swath data collected during the voyage. The bathymetry and sidescan data received was in Reson 6042 proprietary format that can only be read using this software, and as Geoscience Australia does not own this software we did not have any way of reading the data. This problem necessitated data conversion routines to be written and large amounts of disk space were required. Eventually, the depth data from areas B and C were provided in XTF format which was analysed using Carribes™ software. Backscatter data and depth data from Area A have not been provided in a useable format by James Cook University and hence it has not been processed at the time of writing this report (August, 2002).

The depth data from Areas B and C contain a persistent roll bias of 0-10 degrees, giving rise to a corrugated effect between adjacent lines. Removing this roll bias required significant work writing additional data correction routines. Tide corrections were performed during post-processing at GA using predicted tidal heights provided by the National Tidal Facility (NTF) at Flinders University, South Australia. The tidal heights were derived from a computer tide model and relate to the centre positions of the swath survey areas (A, B and C).

2.2 CHIRP SEISMIC DATA

A Datasonics™ 3.5 kHz Chirp Sub-bottom profiler, recorder model no. DSP 661/66 and tow fish model TTV170S was towed behind the ship throughout the survey. The trigger interval was 0.5 to 0.25 seconds (0.25 to 180 metres, 0.5 below 180 M) and the total amount of Chirp data recorded was 30 GB.

2.3 TEMPERATURE, SALINITY AND SUSPENDED SEDIMENTS

The ships Seabird™ SBE911 CTD was deployed along with a Seatech transmissometer, calibrated to measure suspended sediment concentration using surface and near-bed water samples. Two-litre water samples were filtered through pre-weighed 0.45 µm filter papers using a vacuum system to obtain mass concentration values. On return from the voyage, the filter papers were oven dried @ 60°C and re-weighed in the lab to the nearest ±0.0001 g.

2.4 SEDIMENT CORE AND SURFACE GRAB SAMPLES

Seabed sediment samples were collected using a Smith Macintyre grab and the AGSO 1-tonne gravity corer, also rigged to work as a piston corer. Sub-samples of sediment grabs were taken for laboratory analyses, including the collection of "mini-cores" where possible. Mini-cores were taken by pushing a short piece of plastic core liner by hand into the top 10 to 20 cm of the grab sample. The remainder of the grab was sieved and any living material was bagged, labelled and recorded.

2.4.1 Grain Size and Carbonate Analyses

Surface sediment grab samples were analysed for percentage gravel, sand and mud content by the sieve method, using nested 2mm and 63µm analytical sieves.

Carbonate content was determined on the dried sand and mud fractions separately using a carbonate bomb (Muller and Gastner, 1971). A known weight of dried and crushed sediment is placed in a sealed chamber with a pressure gauge fitted. Dilute hydrochloric acid is released inside the chamber and the dissolution of the calcite produces CO_2 gas. The mass of calcium carbonate is then determined by a calibration curve. The method has an estimated precision of ±1%. Values were run on separate grain size fractions (sand and mud) taken from the washed material. The carbonate content of the gravel fraction was determined visually.

2.4.2 Microscope Examination of Gravel and Sand Fractions

The washed residues from the gravel and sand fractions obtained from grain size analysis were used to examine the composition of grab samples. Leitz™ MZ12 stereozoom and Wild™ M32 microscopes were used for examination of samples. Representative views of the sand-sized fraction were photographed using an Olympus™ DP10 or DP11 digital camera top-mounted on the Leitz microscope. Gravel fractions were photographed using a Nikon™ coolpix 950 digital camera. Photographs of representative and unusual biota in the sand and gravel fractions were taken to provide a guide to identification.

Description of the samples was based on the method used by Radke, in Harris et al. (2000). Estimation of bioclast abundance was based on volume percentage, rather than weight, because of the difficulties involved in estimating weights and the likelihood of large errors (Harris et al., 2000). For all samples the whole gravel fraction was examined. Representative samples of s and fractions were obtained using a microsplitter. Estimates of composition were determined separately for each fraction, using a relative scale: abundant (>50%), moderate (20-49%), low (5-19%), minor (1-4%) and trace (<1%). The preservation of the biogenic components in the sand and gravel fraction of each sample was assessed as modern, intermediate or relict. The terminology used was based on that of Radke (in Harris et al., 2000).

The biota present were separated into phyla and identified to class level where possible. In both fractions, where fragments of bioclasts could be clearly recognised they were assigned to the relevant group. Fragments not clearly identifiable were classified as *other bioclasts*. Additional subsamples were collected from the Smith-Macintyre grabs and preserved in ethanol on board ship. In the Sedimentology Laboratory selected samples were washed in distilled water

and stained with varying concentrations of Rose Bengal solution over varying time periods to determine the most effective stain concentration and staining time. The preferred method selected is detailed in the attached notes. These samples were used to identify the presence of protoplasm and to confirm the identification of modern material based on preservation.

2.4.3 Subsurface Sediments

A total of 10 piston cores (PC1 - 10) and 21 gravity cores (GC1-12, 14-19, 21-24) were collected in PVC liners over the study area. The cores ranged in length from <0.2m to 4.03m. To fully characterise the sedimentary environments on the sea floor, cores were recovered from representative marine environments, including: channel beds, sediment drapes, *Halimeda* banks, and the distal part of the Fly River delta. The cores were cut into 1m sections, sealed, and transported to the laboratory for analysis of physical properties, composition, and texture.

2.4.3.1 Physical Properties

After equilibration with the ambient laboratory conditions (between 18 and 23°C), wet bulk density (WBD), P-wave velocity (Vp), magnetic susceptibility (MS), and fractional porosity (FP) were determined at 1 cm intervals down each core using a GEOTEK™ MS2 multi-sensor logger (e.g., Heap et al., 2001).

Wet Bulk Density (WBD) was determined by measuring the gamma attenuation of the sediment from a Cs-137 source. WBD of the sediment is positively correlated with gamma attenuation. The relationship between density and gamma attenuation was initially calibrated using a graduated density standard consisting of 13 water/aluminium density components (e.g., Best and Gunn, 1999). This procedure corrects for gamma attenuation (caused by the PVC liner), count rate effects (e.g., Weber et al., 1997), and the different scattering properties of seawater and sediment (e.g., Gerland and Villinger, 1995). The calibration was undertaken using a water density of 1.001 g cm^{-3}, and aluminium density of 2.71 g cm^{-3}, which is approximately equal to the mineral densities of siliciclastic (2.65 g cm^{-3}) and carbonate (2.67 g cm^{-3}) grains. Using this calibration, repeat density measurements were within 0.05 g cm^{-3}.

P-wave velocity (Vp) was determined by measuring the travel time of a 500 kHz ultrasonic compressional pulse across the core. The pulse propagates through the core from the transmitter and is detected by the receiver. Vp is directly related to changes in the composition and texture of the sediments (e.g., mineral composition, grain shape and size, packing, etc). To prevent variations in the ambient conditions masking differences between sedimentary units, the Vp was also corrected for temperature of the water and sediment and salinity of the interstitial fluid for each core.

Magnetic susceptibility (MS) was determined by measuring variations in the frequency of the AC waveform with a tuned oscillator circuit using a Bartington Instruments MS2 meter and magnetic loop. Variations in the frequency of the AC waveform associated with magnetically susceptible sediment are directly proportional to the MS of the sample (Robinson, 1990). Because magnetically susceptible grains (e.g., magnetite grains) have terrigenous origins, MS can be used as a measure of terrigenous versus marine input. The system was operated with an AC field strength of 80 A/m rms and at a frequency of 0.58 kHz (10s integration time).

Fractional porosity (FP) was calculated directly from the WBD using the equation:

FP = (MGD-WBD)/(MGD-WD)

where FP = fractional porosity, MGD = mineral grain density, GD1 = WBD, and WD = fluid density (i.e., sea water).

This calculation assumes that the sediment was fully saturated with seawater, a mineral density of siliciclastic and carbonate sediments of ~2.65 g cm^{-3}, and a fluid density of 1.024 g cm^{-3}.

2.4.3.2 Sediment Composition

Following analysis with the GEOTEK logger the cores were x-rayed in their PVC liners at Medical Imaging Australasia Ltd in Hobart. The x-radiographs were produced with settings of 30-90 kV and 60-200 mAs. Different combinations of settings were used to reveal internal structures and lithological changes. The cores were then transported to the Geoscience Australia Sedimentology Laboratory in Canberra where they were split, described, photographed, and subsequently sampled for composition and texture.

Samples of approximately 10 to 15g were taken every 5cm from each core for determining grain size distribution and calcium carbonate concentration. The disturbed nature of GC21 required that four samples were collected over the total length of the core. A total of 74 samples of peat, wood, coral, mollusc (bivalve, gastropod), and bulk sediment were also collected for possible radiocarbon age determinations (Table 2.1). Samples of *in-situ* deposits of calcite were also collected from PC3 and PC10 for mineralogical analysis (Table 2.1). Digital photographs of the core archives were taken using a Nikon™ Coolpix® 950 digital camera and provided an image with a resolution of 1,600 x 1,200 pixels. Individual photographs of core sections were then made into whole core composites for display purposes.

Table 2.1. Details of samples collected for C-14 age determination and mineral analysis.

CORE	DEPTH (M)	SAMPLE TYPE	CORE	DEPTH (M)	SAMPLE TYPE
PC1	0	bulk sediment	GC2	0.02	Peat
	0.30	bulk sediment		0.25	peat
	1.70	bulk sediment		0.46	peat
	1.83	bivalve shells (2 valves)		0.75	peat
PC2	0.42	pelecypod (part valve)		0.89	peat
	0.48	bulk sediment		1.17	peat
	0.49	coral		1.40	peat
	0.90	wood		1.51	peat
	1.33	peat	GC4	0.36	wood
	1.52	peat/charcoal	GC5	0.17	shell hash/bryozoan
	1.69	Halimeda/shell hash		1.52	bulk sediment
PC3	0.55	echinoid	GC6	0.02	peat/clay
	0.61	bivalve (articulated)		0.06	organic matter
	1.65	bivalve (single valve)	GC7	0.78	bulk sediment
	1.95	bivalve valve	GC10	0.80	wood
	2.02	shell hash	GC11	0.02	wood
PC4	0.54	shell hash		0.14	wood
	1.53	peat	GC12	0.85	bulk sediment
	1.69	peat	GC14	0.35	gastropod (archive half)
	1.98	bivalve (single valve)		0.97	gastropod (archive half)

CORE	DEPTH (M)	SAMPLE TYPE	CORE	DEPTH (M)	SAMPLE TYPE
PC5	0.45	peat	GC17	0.10	bulk sediment
	1.33	peat		1.03	bulk sediment
	1.58	peat		1.75	shell
	1.95	peat		2.00	bulk sediment
	2.15	peat-rich mud		2.95	bulk sediment
	2.35	peat			
	2.63	peat	**MINERAL ANALYSIS**		
	3.18	peat-rich mud	CORE	DEPTH (M)	SAMPLE TYPE
PC6	1.70	bivalve valve	PC3	0.61	gypsum
	1.82	peat	PC10	0.26	gypsum
	2.34	peat			
	2.73	peat			
	3.19	peat			
PC7	2.16	gastropod			
	2.60	bulk sediment			
	3.40	wood			
	3.65	peat			
	3.98	organic matter			
PC8	0.39	shell			
	0.80	coral			
	0.97	pelecypod			
	1.70	bulk sample			
	2.55	bulk sample			
PC9	0.74	peat			
	1.46	peat			
	1.64	peat			
PC10	0.50	gastropod			
	0.92	organic matter			
	1.24	organic matter			

2.4.4 Foraminifera Analyses

Investigation into the use of foraminifera in habitat characterisation and mapping was undertaken in two parts. Benthic habitats and foraminiferal assemblages were characterised for 12 selected stations to determine whether the foraminiferal assemblages could be used to differentiate the same habitat groups. The 12 stations were selected so as to have at least two stations for each habitat type (Table 2.2) and four stations for each of the three study areas.

The benthic habitats of the twelve sample stations were characterised by the attributes listed in Table 2.2. The habitats were defined so the stations were grouped into the most rational habitat groupings at a scale of tens of metres to kilometres.

Table 2.2. Attributes used for habitat characterisation and their collection method.

ATTRIBUTE	COLLECTION METHOD
Depth	Ship-board Depth Sounder
Grain-Size	Sediment Grab Analysis
Seabed Morphology	Underwater Videography and Chirp sub-bottom profiling (single-channel shallow seismic system)
Sediment Coverage	Underwater Videography
Seabed Slope	Underwater Videography
Seabed Texture	Underwater Videography
Biological Coverage	Underwater Videography
Bioturbation	Underwater Videography

For each of the 12 selected stations, 1 g sub-samples of the sand fractions were collected and further sieved into 62.5 to 150µm and 150µm to 2mm fractions. Foraminiferal abundances were found by 300+ foraminifera systematic picks of the 150µm to 2mm fraction from each of the stations. Statistically, picking 300+ foraminifera ensures a 95% probability of detecting species with abundances of 1% (Dennison & Hay, 1967). Partial or broken foraminiferal tests were included in the total foraminifera counts, and if the test could be identified and was more than half complete it was also included in the count for the particular species or group. Some foraminifera showed signs of reworking (iron staining and being filled with consolidated sediment), however these were not differentiated from non-reworked or living/recently dead foraminifera.

The systematic picks were augmented with selective picking of the total sand fractions (65µm to 2mm) to include smaller foraminifera in the taxonomic list.

Species were identified based on the descriptions of Ellis & Messina (1940 *et seq*.), Haig (1993), Hottinger et al. (1993), Loeblich and Tappan (1994) and Hayward et al. (1997). To aid identification, digital light micrographs and Scanning Electron Microscope (SEM) images were taken of the foraminifera - the latter taken on the Cambridge S360 SEM at the Australian National University Electron Microscopy Unit (ANU EMU). These images are catalogued in an Extensis Portfolio® image database included in the attached cd-rom, and are searchable by species with the included Portfolio Browser®.

Foraminifera species and groups were broken into the following classes based on their abundances:

- Abundant – 10% or greater at all stations in a habitat
- Minor – between 1 and 10% abundance in at least one station in a habitat
- Absent/Very Low Abundance – 1% or less in all sites in a habitat

Due to time constraints the abundance data was only obtained for the foraminiferal groups, genera and species with estimated abundances greater than 1%. The foraminiferal groups, genera and species (here referred to collectively as ‘foraminiferal groups’) are listed in Table 2.3. Further notes on the collection and processing of the sediment grabs are included in other sections of this record.

Table 2.3. Foraminifera groups (and their constituent species), with estimated abundances greater than 1%, used in the foraminiferal abundance counts. The categories followed by an asterix were used to define assemblages for each of the habitats.

GROUPS	FORAMINIFERAL SPECIES
Amphistegina spp.*	A. papillosa, A. radiata (plus rare A. lobifera/A. lessonii)
Assilina ammonoides*	Assilina ammonoides
Asterorotalia gaimardi or Challengerella persica	Asterotalia gaimardi or Challengerella persica
Elphidium spp.	E. advenum, E. albanii, E. charlottense, E. craticulatum, E. crispum, E. cf. mortonbayense, E. simplex
Fijiella cf. simplex, ?Reussella weberi, Reussella cf. hayasakai	Fijiella cf. simplex, ?Reussella weberi, Reussella cf. hayasakai
Miniacina miniacea*	Miniacina miniacea
Nubeculina advena	Nubeculina advena
Nummulites venosus*	Nummulites venosus
Plotnikovina spp.*	Plotnikovina spp.
Gaudryina attenuata*	Gaudryina attenuata
Quinqueloculina philippinensis	Quinqueloculina philippinensis

GROUPS	FORAMINIFERAL SPECIES
Spiroplectinella pseudocarinata*	Spiroplectinella pseudocarinata
Textularia agglutinans	Textularia agglutinans
Textularia foliacea	Textularia foliacea
Peneroplids*	Peneroplis pertosus, Dendritina striata
Planktics*	Globigerinoides ruber, Neogloboquadrina blowi or Globigerinella siphonifera
Remaining Species	All other species not listed above

2.5 SEABED VIDEO

Video footage of the seafloor was collected to characterise the seabed type and record associated benthic fauna. An underwater video camera was deployed for a minimum of three minutes at each of the stations. The video camera was hired from Dr. Yvonne Bone, University of Adelaide, and comprised an analogue VHS video recorder with two, battery-powered, flood lights. The video frame was set up with a scale bar, mounted within the viewing area. The analogue camera provided real time display of footage, enabling the winch control to maneuver the camera frame as required to view specific seabed features. Seafloor characteristics and the main biota were described on board ship and recorded in the shipboard database. Highlights of the video footage from each station were converted into digital format.

2.6 BENTHIC INSTRUMENT FRAME (BRUCE)

Current, temperature, salinity and turbidity measurements were made using a frame designed for deployment in shelf water depths up to 300 m. The *Benthic Research for Underwater sediment ConcEntrations* probe (BRUCE) was constructed at Geoscience Australia. It comprises a Nortek™ vector acoustic current meter, Benthos™ optical backscatter sensor, Sequoia™ LISST-100 transmissometer – laser particle sizer and Seabird™ CTD. BRUCE was deployed at location 9° 7.364'S, 143° 43.113'E in 31.5 m water depth. Instruments were switched on at 23:21 21-Jan-2002 GMT, and the mooring was deployed at 07:21 22-Jan-2002 GMT. The mooring was recovered at 12:00 6-Feb-2002 GMT. On recovery some biofouling was apparent, however it was not in such significant abundance as to interfere with data recording.

The Nortek vector acoustic current meter (ADV #N4103) was positioned to sample at 100cm above the base of the benthic frame. The ADV was programmed to burst sample every 20 minutes for 90 s at 8 Hz, a time scale that enables turbulence to be resolved. Vector components of velocity (east, north and up) and temperature were logged internally and down-loaded on recovery. Data were checked for consistency and, when necessary, edited to remove clearly erroneous data.

The Benthos optical backscatter sensor (OBS #897) was positioned at 100cm above the benthic frame, facing inwards from one vertical support bar. The OBS was powered by, sampled at the same rate as, and logged to the ADV. OBS output is recorded in counts as an analog input to the ADV. This is converted to volts (5 V = 65535 counts) and subsequently converted to turbidity (ftu).

Turbidity (ftu) = $356.7*(x + 0.002)$

where x is the output in Volts.

The Sequoia LISST-100 transmissometer – laser particle sizer (LISST #104579) was placed 27 cm above the base of the benthic frame. The LISST was programmed to burst sample every 20 minutes for 90 s at 2 Hz. The LISST logged internally until the 2MB memory card was full

(~13 days, or ~2 days short of the total deployment period). Data were down-loaded on recovery in day long segments. Transmissivity, battery voltage and volume concentration for 32 size bins were recorded.

The Seabird CTD (CTD #1620) was also placed at 27cm above the base of the frame. The CTD was programmed to samples at the same rate as the LISST. Temperature and conductivity were logged to the LISST internal memory.

Two 20cm lengths of 9cm diameter plastic pipe were placed in the frame at 30cm and 100cm height above the base of the frame, to serve as sediment traps for the deployment.

Chapter 3. Results

In this chapter, the geophysical and station data collected during the cruise are presented and described. Swath mapping and Chirp sub-bottom profile data were collected along evenly spaced track lines, over a total track length of around 2,000km. A total of 75 stations were occupied (Table 3.1) spread more or less evenly between the three survey areas. Station locations are listed in Table 3.1 and shown in relation to bathymetric maps in Figures 3.2, 3.4 and 3.6. In summary, the following samples were recovered: 64 surface grab samples, 64 CTD's, 125 filter papers (from surface and 2m above the seabed), 10 piston cores, 24 gravity cores, 65 underwater video stations and 2 sediment trap samples. The instrument mooring BRUCE was successfully recovered and, after inspection, was found to have logged all data as per the program.

Table 3.1. List of station locations and operations completed during cruise 234 (Fr 01/02). Operation codes are as follows: CM = current meter; CTD = conductivity, temperature depth profile; CAM = video camera pictures of seabed; GR = Smith Macintyre Grab Sample; PC = piston core; GC = gravity core. Station numbers in parentheses are repeat stations targeted at the same locations.

"Area A, Fly River Delta"

STATION NO	LATITUDE	LONGITUDE	WATER DEPTH	OPERATIONS
"1 (27, 77)"	-9°7.364	143°43.113	31.50	234/1CM1
	-9°7.616	143°43.1	31.50	234/1CTD1
	-9°7.4	143°43.2	31.50	234/1CAM1
	-9°7.3	143°43.1	31.50	234/1GR1
2	-9°7.584	143°40.086	30.50	234/2CAM2
	-9°7.586	143°40.161	30.00	234/2CTD2
	-9°7.58	143°40.085	30.00	234/2GR2
3	-9°8	143°40.518	29.00	234/3CTD3
	-9°8.048	143°40.559	29.00	234/3PC1
	-9°8.048	143°40.559	29.00	234/3GR3
	-9°8.037	143°40.584	29.50	234/3CAM3
4	-9°6.564	143°42.054	23.00	234/4CTD4
	-9°6.576	143°42.038	24.50	234/4GR4
	-9°6.575	143°42.042	24.00	234/4CAM4
5 (22)	-9°7.929	143°40.787	33.00	234/5CTD5
	-9°7.928	143°40.767	34.00	234/5CAM5
	-9°7.964	143°40.779	33.50	234/5GR5
6	-9°7.691	143°41.769	28.00	234/6CAM6
	-9°7.025	143°41.745	25.50	234/6CTD6
	-9°7.69	143°41.754	28.50	234/6GR6
7 (23)	-9°9.129	143°41.353	32.00	234/7CTD7
	-9°9.122	143°41.342	32.50	234/7GR7
	-9°9.135	143°41.334	32.50	234/7CAM7
8	-9°10.291	143°41.677	31.50	234/8GR8
	-9°10.271	143°41.684	31.50	234/8CTD8
	-9°10.255	143°41.713	31.50	234/8CAM8
9 (24)	-9°9.11	143°42.88	31.50	234/9CAM9
	-9°9.002	143°42.891	31.50	234/9CTD9
	-9°9.11	143°42.871	32.00	234/9GR9
10	-9°9.087	143°42.158	32.50	234/10CTD10
	-9°9.114	143°42.153	33.00	234/10GR10
	-9°9.107	143°42.131	33.00	234/10CAM10

STATION NO	LATITUDE	LONGITUDE	WATER DEPTH	OPERATIONS
11 (25)	-9º8.08	143º43.874	33.50	234/11CAM11
	-9º8.111	143º43.90	33.50	234/11CTD11
	-9º8.074	143º43.872	34.00	234/11GR11
12	-9º9.01	143º43.817	35.00	234/12CAM12
	-9º8.98	143º43.829	34.50	234/12GR12
	-9º9.016	143º43.827	35.00	234/12CTD12
13 (26)	-9º7.527	143º45.209	33.50	234/13GR13
	-9º7.537	143º45.194	33.50	234/13CTD13
	-9º7.511	143º45.215	33.50	234/13CAM13
14 (76)	-9º7.08	143º44.787	33.00	234/14GR14
	-9º7.08	143º44.796	32.50	234/14CTD14
15	-9º7.552	143º42.917	32.50	234/15GR15
	-9º7.527	143º42.943	32.50	234/15PC2
	-9º7.554	143º42.918	33.00	234/15CAM15
	-9º7.526	143º42.902	32.50	234/15CTD15
16	-9º7.022	143º42.561	30.00	234/16GR16
	-9º7.064	143º42.552	31.00	234/16CTD16
	-9º6.98	143º42.541	29.50	234/16CAM17
	-9º7.057	143º42.549	30.50	234/16CAM16
17	-9º6.222	143º43.513	30.00	234/17CTD17
	-9º6.287	143º43.469	30.00	234/17CAM18
	-9º6.178	143º43.495	30.50	234/17GR17
	-9º6.065	143º43.546	29.50	234/17PC3
18	-9º6.135	143º44.082	29.00	234/18CAM19
	-9º6.15	143º44.081	29.50	234/18CTD18
	-9º6.131	143º44.082	29.00	234/18GR18
19	-9º5.216	143º43.883	29.50	234/19CAM20
	-9º5.217	143º43.879	29.50	234/19CTD19
	-9º5.187	143º43.883	29.50	234/19PC4
	-9º5.206	143º43.876	29.00	234/19GR19
20	-9º5.726	143º42.672	29.00	234/20CAM21
	-9º5.706	143º42.68	28.50	234/20CTD20
	-9º5.713	143º42.675	29.00	234/20GR20
21	-9º7.019	143º40.816	29.50	234/21GR21
	-9º7.013	143º40.816	30.00	234/21PC5
	-9º7.014	143º40.814	29.50	234/21CAM22
	-9º7.014	143º40.817	29.50	234/21CTD21
22 (5)	-9º7.924	143º40.738	34.50	234/22PC6
23 (7)	-9º9.132	143º41.358	34.00	234/23PC7
24 (9)	-9º9.093	143º42.88	32.50	234/24PC8
25 (11)	-9º8.109	143º43.886	33.00	234/25PC9
26 (13)	-9º7.49	143º45.224	31.00	234/26PC10
"27 (1, 77)"	-9º7.537	143º42.927	30.50	234/27CTD22
76 (14)	-9º7.086	143º44.781	31.00	234/76CAM66
77 (1)	-9º7.359	143º43.234	31.00	234/77CTD65

"Area B, Torres Strait"

STATION NO	LATITUDE	LONGITUDE	WATER DEPTH	OPERATIONS
28	-9º29.196	143º56.749	56.00	234/28CAM23
	-9º29.13	143º56.704	51.50	234/28CTD23
	-9º29.176	143º56.733	55.00	234/28GR22
	-9º29.144	143º56.734	53.00	234/28GC1
29	-9º28.098	143º58.586	46.00	234/29CTD24
	-9º28.096	143º58.587	46.00	234/29GR23
	-9º28.104	143º58.587	47.40	234/29CAM24

STATION NO	LATITUDE	LONGITUDE	WATER DEPTH	OPERATIONS
30	-9º29.551	144º0.264	54.00	234/30CTD25
	-9º29.586	144º0.258	54.00	234/30GR24
	-9º29.81	144º0.26	54.00	234/30CAM25
31	-9º28.506	144º1.04	51.50	234/31CTD26
	-9º28.465	144º1.004	52.00	234/31GR25
	-9º28.483	144º1.017	52.00	234/31CAM26
32 (53)	-9º27.565	143º59.729	131.50	234/32GR26
	-9º27.566	143º59.73	132.30	234/32CTD27
	-9º27.558	143º59.728	132.00	234/32CAM27
33	-9º27.844	143º57.818	50.50	234/33CTD28
	-9º27.835	143º57.823	50.50	234/33CAM28
	-9º27.826	143º57.816	50.50	234/33GR27
34 (52)	-9º27.431	143º57.134	90.00	234/34GR28
	-9º27.429	143º57.119	86.00	234/34CTD29
	-9º27.446	143º57.119	86.00	234/34CAM29
35 (51)	-9º26.083	143º57.365	103.00	234/35GR29
	-9º26.081	143º57.361	103.00	234/35CAM30
	-9º26.071	143º57.369	103.00	234/35CTD30
36 (50)	-9º26.776	143º59.182	84.00	234/36CAM31
	-9º26.748	143º59.153	85.50	234/36GR30
	-9º26.771	143º59.171	84.00	234/36CTD31
37	-9º26.865	144º1.292	51.50	234/37CTD32
	-9º26.899	144º1.291	49.00	234/37CAM32
	-9º26.882	144º1.301	50.00	234/37GR31
38	-9º25.68	144º0.731	55.50	234/38GR32
	-9º25.651	144º0.736	56.50	234/38CTD33
	-9º25.658	144º0.725	56.50	234/38CAM33
39 (49)	-9º23.823	144º0.655	59.50	234/39CTD34
	-9º23.87	144º0.661	60.00	234/39CAM34
	-9º23.867	144º0.646	60.00	234/39GR33
40	-9º24.049	144º2.021	57.50	234/40GR34
	-9º24.032	144º2.017	58.50	234/40CAM35
	-9º24.017	144º2.046	54.00	234/40CTD35
41	-9º24.66	144º0.689	58.50	234/41CTD36
	-9º24.705	144º0.695	58.00	234/41CAM36
	-9º24.65	144º0.668	59.50	234/41GR35
	-9º24.653	144º0.71	59.00	234/41GC2
42	-9º24.456	143º58.807	80.50	234/42GR36
	-9º24.551	143º58.774	77.00	234/42GC3
	-9º24.524	143º58.736	80.50	234/42CTD37
	-9º24.522	143º58.752	78.50	234/42CAM37
43	-9º23.043	143º58.768	80.00	234/43GR37
	-9º23.032	143º58.778	81.00	234/43GC4
	-9º23.052	143º58.767	80.00	234/43CAM38
	-9º23.054	143º58.768	80.00	234/43CTD38
44	-9º22.546	144º1.073	90.00	234/44CAM39
	-9º22.557	144º1.078	85.00	234/44GC5
	-9º22.548	144º1.073	88.50	234/44CTD39
	-9º22.552	144º1.077	87.00	234/44GR38
45	-9º22.367	144º2.162	91.50	234/45CTD40
	-9º22.356	144º2.161	91.50	234/45GR39
	-9º22.357	144º2.16	91.50	234/45GC6
	-9º22.958	144º2.165	91.50	234/45CAM40

STATION NO	LATITUDE	LONGITUDE	WATER DEPTH	OPERATIONS
46	-9º21.029	144º2.137	62.00	234/46CTD41
	-9º21.036	144º2.138	63.00	234/46CAM41
	-9º21.038	144º2.139	63.50	234/46GR40
	-9º21.039	144º2.144	63.00	234/46GC7
47	-9º19.911	144º0.913	57.50	234/47GR41
	-9º19.909	144º0.912	57.50	234/47CTD42
	-9º19.91	144º0.114	57.50	234/47CAM42
	-9º19.908	144º0.908	57.50	234/47GC8
48	-9º20.655	143º58.77	57.00	234/48GC9
	-9º20.66	143º58.763	57.00	234/48GR42
	-9º20.654	143º58.768	57.00	234/48CAM43
	-9º20.649	143º58.76	57.00	234/48CTD43
49 (39)	-9º23.849	144º0.687	57.00	234/49GC10
50 (36)	-9º26.754	143º59.151	79.80	234/50GC11
51 (35)	-9º26.056	143º57.351	104.00	234/51GC12
52 (34)	-9º27.433	143º57.124	86.50	234/52GC13
53 (32)	-9º27.561	143º59.726	131.50	234/53GC14

"Area C, Gulf of Papua"

54	-9º22.765	144º16.838	113.50	234/54GC15
	-9º22.865	144º16.72	114.50	234/54CAM44
	-9º22.816	144º16.718	119.00	234/54GR43
	-9º22.812	144º16.752	121.00	234/54CTD44
55	-9º24.591	144º16.578	66.00	234/55CTD45
	-9º24.589	144º16.582	65.50	234/55CAM45
	-9º24.581	144º16.57	64.50	234/55GR44
	-9º24.562	144º16.564	63.50	234/55GC16
56	-9º25.278	144º17.058	26.00	234/56CTD46
	-9º25.283	144º17.055	29.50	234/56CAM46
57	-9º25.029	144º18.503	49.50	234/57CTD47
	-9º25.041	144º18.508	50.00	234/57GR45
	-9º25.034	144º18.506	49.50	234/57CAM47
58	-9º24.481	144º19.325	103.50	234/58CAM48
	-9º24.48	144º19.334	104.50	234/58GR46
	-9º24.478	144º19.33	103.50	234/58GR47
	-9º24.491	144º19.342	103.00	234/58CTD48
59	-9º23.376	144º21.946	75.00	234/59CTD49
	-9º23.421	144º21.977	76.00	234/59GR48
	-9º23.464	144º21.975	78.50	234/59GC17
	-9º23.476	144º22.154	80.00	234/59CAM49
60	-9º25.348	144º21.127	95.50	234/60CTD50
	-9º25.335	144º21.124	96.00	234/60GR49
	-9º25.336	144º21.121	96.00	234/60CAM50
61	-9º26.671	144º21.444	90.00	234/61CAM51
	-9º26.683	144º21.445	92.00	234/61GC18
	-9º26.685	144º21.447	92.00	234/61GR50
	-9º26.664	144º21.439	89.00	234/61CTD51
62	-9º27.821	144º21.445	104.00	234/62GC19
	-9º27.818	144º21.445	103.50	234/62GR51
	-9º27.825	144º21.447	104.00	234/62CTD52
	-9º27.805	144º21.446	103.50	234/62CAM52
63	-9º30.542	144º21.57	91.00	234/63GC20
	-9º30.555	144º21.578	90.50	234/63GR52
	-9º30.534	144º21.582	90.00	234/63CAM53
	-9º30.526	144º21.58	90.00	234/63CTD53

STATION NO	LATITUDE	LONGITUDE	WATER DEPTH	OPERATIONS
64	-9°31.278	144°20.417	117.00	234/64GR53
	-9°31.255	144°20.42	119.00	234/64GC21
	-9°31.26	144°20.398	112.50	234/64CAM54
	-9°31.258	144°20.389	113.00	234/64CTD54
65	-9°30.584	144°19.08	52.50	234/65GR54
	-9°30.591	144°19.123	43.00	234/65CAM55
	-9°30.585	144°12.12	41.50	234/65CTD55
66	-9°28.433	144°18.971	82.50	234/66GR55
	-9°28.418	144°18.974	83.00	234/66GC22
	-9°28.388	144°18.97	82.50	234/66CAM56
	-9°28.395	144°18.974	82.50	234/66CTD56
67	-9°27.267	144°19.813	79.50	234/67CAM57
	-9°27.253	144°19.808	80.00	234/67CTD57
	-9°27.277	144°19.805	79.00	234/67GR56
68	-9°26.277	144°17.859	88.50	234/68CTD58
	-9°26.267	144°17.355	89.00	234/68GR57
	-9°26.319	144°17.855	88.50	234/68CAM58
69	-9°29.331	144°18.15	109.00	234/69GR58
	-9°29.335	144°18.15	109.50	234/69CAM59
70 (71)	-9°31.94	144°16.533	50.50	234/70GR59
	-9°32.045	144°16.526	48.50	234/70CTD60
	-9°31.988	144°16.541	50.00	234/70CAM60
71 (70)	-9°32.033	144°16.488	48.50	234/71CAM61
72	-9°30.144	144°16.031	171.50	234/72GR60
	-9°30.146	144°16.034	172.00	234/72CAM62
	-9°30.143	144°16.041	173.00	234/72CTD61
73	-9°26.682	144°16.673	117.00	234/73GC23
	-9°29.677	144°16.665	116.00	234/73GR61
	-9°29.659	144°16.677	117.00	234/73CAM63
	-9°29.66	144°16.667	116.50	234/73CTD62
74	-9°28.83	144°17.194	90.00	234/74GR62
	-9°28.828	144°17.196	90.00	234/74GC24
	-9°28.827	144°17.196	90.00	234/74CAM64
	-9°28.834	144°17.197	90.00	234/74CTD63
75	-9°33.59	144°20.018	219.50	234/75GR63
	-9°33.055	144°20.014	220.00	234/75GR64
	-9°33.058	144°20.006	220.50	234/75CTD64
	-9°33.058	144°20.016	221.00	234/75CAM65

3.1 SWATH BATHYMETRY DATA

Swath mapping and Chirp sub-bottom profile data were collected along evenly spaced track lines. In Area A, the track lines were aligned 55° from true north (Fig. 3.1), such that the survey lines were parallel to the regional 20 and 30m contours (taken from chart AUS 378).

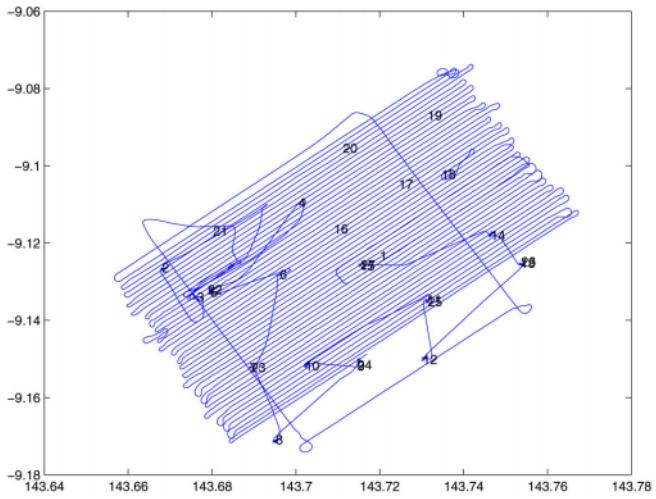

Figure 3.1. *Survey track lines completed in Area "A", adjacent to the Fly River Delta (see Fig. 1.1).*

The bathymetry of Area A shows a gently seaward-dipping ramp (Fig. 3.2), forming a distal section of the Fly River Delta. The water depths in Area A range from about 26 to 35 m and the overall slope dips seawards at 0.07°. Low relief (±2 m) ridges and swales which trend parallel to the regional bathymetric contours, can be detected in Figure 3.2. Other notable bathymetric features in Area A include a shallow (±3 m) gully, having its axis aligned normal to the regional isobaths (i.e. trending northwest-southeast), extending between stations 5/22 and 7/23 (Fig. 3.2). Further to the northeast, a linear rocky ridge also trending northwest-southeast across the area, rises up to about 5m above the level of the surrounding seabed in the vicinity of stations 14/76.

Survey lines in Area B were aligned north-south in the northern part of the area, and east-west in the southern part (Fig. 3.3). The survey in this area confirmed the presence of a submarine valley system, trending east-west across the shelf (Fig. 3.4), as described by Harris et al. (1996). The valley comprises two separate limbs, which appear to have branched around a rocky pinnacle reef, which occurs in the west-central part of the study area.

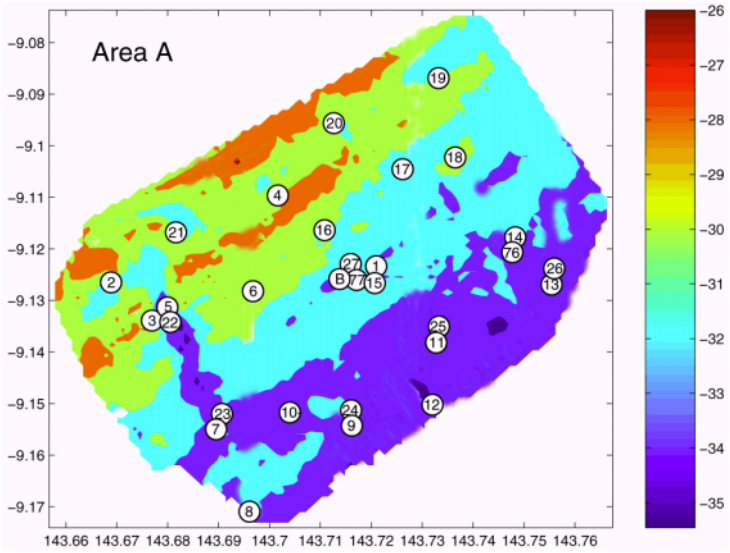

Figure 3.2*. Location of stations occupied in Area "A" in relation to regional bathymetry. The position of current meter station (B), in the centre of the study area, is indicated.*

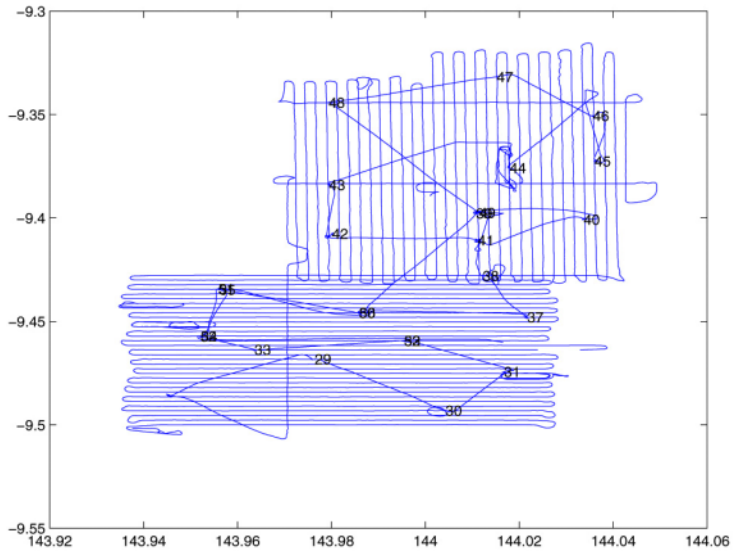

***Figure 3.3**. Survey track lines completed in Area "B", on the middle part of the Torres Strait shelf (see Fig. 1.1).*

The valleys in Area B are as deep as 130m below sea level, and the overall depth range in the areas surveys ranged from around 40 to 130m. Shoal reefs were found in the southernmost section of Area B, where reef pinnacles were mapped to within 9m of the sea surface. Smaller, low-relief (±10m) gullies drain into the larger valleys from the shallow area located along the valley margins.

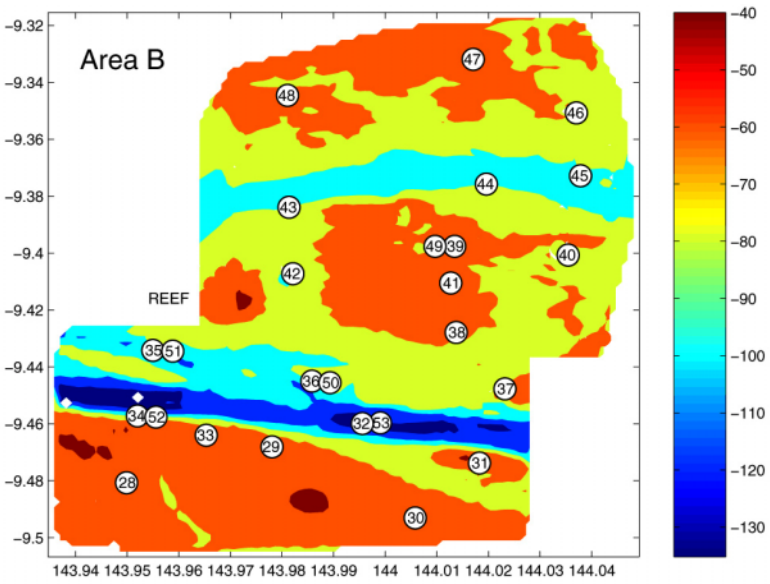

***Figure 3.4.** Location of stations occupied in Area "B" in relation to regional bathymetry.*

In area C, the survey lines were run north-south, apart from a small area in the southern part of the area, where some east-west lines were run (Fig. 3.5). The changed orientation of lines in this area was to assist with the navigation of the vessel while it was working in the shoal reef areas that occurred in that section of Area C. The survey in this area confirmed the presence of a submarine valley system, trending east-west across the shelf (Fig. 3.6), as described by Harris et al. (1996). The valley comprises two separate limbs, located to the north and south of East Cay.

The valley floors in Area C are as deep as 220m and exhibit local over deepening with closed contour lines. The overall alignment of the valleys is distinctly WNW-ENE (Fig. 3.6).

A second major feature of Area C is the shallow (30-50m depth) platform reef which extends eastwards from East Cay. The platform is cut by localised channels (eg in the vicinity of station 59; Fig. 3.6). The shoal area in the south (i.e. south of stations 70-71; Fig. 3.6) is the northward extension of the Great Barrier Reef platform complex.

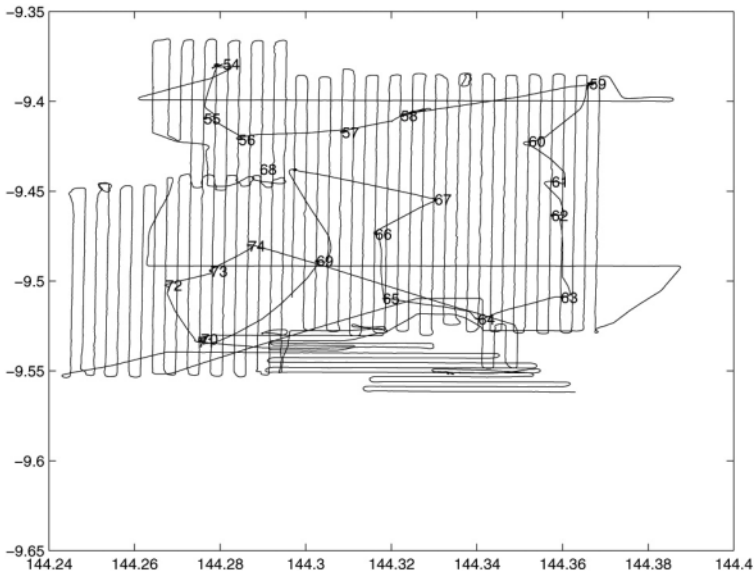

Figure 3.5. *Survey track lines completed in Area "C", outer shelf of the Gulf of Papua, adjacent to East Cay (see Fig. 1.1).*

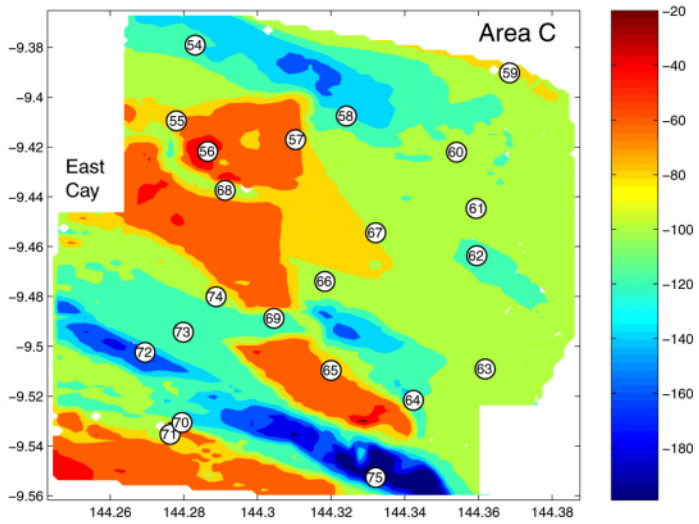

Figure 3.6. *Location of stations occupied in Area "C" in relation to regional bathymetry.*

3.2 CHIRP SEISMIC DATA

Chirp seismic data were collected along all of the swath bathymetry survey lines (Figs. 3.1, 3.3 and 3.5). The data were interpreted during the cruise and the information was recorded onto large format (1:10,000 scale) "collector" maps. Both surface acoustic character and subsurface features were recorded. Copies of the data are included on the attached CD-ROM as Appendix B.

The main features observed in Area A are sub-surface; infilled channels and planar reflectors typically 2 to 3m below the seabed are common (Figs. 3.7; 3.8). Three separate infilled channels trend north-south across the area, in which infilling is typically 8 to 10m, reaching a maximum thicknesses of 22m. In some locations, the acoustic basement reflector crops out on one side of the channel, forming a rocky pinnacle. These pinnacles are commonly around 2m in vertical relief, although some may reach heights of up to 7m above the level of surrounding seabed. Minor features observed in Area A include rocky bottoms (Fig. 3.8), pockmarks and (along the southeastern margin of the area) some low-relief (~2 m amplitude) sandwaves.

Area B is characterised by two east-west trending shelf valleys, which separate three elevated platforms, each having its own distinct assemblage of acoustic features (Fig 3.9). The valley floors are commonly featureless and acoustically opaque (Figs. 3.10A and B). The southernmost platform is 40-50m deep and is dominated by rocky reefs (coral bombies) which locally rise up to the sea surface (9 m below the surface; Fig. 3.10B). The largest of these reefs are located adjacent to the southern side of the shelf valley. The southern platform also exhibits localised infilled channels and erosional notches and incisions.

The central platform of Area B lies in 60-80m water depth, flanked on its northern and southern sides by deep shelf valleys. It includes a large un-named patch reef on its western margin (Fig. 3.9). The elevated middle part of the central platform exhibits widespread erosional notches and incisions, with some rocky reefs along the eastern part of the surveyed area (Fig. 3.10B). The other prominent feature of the central platform is the occurrence of subsurface reflectors located along both of the valley margins. These subsurface reflectors are commonly low-relief and gently dipping towards the south. To the south of the un-named reef, the thickness of sediment overlying the reflectors is around 20m (Fig. 3.9).

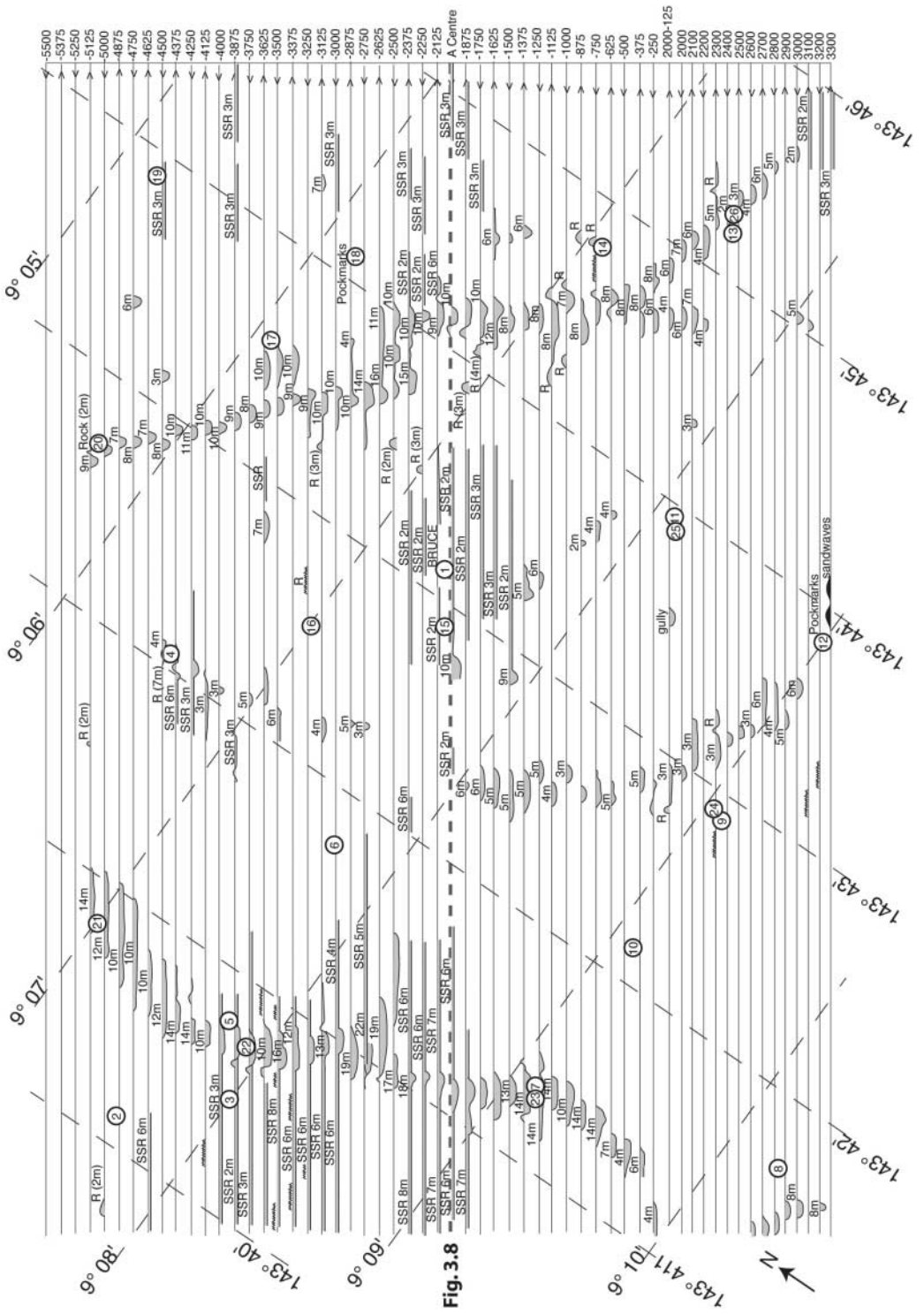

Figure 3.7. *Track map and interpreted features based on Chirp profiles collected in Area A. Numbers refer to the depth of sub-surface reflectors (SSR) and to the thickness of sediment within the infilled channels (not drawn to scale). The locations of rough, rocky bottoms, rock outcrops, pockmarks and sandwaves are also indicated. Dashed track line shows position of Figure 3.8.*

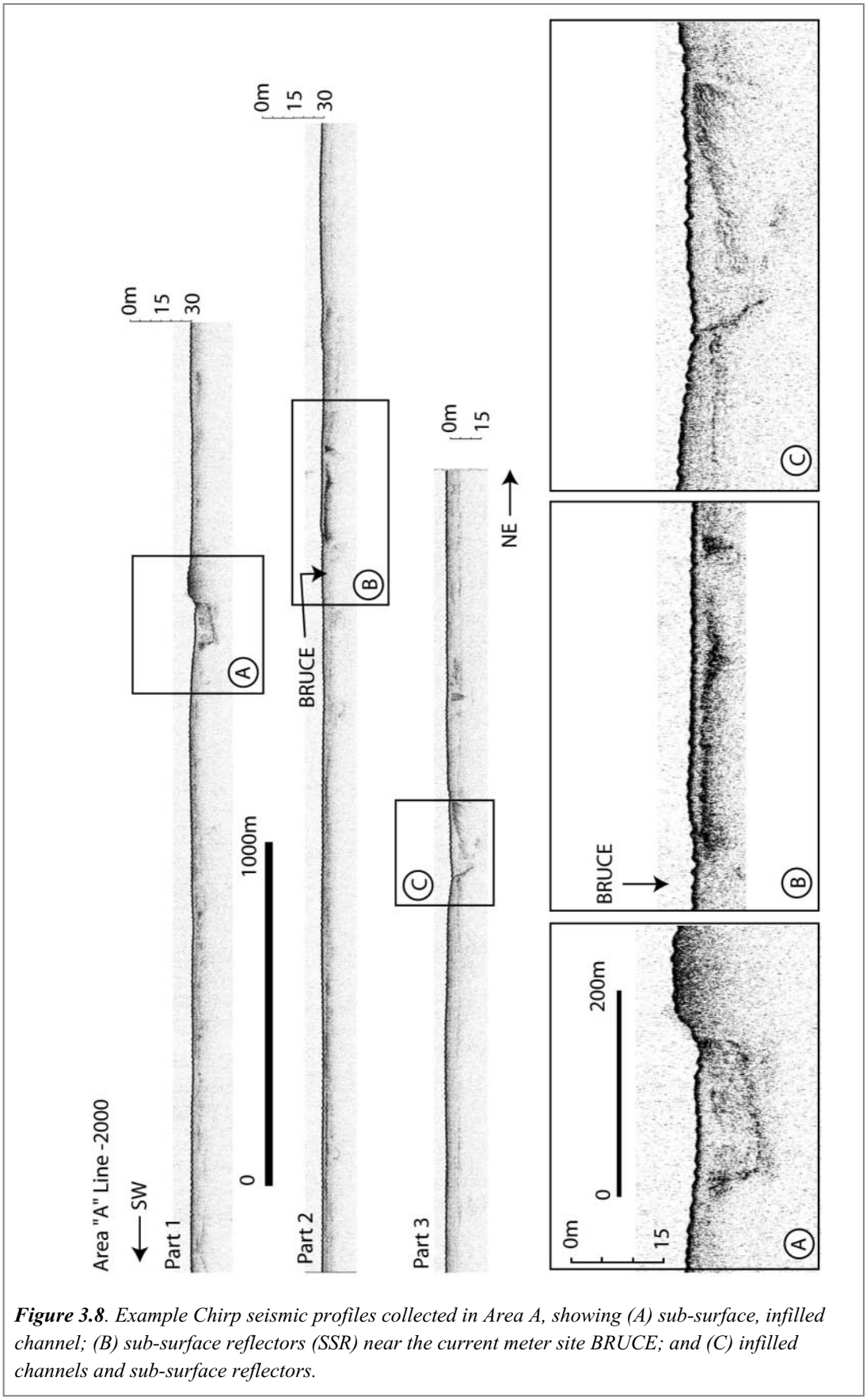

***Figure 3.8**. Example Chirp seismic profiles collected in Area A, showing (A) sub-surface, infilled channel; (B) sub-surface reflectors (SSR) near the current meter site BRUCE; and (C) infilled channels and sub-surface reflectors.*

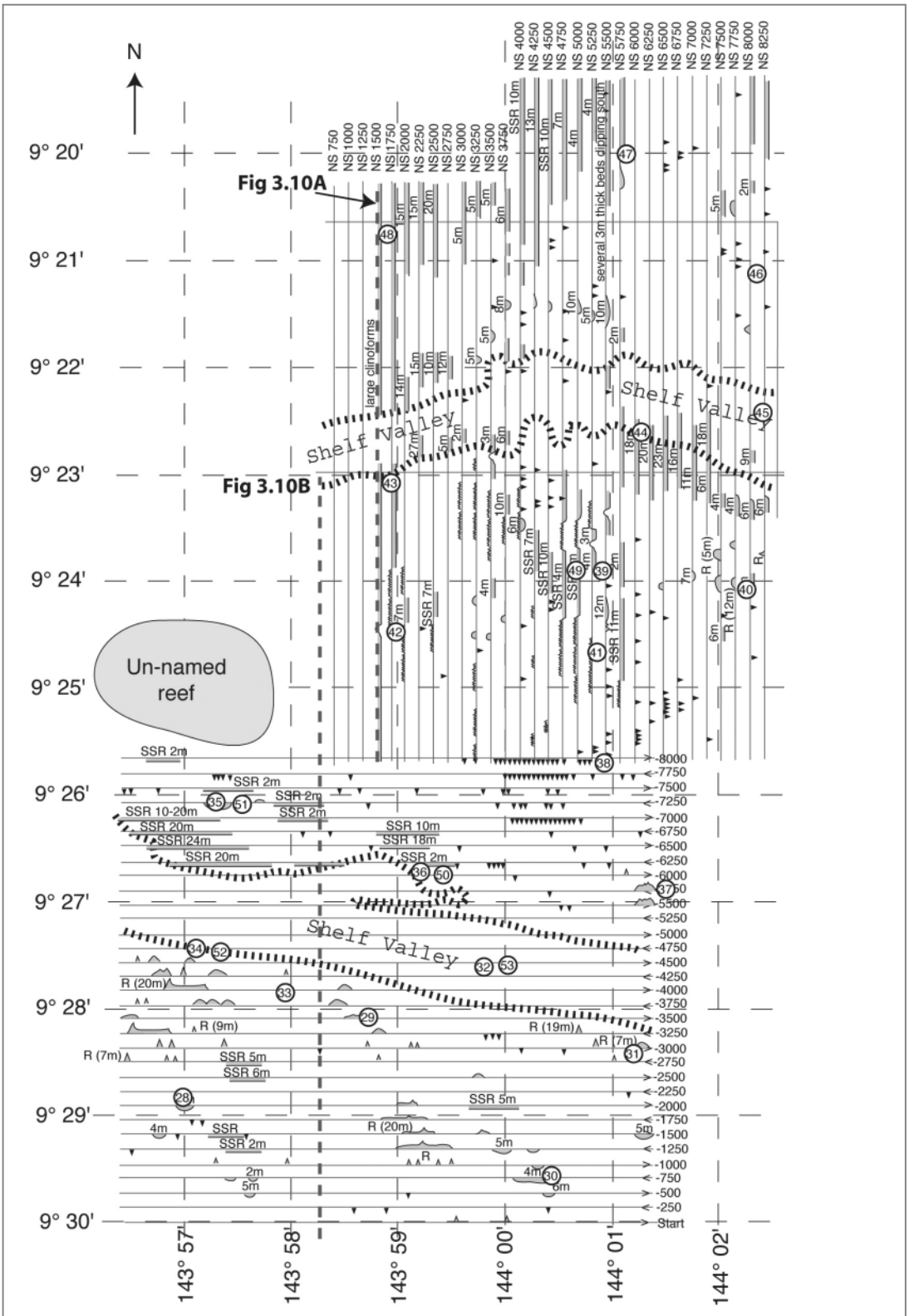

Figure 3.9. *Track map and interpreted features based on Chirp profiles collected in Area B. Numbers refer to the depth of sub-surface reflectors (SSR) and to the thickness of sediment within the infilled channels (not drawn to scale). The heights of rocky reef pinnacles above the seabed are indicated in parentheses. The locations of rough, rocky bottoms, rock outcrops, and incisions into the seabed are also indicated. Dashed track lines show positions of Figures 3.10A and 3.10B.*

The northern platform of Area B lies in 60-80m water depth. Its southern flank dips southward into the northern of the shelf valleys. The eastern part of the northern platform exhibits widespread erosional notches and incisions (Fig. 3.10), but the most prominent feature of the northern platform is the widespread occurrence of subsurface reflectors. The subsurface reflectors are most common in the west, and comprise clinoforms gently dipping towards the south on the northern flank of the shelf valley (Fig. 3.10A).

The acoustic character of Area C contains several contrasting seabed types, ranging from erosional, rough seabed to reefs and subsurface reflectors (Fig. 3.11). The west-central part of the area contains a large reef platform, which extends eastwards from East Cay. This reef platform lies in ~50m depth and is characterised by a hard, rocky seabed. Further to the east in water depths of ~100m there is an extensive sandwave field. These sandwaves rise about 4-6m above the level of surrounding seabed and appear to have their steep faces oriented towards the south. They tend to have well rounded crests and no internal stratification was visible in our chirp records (Fig. 3.12A). To the south of East Cay lies a shelf valley up to 220m deep. It is flanked on its southern and eastern margins by rough, rocky-reef seabed that is acoustically opaque (Fig. 3.12B). Towards the west, however, and just south of East Cay, the Chirp seismic data reveal localised areas of thick sediment accumulation. There are several examples of isolated, lobate to mound-shaped deposits (Fig. 3.12B).

Sub-horizontal, subsurface reflectors can be seen at around 80-100m water depth, buried beneath several metres of acoustically transparent sediments (Fig. 3.12B). In some cases, these reflectors exhibit a rough, erosional appearance suggesting they were subaerially exposed at some time in the past. They appear to crop out on the sides of channels and to correspond to a step-like bathymetric profile (shown by arrows in Figure 3.12B).

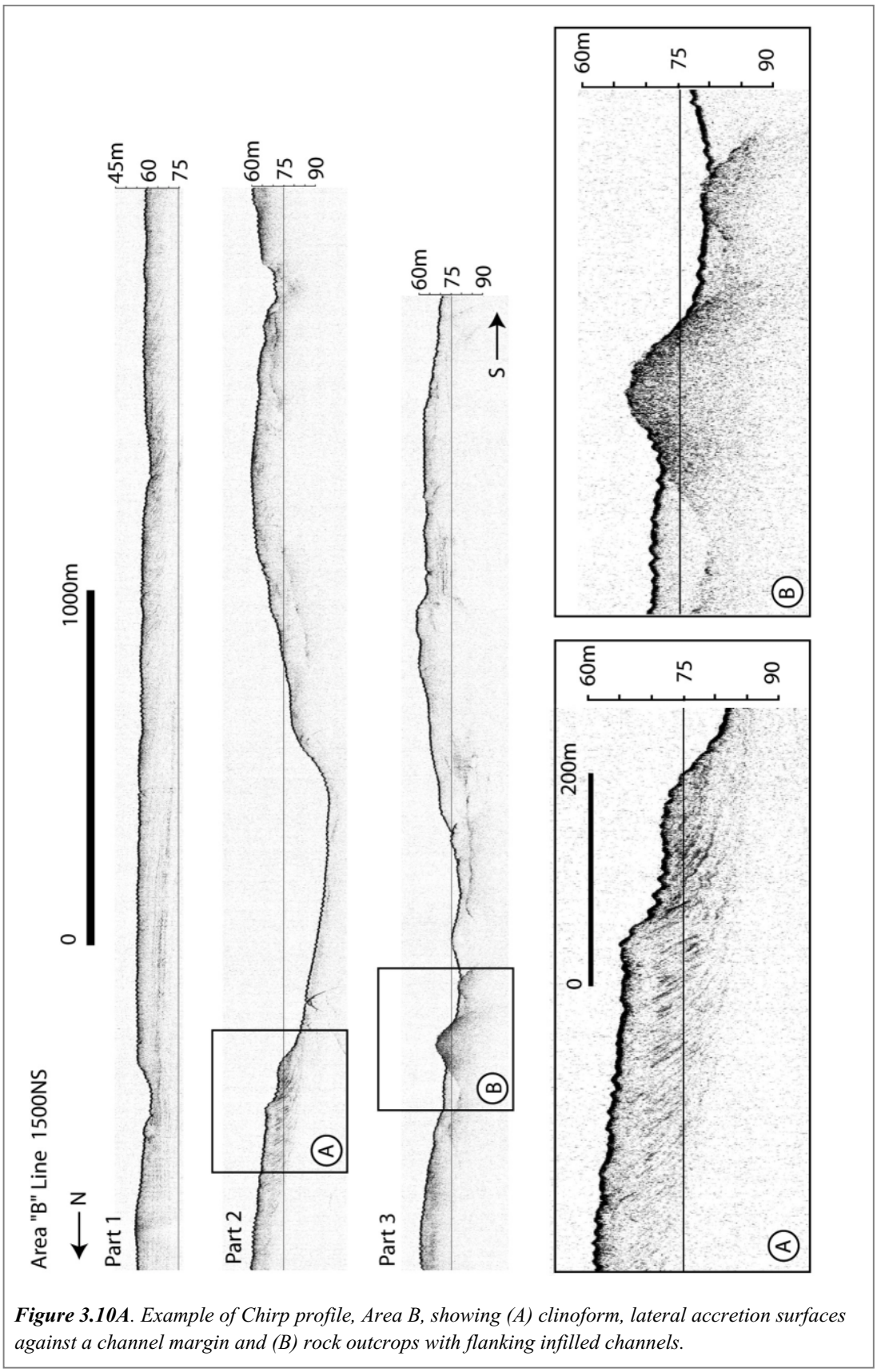

Figure 3.10A. *Example of Chirp profile, Area B, showing (A) clinoform, lateral accretion surfaces against a channel margin and (B) rock outcrops with flanking infilled channels.*

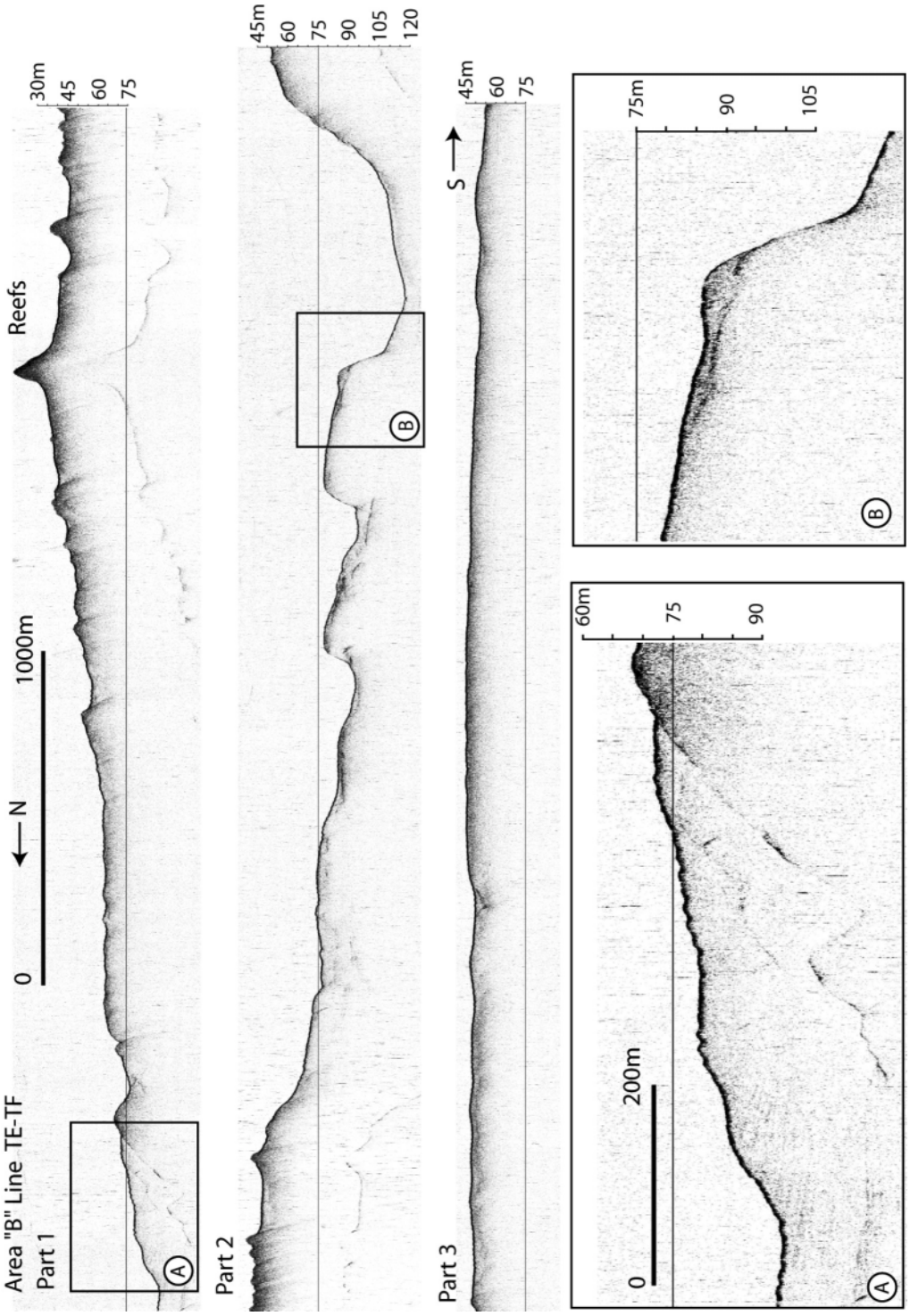

Figure 3.10B. *Example of Chirp profiles, Area B, showing rocky reefs (A) clinoform, lateral accretion surfaces against a channel margin and (B) rock outcrops with flanking infilled channels.*

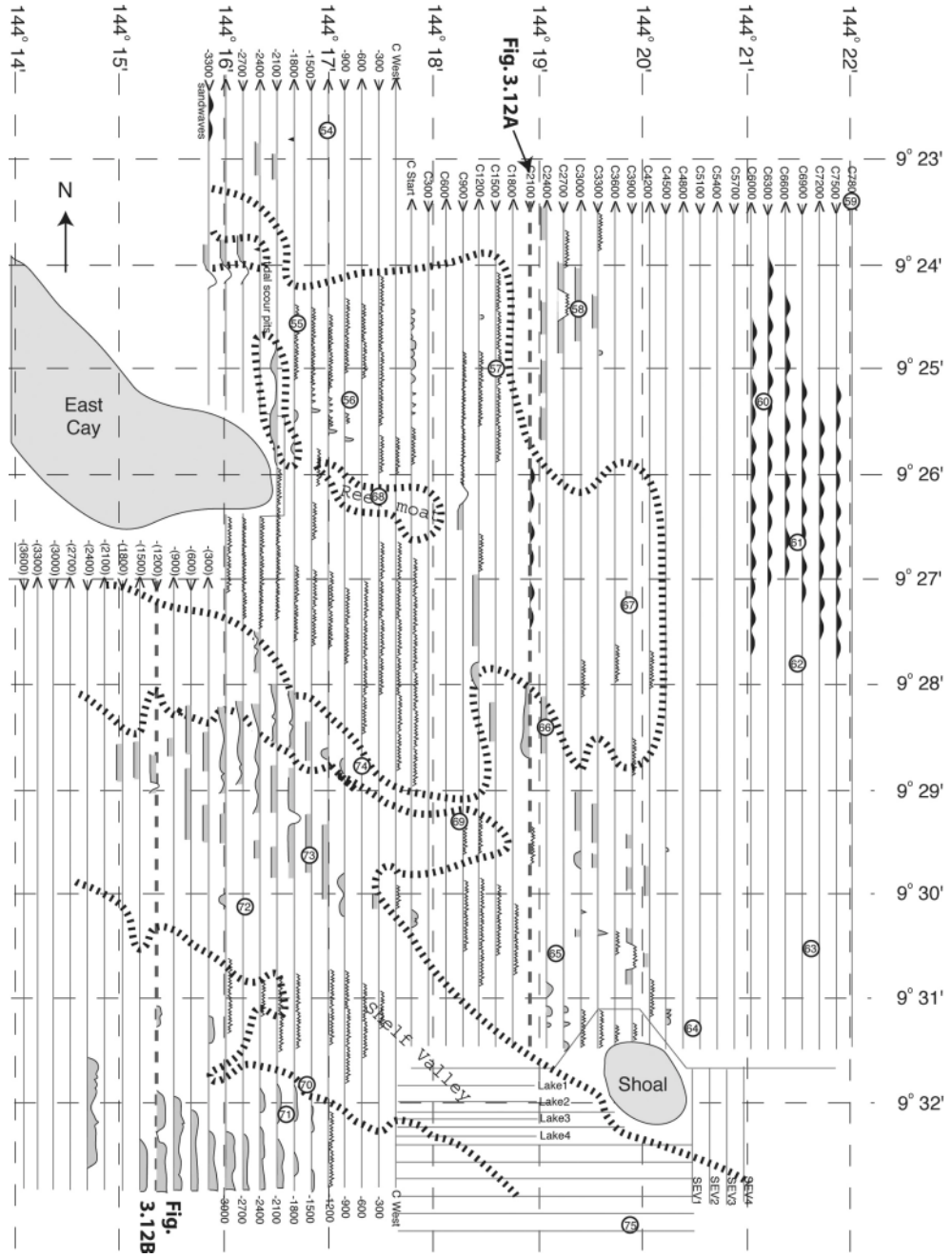

Figure 3.11. *Track map and interpreted features based on Chirp profiles collected in Area C. Numbers refer to the depth of sub-surface reflectors (SSR) and to the thickness of sediment within the infilled channels (not drawn to scale). The heights of rocky reef pinnacles above the seabed are indicated in parentheses. The locations of rough, rocky bottoms, rock outcrops, and incisions into the seabed are also indicated. Dashed track lines show positions of Figures 3.12A and 3.12B.*

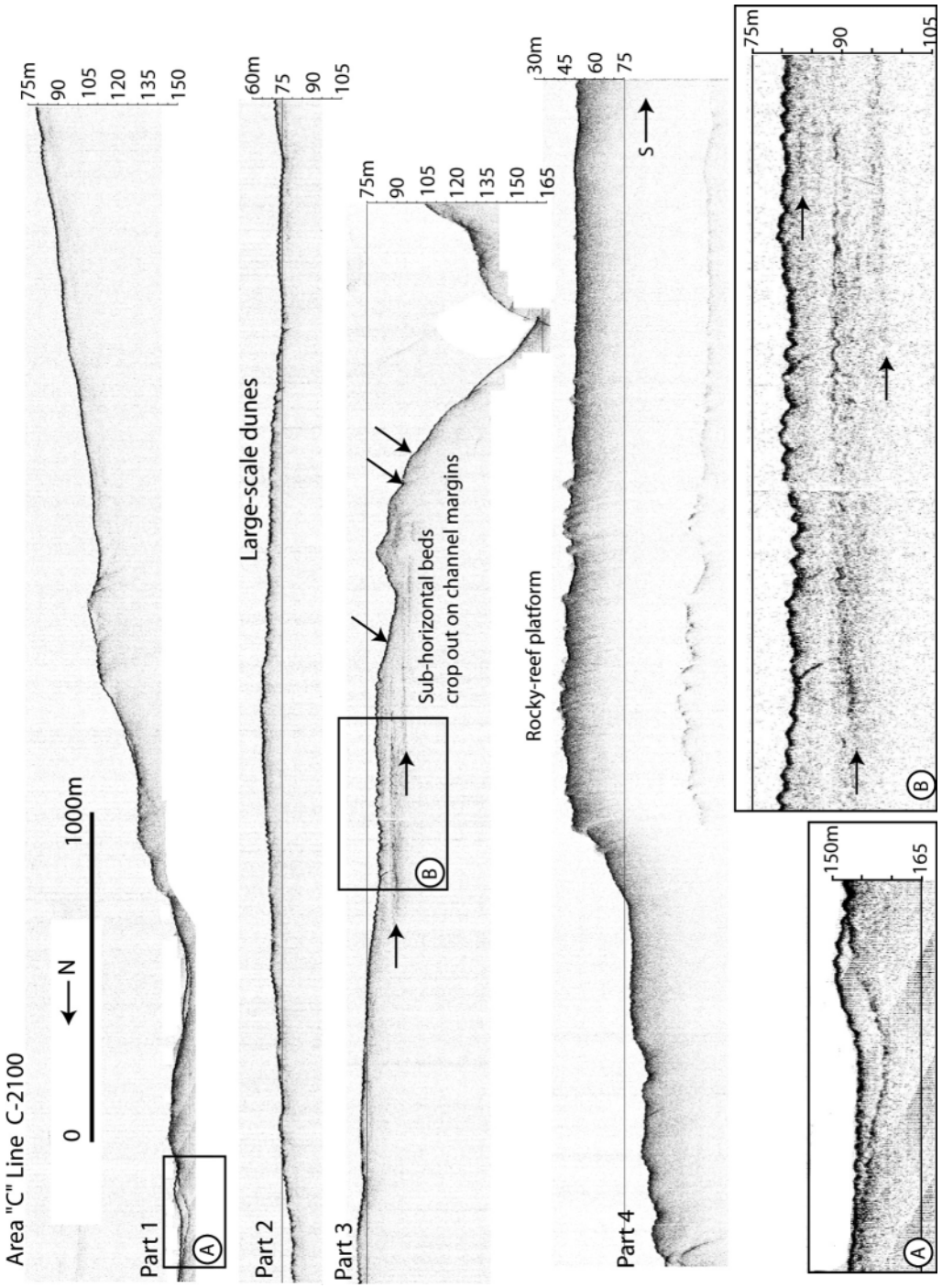

Figure 3.12A. *Examples of Chirp profiles collected in Area C, showing large-scale dunes (sandwaves), rocky reef platform and outcrops of sub-horizontal beds along channel margins. Close up views show (A) over-filled channel with flanking mounded deposit; and (B) rough, rocky bottoms underlain by sub-horizontal beds, some of which also exhibit a rough surface.*

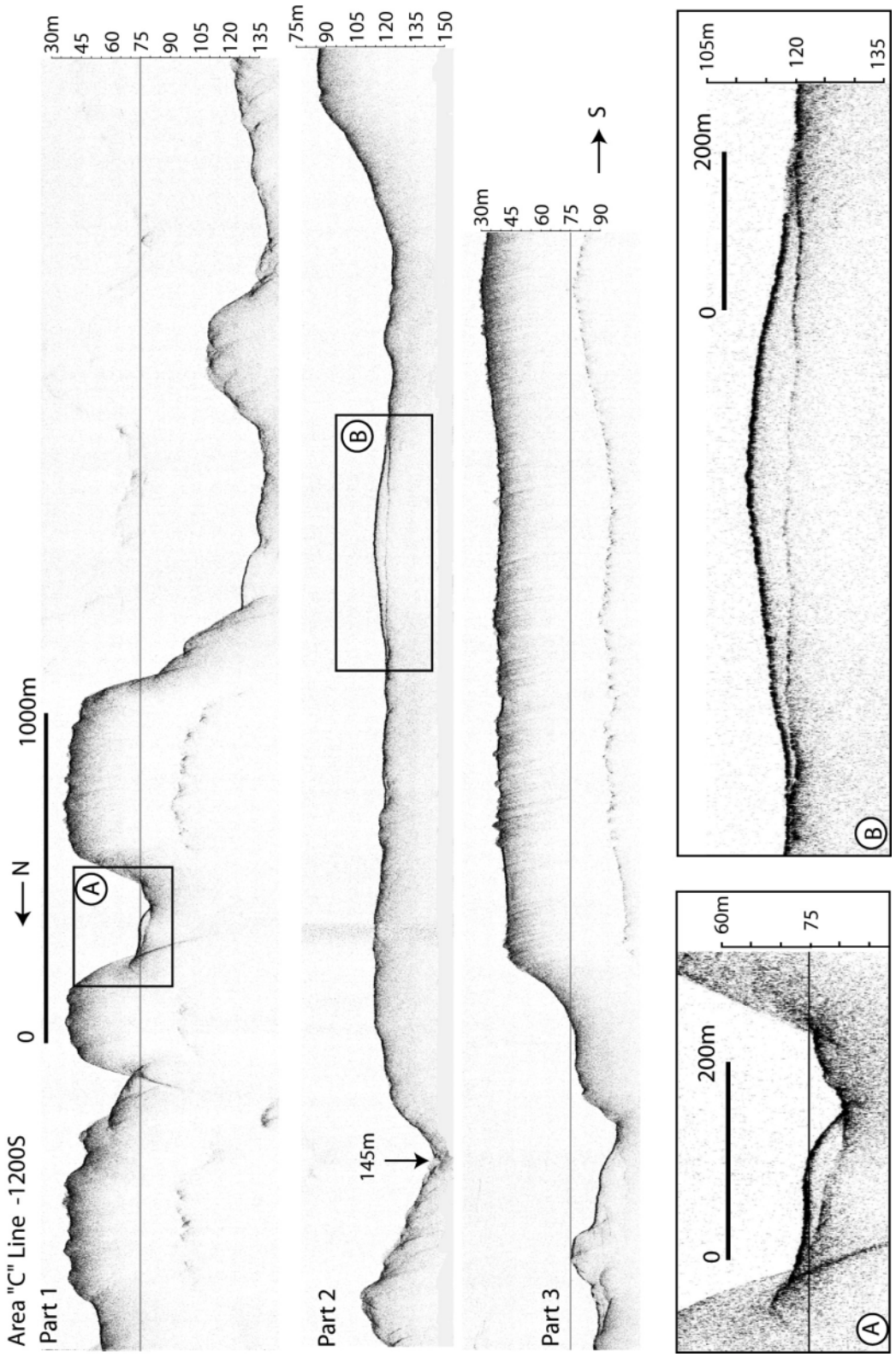

***Figure 3.12B**. Examples of Chirp profiles collected in Area C, showing incised, rocky reef platform and –145m deep channel, south of East Cay. Close up views show (A) lobate channel margin deposit and (B) mounded mid-channel deposit contained in local bathymetric valleys.*

3.3 CTD AND SUSPENDED SEDIMENTS

3.3.1 Water Mass Properties

CTD data collected over the three areas are attached in Appendix C (see Table 3.1 for list of CTD stations). The data show the mixing of warm, fresh surface waters adjacent to the Fly River delta with cooler, more saline waters characterising the outer shelf regions, where the influence of the Coral Sea is greatest (Fig. 3.13). Water masses in Area A exhibit the greatest range in salinity whereas Area C exhibits the largest range in temperature. Stations in Area B exhibited the smallest variation in temperature and salinity (Fig. 3.13).

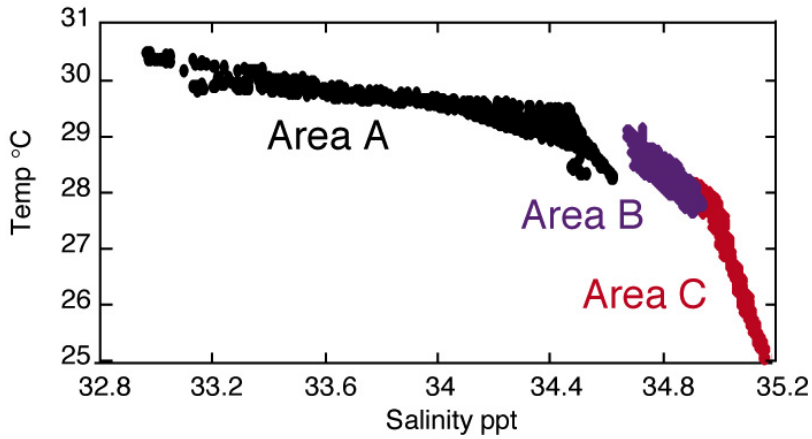

Fig. 3.13. *Temperature-salinity plot of all CTD data collected on the cruise, comprising about 20 stations in each of Areas A, B and C. The plot shows the mixing of warm/fresh waters near the Fly River Delta (Area A) with cooler saline waters from the Coral Sea (Area C).*

CTD data collected in Area A (Fig. 3.14) illustrates the presence of a density interface at around 15-20m water depth. Surface water (i.e. from 0-15m) is typically ~30°C and ~33.5ppt whereas bottom water is 28.5°C and 34.5ppt. The surface waters are not well mixed laterally, however, as shown by the broad scatter particularly in surface and bottom water temperature, which range over ±1°C (Fig. 3.14). The density interface is most clear in the transmissometer profiles, which exhibit a sharp decrease below 15m water depth.

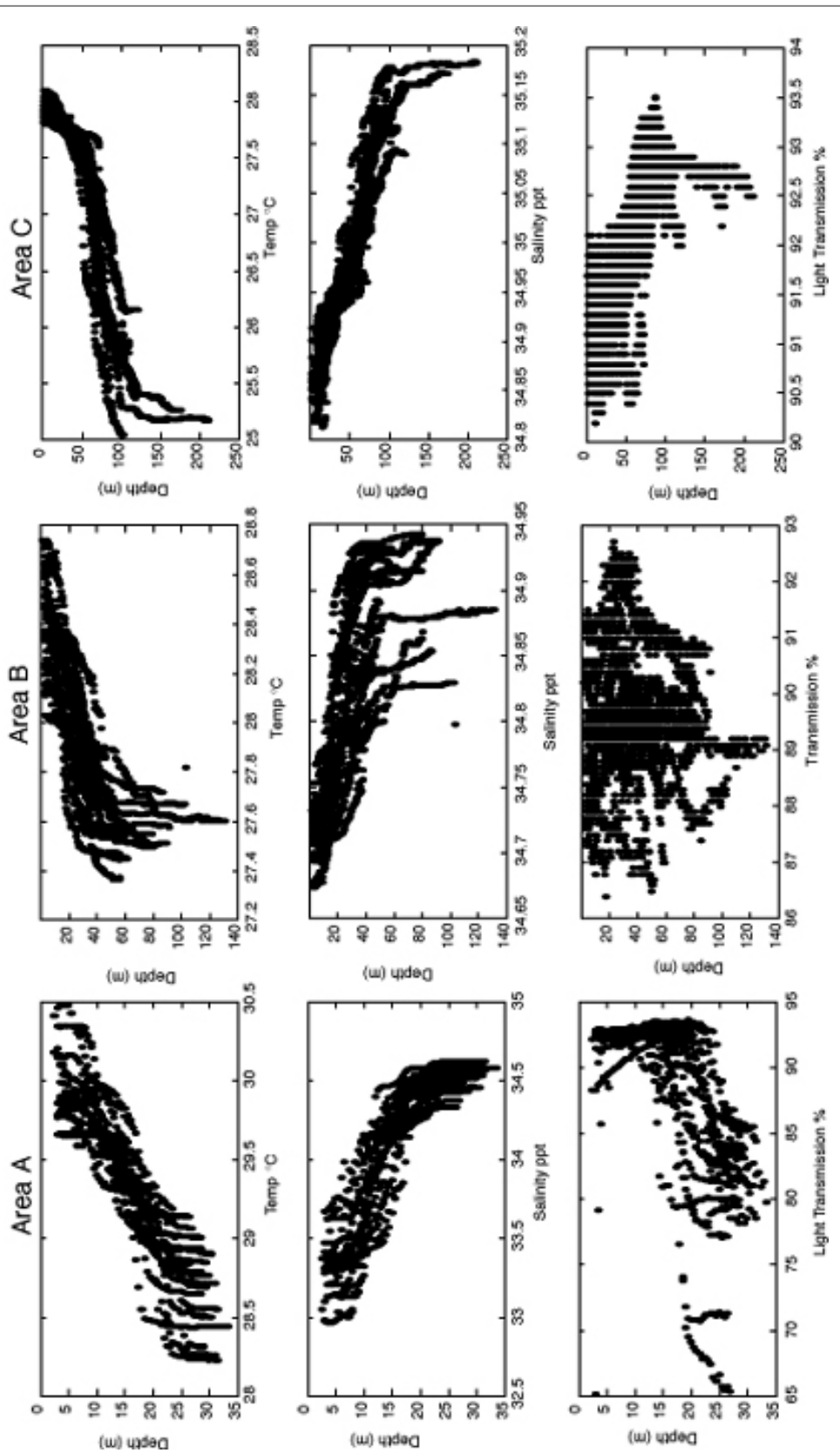

***Figure 3.14**. Plots of temperature, salinity and transmissivity versus depth for all (~20) CTD profiles taken in Areas A, B and C. Note the depth scales are different for each area.*

The depth plots for Area B show a similar overall pattern to Area A, with an increase in salinity and decrease in temperature with depth. There are indications of a surface mixed layer from around 0-20m. Below this depth temperature and salinity change gradually until at around 40m depth, below which the profiles become vertical, indicating mixing of the bottom waters. As in Area A, however, there is a fairly broad range in the surface temperature and salinity between stations, suggesting that lateral salinity and temperature gradients occur. However, since the CTD data were collected over a period of several days, and as we may expect tidal excursion lengths of ~10km, mapping of these surface properties was not attempted.

Area C has the best-mixed surface and bottom water masses out of the 3 areas studied. The lateral mixing is shown by the clustering of surface temperature and salinity profiles (Fig. 3.14). Vertical mixing is particularly evident in the stations from the deep shelf valleys, where the temperature and salinity profiles are nearly vertical between 0-50m and below a depth of about 100m.

3.3.2 Transmissometer Profiles of Suspended Sediments

Suspended sediment concentrations measured by transmissometer during the CTD casts were calibrated by the filtration of surface and near-bottom water samples (data are listed in Appendix D). Area A had the highest bottom suspended sediment concentration of 6.3 mg l^{-1} (Table 3.2). Surface waters in Areas B and C had higher suspended sediment concentrations than Area A, attributed to higher productivity of plankton in the outer shelf surface waters (Table 3.2; see also description of suspended sediments in section 3.3.3, below).

The vertical profiles of transmissivity (Fig. 3.14) differ between the three areas. In Area A, turbidity was highest in the water closest to the seabed, which implies sediment transport processes are operating in this area (i.e. local resuspension and advection of bottom sediment).

In Area B, the transmissivity in surface and bottom waters ranged from ~86% to ~93% (Fig. 3.14) and there is no clear pattern in the vertical profiles (i.e. neither bottom or surface waters were clearly the most turbid). Based on our calibration data (Fig. 3.15, Table 3.2), the maximum suspended sediment concentration in Area B is ~2.9 mg l^{-1}, and there is no detectable difference in the values measured from the surface and the bottom water samples.

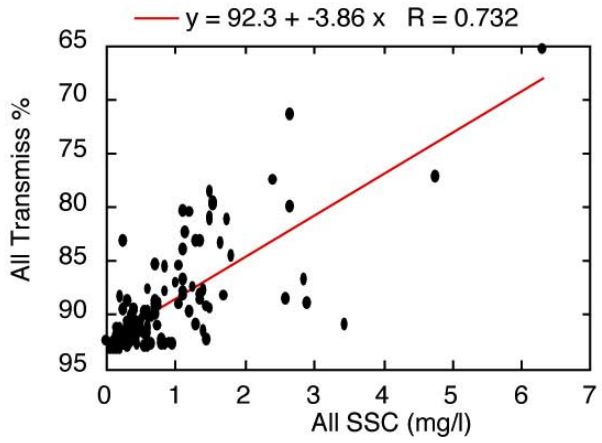

Figure 3.15. *Plot of measured suspended sediment concentrations versus transmissometer measurements for all CTD stations (Areas A, B and C). The data show that concentrations are less than 1 l^{-1}.*

In Area C, the transmissivity in surface and bottom waters ranged only from ~90% to ~93% (Fig. 3.14). Based on our calibration data (Fig. 3.15; Table 3.2), the mean suspended sediment concentration in Area C was everywhere less than ~1 mg l^{-1}. The surface waters appear to be somewhat more turbid than bottom waters in this area (Fig. 3.14), although it is noted that the measured suspended sediment values are very low.

Table 3.2. Statistics of suspended sediment concentrations measured by filtration. The number of sample points varies where bottles misfired, samples were lost or where filtration was unsuccessful. "Top" and "Bottom" refers to surface and near-bed water samples taken for the indicated area.

AREA	MEAN MG L^{-1}	MAX. MG $L^{-1}L$	MIN. MG L^{-1}	SD	NO. POINTS
A (Top)	0.36	0.90	0.10	0.28	18
A (bottom)	1.77	6.30	0.25	1.34	22
B (Top)	0.94	2.90	0.25	0.59	21
B(Bottom)	0.99	2.85	0.35	0.69	20
C (Top)	0.63	3.45	0.15	0.72	21
C (Bottom)	0.48	1.45	0.05	0.34	18

3.3.3 Scanning Electron Microscope Analyses of Suspended Sediments

3.3.3.1 Characterisation of Suspended Particles

Two 9mm by 9mm squares were cut from the filter paper and placed on to scanning electron microscope (SEM) stubs. One of the stubs were gold covered for purposes of image enhancement on the SEM, the second was carbon coated to aid and enhance the Energy Dispersive X-ray spectrum (EDX) in elemental identification. Material on the filter paper is largely made up of 3 components: terrigenous, calcareous biogenic and siliceous biogenic material.

Terrigenous material of clay sized fraction is largely composed of clay minerals (mica) and quartz (Fig. 3.16). Particles of silt size fraction were usually quartz. On the filter papers analysed, the bottom water sample from site 19 in area A contained by far the highest amounts of silt and clay. Site 35 contained 6 times less terrigenous material than site 19, but is still significantly higher than the other samples filtered. Little terrigenous material was filtered surface water samples.

Calcareous biotic material was dominated in all cases by coccoliths *Gephyrocapsa oceanica* and the slightly less abundant *Emiliania huxleyi* (Fig. 3.16). One or two small foraminifera were seen in each sample. Calcareous material is highest in both surface and bottom waters from area B. The bottom water sample from site 35 contains particles containing the highest amount of calcareous material, while the lowest proportions recorded were from surface waters in area A at site 6.

Siliceous biotic material was in all cases dominated by diatoms. Sponge spicules were also relatively common. Silicaflagellates were rare and only occurred in samples from Area C. Surface waters were dominated by species from the genera *Chaetoceros, Cerataulina, Guinardia, Rhizosolenia, Proboscia* and *Bactariastrum. Thalassionema, Thalassiosira* and *Eucampia* were less abundant genera. In bottom waters these species were joined by benthic species from the genera *Nitzschia, Diploneis, Surirella* and *Plurosigma.*

Dinoflagellates occurred occasionally in samples from areas B and C. Other rare occurrences included calcareous crystals in bottom samples, an Achantharian, juvenile shell fish and starfish, fish scales, tentacles of unknown origin and copepods (Fig. 3.16).

3.3.3.2 Energy Dispersive X-Ray Spectrum Analyses

Energy Dispersive X-ray spectrum (EDX) summary counts given in Table 3.3 are based on an average of 10 readings taken at 100 x magnification in 1mm x 1mm squares at different locations on the filter papers. Studies of the filtrate from surface and bottom samples using the Scanning Electron Microscope provide a general overview of the character of suspended sediments (Table 3.3).

In surface samples (CTD-Top, Table 3.3) the relative proportion of Carbon and Calcium increases with distance seawards. Aluminium and Magnesium are largely indicators of fluvially derived clay minerals and hence they tend to decrease with distance from shore in bottom waters. Iron, which is also an indicator of clays, is only found in abundance in the bottom waters from area A.

In bottom water filter papers, Calcium exhibits no clear onshore-offshore trends. The source of silica is a combination of siliciclastic terrigenous material and biogenic silica (largely diatoms). Silica content is relatively constant in surface waters but decreases with distance offshore in bottom waters. Silica Iron and Aluminium are an order of magnitude higher in the near-bed sample from area A (18CTD19; Table 3.3) than at other stations. We attribute this peak to the dominance of suspended terrigenous material in this area.

Sodium and Chlorine (NaCl) concentration variations are related to how well (or otherwise) the filter paper was rinsed with distilled water after each filtration at sea. During the cruise, the distilled water source was found to have become contaminated by seawater, which appears to have affected some of these values (see also suspended sediment measurements).

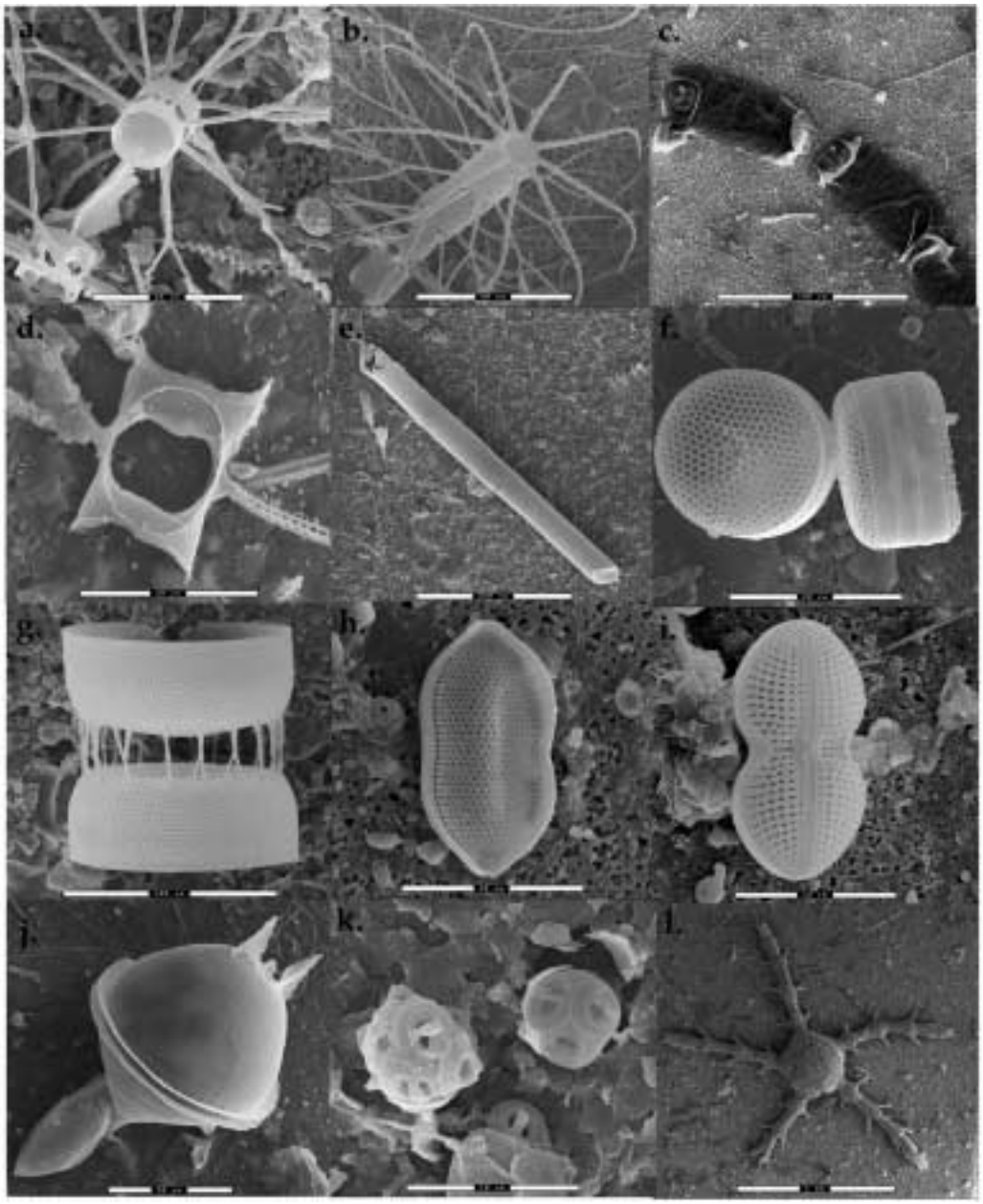

Figure 3.16. *Scanning electron microscope photographs of phytoplankton from the water column samples in Torres Strait. (a. - g.) Planktonic diatom species. (a). Bacteriastrum sp. (b). Bacteriastrum furcatum (c). Cerataulina c.f. bicornis (d). Chaetoceros sp., (e). Rhizosolenia striata, (f). Thalassiosira c.f. oestrupii, (g). Stephanopixsis palmeriana. (h) and (i) are resuspended benthic species Nitzschia panduriformis and Diploneis wiesflogii respectively. (j) is an unknown dinoflagellate, (k) is the common coccolithophorid Gephyrocapsa oceanica and (l). a juvenile sea star. Photos by Nerida Bleakley.*

Table 3.3. Average Energy Dispersive X-ray Spectrum (EDX) data collected using the Scanning Electron Microscope, based on 10 surveys of elemental counts taken for each sample. Samples are listed as surface (top) or near-bed samples (bottom) and are in order with respect to areas A, B and C.

SAMPLE	C	O	NA	MG	AL	SI	S	CL	K	CA	FE
6CTD6Top	1374	2103	174	123	136	304	108	286	55	58.4	24
40CTD35Top	1478	2261	146	119	146	441	147	176	67.8	129	Tr
57CTD47Top	1000	1825	1138	320	141	334	321	2322	107	140	20
18CTD19Bottom	431	2524	865	430	1427	3566	216	1388	316	275	159
35CTD30Bottom	1203	2388	276	184	326	770	116	393	81.1	372	Tr
57CTD47Bottom	1143	1843	384	141	138	360	129	706	68.8	151	18

Brief summaries of the results for each area are as follows:

- Area A 6CTC6 Top Sample dominated by coccoliths and diatoms *Chaetoceros, Bactariastrum*, *Eucampia* and *Cerataulina.* Minimal clastic material seen.
- Area A 19CTD19 Bottom Sample dominated by clastic terrigenous material including clays (giving high Si, Mg, Al and Fe readings) and quartz silt (also high Si). Relatively high proportions of coccoliths and both benthic and planktonic diatoms are present, often smothered by clastic material. One dinoflagellate, one planktonic and one benthic foram identified.
- Area B 40CTD35 Top Sample dominated by diatoms *Cerataulina, Guinardia, Chaetoceros, Proboscia Rhizosolenia* and *Bactariastrum.* Coccoliths also abundant. Minimal clastic material present.
- Area B 35CTD30 Bottom Sample dominated by terrigenous clay and coccoliths. Diatoms, both planktonic and benthic forms are also abundant but not as high in abundance as the former.
- Area C 57CTD47 Top Dominated by diatoms *Cerataulina*, *Chaetoceros* and *Proboscia.* Coccoliths also present in smaller proportions. Three dinoflagellates were also identified. Two from the genus *Ceratium.* Particularly high salt or chloride (Cl, Na, Mg and K) readings from filter paper.
- Area C 57CTD47 Bottom Paper contains high proportions of coccoliths dominated by *Gephyrocapsa oceanica*. Both planktonic and benthic diatoms are also in high proportion. Most abundant species include those from the genera *Chaetoceros, Cerataulin, Rhizosolenia, Nitzschia, Navicula*. Minimal clastic material present.

3.4 SURFACE SEDIMENTS

3.4.1 Grain Size and Carbonate Distribution Patterns

3.4.1.1 Area A, Fly River Delta

Samples in this area are typically comprised of muddy sands, with mud content ranging from 11% to 44% and gravel content in the range of 2-18%. One sample, 4GR4A, comprises a sandy gravel with a high carbonate content in the gravel fraction, reflecting the presence of reworked limestone (see section on Surficial Sediment Composition). Mud content is highest in the northern corner of the area and generally decreases to the east and south, reflecting the source of terrigenous material, the Fly River delta (Fig. 3.17).

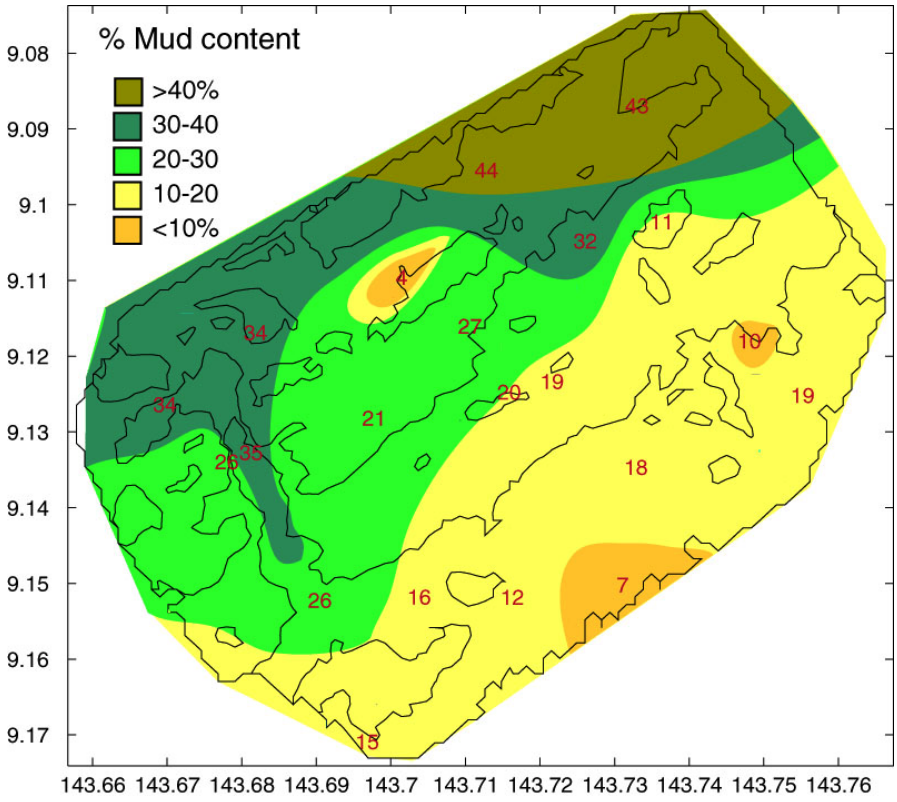

***Figure 3.17**. Distribution of mud in surficial sediments for Area A.*

Carbonate values in the gravel fraction are typically high, with at least 60% carbonate and typically 85% to 97.5%, reflecting a predominantly biogenic origin. The carbonate content of the sand fraction shows greater variation, ranging from 47% to 89%. The mud fraction is low in carbonate (6%-23%), reflecting the high content of terrigenous mud in this area. The spatial distribution of carbonate is similar to the pattern of mud content in samples, reflecting terrigenous input (Fig. 3.18). Peaks of increased carbonate are for the most part associated with samples containing reworked limestone (see section 3.4.2).

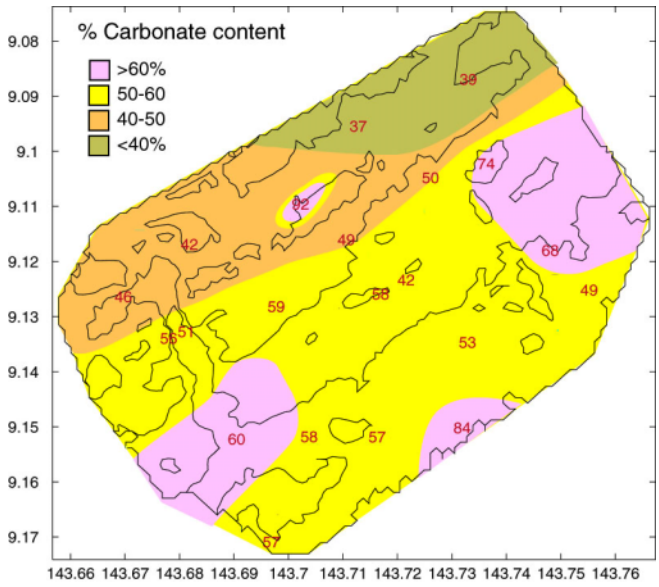

***Figure 3.18**. Distribution of carbonate in surficial sediments for Area A.*

3.4.1.2 Area B, Torres Strait

The sediments of Area B vary between muddy sands and gravelly sands. The more gravelly sands correspond with sites where reef build-ups are present (29CAM24, 37GR31A and 40GR34A) in sediments from valley sides (34GR28A, 36GR30A and 44GR38A) and associated with a sediment mound (42GR36A). Sediments with a high mud content are associated with an incised bed (28GR22A, a valley floor (32GR26A), and channel fills (35GR29A and 43GR37A). Their distribution is consistent with transport through the two main east-west trending channels (Fig. 3.19). There does not appear to be a consistent pattern of coarser sediment in sites which contain bedforms, confirming other evidence that some of these areas may not presently be active.

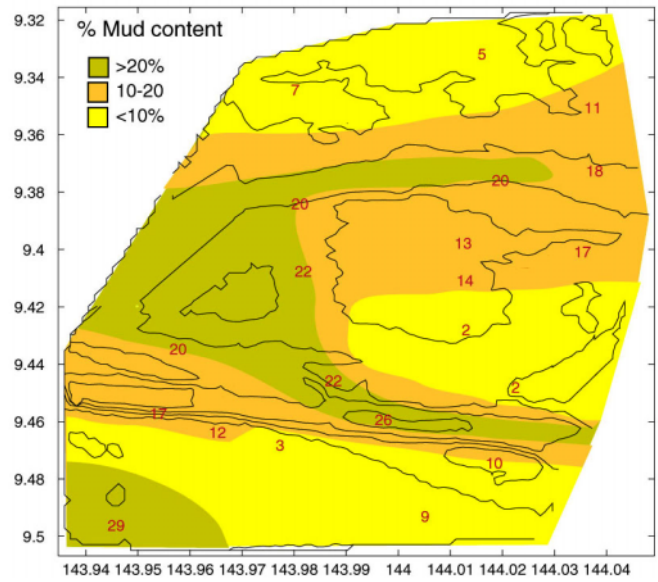

***Figure 3.19.** Distribution of mud in surficial sediments from Area B.*

Carbonate content in the gravel fraction varies from 40% to 97.5%. The sand fraction carbonate content varies from 21% to 91%. The non-biogenic component of both sand and gravel fractions is generally comprised of lithics, although three samples contain peat or woody material. Minor wood or peat is present in 39GR33A and 42GR36A, while 41GR35A contains large quantities, hence the low carbonate values in that sample. Overall, the carbonate content of the mud fraction in Area B is moderate to high, ranging from 24% to 80%.

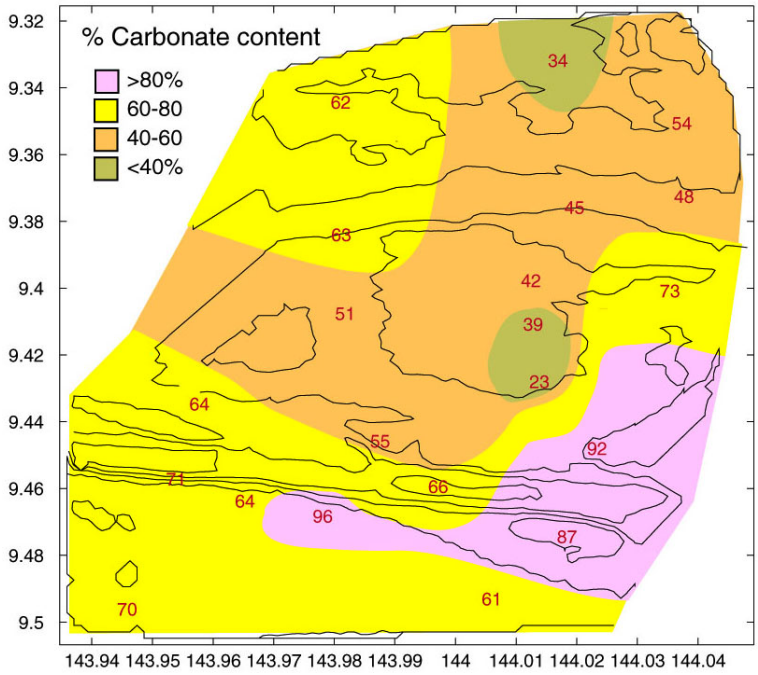

***Figure 3.20**. Distribution of carbonate in surficial sediments for Area B.*

The link between carbonate content and mud content is less clear than in Area A (Figs. 3.19 and 3.20), reflecting the different distribution of terrigenous material across the size fractions. Highest carbonate values are associated with reefs in the south-eastern corner of the area. At least two of these are established on older limestone outcrops (sites 29 and 37; see also Fig. 3.9).

3.4.1.3 Area C, Gulf of Papua

The sediments of Area C show a wide variation in grainsize, with mud content ranging from 0 to 52% (Fig. 3.21). Muddy sands are most abundant; gravelly sands and a sandy mud are also present. Three samples contain gravels (58GR46A, 59GR48A and 65GR54A). All three are associated with rocky or reef sites. The gravelly sands are associated with deep holes (72GR60A, 75GR63A and 75GR64A), rocky reef (57GR47A, 69GR58A) or valley floor (69GR58A). The two samples which targeted sand waves (60GR49A and 61GR50A) both contained muddy sands and are consistent with the lack of video evidence of modern sand mobilisation.

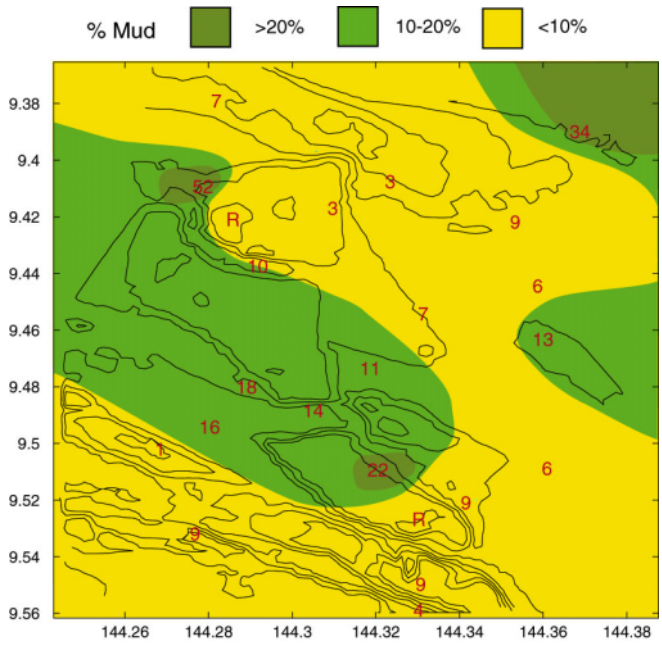

Figure 3.21. *Distribution of mud in surficial sediments from Area C.*

The carbonate content of gravel fractions is high, 65% to 97.5%. Sand fractions show a wider range of variation from 33% to 98%. The dominant non-biogenic component in the sand fraction is lithic grains, while mud clasts are more common in the gravel fraction. The carbonate content in the mud fraction is high, 71% to 90%, indicating that bioerosion and physical erosion processes are generating the bulk of the material. Overall, the carbonate content of sediments in this area is higher than in Areas A and B (Fig. 3.22). The lack of similarity between the distribution of mud content and carbonate values reflects the dominant occurrence of lithic grains in the sand fraction.

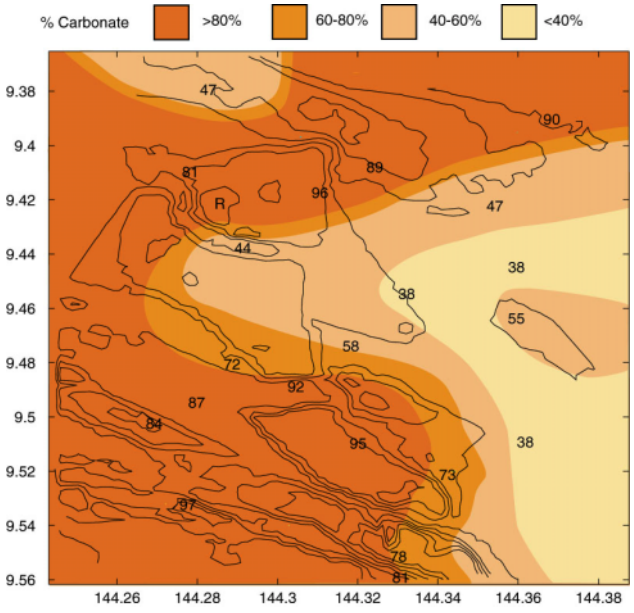

Figure 3.22. *Distribution of carbonate in surficial sediments for Area C.*

3.4.2 Surface Sediment Composition

3.4.2.1 Area A, Fly River Delta

A summary of the composition of samples in Area A is shown in Table 3.4 (See Appendix E for full documentation of surface sample composition). The gravel fractions of all samples in Area A are dominated by bivalves. Other moderately abundant bioclasts include gastropods, benthic foraminifera and arthropods (both decapods and barnacles). Pteropods are locally abundant, particularly in 17GR17A (>40%). Minor echinoids, both regular and irregular, *Halimeda* and corals are present in low abundances. Preservation in the gravel fraction is typically a mix of intermediate to relatively modern and relict material. Relict material typically includes bivalves and benthic foraminifera with less common bryozoans and minor *Halimeda* (See Appendix F for photographs of the gravel fraction in every sample).

Lithics are present in minor to moderate abundances. These comprise terrigenous mudclasts, partially to moderately lithified. Carbonate-cemented clasts containing rounded terrigenous sand grains are also present in a number of samples. Reef limestone, reworked from older material, is present in minor amounts in a number of samples (6GR6A, 9GR9A, 12GR12A, 18GR18A and 21GR21A) but abundant (65%) in sample 4GR4A. In this sample the limestone is less heavily calcified than in most other samples and is extensively bioeroded and encrusted.

The sand fractions of these samples are typically dominated by benthic foraminifera. Other moderately abundant components are bivalves, bryozoan, gastropods and echinoids. Minor components include ostracods, arthropods (decapod crustaceans and barnacles), sponge spicules and soft coral spicules. Lithics are present in variable quantities. These are mostly in the form of mud clasts or mud infill of tests, but lithic grains are also present in a number of samples. Fragments of reworked limestone are present in several samples, including 4GR4A and 12GR12A.

Preservation in the sand fractions is intermediate to relict. Benthic foraminifera were most obviously relict. The presence of relatively fresh juvenile bivalve valves indicates that at least some of the material is modern.

3.4.2.2 Area B, Torres Strait

Table 3.4 contains a summary of the composition of samples in Area B. In Area B, the gravel fractions of samples are similar in overall composition to those of Area A. Corals and coralline algae are more frequently present in samples, but still in low abundance (around 5%). There is an increase in the presence of relict shell, typically derived from bivalves and other taxa, such as bryozoans. Relict material is heavily encrusted and bioeroded.

The lithic component present in many samples includes mudstone clasts, limestone and carbonate-cemented sand clasts. Reef limestone, reworked from older material, is present in about one-third of the samples, but abundant (20% or greater) in samples 29GR23A and 37GR31A. Woody fragments comprise 50% of the gravel fraction in 41GR35A and are present in minor amounts in 39GR33A and 42GR36A.

The sand fractions from samples in Area B are typically dominated by bivalves and benthic foraminifera, with less abundant bryozoa, gastropods, echinoids and soft coral spicules. Minor components present in some samples include decapod crustaceans, ostracods and agglutinated worm tubes. Pteropods are locally abundant, particularly in samples 45GR39A and 32GR26A. Wood fragments are abundant in the sand fraction of 41GR35A.

Lithic grains are present in minor to high abundance. They are most frequently in the form of rounded, polished grains of variable composition. Mud clasts are present in a number of samples, but are much less abundant than lithic grains. Samples with high lithic content can be readily distinguished by their finer grain size and darker colour.

3.4.2.3 Area C, Gulf of Papua

A summary of the composition of samples in Area C is shown in Table 3.4. The gravel fractions of samples show a greater variety than in samples from areas A and B. Several samples are located in or adjacent to reefs or bioherms. Samples 59GR48A and 65GR54A are dominated by *Halimeda.* Living *Halimeda* is evident also in video footage from these sites. Samples 55GR44A, 57GR45A and 70GR59A contain moderate abundances (15-30%) of *Halimeda*, together with moderate to high benthic foram abundances (20%-65%). *Halimeda* is otherwise rare or absent in Area C samples. Hard corals are present but not abundant (<10%) in samples.

Sample 58GR46A from a deep channel area is dominated by boundstone clasts, covered in a variety of fresh encrusting organisms including coralline algae, sponges and benthic foraminifera. The abundance of living material suggests proximity to a reef, although the water depth is too great to support a coral reef. In contrast, the adjacent sample 58GR47A shows little evidence of living material.

The remaining samples from channels and inter-reef areas are generally dominated by eroded bioclasts and carbonate-cemented intraclasts. Bivalves, benthic foraminifera, gastropods, bryozoa and arthropods are often abundant, as are corals in inter-reef samples. Minor components include serpulids, echinoids and agglutinated worm tubes. The lithic component of these gravels is low (<5%) and usually consists of mud clasts. Some samples include lithic sand grains as cemented clasts or incorporated into intraclasts. The relict component of the gravel fractions is typically dominated by bioeroded, abraded clasts. The remainder of the material is intermediate with a minor modern component often present.

The sand fraction of samples from this area can be divided into samples with a high terrigenous content and those dominated by biogenic carbonate. Samples can be readily distinguished on the basis of colour. The samples containing abundant lithic material (54GR43A, 60GR49A to 63GR52A, 66GR55A to 68GR57A) occur in channel and inter-reef environments in the north-western corner and in a tongue extending from the eastern part of Area C. Their distribution can be seen from the map of % carbonate (see Fig. 6 in the section on grain size and carbonate content of surficial sediments). Other components of the sand fraction of these samples include bivalves, gastropods, including pteropods and benthic foraminifera. Minor sponge spicules and planktonic foraminifera are present in some samples. Inter-reef and channel samples from the southern part of Area C show similar composition, but with lithic content of less than 30%.

The highest carbonate values are associated with samples from reefs and bioherms. The sand fraction of these samples generally dominated by benthic foraminifera or *Halimeda* fragments with less abundant corals, echinoids, bivalves, sponge spicules and soft coral spicules. Planktonic foraminifera are abundant in some samples. Preservation in the sand fraction is generally intermediate with a minor modern component.

3.4.2.4 Rose Bengal Stained Material

The most effective staining procedure was obtained using 1gr of Rose Bengal in 100ml distilled water for a period of one hour. Uptake of the stain was greatest in material containing protoplasm, particularly encrusting foraminifera and calcareous algae. Stain in the final chambers of some benthic foraminifera was visible when examined wet. Uptake of stain occurred to a lesser degree on relict material and on some types of carapace, e.g. decapod crustaceans. This suggests either that the stain is more readily absorbed on such material or that coatings of microalgal or other biogenic material are present (Boltovskoy & Wright, 1976).

The lack of stained material may be in part a reflection of the difficulty in preserving very small amounts of protoplasm over a relatively long storage period; in this case approximately six months (Murray & Bowser, 2000; Gustaffson & Nordberg, 2001). Analysis of samples soon after collection, preferably on-board ship, would alleviate this problem.

In general the degree of such staining suggests that there was little living material in the samples. The problem with the use of Rose Bengal is that it identifies material *living* at the time of collection. For studies such as this, where a broader identification of modern material, rather than actual living material, is required, techniques such as assessment of preservation, together with carbon 14 dating of selected samples, are probably more useful. The Rose Bengal staining confirmed that assessment of the material based on preservation characteristics, such as colour, surface condition and presence of soft tissue, is a reliable guide to the identification of fresh biogenic material.

Table 3.4. Summary descriptions of the composition of surficial sediment samples (See Appendix E for full details).

Area A

SAMPLE NUMBER	WATER DEPTH	SEDIMENT DESCRIPTION	WEIGHT % GRAINSIZE			%CACO3			TOTAL
			GRAVEL	SAND	MUD	GRAVEL	SAND	MUD	
1GR1A	31.50	Sandy calcareous mud, dark grey (5Y 4/1), with abundant shell hash (predominantly abraded bivalves).	2.92	77.76	19.32	95	47	13	41.8
2GR2A	30.00	Sandy mud with moderate shell hash (abraded bivalves, gastropods), dark grey (2.5Y 4/1).	2.68	63.66	33.66	95	63	9	45.7
3GR3A	29.00	Sandy dark grey (2.5Y 4/1) mud with moderate shell hash and rare pebble-sized bioclasts (bivalves, gastropods).	18.33	55.84	25.83	60	75	14	56.5
4GR4A	24.50	Coarse muddy gravel with abundant pebble sized bioclasts (abraded bivalves) and cobble-sized cemented carbonate clasts, dark greyish brown (2.5Y4/2). Abundant forams.	69.60	26.73	3.68	97.5	89	12	92.1
5GR5A	33.50	Sandy dark grey (2.5Y 4/1) mud with minor shell hash, predominantly bivalves and gastropods.	3.03	62.18	34.79	95	70	12	50.6
6GR6A	28.50	Dark grey (5Y 4/1) muddy sand with abundant sand-sized shell hash and abraded pebble-sized bioclasts (bivalves, gastropods).	5.45	73.74	20.81	75	70	14	58.6
7GR7A	32.50	Muddy sand, olive grey colour (5Y 4/2) with abundant forams.	2.53	71.80	25.66	95	75	15	60.1
8GR8A	31.50	Olive grey (5Y 5/2) muddy sand, med. to coarse, with minor shell hash, predominantly bivalves.	2.09	83.26	14.65	85	63	22	57.5
9GR9A	32.00	Dark grey (5Y 5/2) calcareous sandy mud, with moderate shell hash and rare pebble-sized bioclasts (predominantly bivalves).	4.93	83.10	11.97	85	60	21	56.6
10GR10A	33.00	Olive grey (5Y 4/2) muddy fine to medium sand with rare granule-sized bioclasts (bivalves, gastropods).	3.98	80.22	15.80	90	63	23	57.8
11GR11A	34.00	Olive grey (5Y 4/2) muddy fine-medium sand with rare pebble-sized bioclasts (bivalves); moderately abundant forams.	9.77	72.27	17.97	85	57	17	52.5

SAMPLE NUMBER	WATER DEPTH	SEDIMENT DESCRIPTION	WEIGHT % GRAINSIZE			%CACO3			TOTAL
			GRAVEL	SAND	MUD	GRAVEL	SAND	MUD	
12GR12A	34.50	Olive brown (2.5Y 5/3) muddy calcareous coarse sand with moderate shell hash, rare pebble-sized bioclasts (bivalves) and cobble-sized cemented carbonate clasts.	18.13	75.05	6.83	95	88	18	84.5
13GR13A	33.50	Dark greyish brown (2.5Y 4/2) calcareous muddy medium sand with moderate shell hash (bivalves).	3.77	77.59	18.64	90	56	14	49.5
14GR14A	33.00	Dark greyish brown (2.5Y 4/2) calcareous coarse muddy sand with abundant shell hash (bivalve, gastropod).	7.52	82.56	9.92	85	73	14	68.1
15GR15A	32.50	Olive grey (5Y 4/2) calcareous muddy medium sand.	2.73	77.28	19.99	90	68	16	58.2
16GR16A	30.00	Medium to coarse muddy sand, dark grey colour (5Y 4/1).	8.73	64.08	27.19	70	61	12	48.5
17GR17A	30.50	Dark grey (5Y 4/1) calcareous sandy mud with muddy intraclasts and abundant shell hash (gastropod, bivalve).	5.20	62.42	32.38	85	68	9	49.8
18GR18A	29.00	Dark greyish brown muddy sand (2.5Y4/2) with abundant forams and shell hash, with rare pebble-sized bioclasts (gastropods).	5.81	82.75	11.45	95	81	10	73.7
19GR19A	29.00	Dark grey (5Y 4/1) sandy mud with abundant mud clasts and rare abraded pebble-sized bioclasts (bivalves).	3.86	52.91	43.23	95	61	7	39.0
20GR20A	29.00	Dark grey sandy mud (5Y 4/1) with rare abraded pebble-sized bioclasts (bivalves, gastropods).	2.50	53.19	44.31	90	61	6	37.4
21GR21A	29.50	Dark olive grey sandy mud (5Y 3/2).	1.98	64.41	33.61	95	59	7	42.2

Area B

SAMPLE NUMBER	WATER DEPTH	SEDIMENT DESCRIPTION	WEIGHT % GRAINSIZE			%CACO3			TOTAL
			GRAVEL	SAND	MUD	GRAVEL	SAND	MUD	
28GR22A	55.0	Olive grey (5Y5/2) muddy caclcareous medium to coarse sand, with minor pebble-sized clasts (bivalves, gastropods, terrigenous rock). Live Callianassid crab, shrimp on sediment surface.	5.92	64.61	29.47	75	67	77	70.4
29GR23A	46.0	Light brownish grey (2.5Y 6/2) calcareous sandy gravel with very abundant coarse sand to granule-sized shell hash (predominantly bivalves). Living *Lithothamnion* and hydroids on cobble surface.	22.83	74.12	3.05	97.5	96	75	95.7
30GR24A	54.0	Olive grey (5Y 5/2) muddy calcareous medium-coarse sand with abundant coarse sand to granule-sized shell hash (predominantly bivalves). Live crabs and juvenile fish on recently dead spiny scallop shell present on sediment surface.	6.32	84.89	8.79	90	57	80	61.1
31GR25A	52.0	Coarse, poorly-sorted, pale olive (5Y 6/3) calcareous sand with minor mud and abundant shell hash, moderate forams. 10cm (juvenile) garden eel, 3mm spider crab and infaunal polychaete worm live in sample.	5.31	84.32	10.37	80	89	77	87.3
32GR26A	131.5	Muddy fine-medium olive grey (5Y 5/2) sand. Live 7cm sipunculid worm present in sediment. Minor forams present.	0.25	73.61	26.15	97.5	63	76	66.5
33GR27A	50.5	Muddy calcareous olive grey (5Y 5/2) medium sand with coarse to gravel size shell fragments and gravel-size clasts of carbonate-cemented material.	5.77	82.57	11.66	60	63	76	64.3
34GR28A	90.0	Calcareous olive grey (5Y 5/2) muddy sand, gravel-sized clasts, many calcarenite fragments, comminuted shells, weathered shells abundant.	27.57	55.54	16.89	55	78	76	71.3
35GR29A	103.0	Calcareous olive grey (5Y 5/2) muddy sand with gravel clasts.	5.70	74.07	20.23	80	62	67	64.0
36GR30A	85.5	Muddy olive grey (5Y 5/2) sand with pebble-sized gravel bioclasts.	23.04	55.31	21.64	65	47	63	54.6
37GR31A	50.0	Calcareous light yellowish brown (2.5Y 6/3) sandy gravel, abundant granule-sized shell fragments. Moderate forams present.	31.90	65.49	2.60	95	91	70	91.7
38GR32A	55.5	Muddy fine-medium dark olive grey (5Y 3/2) sand with gravel sized shell fragments. Minor forams present.	1.16	96.58	2.26	90	21	63	22.7
39GR33A	60.0	Calcareous very muddy olive grey (5Y 4/2) sand, medium-coarse sand with coarse shell fragments and woody organic matter. Fish caught 25mm length (thrown back, not legal size!)	3.27	83.98	12.75	75	37	63	41.6

SAMPLE NUMBER	WATER DEPTH	SEDIMENT DESCRIPTION	WEIGHT % GRAINSIZE			%CACO3			TOTAL
			GRAVEL	SAND	MUD	GRAVEL	SAND	MUD	
40GR34A	57.5	Olive grey (5Y 4/2) muddy coarse calcareous sand cobble-sized carbonate cemented shell fragments. Minor forams present.	22.35	60.58	17.07	75	75	63	73.0
41GR35A	59.5	Dark olive grey (5Y 5/2) calcareous medium-coarse gravelly sand with abundant shell hash (predominantly bivalve) overlying dark grey (2.5Y 4/1) firm mud with abundant wood fragments. Live polychaete in burrow through clay.	7.37	78.88	13.75	40	41	24	38.6
42GR36A	80.5	Gravelly calcareous muddy sand,olive grey (5Y 4/2) with abundant pebble-cobble sized shell hash (bivalves) and rare wood fragments. Mud content increasing with depth in substrate.	25.69	52.00	22.31	70	35	66	50.9
43GR37A	80.0	Olive grey (5Y 5/2) calcareous gravelly sand with moderate coarse sand to pebble-size shell hash (predominantly bivalves). Live hydroid, polychaete slime, mantis shrimp and golf ball sponge in grab.	4.39	75.12	20.49	70	64	60	63.4
44GR38A	87.0	Gravelly calcareous olive grey (5Y 4/2) calcareous sand with minor mud. Abundant pebble-sized lithoclasts, rare cobble-sized cemented carbonate clasts. Live soft coral, crab, and hard coral, attached to carbonate clasts, present on sediment surface.	13.80	66.53	19.67	75	38	47	44.9
45GR39A	91.5	Muddy fine-medium olive grey (5Y 4/2) sand with rare pebble-sized bioclasts (predominantly bivalves). Minor forams present.	1.39	80.37	18.23	60	49	42	47.9
46GR40A	63.5	Calcareous olive grey (5Y 4/2) muddy medium-coarse sand with abundant coarse sand to granule-sized shell hash.	7.50	81.27	11.23	80	51	54	53.5
47GR41A	57.5	Calcareous olive grey(5Y 4/2) gravelly coarse sand with abundant shell hash.	3.50	91.36	5.14	70	32	54	34.5
48GR42A	57.0	Calcareous, muddy, olive grey (5Y 4/2) coarse sand with pebble-sized shell fragments.	7.40	76.47	16.13	85	60	59	61.7

Area C

SAMPLE NUMBER	WATER DEPTH	SEDIMENT DESCRIPTION	WEIGHT % GRAINSIZE			%CACO3			TOTAL
			GRAVEL	SAND	MUD	GRAVEL	SAND	MUD	
54GR43A	119.00	Gravelly calcareous dark greyish brown medium-coarse sand (2.5Y 4/2) with minor mud. Abundant coarse sand to granule-sized shell hash and cemented carbonate sand clasts. Abundant live infaunal shrimp in sediment, active burrowers, males and gravid females	8.81	84.53	6.67	80	41	82	47.2
55GR44A	64.50	Gravelly medium-coarse calcareous olive sand (5Y 5/3) with abundant granule to pebble-sized bioclasts and cemented sandy carbonate clasts. *Halimeda* and forams abundant. Live sponge, sipunculid and crustacean in grab.	7.35	40.87	51.78	95	87	75	81.4
57GR45A	50.00	Calcareous sandy gravel, light grey (2.5Y 7/2), dominated by *Halimeda* and foram shell hash. Abundant pebble to cobble sized bioclasts on surface, consisting of cemented sand & gravel-sized calcareous grains with live *Lithothamnion,*sponges and coralline re	28.60	68.17	3.23	97.5	96	81	95.9
58GR46A	104.50	Calcareous muddy gravel, light yellowish brown (2.5Y 6/3), predominantly pebble-sized bioclasts (shell hash).	90.63	6.80	2.58	97.5	80	71	95.6
58GR47A	103.50	Muddy medium olive sand (5Y 5/3) with minor gravel bioclasts.	12.38	78.30	9.33	85	76	83	77.8
59GR48A	76.00	Calcareous muddy olive gravel (5Y 5/3) with fine-medium sand. Gravel fraction dominated by pebble-sized Halimeda flakes. Live *Lithothamnion* and soft coral on surface.	36.82	29.00	34.18	97.5	92	80	89.9
60GR49A	96.00	Dark grey (5Y 4/1) moderately sorted sand with minor calcareous granule to pebble sized shell hash. Live sponge present in sample.	1.16	89.45	9.39	85	43	82	47.1
61GR50A	92.00	Moderately sorted medium-coarse olive grey sand (5Y 4/2). Live sipunculid in grab, worm tubes present.	2.14	91.42	6.44	85	34	85	38.4
62GR51A	103.50	Muddy medium-fine sand, light olive grey (5Y 6/2).	1.60	85.59	12.81	80	51	82	55.4
63GR52A	90.50	Calcareous, muddy medium-fine olive grey sand (5Y 5/2) with some gravel-sized shell detritus.	4.85	89.64	5.51	80	33	84	38.1
64GR53A	117.00	Slightly muddy medium-coarse calcareous pale olive (5Y6/3) sand. Abundant gravel-sized shell detritus.	5.79	85.04	9.16	80	72	82	73.4

SAMPLE NUMBER	WATER DEPTH	SEDIMENT DESCRIPTION	WEIGHT % GRAINSIZE			%CACO3			TOTAL
			GRAVEL	SAND	MUD	GRAVEL	SAND	MUD	
65GR54A	52.50	Reef fragment recovered. Pale olive mud (5Y 6/3) amongst coarser calcareous fragments, detritus and abundant live material, *Halimeda* and large bits of coral.	46.70	31.53	21.77	97.5	96	90	95.4
66GR55A	82.50	Muddy coarse calcareous olive grey sand (5Y 5/2).	1.17	87.20	11.63	85	54	83	57.7
67GR56A	79.00	Muddy medium dark olive grey sand (5Y 3/2).	0.37	92.40	7.23	95	33	82	36.8
68GR57A	89.00	Olive grey calcareous, fine-medium sand (5Y 4/2) with abundant shelly gravel clasts.	6.22	83.44	10.35	80	36	85	43.8
69GR58A	109.00	Light olive calcareous sandy gravel (5Y 6/3). Abundant *Halimeda* fragments; soft corals, shrimp? live in sample.	19.29	66.79	13.92	95	93	83	92.0
70GR59A	50.50	Calcareous sandy olive grey gravel (5Y 5/2) with some mud present. Abundant *Halimeda*. Live sipunculids (2) in sample.	33.95	56.84	9.21	97.5	98	85	96.6
72GR60A	171.50	Calcareous gravelly med-v. coarse light olive brown sand (2.5Y 5/3). Live spanner crab, worm, shrimp on surface. Agglutinated worm tube in sediment.	17.96	80.70	1.34	65	88	82	83.8
73GR61A	116.00	Muddy calcareous medium-coarse olive grey sand (5Y 5/2). Abundant polychaete slime tubes, live hydroid on surface.	0.82	82.81	16.38	90	87	87	87.0
74GR62A	90.00	Muddy calcareous olive medium-coarse sand with abundant granule-pebble size clasts, predominantly cemented carbonate. Minor bivalves, sand dollars.	6.18	75.47	18.35	75	70	81	72.3
75GR63A	219.50	Gravelly calcareous medium-v. coarse olive sand (5Y 5/3) with abundant granule-pebble shell hash. Minor mud. Live sponge, hydroid, crab, mysid shrimp and polychaete in sample.	25.21	70.72	4.07	80	81	85	80.9
75GR64A	220.00	Gravelly calcareous medium-v. coarse olive grey sand (5Y 4/2) with abundant coarse sand to pebble shell hash. Live polychaetes amd brittle stars in sample.	14.97	75.72	9.31	75	78	87	78.4

3.4.3 Foraminifers as Indicators of Habitat Type

3.4.3.1 Foraminiferal Assemblages

The foraminiferal assemblages for each of the five habitats identified are listed in Table 3.5 (see Appendix G for a full taxonomic list). The assemblages for each of the habitats are quite distinct, with only the Channel Floor Muddy-Sand and Open Shelf Flat Sand having the same foraminiferal group as abundant (Planktics). The similarity of these two habitats in terms of foraminiferal assemblages is not surprising as they are also very similar in environmental attributes – the two only differentiated by the greater percentage of mud in the Channel Floor Muddy-Sand habitat and the different broad-scale morphologies of the two habitats. Despite these habitats having the same abundant foraminiferal group, it is important to note that differentiation is still possible on the basis of the foraminiferal groups with minor abundance.

Table 3.5. The foraminiferal assemblages for each of the five habitats. The abundance range in the habitat is given in parentheses after the group. Groups listed in the Absent/Very Low Abundance category were absent from the sample unless an abundance figure is given.

Habitat: Delta-Proximal Muddy-Sand Sites: Area A - 7, 11, 17, 20 Foraminiferal Assemblage: Abundant: *Amphistegina* spp. (20-25%), *Assilina ammonoides* (13-20%) Minor: *Nummulites venosus* (7-11%), Peneroplids (1-6%) Absent/Very Low Abundance: *Gaudryina attenuata*, *Spiroplectinella pseudocarinata*, *Plotnikovina* sp., Planktics (≤1%), *Miniacina miniacea*
Habitat: Channel Floor Muddy-Sand Sites: Area B - 32, 35 Foraminiferal Assemblage: Abundant: Planktics (10-22%) Minor: *Amphistegina* spp. (2-8%), *Plotnikovina* sp. (2-3%), *Gaudryina attenuata* (1-3%) Absent/Very Low Abundance: Peneroplids (<1%), *Spiroplectinella pseudocarinata, Miniacina miniacea*
Habitat: Reef-Proximal Gravelly-Sand Sites: Area B - 37, 40 Foraminiferal Assemblage: Abundant: *Amphistegina* spp. (21-33%) Minor: *Assilina ammonoides* (6-11%), *Nubeculina advena* (3-6%), Planktics (2-9%) Absent/Very Low Abundance: Peneroplids, *Plotnikovina* sp. (<1%), *Spiroplectinella pseudocarinata, Miniacina miniacea*
Habitat: Reef-Proximal Sandy-Gravel Sites: Area C - 59, 65 Foraminiferal Assemblage: Abundant: *Amphistegina* spp. (14-16%), Planktics (14-31%), Minor: *Assilina ammonoides* (1-2%), *Miniacina miniacea* (3-11%), *Plotnikovina* sp. (1-2%), *Gaudryina attenuata* (1-2%) Absent/Very Low Abundance: Peneroplids, *Nubeculina advena* (<1%), *Spiroplectinella pseudocarinata*,
Habitat: Open-Shelf Flat Sand Sites: Area C - 67, 68 Foraminiferal Assemblage: Abundant: Planktics (12-21%) Minor: *Amphistegina* spp. (4-11%), *Assilina ammonoides* (4%), *Nubeculina advena* (4-6%), *Gaudryina attenuata* (2-4%), *Spiroplectinella pseudocarinata* (3-5%) Absent/Very Low Abundance: Peneroplids, *Miniacina miniacea*

Due to the small number of replicate stations for each habitat, no attempt was made to define the foraminiferal assemblages separately to the habitats. In future studies, with larger numbers of samples, foraminiferal assemblages may be characterised independently by statistical methods, such as hierarchical cluster analysis (e.g. Glenn-Sullivan & Evans, 2001; Renema & Troelstra, 2001). With large

numbers of samples, statistical methods such as this may be the only feasible way of grouping of foraminiferal assemblages independent of habitats.

3.4.3.2 Indicator Species

Figure 3.21 shows the abundances of four selected foraminiferal groups plotted against depth and stations, the latter in order of increasing depth. Two trends are evident from Figure 3.21; the first is a general decrease in abundance with depth of the larger benthic foraminifera (*Assilina ammonoides*, *Amphistegina* spp., *Nummulites venosus*) and the second a general increase in abundance of the planktic foraminifera with depth. This decrease in the benthic to planktic foraminifer ratio with depth is common, and is attributable to two main factors (Murray, 1991):

- Decreasing sedimentation rates of benthic foraminifera with depth, due to either lower *in situ* rates of benthic foraminifera production or reduced transport of benthic foraminifera into the deeper sites or a combination of the two.
- Increasing sedimentation rates of planktic foraminifera with depth, due to either higher abundances of planktic foraminifera in the water column or increased deposition because of different current configuration in deeper water.

Two methods were used to attempt to identify whether transport of benthic foraminifera into the deeper stations is a major source of sedimentation. The first method is to compare the published depth ranges of the indicator species to their depth ranges in the study site. If there are large abundances of the species below their published maximum living depth, this may be indicative of transport. In the case of the foraminifera selected in this study, their depths are within published maximum depth ranges in the region (Murray, 1991; Hohenegger et al., 1999; 2000), so no transportation from shallower areas can be detected.

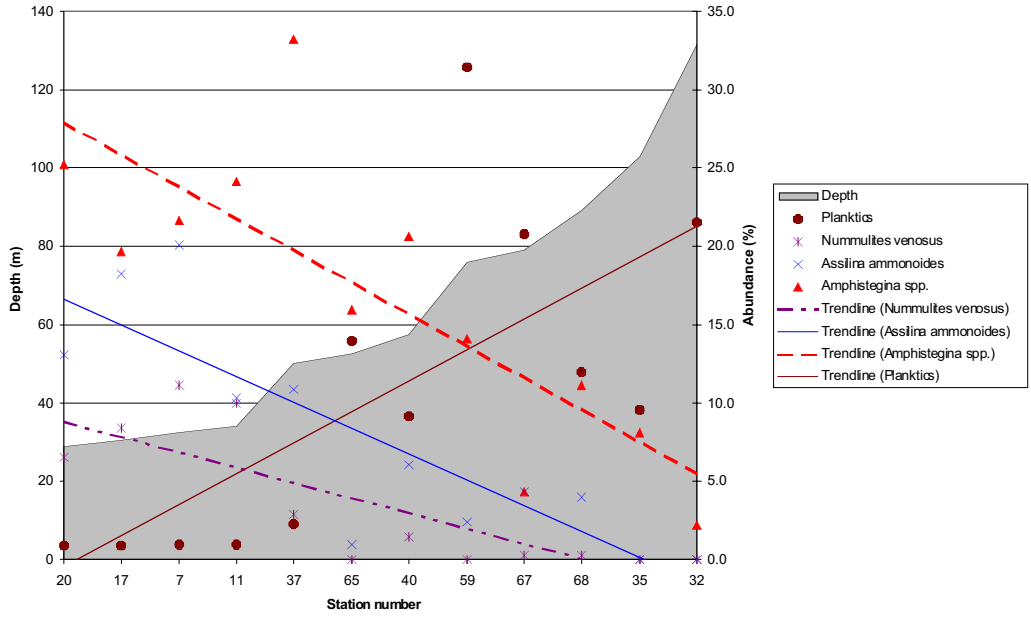

Figure 3.23. *Abundance of selected species graphed against station depths. The trendlines are for the species listed in brackets. Note the general decrease in abundance of* N. venosus, A. ammonoides *and* Amphistegina *spp. and the general increase in the abundance of planktic foraminifera (Planktics).*

Caution should be noted on two counts; firstly, the depth ranges of species may vary slightly with locality and environmental parameters. For example, the main control on the maximum depth of larger foraminifera is light intensity, so the maximum depth will vary with turbidity (Hohenegger, 1995), with species able to live at greater depths at sites with lower turbidities (clearer water). Thus, unless the foraminifera are far below their maximum depth range, this will only give an indication that transport may be occurring. Secondly, some care should be taken that the foraminifera are not reworked or relict from periods of different sea-level. If this is the case, the seafloor assemblage will not be a reflection of the recent seafloor environment. In reality, reworked or relict foraminifera are usually easily identified by iron-staining, infilling with consolidated sediment and poor preservation, so this is not usually a problem.

The second method is by investigating the distribution of species that have specific habitat requirements. *Miniacina miniacea* is an example of a species with a specific habitat requirement from this study region - being an encrusting foraminifera, it requires a hard substrate (generally rock outcrop or coral). If *M. miniacea* were present in a habitat with only soft substrate, such as sand, the tests must have been transport from an area with hard substrate. In the case of this study, *M. miniacea* was only present in the Reef-Proximal habitats; therefore, no inter-habitat transport was indicated.

Further evidence for determining whether the foraminifera at a site were produced *in situ* or were transported into it may be given by use of a protoplasmic stain such as Rose Bengal. These stains allow separation of the living/recently dead assemblage from the death assemblage. Low numbers of living/recently dead foraminifera would indicate either very low production rates or transport of the foraminifera into the site.

3.5 CORE SAMPLES

The results listed here accompany the core logs contained in Appendix H. A total of 10 piston cores were recovered from Area A – Fly River Delta (PC1-10), 13 gravity cores were recovered from Area B – Torres Strait (GC1-12, 14), and 8 gravity cores were recovered from Area C – Gulf of Papua (GC15-19, 21, 23-24; see Table 3.1). Cores from Area A were collected from water depths of 29 to 35 m and range in length from 1.27 to 4.03m. Cores from Area B were collected from water depths of 55 to 131.5m and range in length from 0.07 to 2.99m. Cores from Area C were collected from water depths of 64 to 119m and range in length from 0.03 to 2.96m.

3.5.1 Physical Properties – Area A, Fly River Delta

3.5.1.1 Wet Bulk Density

Wet bulk densities (WBD) range from 1.3 – 2.5 g cm^{-3} for all cores. Densities are variable downcore but generally increase with depth, associated with increased sediment compaction. Highest WBD of 2.52 g cm^{-3} occur in 21PC5 and are associated with coarser sediment, which is comprised mostly of carbonate sand and in the case of 15PC2 *Halimeda* gravel. Lowest WBD values of <1.6 g cm^{-3} occur in the top 0.5 m of 15PC2 and are associated with poorly sorted calcareous muddy gravel. In the other cores collected from this area low WBD values of ~1.65 g cm^{-3} are generally associated with fine-grained sediment, including clay and silt beds. Cores 17PC3, 19PC4, 21PC5, 22PC6, and 23PC7 exhibit cyclic variations that appear to have good agreement with lithological changes downcore associated with alternating silt and clay beds.

3.5.1.2 P-Wave Velocity

P-wave velocities (Vp) range from 1.1 – >3.0 km s^{-1} for all cores (average ~1.4 km s^{-1}). Downcore VP values are highly variable and display no consistent trends with depth or between the cores.

Highest Vp values of 3.3 km s^{-1} occur in 15PC2 and are associated with coarse grained *Halimeda* gravel beds (typically calcareous gravels) and large lithic fragments. Lowest Vp values of 1.1 km s^{-1} occur in PC5 and are associated with fine-grained organic-rich material. In other cores collected from this area, fine-grained material (i.e., clay and silt) generally has lower Vp values than coarse-grained material (i.e., sand and gravel). Cores 17PC3, 19PC4, 21PC5, 22PC6, and 23PC7 exhibit cyclic variations that have good agreement with lithological changes downcore associated with alternating silt and clay beds. Significant variability in Vp values occurs at the ends of the core sections, and these data should be interpreted with caution.

3.5.1.3 Magnetic Susceptibility

Magnetic susceptibility (MS) range from <10 – >250 cgs for all cores collected from this area. Downcore MS values are highly variable containing few consistent trends with depth or between the cores. Highest MS values of >250 cgs occur in PC3 and are associated with a bed of shell and coarse sand at the base of the core. However, in cores collected from this area terrigenous dominated material composed of fine-grained beds (e.g., clay beds) have higher MS values than beds composed of calcareous sands and gravels. Lowest MS values of <10 cgs occur in 17PC3 and 19PC4 and are associated with sandy mud units. In cores 19PC4, 22PC6, 23PC7, and 24PC8 MS values peak just above the contact between a unit of carbonate dominated marine sediment and an underlying unit of siliciclastic dominated (terrigenous?) sediment. In all other cores collected from this area, the underlying unit contains higher MS values.

3.5.1.4 Fractional Porosity

Fractional porosity (FP) values range from 0.4 – 0.8 (most occur between 0.6 – 0.65) for all cores. Downcore FP values are variable but do display a general reduction with depth due to sediment compaction. Generally, highest FP values occur at the tops of the cores collected in this area and correspond to the most unconsolidated sediment, with the highest FP values of 0.8 occurring towards the tops of 15PC2, 19PC4, 24PC8, and 26PC10. However, higher FP values are generally associated with beds comprised of coarse sediment, while lowest FP values are generally associated with beds comprised of fine-grained sediment. Cores 17PC3, 19PC4, 21PC5, 22PC6, and 23PC7 exhibit cyclic variations in P values that can be correlated with downcore lithological changes associated with alternating silt and clay beds.

3.5.2 Physical Properties – Area B, Torres Strait

3.5.2.1 Wet Bulk Density

WBD values range from <1.0 - >2.0 g cm^{-3} for all cores collected from this area. Densities are highly variable downcore but generally increase with depth due to increased sediment compaction. Highest WBD values of >2.4 g cm^{-3} occur in cores 28GC1 and 41GC2 and coincide with coarse-grained calcareous units. Lowest WBD values are generally associated with fine-grained siliciclastic units. These trends are reflected in all cores recovered in this area, with the addition that lowest WBD values generally occur within the top 0.5 m of the cores. Below 0.5 metres below sea floor (mbsf) in 46GC7, WBD values display good agreement with a 2.5 m thick sequence of siliciclastic sediment containing numerous fine-grained laminations.

3.5.2.2 P-Wave Velocity

Vp values range from 1.1 – 1.9 km s^{-1} for all cores collected in this area, but most Vp values are between 1.4 – 1.5 km s^{-1}. Downcore Vp values are highly variable and display no consistent trends with depth or between the cores. Generally, highest Vp values are associated with coarser sediment units, but the data quality was severely compromised because of poor core condition. In many instances, the significant variability in the cores was caused by air space between the core liner and sediment, thus masking

variations relating to lithological changes. Below 0.5 mbsf in 46GC7 Vp values display good agreement with fine-grained laminations contained in a 2.5 m thick sequence of siliciclastic sediment.

3.5.2.3 Magnetic Susceptibility

MS values range from <10 - >200 cgs for all cores collected in this area, but most MS values are <100 cgs. Downcore MS values are highly variable and display no consistent trends with depth or between the cores. Highest MS values of >150 cgs are associated with muddy, gravely calcareous sands (e.g., tops of cores 41GC2 and 43GC4), although high values also occur in association with organic-rich laminated siliciclastic sediments (e.g., 46GC7, 50GC11). In cores 43GC4, 44GC5, and 46GC7 MS values exhibit distinct changes downcore, with the top muddy calcareous sand unit containing significantly more magnetically susceptibility material than underlying units.

3.5.2.4 Fractional Porosity

FP values range from 0.2 – 0.8 for all cores collected in this area, but are mostly between 0.5 – 0.6. FP values are variable downcore. In the cores collected from this area, fine-grained sediments generally have lower porosities while coarse-grained sediments generally have higher porosities. Despite this, there are no consistent trends across all cores collected in this area.

3.5.3 Physical Properties – Area C, Gulf of Papua

3.5.3.1 Wet Bulk Density

WBD values range from 1.0 – 2.1 g cm^{-3} for all cores collected in this area. Densities are highly variable and exhibit no consistent trends downcore or across all the cores. Highest WBD values of 2.1 g cm^{-3} and 1.85 g cm^{-3} occur in GC15, where they are associated with units of calcareous sand, and in GC17, where they coincide with *Halimeda* gravel beds, respectively.

3.5.3.2 P-Wave Velocity

Vp values range from 1.1 – >1.7 km s^{-1} for all cores collected in this area, but are mostly between 1.35 – 1.4 km s^{-1}. Downcore Vp values are highly variable and exhibit no consistent trends across all the cores. Highest Vp values of 1.75 km s^{-1} occur in 59GC17 and coincide with coarse *Halimeda* and benthic foraminiferal gravel beds. Lowest Vp values of 1.1 km s^{-1} occur in 54GC15 and are associated with calcareous sand. The quality of the data was severely compromised by poor core condition. In many instances, the significant variability in the cores was caused by air space between the core liner and sediment, thus masking variations relating to lithological changes. However, due to the shortness of the cores in this area, variability in the Vp values caused by end effects was negligible.

3.5.3.3 Magnetic Susceptibility

MS values range from <5 - >200 cgs for all cores collected in this area, but are mostly between 10 – 70 cgs. Downcore MS values are highly variable. In all but four of the cores (61GC18, 62GC19, 73GC23, 74GC24) the MS values exhibit a slight increase with depth. Although the MS profiles in those four cores was severely compromised due to poor core condition. There is no consistent relationship with MS and sediment type.

3.5.3.4 Fractional Porosity

FP values range from 0.4 – 0.8 for all cores collected in this area, but are mostly between 0.55 – 0.65. Downcore FP values are highly variable with no consistent trends between cores. Lowest FP values generally coincide with fine-grained sediments. Gravels generally have greater FP values that coarse or medium sand.

3.5.4 Sediment Composition Observed in Cores

A total of 10 sediment types occur across the three study areas (see core legend in Appendix F). They are: gravel, sandy mud, silt, clay, muddy gravely fine to coarse sand, and fine to coarse sand. While individual cores show specific compositional variations, some general patterns occur. In all cases, the dominant component of the sediment at the tops of the cores is carbonate, with poorly-sorted calcareous fine to medium sands being the most abundant facies. The cores contain a variety of sedimentary features including: shell hash beds, woody and organic fragments, articulated and disarticulated bivalves. Overall, the most abundant sedimentary structures are laminations and burrows. Unconformities between sediment facies of sedimentary environments, and possible different ages, are also present in several cores from each of the study areas. In general, the fossil content of the cores is typical for shallow tropical marine settings in Australia, and included: benthic foraminifers, bivalves, gastropods, bryozoans, corals, echinoids, *Halimeda*, worm tubes, scaphopods, and crustaceans in decreasing abundance. The salient features of the sediment composition contained in cores collected from the three study areas are now described.

3.5.4.1 Sediment Composition – Area A, Fly River Delta

Poorly-sorted calcareous muddy gravely medium to coarse sand occurs at the tops of the cores recovered from Area A, except for 19PC4 and 21PC5 where sandy mud and mud and sand interbeds crop out at the surface, respectively (Appendix H). The calcareous muddy gravely sand attains a minimum thickness of 0.25 m in 3PC1 and a maximum thickness of 2.5 m in 23PC7. The base of this unit was not sampled in cores 25PC9 and 26PC10, and the unit may be thicker at these sites. Visual inspections of the fossil content of the bulk sediment indicate that benthic foraminifers, bivalves, and bryozoans are generally more common than coral and algal fragments. Apart from extensive burrowing (the burrows are comprised of moderately sorted mud and silty sand), the unit is generally devoid of sedimentary structures. In core 15PC2, a bed of coarse shell hash and calcareous sand occurs at the base of this unit.

An unconformity separates the calcareous muddy gravely sand unit from an underlying siliciclastic dominated silt and clay unit, where both units occur in the cores. The lower fine-grained silt and clay unit attains a minimum thickness of 0.30m in 15PC2 and a maximum thickness of 3.2m in 22PC6, although only cores 15PC2, 17PC3 and 19PC4 sampled the base of this unit. Fossils are generally rare, but bivalves and benthic foraminifers do occur in this unit in cores 3PC1, 17PC3, and 24PC8. Peat and wood fragments are abundant throughout, and occasional sandstone and mudstone clasts are preserved. Laminations or interbeds of silt, clay and some sand are the dominant sedimentary structures in this unit as can be observed in X-radiographs taken from the core (Fig. 3.24, Appendix I). Except for core 19PC4, the laminations and interbeds generally have sharp bottom contacts and fine-upwards from fine sand to clay (e.g., core 21PC5) and are spaced relatively regularly down each core. In 19PC4, between 0.63 and 1.08 mbsf, a total of 22 sand-mud couplets occur that have a mud layer that gradually coarsens upwards into a sand layer with a sharp upper contact (Fig. 3.24). Below these sand-mud couplets, between 1.08 and 1.81 mbsf, the more widespread fining upward laminations occur. In core 15PC2, below 1.35 mbsf, the fine-grained muddy unit contains extensive burrows comprised of silty fine sand and is truncated at its base by *Halimeda* gravel containing several distinct gravel beds with a grain alignment dipping at approximately 30°. A bed of bioturbated muddy calcareous coarse sand 0.04m and 0.19m thick, respectively, containing abundant shell fragments occurs at the base of cores PC3 and PC4. Interestingly, abundant calcite occurs in cores 3PC1 and 24PC8, where it appears to have precipitated *in-situ* between two bedding planes.

3.5.4.2 Sediment Composition - Area B, Torres Strait

Poorly-sorted calcareous muddy gravely fine to medium sand occurs at the tops of the cores recovered from Area B, except for 50GC11 where siliciclastic-dominated mud crops out at the surface (Appendix F). The calcareous muddy gravely sand unit attains a minimum thickness of <0.05m in 45GC6 and a maximum thickness of 1.17m in 42GC3. However, the base of this unit was not sampled in cores 42GC3, 47GC8, 49GC10, 51GC12, and 53GC14, and could be thicker at these sites. Visual inspections of the fossil content of the bulk sediment indicate that benthic foraminifers, bivalves, gastropods, and bryozoans are generally more abundant than coral and algal fragments. Apart from occasional burrowing (the burrows are comprised of finer sediment, e.g., mud), the unit is generally devoid of sedimentary structures. Abundant shell hash occurs at the contact between this unit and an unconformable lower fine-grained unit in cores 28GC1, 44GC5, and 47GC8.

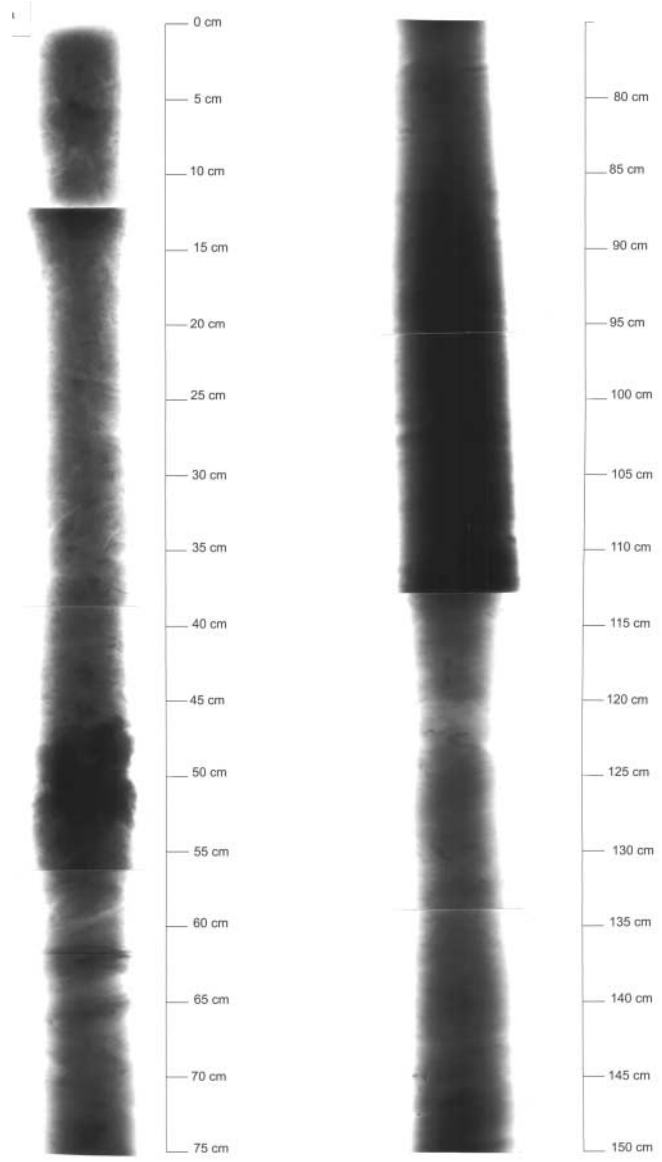

Figure 3.24. *X-radiograph of the upper 150cm of sediment core 19PC4. Note the transition from calcareous to terrigenous-laminated facies at 45-50cm depth down-core is accompanied by an increase in density, as shown by dark tones in the X-radiograph. Laminations are abundant below 63cm in this core.*

A fine-grained, organic-rich, siliciclastic dominated unit, comprised of grey clay to black mud, underlies the upper unit in cores 28GC1, 41GC2, 43GC4, 44GC5, 46GC7, 48GC9, and 51GC12, but crops out at the surface in 50GC11. The lower fine-grained unit attains a minimum thickness of 0.10 m in 28GC1 and a maximum thickness of 2.55 m in 46GC7, although none of our cores sampled the base of this unit. Fossils are extremely rare, but benthic foraminifers occur in this unit in 43GC4. In all cores containing this unit peat deposits and wood fragments occur throughout but are they are especially abundant in 41GC2. Laminations occur throughout and are comprised of either mud or discontinuous whispy sand with sharp upper boundaries (44GC5). Laminations are most abundant in 46GC7 where the sand laminae are locally discontinuous and burrowed with sharp upper surfaces and overlain by mud drapes. They are also occasionally associated with terrigenous fine sand. The laminations range in colour from green-grey (44GC5, 46GC7, 50GC11) to reddish brown (43GC4). Burrows comprised of silty sand to fine sand are common throughout.

3.5.4.3 Sediment Composition – Area C, Gulf of Papua

Poorly-sorted calcareous muddy gravely fine to medium sand comprises the total length of five cores (54GC15, 55GC16, 64GC21, 73GC23, 74GC24) and well-sorted sand occurs comprises the total length of two cores (61GC18, 62GC19) recovered from Area C (Appendix F). The remaining core, 59GC17, is entirely comprised of a 2.96 m thick sequence of *Halimeda* gravel that also contains abundant very large benthic foraminifera disks. The calcareous muddy gravely fine to medium sand attains a minimum thickness of 0.06 m in 73GC23 and a maximum thickness of 0.52 m in 55GC16. The well-sorted sands attain a minimum thickness of 0.03 m in 61GC18 and a maximum thickness of 0.10 m 62GC19. However, it must be stressed that none of our cores sampled the base of these units from Area C. Visual inspections of the fossil content of the bulk sediment indicate that benthic foraminifers, bivalves, gastropods, bryozoans, and echinoids are generally more abundant than coral and algal fragments. Except for indistinct laminations 59GC17 and 74GC24, sedimentary structures are absent, with the sediment in 64GC21 being disturbed throughout. Pebble-sized clasts of sandstone and other lithics occur in two cores (54GC15, 55GC16), but they are relict in appearance, being encrusted with worm-tubes. Preserved burrows are rare, but occur occasionally in 59GC17 as mottles of olive coloured silt.

3.5.5 Stratigraphic Interpretations

Below is a brief stratigraphic and environmental interpretation of the sub-surface sediment contained in the cores. Sediment facies contained in several cores recovered from Areas A and B indicate a change in depositional conditions through time, while sediment facies contained in cores from Area C indicate depositional conditions similar to present-day.

3.5.5.1 Highstand Sequence

The calcareous muddy gravely sands that dominate the tops of cores from Area A are consistent with the surface samples collected from the sea floor, and other geological studies of the Holocene sediments for Torres Strait and Gulf of Papua shelf (Harris, 1988; Harris et al., 1996) and the Great Barrier Reef (GBR) platform (e.g., Maxwell, 1968; Harris et al., 1990; Orpin and Woolfe, 1999; Dunbar et al., 2000; Heap et al., 2001). This facies is inferred to represent highstand deposition in open shallow marine settings at the distal part of the Fly River delta. Carbonate fragments dominate the coarse fraction. Because the coarse fragments occur in conjunction with fine-grained mud and clay, it is likely that much of the carbonate material in these units is produced *in-situ*, and has not been transported in from elsewhere. The fine-grained component is a mixture of carbonate and siliciclastic material, implying multiple sources, possibly terrigenous sediment from the Fly River. As with other parts of the GBR platform, it is likely that relict sediment deposited during the lowstand has also been mixed with modern sediments, although the contribution of the relict sediment has not been reliably estimated for this region. Interestingly, the same muddy gravely sand facies occurs at the tops of several cores recovered from areas A and C, indicating that the similar open shelf conditions occur throughout the region. It is inferred from this that,

despite being located at the distal part of the delta, the influence of the Fly River is significantly reduced at Area A, and that present-day depositional conditions are more representative of an open marine shelf environment with some tidal influence. Included in this shelf setting are *Halimeda* banks (sampled in 59GC17), which show evidence of uninterrupted deposition of *Halimeda* gravels that contain an abundance of benthic foraminifers in an outer shelf setting. The physical properties (bulk density, p-wave velocity, magnetic susceptibility, fractional porosity) are all comparable with values obtained for modern-day sediment on the GBR platform (e.g., Heap et al., 2001).

3.5.5.2 Transgressive Sequence

Siliciclastic dominated clay and mud units occur below the highstand shelf deposits in several cores recovered from Areas A and B. In all cases, these underlying units are separated from the highstand units by an unconformity. Because this unconformity separates sediment facies of very different composition and physical properties it probably also marks a time line associated with a significant change in depositional environments at these locations on the shelf. The units are dominated by fine-grained siliciclastic clay and silt and contain abundant peat and woody fragments, with laminations and interbeds composed of siliciclastic silt and sand that occur throughout the sequence. Their physical structures and composition are remarkably similar to the modern deposits that have been described from the adjacent Fly River Delta distributary channels (Baker et al., 1995; Dalrymple et al., 2002). Also, physical properties from this unit are consistent with values obtained for siliciclastic dominated estuarine and shallow embayment deposits on the GBR platform. It is inferred from these features that the lower units in the cores accumulated in a marginal marine environment, probably influenced by river or estuarine processes. Given that these siliciclastic-dominated units occur in the vicinity of the Fly River at between 29 to 85m below present-day sea level, it follows that they were formed during the last post-glacial transgression and represent a transgressive sequence of a palaeo-river system (Fly River?), deposited in the estuary or lower river reaches. Consequently, the unconformity at the top of this transgressive sequence would represent an erosional surface formed sometime soon after the onset of the Holocene highstand.

3.6 SEABED CHARACTER OBSERVED IN UNDERWATER VIDEO

3.6.1 Area A, Fly River Delta

A summary of the video sites, their characteristic seafloor types and biota is provided in Table 3.6 (video clips from every station are included in Appendix J). Area A is strongly influenced by terrigenous sediments, probably derived from the Fly River. Video footage shows that the sediments are fine-grained. The seafloor in this area is generally flat to occasionally undulating. Pits and pockmarks, varying from small (5-10 cm) to large (40 cm) diameter, were present at sites 1CAM1, 3CAM3, 11CAM11, 15CAM15, 21CAM22 and 76CAM66. Low irregular ridges of 2-3cm elevation and cracks up to 2 cm wide were observed at site 10CAM10, while large holes were present at site 19CAM20 (Table 3.6). Some of these features may be due to bioturbation; others are possibly gas escape features. Additional evidence suggestive of gas escape was observed in seismic sections.

The biota is generally sparse, although moderate to extensive bioturbation and burrows at most sites suggest a relatively rich infauna. Distinctive Callianassid burrows are low in abundance, but present in many of the sites. Live Callianassids were retrieved in several grab samples. The fauna most commonly observed on the sediment surface is soft corals, sponges, fish and sea whips. Other biota includes shrimp, sea cucumber, hard coral, heart urchin and worm. Three sites show a much higher faunal abundance: 4CAM4, 18CAM19 and 76CAM66. All three sites show an increase in relief, suggesting a causal relationship between greater seabed relief and the abundance of faunal cover.

Abundant marine snow was present in the water column at a number of sites: 2CAM2, 5CAM5, 7CAM7, 9CAM9, 11CAM11 and 12CAM12. The water column was turbid at sites 3CAM3, 12CAM12, 18CAM19, 19CAM20, 20CAM21 and 76CAM66. A strong current was observed at some of the sites in the deeper area to the south-east: 11CAM11, 12CAM12 and 13CAM13.

3.6.2 Area B, Torres Strait

The seafloor in this area is flat or relatively flat at the majority of sites. Flat seafloor with sloping areas is present in 44CAM39. Rocky or patchy reef occurs in sites 29CAM24, 37CAM32 and 40CAM35. Reefs were targeted at two additional sites, but were not traversed. At site 29CAM24 coral rubble was evident, but no reef build-up was observed. At site 31CAM26, the ship was unable to drift across the reef (Table 3.6).

Bedforms, predominantly ripples, were observed in a number of sites: 38CAM33, 41CAM36, 42CAM37 and 45CAM40. At site 41CAM36 small dunes were also present. The presence of faint bedforms at site 47CAM42 suggests that sediment transport is weak or inactive at some of these sites. Currents were present at nearly half the sites in this area, including 28CAM23, 30CAM25, 342CAM37, 43CAM38, 44CAM39 and 47CAM42. Strong to very strong currents were present at sites 32CAM27, 36CAM31, 38CAM33, 39CAM 34 and 40CAM35.

Sediments in the area are typically muddy sands. Coarser sands are present in inter-reef flats, as well as one flat area (39CAM34). Rubble and gravel are evident near reefs, inter-reef areas, in an incised bed (28CAM23) and on the floor of the channel (45CAM40).

Burrows, small to large in size (2-10cm) were present in about half the sites: 28CAM23, 29CAM24, 30CAM25, 33CAM28, 35CAM30, 36CAM31, 41CAM36, 42CAM37, 43CAM38. Other evidence of bioturbation included colour changes and feeding trails (30CAM25, 47CAM42). Pits, including possible scour pits were observed at a few sites (29CAM24, 36CAM31, 48CAM43). These vary from 3cm to greater than 20cm diameter. Faunal abundance is very rare to low at most sites, particularly those subject to strong currents. More abundant faunas were found at sites with bommies or rocky reef patches (29CAM24, 37CAM32 and 40CAM35). The presence of burrowing in many sites suggests an abundant infauna.

Reef and bommie sites contain sponges, soft corals, gorgonians, sea whips, hydroids and associated gastropods and starfish. Hard corals were not observed in any of these sites. Elsewhere the biota includes sponges, polychaetes, sea urchins, prawns, shrimp, soft corals, crabs brittle stars, spider shell, crinoid, including sea lily, anemones, sea whips, hydroids, sea cucumbers, gorgonians and fish, including fusiliers, lizard fish, gobies and eel. Fish, ctenophores and jellyfish were observed in the water column at a number of sites.

Marine snow was low to abundant in the water column at sites 28CAM23, 29CAM24, 30M25, 38CAM33, 42CAM37, 43CAM38, 44CAM39 and 46CAM41.

3.6.3 Area C, Gulf of Papua

The seafloor is flat to relatively flat throughout most of the area. Uneven to rough seafloor was observed at site 59CAM49. Reef areas were present at sites 56CAM46, 57CAM47, 70CAM60, 71CAM61, 65CAM55 and 75CAM65 (Table 3.6). For the most part these are uneven rocky outcrops or bommies. Modern growth at site 57CAM47 is clearly established on a base of older, eroded reef.

Sediments for the most part are sandy; muddy sand and sandy mud are less common. Rubble is evident in areas adjacent to reefs. Bedforms were targeted at two sites (60CAM50 and 61CAM51). Some change in elevation was observed at 60CAM50, but otherwise there was little evidence of active bedforms from

the video footage. Ripple marks were observed at site 66CAM56. Currents were only observed at one site: 62CAM52.

Burrows are small, between 2 and 5cm diameter, and rare to moderate in abundance, present at only a small number of sites. Other possible evidence of bioturbation includes pock marks, pits, mounds and rare cracks up to 10cm diameter in sites 54CAM44, 60CAM50, 61CAM51, 66CAM56, 67CAM57, 74CAM64 and 73CAM63.

Faunal abundance varies from rare to moderate and shows a greater variety than observed in Areas A or B. Continuous cover was present only at the coral reef at 56CAM46 and across the top of the *Halimeda* bioherm at 65CAM55. Other reef areas typically show patchy cover dominated by soft corals and other soft biota, including sponges, gorgonians, sea whips and hydroids. Associated fauna includes starfish, crabs, baler shell, sea cucumbers, sea urchins, crinoids and sea lilies, sea pens, polychaetes and fish, including angelfish, surgeon fish, gobies and *Chaetodon* species associated with reefs, and elsewhere flounder, moray eel and cardinal fish. Hard corals were not common, being present at only one site 71CAM61 in addition to the coral reef site (56CAM46). Marine snow was moderate to abundant at two stations in the north: 58CAM48, 23461CAM51, and several in the south: 72CAM62, 73CAM63, 74CAM64 and 75CAM65.

Table 3.6. Descriptions of seafloor features observed in underwater video images (clips from each station are included in Appendix J).

Area A.

VIDEO NO.	START LAT	START LONG	END LAT	END LONG	START WATER DEPTH	END WATER DEPTH	VIDEO DESCRIPTION	COMMENTS
1CAM1	-9.123	143.720	-9.123	143.719	31.5		Flat seafloor, with fine-grained muddy sediment, extensively burrowed. Occasional pock marks (5-40cm diameter) and rare Callianassid burrows present. Other fauna includes rare soft corals, fish (flounder).	Target site: site for deployment of Bruce (current meter). Water depth taken as station depth (not recorded for video times).
2CAM2	-9.126	143.668	-9.127	143.668	30.5	30.5	Abundant snow in water column. Flat, muddy seafloor with rare Callianassid burrows and other faunal burrows (2-5cm diameter) abundant.	Target site: flat area.
3CAM3	-9.134	143.676	-9.134	143.677	29.5	29.0	Very turbid in water column. Moderately abundant biota, including soft corals, sponges. Seafloor undulating, moderately burrowed. Large mounds/burrows (~10cm diameter) and uncommon pits (>30 cm diameter) also present.	Target site: flat area with subsurface reflectors.
4CAM4	-9.110	143.701	-9.110	143.701	24.0	23.5	Abundant soft corals, large sponges, cardinal fish, sea whips, gorgonians. ~70-80% coverage of seafloor by biota. Little fine-grained sediment, seafloor relatively consolidated.	Target site: rock Ship's heading during filming: 270.
5CAM5	-9.132	143.679	-9.132	143.680	34.0	33.5	Abundant snow in water column. Flat, muddy bottom with occasional burrows, including Callianassid burrows. Biota not abundant, includes cardinal fish.	Target site: channel fill.
6CAM6	-9.128	143.696	-9.128	143.696	28.0	28.0	Irregular seafloor with moderate to extensive burrowing (2-5cm diameter). Sediment muddy. Biota rare, includes sponges, fish, shrimp.	Target site: flat area.
7CAM7	-9.152	143.689	-9.152	143.689	32.5	32.5	Moderate snow in water column. Relatively flat seafloor, moderately burrowed (2-5cm diameter), muddy sediment. Rare biota includes ?sponges, fish (flounder).	Target site: channel fill.
8CAM8	-9.171	143.695	-9.171	143.695	31.5	31.5	Seafloor relatively flat, with low to moderate burrowing (3-10cm diameter), sediment muddy. Rare fauna includes sea cucumber, rare soft coral, ?hard coral, heart urchin.	Target area: flat area.
9CAM9	-9.152	143.715	-9.152	143.715	31.5	31.5	Moderate snow in water column. Seafloor relatively flat, moderately burrowed (2-10cm diameter), with occasional Callianassid burrows. Sediment muddy. Other rare fauna includes worm, soft corals, sponges.	Target site: outcrop of reflector.
10CAM10	-9.152	143.702	-9.152	143.702	33.0	33.0	Seafloor flat to slightly undulating, rare burrows (3-5cm diameter). Irregular low ridges (2-3 cm elevation) and cracks ~2cm width. No fauna evident.	Target site: flat area.

VIDEO NO.	START LAT	START LONG	END LAT	END LONG	START WATER DEPTH	END WATER DEPTH	VIDEO DESCRIPTION	COMMENTS
11CAM11	-9.135	143.731	-9.135	143.731	33.5	33.0	Snow very abundant in water column. Seafloor relatively flat with occasional burrows (2-5cm diameter) and rare large Callianassid burrows (up to 20cm diameter). Occasional pits of 15-20 cm diameter present. Strong current evident. Rare soft corals.	Target site: Subsurface reflectors.
12CAM12	-9.150	143.730	-9.150	1433.723	35.0	35.0	Abundant snow and suspended particles in water. Seafloor gently undulating to uneven. Sediment muddy; appears to be abundant algal growth in areas. Strong current present.	Target site: sandwaves. Camera brought up early because cable went under ship.
13CAM13	-9.125	143.754	-9.125	143.754	33.5	33.5	Seafloor uneven with moderate burrowing (1-5cm diameter). Sediment muddy. Rare biota includes soft corals, sponges. Strong current present.	Target site: channel fill Difficulty in keeping camera on bed due to ship heave.
14CAM14							No bottom footage recorded.	Target site: rock Deployment aborted due to currents pushing camera near ship's propeller. Camera did not reach bottom. Repeat video taken as 76CAM66.
15CAM15	-9.126	143.715	-9.127	143.715	33.0	33.0	Muddy sand. Seafloor irregular, moderately to heavily burrowed with small pock-marks/burrows <5 cm diameter. Large pock marks (up to 20cm diameter) and rare Callianassid burrows also present.	Target site: subsurface reflectors.
16CAM17	-9.116	143.709	-9.116	143.709	29.5	29.5	Fine muddy sediment with abundant mud clasts. Uneven seafloor characterised by burrows, including Callianassid burrows. Biota not abundant.	Target site: flat area. Repeat video deployment at station 16. Ship's heading during filming: 254.
17CAM18	-9.105	143.724	-9.105	143.725	30.0	30.0	Seafloor uneven with abundant burrows present (small, 1-5cm and large~10cm diameters). Very muddy sediment. Biota includes rare soft & hard corals, fish.	Target site: channel.
18CAM19	-9.102	143.735	-9.102	143.734	29.0	27.5	Sea floor irregular, moderately burrowed, characterised by large depressions >1m, with increased relief (~10-20cm) at margins. Sediment muddy. Moderate fauna (sea whips, soft corals). Fauna most abundant on areas of higher relief, rare to moderate elsewhere.	Target site: rock, pockmarks.
19CAM20	-9.087	143.731	-9.087	143.731	29.5	29.5	Very turbid in water column, Seafloor relatively flat to irregular, with some large holes present (size?). Abundant burrows (2-5cm diameter), including Callianassid burrows. Other fauna includes soft corals. Sediment muddy.	Target site: subsurface reflectors. Ship's hading during filming: 235.
20CAM21	-9.095	143.711	-9.095	143.711	29.0	28.5	Very turbid water. Seafloor relatively flat with burrows (~2-8cm diameter). Rare soft corals, seawhips present. Sediment sandy mud.	Target site: valley with subsurface reflectors Ship's heading during filming: 222.

VIDEO NO.	START LAT	START LONG	END LAT	END LONG	START WATER DEPTH	END WATER DEPTH	VIDEO DESCRIPTION	COMMENTS
21CAM22	-9.117	143.680	-9.117	143.680	29.5	29.5	Seafloor relatively flat moderately burrowed (1-5cm diameter), with rare Callianassid burrows and small pock marks (~5-10cm diameter). Sediment fine-grained, muddy.	Target site: valley fill.
76CAM66	-9.118	143.746	-9.117	143.747	31.0	30.0	Water turbid. Sediment muddy. Seafloor relatively flat through most of transit, with large pits 6-10cm diameter and abundant burrows. Moderate faunal cover including soft corals, shells, fish. Rocky outcrops present with increased cover, including soft corals.	Target site: rocky area (original station 14).

Area B

VIDEO NO.	START LAT	START LONG	END LAT	END LONG	START WATER DEPTH	END WATER DEPTH	VIDEO DESCRIPTION	COMMENTS
28CAM23	-9.487	143.946	-9.487	143.946	56.0	56.0	Water column very clear, minor plankton snow. Seafloor relatively flat, moderately burrowed (small-large burrows 2-10cm diameter. Sediment calcareous coral rubble. Fauna rare, includes polychaete, fish (in water column), sponge. Current running.	Target site: incised bed.
29CAM24	-9.468	143.976	-9.468	143.977	47.4	44.5	Abundant snow in water column. Seafloor relatively flat, moderate burrowing (2-5cm diameter) with large pits >20cm diameter, abundant coral rubble. Occasional fauna includes sponges, fish, sea urchin, goby/prawn, shrimp. Large coral bommie present (2m+).	Target site: reef buildups.
30CAM25	-9.497	144.004	-9.493	144.004	54.0	54.0	Low marine snow in water column. Flat seafloor, with rare small burrows (~2cm diameter) evident. Evidence of low to moderate bioturbation: colour changes suggest it is recent. Biota include shrimp, fish (fusiliers), soft coral, spider shell, crab.	Target site: flat area with subsurface reflectors.
31CAM26	-9.475	144.017	-9.475	144.017	52.0	52.0	Flat featureless bottom. Biota rare, includes 3 fish, small crab, ?polychaete tube worms, lizard fish, sponge, soft coral, ctenophores in water column. Little evidence of burrowing.	Target site: reef. Unable to drift across reef site.
32CAM27	-9.459	143.995	-9.459	143.995	132.0	131.5	Flat seafloor. Biota very rare: several jellyfish, brittle star. Strong current running.	Target site: submarine valley floor.
33CAM28	-9.464	143.964	-9.464	143.964	50.5	50.5	Flat seafloor with sandy sediment, occasional gravel-sized clasts and shelly debris, burrows 2-5cm diameter. Biota very sparse, crinoids/anemone, fish including gobies.	Target site: inter-reef flat.
34CAM29	-9.457	143.952	-9.457	143.952	86.0	87.0	Flat bottom with muddy sand. Biota includes soft corals, sponges, crinoids, small fish, sea whips.	Target site: valley side.

VIDEO NO.	START LAT	START LONG	END LAT	END LONG	START WATER DEPTH	END WATER DEPTH	VIDEO DESCRIPTION	COMMENTS
35CAM30	-9.435	143.956	-9.435	143.956	103.0	103.0	Flat bottom with muddy sand, occasional burrows ~2cm diameter. Biota very sparse; some soft corals/sponges. Moderately abundant fish, including eel?	Target site: channel fill.
36CAM31	-9.446	143.986	-9.447	143.986	84.0	88.5	Flat bottom with muddy sand. Rare scour pits or burrows around 5cm diameter and >20cm. Biota very sparse, some soft corals, hydroids. Strong current running.	Target site: valley side.
37CAM32	-9.448	144.022	-9.448	144.022	49.0	49.0	Rocky reef (patchy distribution) with intervening flat bottom comprised of calcareous muddy sand. Reef surface eroded, probably karst. Abundant faunal cover on rocky reef: sponges, soft corals, gorgonians, sea whips.	Target site: reef.
38CAM33	-9.428	144.012	-9.428	144.012	56.5	55.5	Very abundant snow in water column. Ripples present on seafloor. Biota very sparse: sea whip? Very strong current flowing.	Target site: rough seabed.
39CAM34	-9.398	144.011	-9.397	144.011	60.0	60.0	Flat sandy bottom. High levels of turbidity in water column. Very strong current running.	Target site: flat area with subsurface reflectors. Cable going under ship. Ship's heading altered to 311; couldn't stay on station.
40CAM35	-9.401	144.034	-9.401	144.034	58.5	59.5	Flat sandy bottom between rocky patches with good faunal cover: seawhips, sponges, hydroids, gastropod, starfish, soft corals. Strong current running.	Target site: reef.
41CAM36	-9.412	144.012	-9.413	144.011	58.0	58.0	Sandy sea floor with ripples and small dunes. Biota very sparse: crab, goby, hydroid, polychaete tubes, sea whip. Small burrows present (2cm diameter).	Target site: rough bed (bowties on seismic). Camera cable under boat, ship's heading changed to 229.
42CAM37	-9.409	143.979	-9.409	143.479	78.5	78.5	Jellyfish and fish (fusiliers) in water column. Abundant marine snow in water column at depth. Relatively flat seafloor. Ripples with colour 3D patterns present. Burrows not abundant, both small ~2cm diam and medium 4-5 cm diam present. Current running.	Target site: sediment mound.
43CAM38	-9.384	143.979	-9.384	143.980	80.0	79.5	Jellyfish & fish in water column with moderately abundant snow. Flat seafloor with rare small-medium burrows (scale bar not present). Biota includes soft corals, sea cucumbers, tube worms, sea urchins with (commensal?) fish present. Current running.	Target site: eroded edge of channel.
44CAM39	-9.376	144.018	-9.376	144.018	90.0	89.9	Flat and sloping seafloor areas crossed. Jellyfish and moderate snow in water column. Moderately abundant fauna: gorgonians, soft corals, sea whips, crinoids, sea lily? Burrows rare, <5cm diameter. Current present.	Target site: valley wall.
45CAM40	-9.383	144.036	-9.373	144.036	91.5	91.0	Flat seafloor with ripples (<5cm length). Coral rubble present. Fauna not abundant; soft corals, fish, large sponges (10-15 cm high), shrimp.	Target: Floor of wide channel

VIDEO NO.	START LAT	START LONG	END LAT	END LONG	START WATER DEPTH	END WATER DEPTH	VIDEO DESCRIPTION	COMMENTS
46CAM41	-9.351	144.036	-9.351	144.036	63.0	63.0	Moderate snow in water column. Small fish and shrimps present above seafloor. Flat seafloor with little evidence of burrowing. Burrows present are small (2-5cm in diameter). Moderate amount of fauna; sea whips, fish (incl. lizard fish), crabs, starfish.	Target site: incised bed.
47CAM42	-9.332	144.002	-9.332	144.015	57.5	57.5	Moderate snow in water column. Flat seafloor, faint bedforms, feeding trail visible. Fauna not abundant; fish (fusiliers), sea whips. Current running.	Target area: sediment wedge.
48CAM43	-9.344	143.979	-9.344	143.979	57.0	57.0	Abundant snow in water column. Flat seafloor with muddy sand. Biota rare includes fish, sponges, soft corals, hydroids. Rare pits ~3cm diameter.	Target site: sediment wedge.

Area C

VIDEO NO.	START LAT	START LONG	END LAT	END LONG	START WATER DEPTH	END WATER DEPTH	VIDEO DESCRIPTION	COMMENTS
54CAM44	-9.381	144.279	-9.382	144.278	114.5	111.0	Seafloor flat with burrows (~5cm diameter) and pock marks >15-20cm diam. Fauna low-moderate abundance, includes sponges, fish, sea whips, polychaete, sea pen, starfish.	Target site: incised surface. Heading 272. Mixed layer in water column near seafloor.
55CAM45	-9.410	144.276	-9.410	144.277	65.5	66.0	Seafloor flat, rubbly. Abundant fauna, including soft corals, sponges, sea whips, gorgonians, hydroids, baler shell, rare hard coral. Burrows rare, small (2-5cm diameter).	Heading 315 deg. Target site: onlap sediment wedge, flat floor adjacent to rocky area.
56CAM46	-9.421	144.284	-9.421	144.284	29.5	29.0	Coral reef, 100% faunal coverage, predominantly hard corals with soft corals, fish (surgeon fish, *Chaetodon* sp.), sea star (?*Linkia*). Relief of at least several meters.	Target site: reef. Heading 302 degrees.
57CAM47	-9.417	144.308	-9.417	144.308	49.5	49.5	Seafloor very uneven: large bommies and cave in older-looking coral base. Fauna includes *Lithothamnion*, soft corals, sea whips, fish, including angelfish. Adjacent area low relief with sandy floor, patchy cover including soft corals, sponges, hydroids.	Target site: hard rocky bed. Video dropped out of record over bommie area. Some footage lost, including cave. Heading 286 deg.
58CAM48	-9.408	144.322	-9.409	144.323	103.5	107.5	Moderate snow in water column. Seafloor flat and muddy in areas, elsewhere topography is rugged with small bommies. Relatively abundant fauna over rough area includes soft corals, sea whips, gorgonians, sponges, fish. Fauna on muddy areas much less abundant.	Target site: hard ground ~100m water depth.

VIDEO NO.	START LAT	START LONG	END LAT	END LONG	START WATER DEPTH	END WATER DEPTH	VIDEO DESCRIPTION	COMMENTS
59CAM49	-9.391	144.369	-9.389	144.366	80.0	78.5	Moderate snow in water column. Seafloor uneven, rough, with rare burrows ~2cm diameter. Moderately abundant fauna: hydroids, soft corals, sea whips.	Target site: outer shelf mesa (possible *Halimeda* bed). Heading 272.
60CAM50	-9.422	144.352	-9.422	144.422	96.0	96.0	Seafloor sandy, burrows rare ~2cm diameter, mounds rare. Rare biota includes fish (flounder, cardinal fish), crab, soft coral, sponges, sea whips. Change in elevation apparent across one section. Otherwise little evidence of sandwaves, no evidence of activity.	Target site: sandwaves. Heading 287deg.
61CAM51	-9.445	144.357	-9.444	144.357	90.0	91.0	Small fish abundant in water column and over seafloor. Moderate snow in w. column. Seafloor appears flat, occasional mounds and pits >10cm across/diameter. Fauna moderately abundant, includes hydroids, soft coral, sea whips, crinoids, moray eel.	Target site: sandwaves.
62CAM52	-9.463	144.357	-9.463	144.357	103.5	103.5	Planar bed with rare burrows ~2cm diameter. Biota rare, includes soft corals, sea whips, hydroids, sponges. Current running.	Target site: flat area with subsurface reflectors.
63CAM53	-9.509	144.360	-9.509	144.360	90.0	90.5	Generally planar bed with isolated benthic life: sponges, soft corals, ?sea cucumber, hydroids, starfish.	Target site: flat bed.
64CAM54	-9.521	144.340	-9.521	144.340	112.5	112.0	Flat bed covered in coarse lag material. Isolated occurrences of benthic life, widely separated, includes soft corals, hydroids, sponges, sea whips, crinoids.	Target site: SE channel outlet.
65CAM55	-9.510	144.319	-9.510	144.319	43.0	45.5	Reef top, abundant benthic organisms, *Halimeda*-dominated. 100% cover over reef top. Additional fauna includes soft corals and crinoids. Sedimented areas show abundant *Halimeda* flakes.	Target site: bommie reef.
66CAM56	-9.473	144.316	-9.474	144.316	82.5	82.5	Flat bed, featureless. Moderate burrows, mounds 3-10cm diameter. Ripple marks. Rare biota includes starfish, hermit crab, sea whip, fish.	Target site: valley side (subsurface reflectors).
67CAM57	-9.454	144.330	-9.455	144.330	79.5	79.0	Jellyfish in water column. Featureless flat sandy bed; few burrows and cracks ~3cm diameter. Biota very rare, includes seawhip, crinoid?	Target site: flat bed.
68CAM58	-9.439	144.298	-9.438	144.297	88.5	90.5	Flat featureless sandy mud on seafloor. Sparse small burrows (<5cm diameter). Biota includes sea urchins, sponges, soft corals, crinoid, sea pen.	Target site: valley floor.
69CAM59	-9.489	144.303	-9.489	144.302	109.5	109.0	Relatively flat seafloor, sandy sediment, with few burrows, <5cm diameter. Fauna includes sea cucumber, sponges, soft corals, hydroids. Low to moderate faunal cover.	Target site: valley floor.
70CAM60	-9.533	144.276	-9.533	144.276	50.0	51.0	Reef, patchy coverage.	Target location: reef. Video footage poor, lights low. Video repeated as station 71, see 71CAM61.

VIDEO NO.	START LAT	START LONG	END LAT	END LONG	START WATER DEPTH	END WATER DEPTH	VIDEO DESCRIPTION	COMMENTS
71CAM61	-9.534	144.275	-9.534	144.275	48.5	48.0	Seafloor uneven with rubble. Bommies with high relief (1-2m), eroded, also present. Fauna patchy cover (~30-40%) on flatter areas, includes *Lithothamnion*, soft coral, sponges, fish (including goby), mushroom coral, hydroids. Bommies show increased coverage.	Target site: reef. Heading:299 degrees. Live material brought up on camera frame included large sponge (~30cm length), hydroids and small ophiuroids (brittle stars).
72CAM62	-9.502	144.267	-9.502	144.267	172.0	172.5	Abundant snow in water column. Water very clear above seafloor. Sediment coarse - no fines thrown up by camera. Biota very rare: fish, crinoids, other indeterminate taxa. Rare pits.	Target site: deep hole. Heading:323 degrees.
73CAM63	-9.494	144.278	-9.495	144.278	117.0	114.0	Moderate snow in water column. Seafloor relatively flat with mounds/burrows (1-5cm diameter), ridge. Occasional pits ~2-5cm diameter. Seafloor heavily bioturbated. Biota not abundant: soft corals, polychaetes.	Target site: low relief area with subsurface reflectors.
74CAM64	-9.480	144.287	-9.480	144.287	90.0	90.0	Moderate snow in water column. Seafloor flat, with rare burrows ~10cm diameter. Fauna not abundant: polychaete tubes, sponges, soft corals, sea whips, hydroids.	Target site: valley side. Heading 277 degrees.
75CAM65	-9.551	144.334	-9.552	144.334	221.0	188.5	Abundant marine snow and rare fish in water column. Seafloor relatively flat with rare burrows and pits ~5cm diameter. Biota sparse, includes soft corals, hydroids, sponges. Small rocky outcrops present, with increased faunal cover.	Target site: deep hole, channel floor.

3.7 WATER AND SEDIMENT TRANSPORT MEASURED BY BRUCE

Data recorded on the BRUCE instrument frame were analysed at the Antarctic CRC in Hobart. Energy levels at the high wave and turbulence frequencies were low. As a result, the acoustic Doppler velocity-meter (ADV) data were burst averaged to generate time series plots of currents, temperature, progressive current vector plots and pressure (sea level; Fig. 3.25). Each burst file from the pressure record was used to determine a wave spectrum. Energy levels at wave frequencies in the u & v components of velocity were too low (amongst noise levels) to compute a directional wave spectrum. For each burst spectrum, the Significant wave height was determined:

$$Hs = 4\sqrt{(\int F(\sigma)d\sigma)}$$

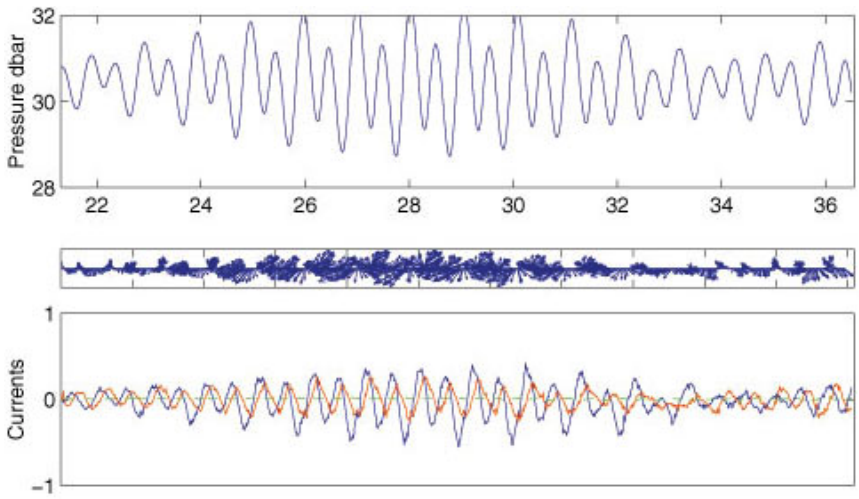

Figure 3.25. *Time series plots (Julian days, 2002) of pressure (sea level height), current vector and current amplitudes recorded by the Nortek acoustic current meter mounted on BRUCE. Current amplitudes are plotted as east-west components (red), north-south components (yellow) and combined (blue).*

Low frequency (sub-tidal) currents and pressure levels were estimated by applying a frequency domain, 40hr low-pass filter to the ADV data. OBS data were also burst-averaged, converted to turbidity (NTU), and plotted as a time series.

LISST data were burst averaged, and time series plots of transmissivity and the grain-size distribution spectra are shown. The grain-size distribution spectra were used to compute time series of grain size statistics: Mean, Sorting, Skewness and Kurtosis.

CTD data were burst averaged and time series of temperature and salinity were produced. Bedload transport rates are estimated using a variation of Bagnold's bedload equation proposed by Hardisty (1983), given as:

$$q = k_1 (U_{100} - U_{100cr})^2 U_{100}$$

where U_{100} is the current speed measured 100cm above the bed, as measured by the ADV, U_{100cr} is the threshold speed at which bedload transport commences, and k_1 is an empirically derived coefficient, dependent only upon grain size:

$$k_1 = (6.6 \times D_{mm}^{1.23})^{-1} \times 10^{-5}\ gcm^{-4}s^2$$

in which D_{mm} is the sediment grain size in millimeters. The threshold speed U_{100cr} was selected as 30 cms^{-1} for intercomparison to previous studies (Harris, 1993).

Winds were measured aboard the RV *Franklin* (Fig. 1.2). The Ship was up to 80km distance from the BRUCE deployment at times, however they are considered a good indicator of the regional wind conditions at the BRUCE site for the period of deployment. BRUCE was deployed during a period of abating 10kts SE'erly winds which lasted for approximately two days before the lighter NW'erly winds commenced. A period of stronger winds from the NW was observed between days 31-33, when mean exceeded 20kts. Mean winds were directed from the north and reached speeds of 25 knots during the period of deployment (Fig. 1.2).

3.7.1 Sea-Level

ADV recorded sea-level, or pressure, indicates the tidal record for the period of deployment. A 40hr Low pass filter of the pressure record has a maximum deviation from the mean of ~5cm. The recorded maximum tidal range is ~3.5m at spring tides occurring at days 28-29 (Fig. 3.25). The 15 days of deployment began during neap tides at day 21.5, passed through the spring tide during days 28-29, through neaps at day 35. The mooring was recovered on day 36.

3.7.2 Currents

The ADV current record is dominated by the semi-diurnal tides. Maximum bottom currents of speeds ~50 cm/s directed towards the south-west occur during spring tides at day 28 (Fig. 3.25). Rising tides are associated with a current towards the west south-west, falling tides with a current towards the east north-east, with an anti-clockwise rotation.

Low pass filtered currents are relatively weak (~5 cm/s). During the first 2 days of SE'erly winds, weak (< 2 cm/s) non-tidal bottom currents are directed to the north-east. NW'erly winds direct the current to the west (Fig. 3.26). Periods of increased NW'erly winds at days 31-33 increase the non-tidal currents to ~8 cm/s, directing them to the south southwest. During the period of deployment, mean currents were heading towards the southwest, bearing ~265° at ~3 cm/s.

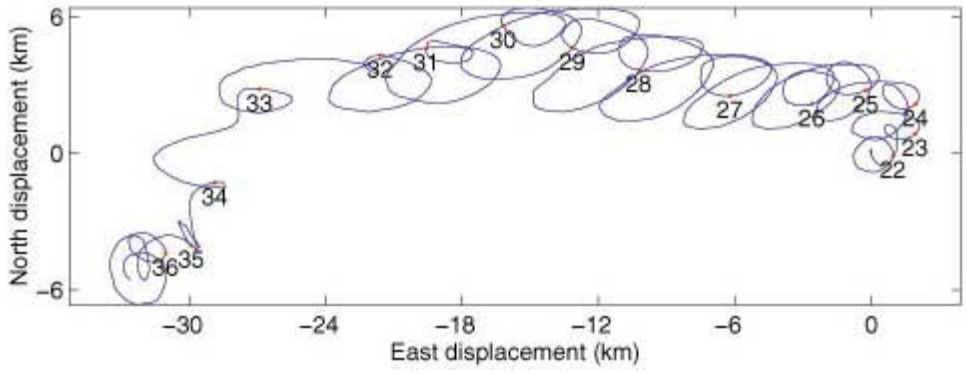

***Figure 3.26**. Progressive vector plot of currents illustrating the predominantly westward residual currents over the BRUCE site. Numbers on the plot refer to Julian Days (2002). Note the acceleration and southward deviation of residual flow that occurs from days 32-35, in response to increased wind speeds during that time.*

3.7.3 Waves

Maximum wave energy is observed at day 24 with a Significant wave height of ~16cm (Fig. 3.27), and a significant wave period of ~8s. The significant wave period is greatest during day 28 at ~11s. During periods of greatest recorded winds, on days 31-33, the wave energy is least (Hs ~ 20cm) suggesting that either the wind direction whilst the winds were strong were such that the fetch was too short for any large waves to be generated, or the wind record taken from the ships log is not a good indicator of winds at the BRUCE deployment site for the given period. Directional wave spectra would be useful to resolve the origins of the waves. Coral sea generated swell waves would be heading to the north-west, whereas locally generated waves would be heading to the south-east. Greater significant wave heights during the early deployment may be left over from southeasterly winds experienced prior to, and during, the early deployment period, having a greater fetch.

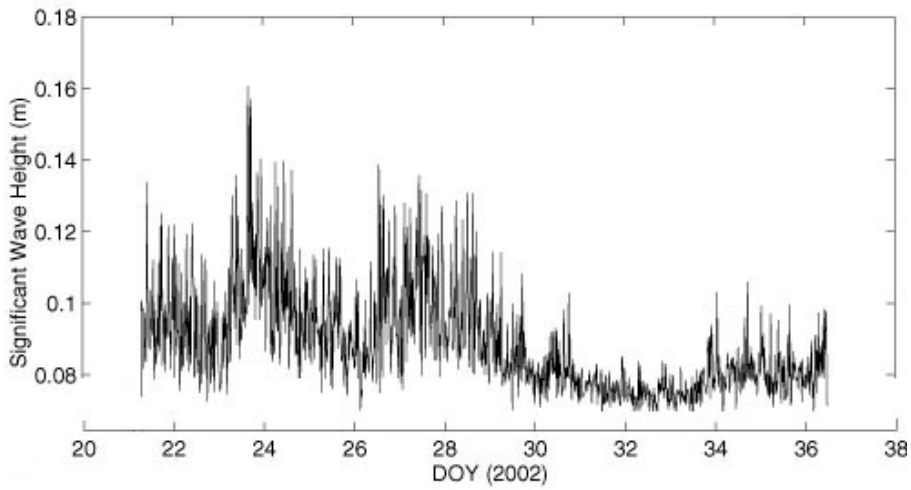

Figure 3.27. *Time series plot of significant wave height measured by the Nortek acoustic current meter installed on BRUCE.*

3.7.4 Salinity and Temperature

The salinity record obtained from the CTD has a semi-diurnal signature associated with the tide. Low salinities are correlated with periods of high tide, and high salinities are observed during low tide. Tidal variation of salinity is of the order of 0.2ppt (Fig. 3.28). Over the two-week period of deployment, the mean near-bed salinity falls from ~34.3 to ~33.7ppt (Fig. 3.28), apparently due to mixing of the water column by the wind event on days 31-33.

Approximately 1 day after deployment of the BRUCE probe, a sharp boundary oceanic front, of less dense fresh water intruding over the more dense, more saline water was observed from the deck of the RV *Franklin*. The ships log of surface salinity shows a drop from ~32.5 psu to ~31psu associated with this front. However, the recorded bottom salinity from BRUCE during this period does not show any significant salinity drop associated with this front. This is consistent with water profile being stratified as observed in the CTD records from Area A (Fig. 3.14), which show a persistent ~1.5psu variation in salinity through the water column. The semidiurnal tidal variation of salinity observed during days 22-26 (when the CTD profiles were collected) is less than the range observed during spring tides (days ~26-31; see Fig. 3.28).

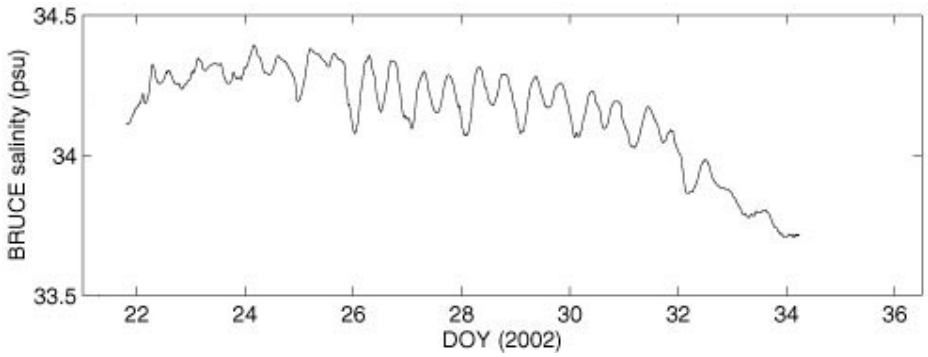

Figure 3.28. *Time series plot of bottom water salinity measured by Seacat CTD installed on BRUCE.*

The temperature record indicates similar trends to the salinity record. Higher temperatures are observed at periods of low tide, and lower temperatures are observed at high tide. Semi-diurnal variation of temperature, of up to 1°C, during periods of spring tide (Day 28) are observed. Over the duration of the deployment, a decrease of ~1°C in mean temperature is observed (Fig. 3.29).

Two instruments record the temperature, the ADV and the CTD. A ~1.3°C offset between the instruments is observed. The ADV records the higher temperatures ranging between 28.8° and 30.5°C, whereas the CTD records temperatures ranging from 27.5° to 29.2°C. This discrepancy is to be resolved by the instruments supplier, IMBROS.

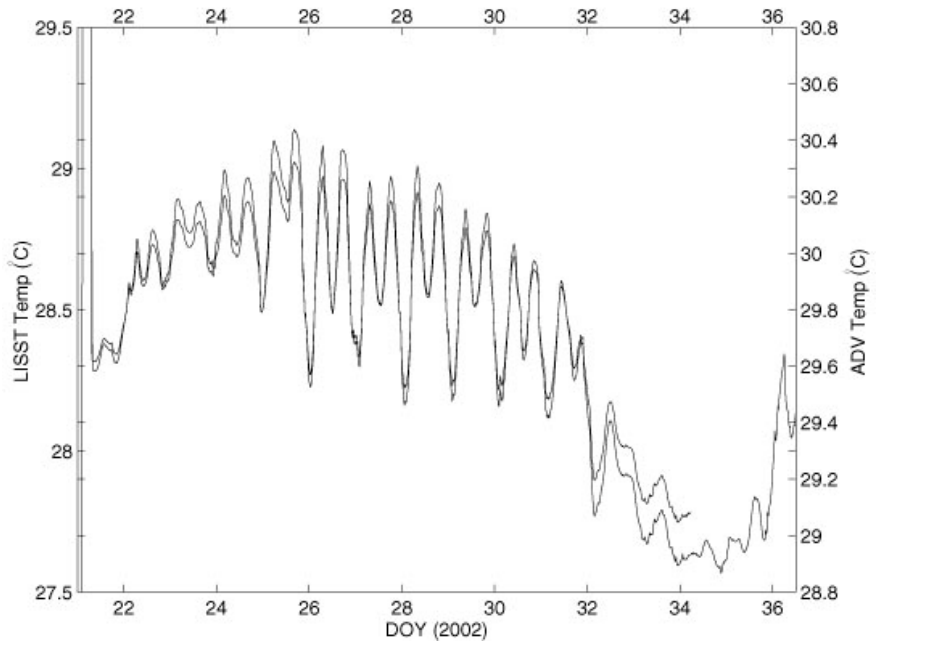

Figure 3.29*. Time series plot of bottom water temperature measured by the Nortek (upper line) and Seacat CTD installed on BRUCE.*

3.7.5 Suspended Material (Transmissivity/Turbidity)

The LISST transmissometer recorded transmissivity for the first period that the LISST was recording, from days 21-34. The memory of the LISST filled up and so data were not recorded over the full deployment period. The water is initially quite clear (Transmissivity 0.85). Transmissivity displays some small semi-diurnal variation (0.05) during the period of spring tides and exhibits a

gradual (downward) trend, decreasing to ~0.50 by the end of recording. This gradual downward trend in transmission is probably a real event, rather than an optical effect of biofouling, because this same gradual trend is exhibited by salinity and temperature time series (Figs 3.28, 3.29).

OBS measured turbidity is below noise levels for the majority of deployment. On day 35, after the LISST stopped recording, turbidity was great enough to be resolved (up to 60 ftu; Fig. 3.30). Semi-diurnal variability seems to be observed in the turbidity record, however only one day of record exists. The OBS record does confirm that the water column had more suspended material at the end of deployment than the start. The lack of overlap between OBS turbidity and LISST transmissivity means that no relationship between the two quantities could be developed (Fig. 3.30).

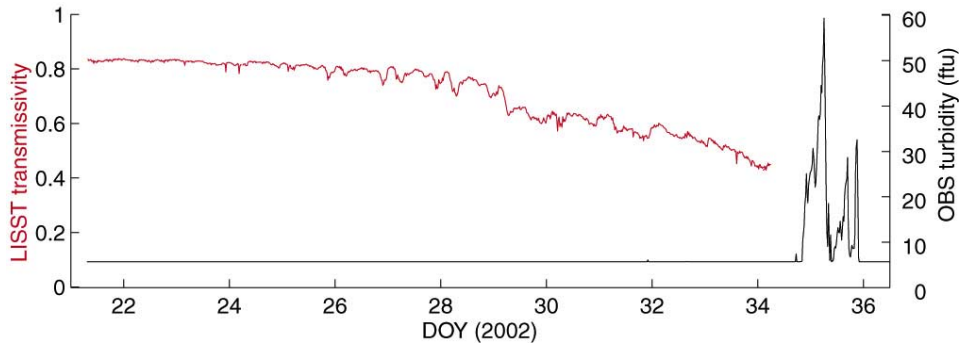

***Figure 3.30**. Time series plot of bottom water transmissivity and turbidity measured by the LISST-100 and OBS sensors installed on BRUCE.*

The product of suspended sediment concentration and current speed indicates that net suspended sediment transport was towards the west (~265°) during the deployment period. The mass flux rate estimated using the LISST (and an assumed grain density of 2.63 g cm^{-3}) was 3.3 x 10^{-2} g cm^{2} sec^{-1} towards 238° (at 30cm above bed). For the OBS sensor, the estimated flux rate was 3.8 x 10^{-3} g cm^{2} sec^{-1} towards 274° (at 100cm above bed).

An interesting question is the cause of the apparent increase in water turbidity over the deployment period (Fig. 3.30). If the bed sediment was resuspended as the result of tides, then a peak in turbidity would have been expected at around the time of springs, on days 28-32 (Fig. 3.25). Or if waves were the dominant process, then the time of maximum significant wave height (days 23-24; Fig 3.27) might be predicted to have been the time of peak turbidity. Instead, turbidity reaches a peak at the very end of the deployment on days 35-36 (Fig. 3.30), when neither tidal or wave energy are at their highest levels.

Some insight into a possible explanation for this paradox is provided by a plot of bed shear stress (T_b). Bed stress was estimated using the ADV data, as:

$T_b = -\rho \overline{u'w'}$

where ρ is water density, *w*' is the turbulent vertical velocity and *u*' is the horizontal streamwise velocity ($u_t - u_{mean}$). An interesting observation is that the estimated bottom stress (Fig. 3.31) reaches a peak on around day 31, just as turbidity levels are rising (Fig. 3.30) but is apparently unrelated to either peak tidal or wave energy (Figs. 3.25 and 3.27). Residual wind-driven flow, however, does appear to correspond to this time, as the progressive vector plot indicates a marked acceleration and change in direction after day 32 (Fig. 3.26). Wind-driven flow and its associated turbulence therefore appear to be key processes in remobilising bed sediments in the vicinity of the BRUCE deployment site.

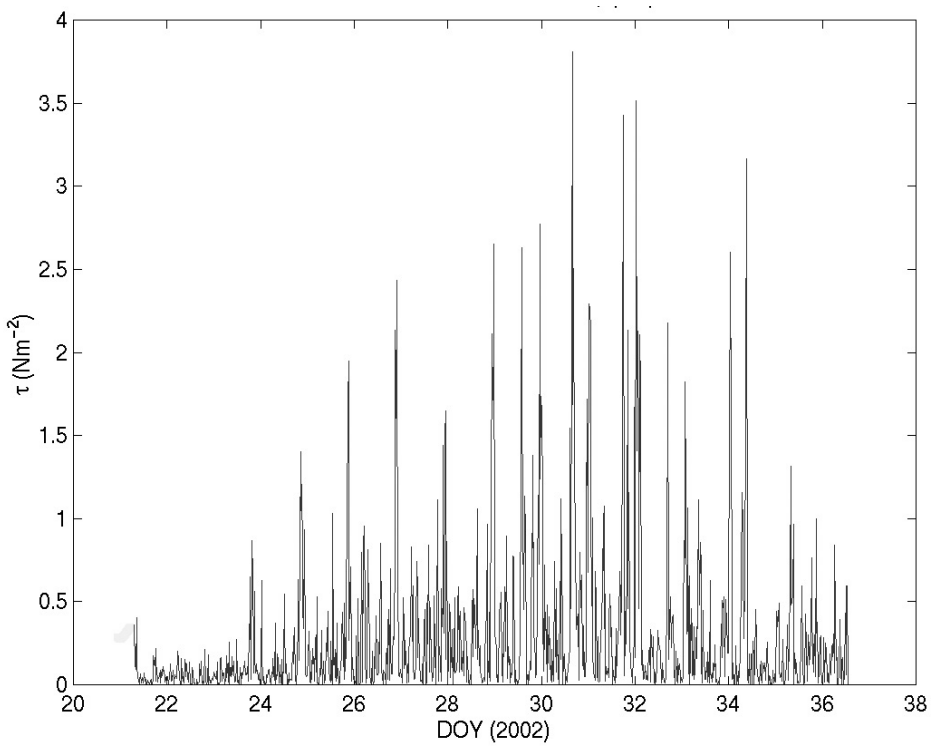

***Figure 3.31**. Time series of bed shear stress estimated using horizontal and vertical (turbulence) components of ADV data.*

3.7.6 Grain Size

The grain size distribution spectrum is noisy for the first 3 days of the record, associated with the low suspended sediment concentration (and thus the small number of reflectors in the water column) for making measurements (Fig. 3.32). Through days 26-29, low volume concentrations over all sizes are observed. Mean grain size is approximately 50µm. Mean grain size and volume concentration over all size bins is observed to increase after day 28, as spring tides begin and current speeds increase. A semi-diurnal tidal variation of mean grain size is evident (Fig. 3.32).

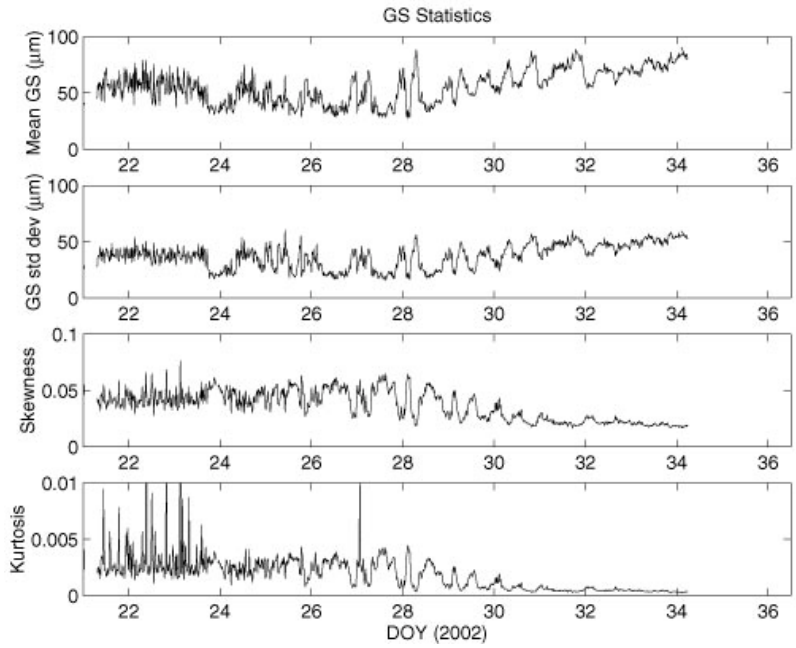

***Figure 3.32**. Time series plot of suspended sediment grain size statistics measured by the LISST.*

Separating the fine and coarse fractions at 63mm, the volume concentrations of the two size fractions suggest differing origins. Both fractions indicate increasing concentrations associated with decreasing transmissivity, salinity and temperature, and the south-westward current as observed by other sensors. However, the semi-diurnal tidal variability is more strongly apparent in the coarse fraction than the fine. Rising tides, with increased currents towards the W-SW are correlated with periods of decreased coarse fraction volume concentrations. Falling tides, with increased currents to the E-NE are correlated with periods of greater coarse fraction volume concentrations. Currents are generally greater on the rising tide.

3.7.7 Bedload Transport

Bedload transport rates are estimated for the period that the LISST was recording. The bedload transport time series plot indicates that the threshold speed of 30cms-1, corresponding to a 0.1mm mean grain size, was exceeded during the period of spring tides only. Bedload transport estimates for the period of deployment are 0.014 g/cm/s at a bearing of 260° (towards the west).

The BRUCE current meter mooring shows a semi-diurnal tide dominated system. Bedload transport of sediments occurs only during the period of maximum tides, and always towards the south-west (on a rising tide). A minor wind-driven effect is observed during the period of deployment. North-westerly monsoon winds appear to push cooler, fresher water of increased suspended sediment load, presumable from the Fly River Delta, toward and past the BRUCE deployment site. Cooler fresher waters are observed during periods of increased NW winds, south-westwards currents, and increased turbidity/decreased transmissivity. Counteracting this effect however, falling tidal currents directed to the NE appear to transport increased loads of coarser sediments past the probe.

Chapter 4. Discussion

The results of Geoscience Australia Cruise 234 have provided new insights into the character of the seafloor in three distinctly different areas at the northern limit of the Great Barrier Reef. It is beyond the scope of this report to provide a detailed synthesis of this information here. However, a few of the most obvious highlights that are worthy of special mention will be briefly discussed. These selected topics are the nature of reefs and associated fauna occurring in the areas; the age and character of sediments in relation to regional transport patterns; the formation of shelf valley systems and the role these have played in the evolution of the region; and cross-shelf sediment transport.

4.1 DEVELOPMENT AND NATURE OF REEFS

The rocky reefs found in Areas A and B are dominated by soft faunas. True coral reefs are limited in distribution and extent and largely restricted to Area C. Reefs in Areas A and B are typically established on areas with increased elevation. At several sites, reef bases consist of older coral reef as evidenced by the presence of karst-style erosion, caves (seen in video images), and the presence of reworked limestone in grab samples. Several of the sites targeting rock outcrop in Area A contained limestone in grab samples, as did reef targets in Area B. This abundance of coral-dominated limestone suggests that the development of coral reefs was far more extensive in the past in both areas. This, in turn, suggests that mud supplied from the Fly River at such times was deposited elsewhere or was eroded and dispersed after the post-glacial sea level rise.

The coral reefs of Area C contain a mix of faunas, particularly in deeper fringing areas, for example at site 234/65. Again there is evidence of some reefs being established on a base of older limestone. Several other reef-like accumulations, located in deeper waters, are dominated by other biota, such as the *Halimeda* bioherm to the north-east (site 234/59) and the sponge-encrusted boundstones at site 234/58.

Another common feature of the reefal mounds in all 3 areas is that they occur in association with erosional valleys, either infilled with sediment (common to Area A) or exhumed (common to Areas B and C). This relationship is most clearly seen in the Chirp seismic data (Section 3.2) and it is also evident in some of the 3D bathymetric imagery recently generated using the swath information collected on the cruise (see below).

4.2 AGE OF THE SEDIMENTS AND TRANSPORT PATTERNS

Relict material forms an important component of sediments in all three areas, suggesting that erosion of older deposits and reworking of sediments are occurring. Sedimentation rates are not high, even in Area A (adjacent to the Fly River Delta). Evidence of slow deposition rates and sediment reworking is provided by the abundance of semi-lithified mud clasts in Areas A and B. Slow rates of modern sediment accumulation in Area A are illustrated by core logs from the area (Fig. 4.1). The thickest Holocene carbonate unit in Area A is ~2.5m, observed in core 23PC7. At most other stations this unit is <1m thick and it is as thin as ~50cm in some locations (Fig. 4.1). These results suggest that the presence of Fly River Delta muds in Area A is related (at least partly) to the erosion and reworking of older deposits. In any event, the deposition of Fly River terrigenous mud in Area A is very limited at the present time.

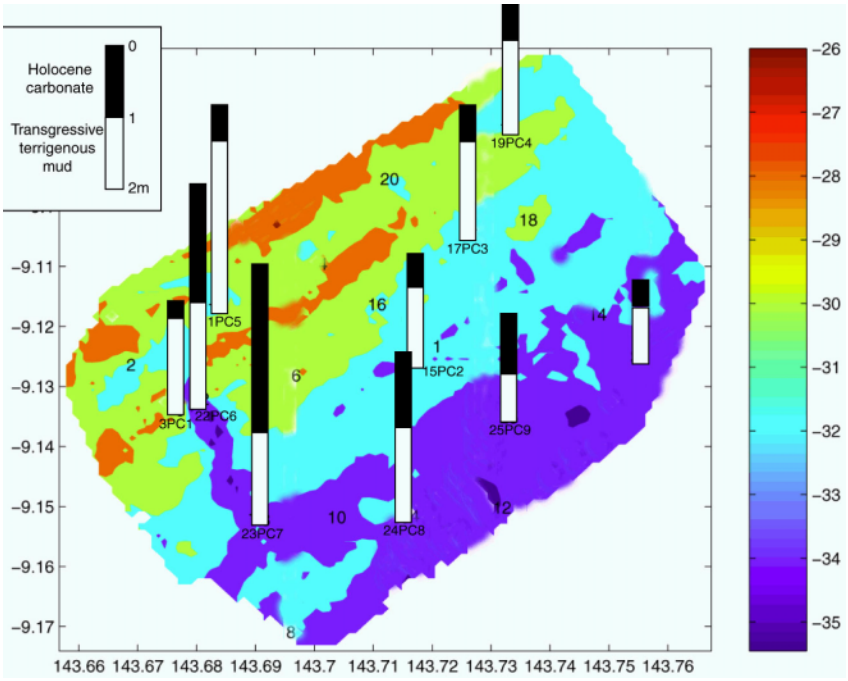

***Figure 4.1**. Bathymetry map showing core lengths collected at stations in Area A. The carbonate Holocene unit is up to 2.5m thick in core 23PC7 but is less than 50cm thick in many other locations.*

Most of the relict material in all three areas appears to be locally derived, since the taxa present are similar to those present in younger material. Obviously reworked limestones are present in a number of sites in all three areas. This material appears to be eroded from older horizons in local deposits.

Transport paths for some of the relict sediment appear to be short judging from the presence of angular surfaces. In several sites older reef could be clearly seen in videos. At some sites outcrop of strong reflectors could be traced on seismic sections. However, the abundance of lithic grains, primarily in the sand fraction in samples from Area C, may be related to earlier periods of transport through the channels. This is consistent with the highly polished and rounded nature of the grains. Their pattern of distribution, as shown by the map of % carbonate (Fig. 3.20), suggests a possible source to the north-west, although the distribution is not continuous. A number of high-carbonate samples in this area contain lithic grains but their abundance is diluted by biogenic carbonate. It is possible that the original distribution has been overwritten by the deposition of more modern material.

Because of the dominance of soft faunas over hard corals and a strong infaunal contribution, the appearance of most of the sediments is more typical of cool-water carbonate sediments than tropical. While the species present are probably tropical in distribution, the main groups contributing to the sediments and their relative abundances are similar to samples from Australia's southern margins (Jones and Davies, 1983; Boreen et al., 1993). Similar trends have been observed in samples from Joseph Bonaparte Gulf, where the mud content of samples is also high (Clarke et al., 2001).

4.3 ORIGIN OF SHELF VALLEYS

The most striking geomorphic feature of Areas B and C are the submarine valley systems which traverse these areas. The bathymetry maps depict at least 2 systems of submarine valleys that extend for more than 80km from eastern Torres Strait across the northern end of the Great Barrier Reef (Figs. 4.2, 4.3).

Furthermore, based on the available information, the evolution of the valley systems appears to have involved two independent processes; fluvial erosion and tidal scour.

Submarine valleys in the north are clearly relict fluvial channels, exhibiting lateral accretion surfaces and incised channels that intersect and truncate underlying strata. The floors of these channels are mostly <100m water depth, hence they were above sea level during the last glaciation when eustatic sea level was ~120m below its present position.

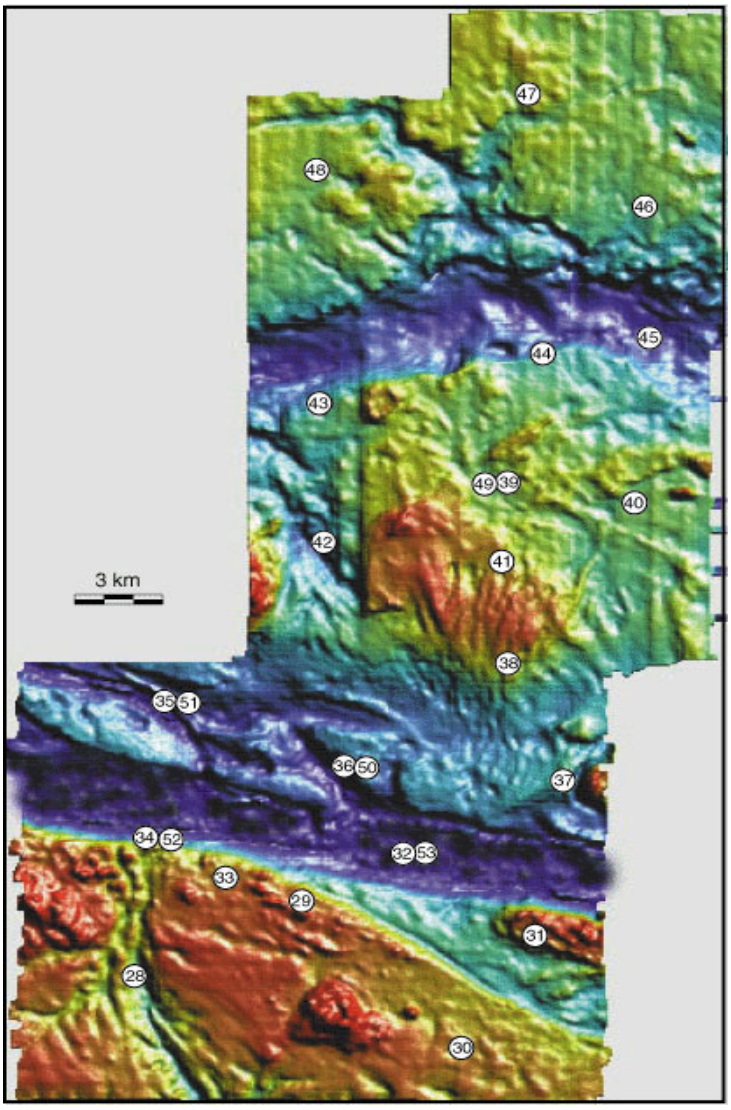

***Figure 4.2**. Colour-shaded bathymetry map of Area B, showing the location of stations in relation to two submarine valley systems which transect the area. The northern valley floor is relatively flat and lies in <100m water depth. The southernmost valley, however, is locally >130m in depth.*

Over-deepened channels in the south, however, appear to have formed by tidal current scour. They exhibit closed bathymetric contours (Fig. 4.3) and are floored with well-sorted carbonate gravely sand (Table 3.4, Stations 72 and 75). The occurrence of strong near-bed currents is also indicated by the occurrence of sandwaves in the eastern part of Area C (vicinity of Station 61; Fig. 4.3).

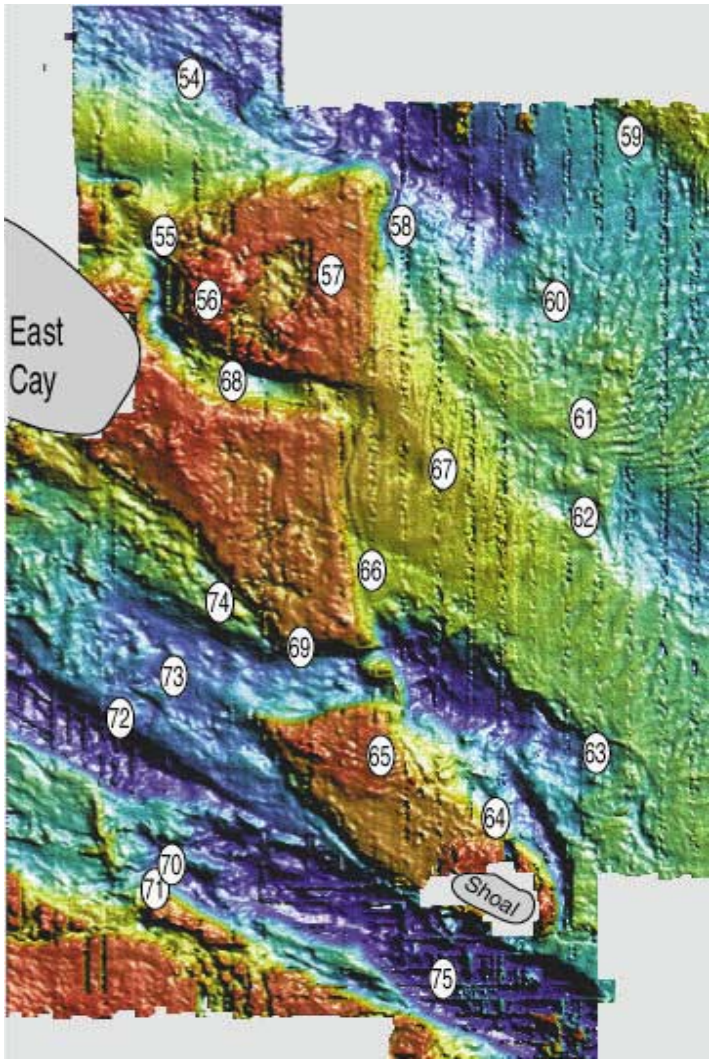

Figure 4.3. *Colour-shaded bathymetry map of Area C, showing the location of stations in relation to submarine valley systems which transect the area. The southernmost valleys exhibit closed contours (localised depressions) and are >220m in depth in the vicinity of Station 75.*

The deepest channels form isolated depressions, and possibly were the sites of lakes during the last ice age, when Torres Strait formed a land-bridge between Australia and Papua New Guinea. However, there is no indication of former lake deposits or of any thick, unconsolidated sediment deposits in the channel bottoms in the Chirp seismic records, and no lacustrine sediments were encountered in our cores. The conclusion is that either these depressions were simply subaerially exposed during the glacial maximum, or that the channels have been exhumed of any fluvial or lacustrine deposits by current erosion following post-glacial sea level rise (and flooding of the shelf).

Oceanographic observations indicate that the channels provide a conduit onto the shelf for cool and saline (and nutrient-rich?) upwelled Coral Sea water (Section 3.3). The CTD profiles taken in Area C during the waning spring tide phase, suggest that the water column is stratified above 50m depth (Fig. 3.14). Also, recent tidal and wind-driven current modelling work carried out for the region by Hemer et al. (in press) suggest that currents in Area C are relatively sluggish. It appears, therefore, that the modern

current regime could not have created the deep shelf valleys that are found in Area C. The question is, when were the valleys formed?

To answer this question, we have carried out a simple tidal modelling exercise. The tidal model used is the one developed for the GEOMAT sediment mobility project and is documented by Harris et al. (2000). The model was run using a fixed bathymetric model for 8 different sea levels at 10m increments below present sea level. The results (Fig. 4.4) indicate that tidal bottom current stress reached a maximum value over the site of the deepest shelf valleys when sea level was ~40m below its present position. This depth is also common to the submerged reef platforms seen in Areas B and C, suggesting that these relict reefs developed at times when sea level was at about 40m below its present position.

We conclude that the over-deepened shelf valleys in Areas B and C are relict features, whose origin is related to periods when sea level was ~40-50m below its present position. The eustatic sea level curve (eg Chappell and Shackleton, 1986) indicates that over the past 150,000 years, sea level has been between 40-50m below its present position for about 36% of the time (Fig. 4.5). Prolonged periods (>10,000 years duration) of sea level within this depth range occurred during isotope stages 3, 4, 5a and 5c (Fig. 4.5). These are most likely to be the times during which the deepest shelf valleys were formed.

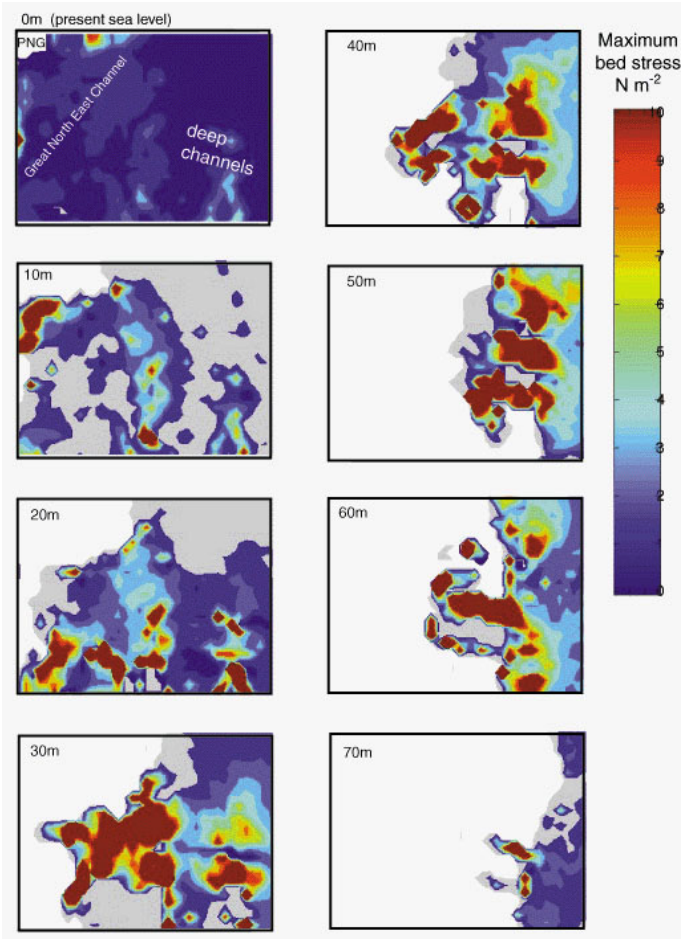

***Figure 4.4**. Results of tidal modelling under 8 different sea level scenarios. Land is shown as white areas. The bottom stress was calculated as the depth-averaged speed times a drag coefficient of 3 x 10^{-3} (eg. Pingree and Griffiths, 1979). Note the maximum bottom stress occurs over the deep shelf valleys when sea level is ~40-50m below present.*

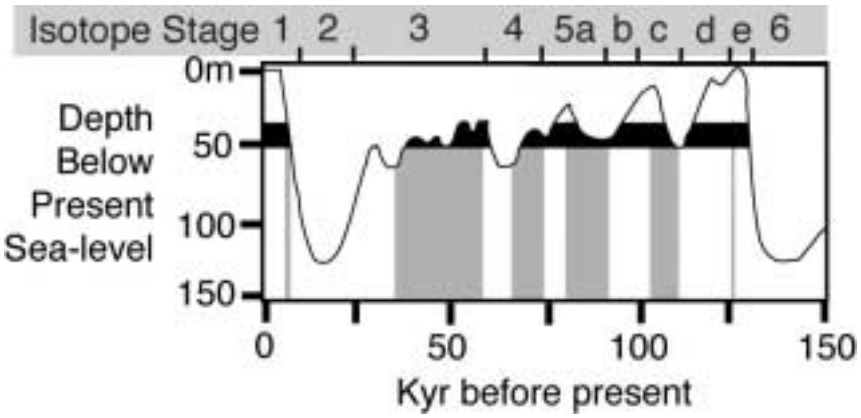

***Figure 4.5**. Sea level curve for the past 150 kyr from Chappell and Shackleton (1986). Gray shading illustrates time periods when sea level has ranged between 40-50m below its present position (highlighted in black). Oxygen isotope stages are after Martinson et al. (1987).*

4.4 CROSS-SHELF SEDIMENT TRANSPORT

An aim of this project was to attempt to find out whether modern oceanographic processes are transporting calcareous and terrigenous sediments from NE Torres Strait to the outer shelf of the Gulf of Papua. Based on the results of this study, we conclude that they are not. Terrigenous sediment supplied by the Fly River is not accumulating in Area A and the only terrigenous sediments found in Areas B and C are interpreted to be relict deposits. Modern surficial sediments in all areas are dominated by coarse-grained, autochthonous biogenic carbonate.

As noted above, oceanographic observations indicate that the deep shelf valleys provide a conduit onto the shelf for cool and saline upwelled Coral Sea water (Section 3.3; Fig. 4.6). However, the bottom waters in the channels are exceptionally clear, with generally >90% light transmission (Fig. 3.14). The stations located in the deep valleys also exhibited very clear bottom waters. Hence the evidence suggests that the shelf valleys are not conduits for fluid muds or terrigenous sediment transport across the shelf.

An interesting result from the BRUCE instrument deployment is that wind events seem to give rise to elevated turbidity and suspended sediment transport on the shelf adjacent to the Fly Delta front (i.e. Area A). This is the first instrument deployment of its kind in the Fly delta region and is also the first observation of a direct sediment transport path linking the Fly River Delta with the Torres Strait. Harris et al. (in press) discussed the processes that control the export of fluid muds with concentrations up to 10 g/l from the distributary channels across the delta front and onto the pro-delta. They described a one-month time series of suspended sediment concentration and current velocity data from the delta front and showed that tidal currents alone are unable to cause significant cross-delta mud transport. They suggest that wave-induced resuspension together with tides, storm surge and barotropic return-flow may play a role in maintaining the transport of fine sediment across the delta front. The data collected by BRUCE (Section 3.7) seems to support his latter suggestion.

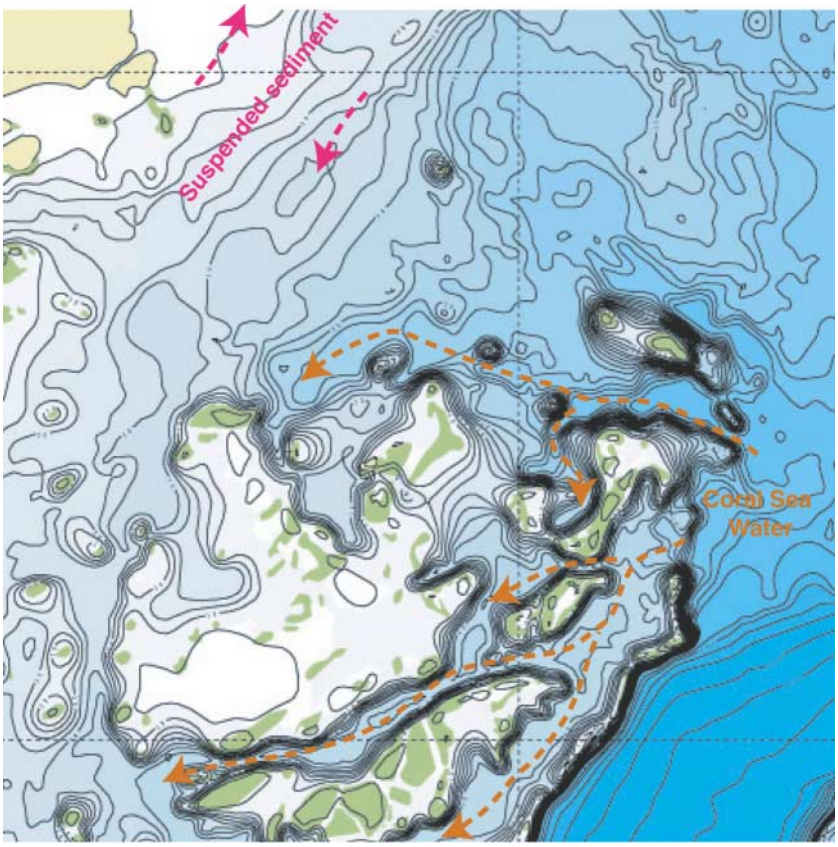

Figure 4.6. *Sketch map showing the interpreted sediment transport pathways in the Fly Delta region and inferred intrusion of Coral Sea water onto the shelf via the deep shelf valleys.*

However, the transport path for sediment exported from the delta front and onto the shelf is not eastwards (offshore) in Area A, but rather it is towards the southwest (towards the Great North East Channel and Torres Strait; see Section 3.7.5). This observation, taken together with the available data for the delta front (Harris et al., in press), suggests that sediment may recirculate between the delta front and distal delta environments (Fig. 4.6). A north-eastward flux of sediment on the delta front gives way to a south-westward flux on the shelf, thus trapping sediment within the prodelta depocentre. Such a recirculation pattern (if true) could have significance for Gulf of Papua-derived sediment input to the northern Great Barrier Reef and Torres Strait regions. However, the transport patterns do not support the concept of cross-shelf transport via the shelf valleys adjacent to the northern margin of the Great Barrier Reef as was postulated in the cruise proposal (Chapter 1).

Acknowledgments

Thanks to the National Facility Steering Committee for making the ship time available and to Geoscience Australia for logistical and financial support. Technical support for the voyage was provided by Eric Madsen and Bernie Heaney (CSIRO), Jon Stratton and Lyndon O'Grady (Geoscience Australia) and Kevin Hooper (James Cook University). Digital conversion of video tape footage was carried out by Kathy Ambrose of the Geospatial Applications and Visualisation Group, Geoscience Australia. Digital copies of the core X-radiographs were made by Brett Ellis, of the Geospatial Applications and Visualisation Group, Geoscience Australia. Preparation of samples was carried out by Alex McLachlan and Neil Ramsay of the Sedimentology Laboratory, Geoscience Australia. Neil Ramsay, Alex McLachlan and Tony Watson compiled the Standard Operating Procedures given as Appendix E. Thanks to Richard Brown and Tony Watson for facilitating processing of the samples by the Laboratory. We would like to offer our special thanks to Captain Ian Sinclair, the officers and crew of the RV *Franklin*. The *Franklin* was sold in 2002, making ours the last voyage undertaken by the ship in Australian waters as the CSIRO National Facility Research Vessel. This report benefited from the critical reviews of Neville and Leanne Armand. Published with the permission of the Executive Director, Geoscience Australia.

References

Baker, E. K., Harris, P. T., Short, S. A., and Keene, J. B. (1995). Patterns of sedimentation in the Fly River Delta. In: B. W. Flemming and A. Bartholoma (Eds.), Tidal signatures in modern and ancient sediments Oxford, Blackwell, pp. 193-211.

Best, A.I. and Gunn, D.E., 1999. Calibration of marine sediment core loggers for quantitative acoustic impedance studies. Marine Geology, 160, 137-146.

Boreen. T., James, N., Wilson, C. and Heggie, D. (1993). Surficial cool-water carbonate sediments on the Otway continental margin, southeastern Australia. Marine Geology 112, 35-56.

Brunskill, G. J., Woolfe, K. J., and Zagorskis, I. (1995). Distribution of riverine sediments on the shelf, slope and rise of the Gulf of Papua, Papua New Guinea. Geo-Marine Letters, 15(3-4), 160-165.

Brunskill, G. J., Nittrouer, C. A., Sternberg, R. W., Aller, A. C., and Milliman, J. D. (2000). RV Franklin Cruise Summary, FR02/00: Tropical River Ocean Processes in Coastal Settings (TROPICS Leg 10) - Biogeochemistry, Benthos, and Sedimentation in the Gulf of Papua Australian Institute of Marine Science, 9 pp.

Chappell, J., and Shackleton, N. J. (1986). Oxygen isotopes and sea level. Nature, 324, 137-140.

Clark, F.E., Patterson, T.R., and Fishbein, E. (1994). Distribution of Holocene Benthic Foraminifera from the Tropical Southwest Pacific Ocean. Journal of Foraminiferal Research, 24(4), 241-267.

Clarke, J.D.A., Bone, Y., Cann, J.H., Davies, M., Macphail, M.K. and Wells, F. (2001). Post-glacial biota from the inner part of southwest Joseph Bonaparte Gulf. Australian Journal of Earth Sciences. 48(1), 63-79.

Cole, A. (1995). The Surficial Sediments and Foraminiferal Taphonomy of Torres Strait. MSc. Thesis, University of Sydney, Sydney, 218pp.

Cole, A., Harris, P.T. and Keene, J.B. (1995). Foraminifers as Facies Indicators in a Tropical, Macrotidal Environment: Torres Strait – Fly River Delta, Papua New Guinea. Special Publication of the International Association of Sedimentologists, 24, 213-223.

Dalrymple, R. W., Baker, E. K., Harris, P. T., and Hughes, M. G. (2002). Sedimentology and stratigraphy of a tide-dominated, foreland-basin delta (Fly River, Papua New Guinea). In F. H. Sidi, H. W. Posamentier, H. Darman, D. Nummedal, and P. Imbert (Eds.), Deltas of Southeast Asia and Vicinity - Sedimentology, Stratigraphy, and Petroleum Geology SEPM Special Publication,

Dennison, J.M. and Hay, W.H. (1967). Estimating the Needed Sampling Area for Sub-Aquatic Ecologic Studies. Journal of Paleontology, 41, 706-708.

Dight, I. J., and Gladstone, W. (1993). Torres Strait baseline study: Pilot study and final report. (Research Publication No. 29). Great Barrier Reef Marine Park Authority, 259 pp.

Dunbar, G.B., Dickens, G.R., and Carter, R.M. (2000). Sediment flux across the Great Barrier Reef Shelf to the Queensland Trough over the last 300 ky. Sedimentary Geology, 133, 49-92.

Ellis, B.F. and Messina, A. (1940 *et seq*.). Catalogue of Foraminifera. American Museum of Natural History, New York.

Gagan, M. K., Chivas, A. R., and Herczeg, A. L. (1990). Shelf wide erosion, deposition and suspended sediment transport during cyclone Winifred, central Great Barrier Reef, Australia. Journal of Sedimentary Petrology, 60(3), 456-470.

Gerland, S. and Villinger, H. (1995). Non-destructive density determination on marine sediment cores from gamma-ray attenuation measurements. Geo-Marine Letters, 15, 111-118.

Glenn-Sullivan, E. and Evans, I. (2001). The Effects of Time-Averaging and Taphonomy on the Identification of Reefal Sub-Environments Using Larger Foraminifera: Apo Reef, Mindoro, Philippines. Palaios, 16(4), 399-408.

Haig, D.W. (1988). Miliolid Foraminifera from Inner Neritic Sand and Mud Facies of the Papuan Lagoon, New Guinea. Journal of Foraminiferal Research, 18(3), 203-236.

Haig, D.W. (1993). Buliminid Foraminifera from Inner Neritic Sand and Mud Facies of the Papuan Lagoon, New Guinea. Journal of Foraminiferal Research, 23(3), 162-179.

Haig, D.W. and Burgin, S. (1982). Brackish Water Foraminiferids from Purari River Delta, Papua New Guinea. Revista Espanola De Micropaleontologia, 14, 359-366.

Hardisty, J. (1983). An assessment and calibration of formulations for Bagnold's bedload equation. Journal of Sedimentary Petrology. 53(3), 1007-1010.

Harris, P. T. (1988). Sediments, bedforms and bedload transport pathways on the continental shelf adjacent to Torres Strait, Australia - Papua New Guinea. Continental Shelf Research, 8, 979-1003.

Harris, P.T., Davies, P.J., and Marshall, J.F. (1990). Late Quaternary sedimentation on the GBR continental shelf and slope of Townsville, Australia. Marine Geology, 94, 55-77

Harris, P.T. (1993). Near-Bed Current Measurements from Torres Strait Obtained During January-March 1993 Aboard R.V. Southern Surveyor. Ocean Sciences Institute. Technical Report No. 29. University of Sydney. 68p.

Harris, P. T. (1995). Muddy waters: the physical sedimentology of Torres Strait. In O. Bellwood, H. Choat, and N. Saxena (Eds.), Recent Advances in Marine Science and Technology '94 Townsville, Qld., James Cook University of North Queensland, pp. 149-160.

Harris, P. T. (2001). Environmental Management of Torres Strait: a Marine Geologist's Perspective. In V. A. Gostin (Ed.), Gondwana to Greenhouse: environmental geoscience - an Australian perspective Adelaide, Geological Society of Australia, Special Publication 21, pp. 317-328.

Harris, P. T., Hughes, M. G., Baker, E. K., Dalrymple, R. W., and Keene, J. B. (in press). Sediment transport in distributary channels and its export to the pro-deltaic environment in a tidally-dominated delta: Fly River, Papua New Guinea. Continental Shelf Research.

Harris, P. T., Pattiaratchi, C. B., Keene, J. B., Dalrymple, R. W., Gardner, J. V., Baker, E. K., Cole, A. R., Mitchell, D., Gibbs, P., and Schroeder, W. W. (1996). Late Quaternary deltaic and carbonate sedimentation in the Gulf of Papua foreland basin: Response to sea-level change. Journal of Sedimentary Research, 66(4), 801-819.

Harris, P. T., Smith, R., Anderson, O., Coleman, R., and Greenslade, D. (2000). GEOMAT - Modelling of Continental Shelf Sediment Mobility in Support of Australia's Regional Marine Planning Process (Record No. 2000/41). Australian Geological Survey Organisation, pp.

Heap, A.D., Dickens, G.R., and Steward, L.K. (2001). Late Holocene sediment in Nara Inlet, central Great Barrier Reef platform, Australia: sediment accumulation on the middle shelf of a tropical mixed clastic/carbonate system. Marine Geology, 176, 39-54.

Hemer, M.A., Harris, P.T., Coleman, R., Hunter, J. (in press) Sediment Mobility due to currents and waves in the Torres Strait - Gulf of Papua region, Continental Shelf Research

Hayward, B.W., Hollis, C.J. and Grenfell, H.R. (1997). Recent Elphidiidae (Foraminifera) of the South-West Pacific and Fossil Elphidiidae of New Zealand. Institute of Geological and Nuclear Sciences Monograph, 16, 170pp.

Hohenegger, J. (1995). Depth Estimation by Proportions of Living Larger Foraminifera. Marine Micropaleontology, 26, 31-47.

Hohenegger, J., Yordanova, E., Nakano, Y. and Tatzreiter, F. (1999). Habitats of Larger Foraminifera on the Upper Reef Slope of Sesoko Island, Okinawa, Japan. Marine Micropaleontology, 36, 109-168.

Hohenegger, J., Yordanova, E. and Hatta, A. (2000). Remarks on West Pacific Nummulitidae (Foraminifera). Journal of Foraminiferal Research, 30(1), 3-28.

Hottinger, L., Halicz, E. and Reiss, Z. (1993). Recent Foraminiferida from the Gulf of Aqaba, Red Sea. Ljubljana, Slovenia, 179 pp.

Jones, H.A. and Davies, P.J. (1983). Superficial sediments of the Tasmanian continental shelf and part of Bass Strait. Bureau of Mineral Resources, Geology and Geophysics Bulletin 218. 25pp.

Lipps, J.H. and Severin, K.P. (1986). *Alveolinella quoyi*, a Living Fusiliform Foraminifera at Motupore Island, Papua New Guinea. Science in New Guinea, 11, 126-137.

Loeblich, A.R. and Tappan, H. (1988). Foraminifera Genera and Their Classification. Van Norstrand Reinhold Company, New York, 970 pp.

Loeblich, A.R. and Tappan, H. (1994). Foraminifera of the Sahul Shelf and Timor Sea. In: A.R. Loeblich and H. Tappan (Editors), Special Publication. Cushman Foundation for Foraminiferal Research, Cambridge. London, 565 pp.

Martinson, D. G., Pisias, N. G., Hays, J. D., Imbrie, J., Moore, T. C. Jr., and Shackleton, N. J. (1987). Age dating and the orbital theory of ice ages: development of a high-resolution 0 to 300,000 years chronostratigraphy, Quaternary Research, 27, 1-29.

Maxwell, W.G.H. (1968). Atlas of the Great Barrier Reef. Elsevier, NY. 258pp.

Muller, G., and Gastner, M. (1971). The "karbonate bombe" a simple device for the determination of the carbonate content in sediments, soils and other materials. Neus Fahrb. Mineral. Monatsh., 10, 466-469.

Murray., J.W. (1991). Ecology and Palaeoecology of Benthic Foraminifera. Longman Science and Technical, Essex. 397pp.

Nittrouer, C. A., and Wright, L. D. (1994). Transport of particles across continental shelves. Reviews of Geophysics, 32(1), 85-113.

Orpin, A.R., and Woolfe, K.J. (1999). Unmixing relationships as a method of deriving a semi-quantitative terrigenous sediment budget, central Great Barrier Reef lagoon, Australia. Sedimentary Geology, 129, 25-35.

Pingree, R. D., and Griffiths, D. K. (1979). Sand transport paths around the British Isles resulting from M2 and M4 tidal interactions. J. Mar. Bio. Assoc. U. K., 59, 497-513.

Renema, W. and Troelstra, S.R. (2001). Larger Foraminifera Distribution on a Mesotrophic Carbonate Shelf in SW Sulawesi. Palaeogeography, Palaeoclimatology, Palaeoecology, 175, 125-146.

Robinson, S.G. (1990). Applications for whole-core magnetic susceptibility measurements of deep-sea sediments: Leg 115 Results. In: Duncan, R.A., Backman, J., Peterson, L.C., et al. (Eds.), ODP. Scientific Results, 115. Ocean Drilling Program, College Station, pp. 737-771.

Semenuik, T.A. (2001). Epiphytic Foraminifera along a Climatic Gradient, Western Australia. Journal of Foraminiferal Research, 31(3), 191-200.

Stride, A. H. (Ed.). (1982). Offshore Tidal sands - Processes and Deposits. London: Chapman and Hall, 222 pp.

Walker, S. J. and Waring, J. R. (1998). MECO Model for Estuaries and Coastal Oceans. Internal report no.omr-118/120, CSIRO Marine Research.

Weber, M.E., Niessen, F., Kuhn, G., and Wiedicke, M. (1997). Calibration and application of marine sedimentary physical properties using a multi-sensor core logger. Marine Geology, 136, 151-172.

Appendix A. Cruise Narrative

RV *Franklin* Cruise 01/-02
Geoscience Australia Cruise 234
Fly River Delta, Torres Strait and Gulf of Papua, Jan-Feb., 2002

Thursday 17-01-02 The RV *Franklin* sailed from Cairnscross Shipyard, Brisbane, @ 1000 hrs local time. Pilot dropped at Caloundra @ 1500 hrs and ship headed north with a brisk following (southerly) breeze.

Friday 18-01-02 Transit

Saturday 19-01-02 The 2nd cook has injured his finger. We must detour to Cairns to take him for treatment.

Sunday 20-01-02 Anchored offshore Cairns @1100 hrs on while 2nd Cook was taken to hospital for treatment. Underway again by 1300 hrs.

Monday 21-01-02 Transit

Tuesday 22-01-02 Arrived in Torres Strait and commenced work at station 1 @1500 hrs. Deployment of CTD, bottom video camera and grab sample were successful and the current meter frame was launched @1720 hrs. The probe has been named BRUCE (for Benthic Research Underwater sediment Concentration Experiment). After two sound velocity profiles were completed we commenced the swath survey @ 1900 hrs.

Wednesday, 23-01-02 By 1200 hrs we had completed 13 10km survey lines. The sea conditions were excellent, quiet and calm, and the Seabat system was operating at its optimum swath width (7 times water depth). Thus we decided to increase the line spacing from 100 to 125 m. This should save us a few hours of survey time.

Thursday, 24-0-02 Continue swath survey of Area "A".

Friday, 25-01-02 Swath survey for Area "A" completed @1630 hrs. Proceeded to conduct a "Patch Test" (swath system calibration) before start of sampling @1900 hrs. Sea conditions remain calm.

Saturday, 26-01-02 After completion of 3 stations including one piston core, an incident occurred @0015hrs when the piston core appeared to slide down the wire mid-way through deployment and come to jolting stop. Inspection of the damaged piston-core, trigger-arm assembly indicated the clamp had failed, although suspected that the winch may have spontaneously paid out wire. Coring was therefore postponed until daylight.

Sunday, 27-01-02 Completed all cores and stations in Area "A" @ 0145 hrs. Transit to Area "B", arriving @0730 hrs. Delay to start of survey @ 1300 hrs caused by failure of air conditioning system and attendant shut-down of all computing systems.

Monday, 28-01-02 Continue surveying Area "B"

Tuesday, 29-01-02 Continue surveying Area "B"

Wednesday, 30-01-02 Complete survey of Area "B" @ 1900 hrs and commenced sampling. After one successful gravity core was collected, the winch again spontaneously paid out wire with the gravity corer hanging just outside of the deployment cradle at the third station @2345 hrs. Coring work postponed until the winch can be made safe.

Thursday, 31-01-02 CTD, camera and grab operations continued at the remaining stations. Ship's engineers and crew declared that the winch may be used again for gravity coring, but not piston coring, operations began @1100 hrs. Sea conditions calm to moderate, with morning nor-westerly winds up to about 15 knots.

Friday, 1-02-02 Final gravity cores collected and station work in Area "B" completed @0430. Transit from Area "B" to Area "C" arriving @ 0900 and commenced swath survey.

Saturday, 2-02-02 Swath survey of Area "C"

Sunday, 3-02-02 Swath survey of Area "C" Strong to moderate nor westerly wind and moderate seas. Chirp tow fish hitting side of ship in larger waves caused the loss of seismic data on about 3 lines.

Monday, 4-02-02 Complete swath survey of Area "C" and commence station work. Sampling sites chosen on the basis of the swath data recorded.

Tuesday, 5-02-02 Station work completed @1900 hrs and swath surveys of selected targets commenced. A deeply scoured channel up to 220 m in depth has been discovered on the outer shelf, in an area marked as shoal on the AUS chart.

Wednesday, 6-02-02 Swath survey and final station work completed @ 1700 hrs and transit to Area "A". Final underwater video and CTD stations completed and current meter mooring BRUCE successfully recovered @2200 hrs. This marks the end of the scientific work for the cruise. Depart Torres Strait headed for Cairns.

Thursday, 7-02-02 Transit to Cairns. Scientific party packing up equipment, completing data entry work and down-loading of moored instrument (current meter) data.

Friday, 8-02-02 Transit to Cairns.

Saturday, 9-02-02 Divers inspect hull at Fitzroy Island, 0600 to 0800 hrs. Arrive Cairns @ 1100 hrs. So ends the final voyage of the RV *Franklin* in Australian waters. After two further voyages this year in international waters, she will have all marine scientific equipment removed and be sold. After almost two decades of service, her departure concludes a chapter in Australian marine science research.

Peter T. Harris
Cruise Leader

Appendix B. Seismic Data

See attached CD-ROM 1.

Files contained in Appendix B are screen dumps obtained from the program Discofocus. These have been saved as tiff files. The filenames follow a number of naming conventions. The beginning of the filename indicates the survey area names [e.g., Area_A1, Area_B_c, Area_C]. Numbers thereafter indicate line offsets or the spacing in meters between the lines [e.g., Area_A1_1000a.tiff, Line_B_1000a.tiff, Area_C_1200a.tiff]). Letters at the end of file names indicate segments of the lines, cut for ease of viewing [e.g., Area_A1_1000a.tiff, Area_A1_1000b.tiff]. Some lines have been named with the word "line" in the name, either at the start or middle of the file name. Some lines have the line orientation included in the name [e.g., line_B_NS_1000a.tiff (north/south) or line_B_EW_Ta_Tba.tiff (east/west)]. T, TL or TR indicates a Transit line [e.g., Area_A1_T1-2a.tiff or CTR_1a.tiff]. Where appropriate, some lines have features in the area listed in the name [e.g., Lake_1.tiff (lake) or SEV_1.tiff (south east valley)].

Appendix C. CTD Data

See Attached CD-ROM 1.

This appendix contains the corrected CTD data stored in Excel format. The filename format is fr0201XXXXcol.xls. The “fr” indicates the data was collected by the R. V. Franklin, “02” is the year the survey took place (i.e., 2002), "01" indicates it was the first survey the ship completed that year, and “19001col” is a sequential file number designated by CSIRO - marine laboratories.

There are 6 lines of header information in the files, including time, latitude, longitude, and water depth. The CTD data includes fields recording corrected depth (m) pressure (decibars), temperature (degrees celicus), salinity (ppt), transmission (%). fluorescence (%), gravity effect and depth correction factors.

Appendix D. Filter Paper Weights

STATION NO	OPERATION	SAMPLE NO	BOTTOM WEIGHT /2L (G)	TOP /2L (G)
1	CTD	1	0.0027	
2	CTD	2	0.0026	0.0016
3	CTD	3	0.0033	
4	CTD	4	0.0005	0.0005
5	CTD	5	0.0030	0.0008
6	CTD	6	0.0035	0.0018
7	CTD	7	0.0022	0.0017
8	CTD	8	0.0014	0.0005
9	CTD	9	0.0021	0.0007
10	CTD	10	0.0017	0.0002
11	CTD	11	0.0036	0.0016
12	CTD	12	0.0031	0.0004
13	CTD	13	0.0030	0.0006
14	CTD	14	0.0030	0.0006
15	CTD	15	0.0024	0.0002
16	CTD	16	0.0023	0.0003
17	CTD	17	0.0031	0.0004
18	CTD	18	0.0095	0.0002
19	CTD	19	0.0126	0.0004
20	CTD	20	0.0053	
21	CTD	21	0.0048	0.0004
27	CTD	22	0.0053	0.0009
28	CTD	23	0.0022	0.0025
29	CTD	24	0.0034	0.0022
30	CTD	25	0.0021	0.0028
31	CTD	26	0.0014	0.0029
32	CTD	27	0.0015	0.0022
33	CTD	28	0.0014	0.0027
34	CTD	29	0.0030	0.0027
35	CTD	30	0.0052	0.0015
36	CTD	31	0.0013	0.0015
37	CTD	32	0.0012	0.0005
38	CTD	33	0.0017	0.0014
39	CTD	34	0.0020	0.0024
40	CTD	35	0.0057	0.0058
41	CTD	36	0.0014	0.0012

STATION NO	OPERATION	SAMPLE NO	BOTTOM WEIGHT /2L (G)	TOP /2L (G)
42	CTD	37	0.0014	0.0014
43	CTD	38	0.0011	0.0012
44	CTD	39	0.0012	0.0010
45	CTD	40	0.0000	0.0012
46	CTD	41	0.0007	0.0007
47	CTD	42	0.0008	0.0008
48	CTD	43	0.0008	0.0008
54	CTD	44	0.0007	0.0012
55	CTD	45	0.0009	0.0007
56	CTD	46	0.0007	0.0015
57	CTD	47	0.0029	0.0069
58	CTD	48	0.0012	0.0009
59	CTD	49	0.0013	0.0028
60	CTD	50	0.0003	0.0010
61	CTD	51	0.0019	0.0012
62	CTD	52	0.0011	0.0006
63	CTD	53	0.0001	0.0009
64	CTD	54	0.0006	0.0010
65	CTD	55	0.0000	0.0004
66	CTD	56	0.0006	0.0003
67	CTD	57	0.0004	0.0006
68	CTD	58	0.0016	0.0011
69	CTD	59	0.0012	0.0006
70	CTD	60	0.0010	0.0026
72	CTD	61	0.0000	0.0009
73	CTD	62	0.0002	0.0006
74	CTD	63	0.0005	0.0003
75	CTD	64	0.0000	0.0005
76	CTD	65	0.0022	0.0000
BRUCE			Sediment Trap (top)	0.1631
BRUCE			Sediment Trap (bot)	3.8266

Appendix E. Composition of Grab Samples

See attached CD-ROM 1.

The Excel spreadsheets in Appendix E contain full descriptions of the samples recovered in the surface grabs. Each sample is listed by its associated filename which consists of GA cruise number/Station number, Operation type (GR = grab), sample number, and a letter associated with the sub-sample taken from the grab (e.g., 234/1GR01A). In all cases the letter "A" refers to a sub-sample of the bulk sediment.

Appendix F. Photographs of Grab Sample Gravel Fractions

See attached CD-ROM 1.

Files in Appendix F are jpegs. The following naming convention applies: a 7 digit GA Sediment Laboratory Number, a space, followed by the GA Survey Number, Station Number, Operation Type (GR = grab), Operation Number and a Letter indicating the sequence in the photos (e.g., 6406765 234_1GR1A.jpg).

Appendix G. Foraminifera Taxonomic List

See attached CD-ROM 1.

The files contained in Appendix G are images taken of Foraminifera, stored as tiff files. The files in the folder lmg_images are digital light micrographs. The file format is as follows, P3250005!.tiff, where the file name is a sequential number generated by the digital camera. The files in the folder sem_images have been taken by a scanning electron microscope (SEM). The file formats are DC1_01.tif where, DC1 is a folder generated by the camera for each camera session and 01 is a sequential file number.

Preliminary list of 107 species of foraminifera identified in this study (See Table G1). Queries signify uncertain identifications and the reference (including plate and figure number) used to make the identification is listed after the species name in square parentheses.

- *Alveolinella quoyi* (d'Orbigny) [Loeblich & Tappan, 1994;107(1-4)]
- *Agglutinella arenata* (Said) [Loeblich & Tappan, 1994; 74(10-13)]
- *Ammomassilina alveoliniformis* (Millet) [Loeblich & Tappan, 1994;5(1-5)]
- *Amphistegina lessonii* or *Amphistegina lobifera*
- *Amphistegina papillosa* Said [Loeblich & Tappan, 1994;339(4-7),341(1-7)]
- *Amphistegina radiata* (Fichtel & Moll) [Loeblich & Tappan, 1994;341(8-11/1-7)]
- *Anomalinella rostrata* (Brady) [Loeblich & Tappan, 1994; 349(1-8)]
- *Anomalinoides* sp.
- *Assilina ammonoides* (Gronovius) [Loeblich & Tappan, 1994;387(7-9)]
- *Asterorotalia gaimardi* (d'Orbigny) [Loeblich & Tappan, 1994;372(1-7)] or *Challengerella persica* Billman [Loeblich & Tappan, 1994;373(1-7)]
- Buliminid sp. 1
- Buliminid sp. 2
- Buliminid sp. 3
- *Calcarina* sp.
- *Cancris auriculus* (Fichtel & Moll) [Loeblich & Tappan, 1994;265(7-10)]
- *Cancris carinatus* (Millett) [Loeblich & Tappan, 1994;266(1-13)]
- *Caribbeanella ogiensis* (Matsunaga) [Loeblich & Tappan, 1994;325(1-10)]
- *Caribbeanella philippinensis* McCulloch [Loeblich & Tappan, 1994;324(1-9)]
- *Clavulina pacifica* Cushman [Loeblich & Tappan, 1994;47(16-24)]
- *Dendritina striata* Hofker [Loeblich & Tappan, 1994;108(5-10)]
- *Discorbia candeiana* (d'Orbigny) [Loeblich & Tappan, 1994; 320(1-10)] or *Gavelinopsis praegeri* (Heron-Allen & Earland) [Loeblich & Tappan, 1994; 281(1-10)]
- *Elphidium advenum* Albani [Hayward et al., 1997;3(1-4)]
- *Elphidium albanii* Hayward [Hayward et al., 1997;6(1-5)]
- *Elphidium charlottense* (Vella) [Hayward et al., 1997;16(13-16)] or *Elphidium advenum* Albani
- *Elphidium craticulatum* (Fichtel & Moll) [Hayward et al., 1997;7(5-12)] or *Elphidium mortonbayense* Albani & Yassini [Hayward et al., 1997;14(6-9)]
- *Elphidium crispum* (Linné) [Hayward et al., 1997;7(13-16),8(1-9)]
- *Elphidium* cf. *mortonbayensis* Albani & Yassini [Hayward et al., 1997;14(6-9)]
- *Elphidium simplex* Cushman [Loeblich & Tappan, 1994;385(1-12)]
- *Eponides repandus* (Fichtel & Moll) [Loeblich & Tappan, 1994;268(10-13)]
- *Fijiella* cf. *simplex* (Cushman) [Loeblich & Tappan, 1994;252(5-6)]
- *Gaudryina attenuata* Chapman [Loeblich & Tappan, 1994;18(1-13)]

- *Glandulina laevigata* (d'Orbigny) [Hottinger et al., 1993;196(1-5,8)]
- *Globigerinoides ruber* (d'Orbigny) [Loeblich & Tappan, 1994;203(1-9)]
- *Placopsilina* sp.
- *Hauerina* cf. *orientalis* Cushman [Loeblich & Tappan, 1994;76(12-14)]
- *Heterolepa margaritifera* (Brady) [Loeblich & Tappan, 1994;358(1-7)]
- *Heterolepa subhaidingeri* (Parr) [Loeblich & Tappan, 1994;359(1-13)]
- *Heterostegina depressa* d'Orbigny [Loeblich & Tappan, 1994;389(1-6),390(1-3)]
- *Homotrema rubrum* (Pallas) [Loeblich & Tappan, 1995;335(5-6)]
- *Lagena annellatrachia* Loeblich & Tappan [Loeblich & Tappan, 1994;142(1-8, 11-12)]
- *Lagena auberi* (d'Orbigny) [Loeblich & Tappan, 1994;278(1-11)]
- *Lagena strumosa* Reuss [Hottinger et al., 1993;190(18-25)]
- *Lamarckina ventricosa* (Brady) [Loeblich & Tappan, 1994;172(1-9)] or *Discorbinella serangodes* Loeblich & Tappan [Loeblich & Tappan, 1994;311(7-9)]
- *Loxostomina costatapertusa* Loeblich & Tappan [Loeblich & Tappan, 1994;234(1-12)]
- *Loxostomina limbata* (Brady) [Loeblich & Tappan, 1994;233(1-8)]
- *Loxostomina porrecta* (Brady) [Loeblich & Tappan, 1994;235(1-7)]
- ?*Loxostomina costulata* (Cushman) [Loeblich & Tappan, 1994;232(12-16)]
- *Mikrobelodontos bradyi* (Barker) [Loeblich & Tappan, 1994;66(1-8)]
- Miliolid sp. 1
- Miliolid sp. 2
- Miliolid sp. 3
- *Miniacina miniacea* (Pallas) [Hottinger et al., 1993;175(9-10),176(1-6)]
- *Neocassidulina abbreviata* (Heron-Allen & Earland) [Loeblich & Tappan, 1994;258(1-7)]
- *Neoeponides bradyi* LeCalvez [Loeblich & Tappan, 1994;279(1-9)]
- ?*Neoeponides procerus* (Brady) [Loeblich & Tappan, 1994; 280(1-4)]
- *Neorotalia* sp.
- *Neouvigerina* sp.
- *Nubeculina advena* Cushman [Loeblich & Tappan, 1994;59(1-12)]
- *Nummulites venosus* (Fichtel & Moll) [Loeblich & Tappan, 1994;388(5-9)]
- *Peneroplis pertosus* Forskål [Loeblich & Tappan, 1994;110(1-5)]
- *Planispirinella exigua* (Brady) [Loeblich & Tappan, 1994;57(7-8)]
- *Planorbulinella larvata* (Parker & Jones) [Loeblich & Tappan, 1994;327(1-7)]
- *Planulina retia* Belford [Loeblich & Tappan, 1994;315(1-11),316(4-7)]
- *Plotnikovina* sp. 1 [Hottinger et al., 1993;18(1-8)]
- *Plotnikovina timorea* Loeblich & Tappan [Loeblich & Tappan, 1994;47(1-10)]
- *Pseudomassilina australis* (Cushman) [Hottinger et al., 1993;41(3-11)]
- *Pyrgo sarsi* (Schlumberger) [Loeblich & Tappan, 1994; 94(1-9)]
- *Pyrgo striolata* (Brady) [Loeblich & Tappan, 1994; 92(9-15)]
- *Quinqueloculina* cf. *Q. adiazeta* Loeblich & Tappan [Loeblich & Tappan, 1994; 85(1-18)]
- *Quinqueloculina bicostoides* Vella
- *Quinqueloculina crassicarinata* Collins [Loeblich & Tappan, 1994;77(4-12)]
- *Quinqueloculina parkeri* (Brady)
- *Quinqueloculina philippinensis* Cushman [Loeblich & Tappan, 1994;81(1-10)]
- *Quinqueloculina quiquecarinata* Collins [Loeblich & Tappan, 1994; 79(13-18)]
- *Quinqueloculina* sp. 1
- *Quinqueloculina* sp. 2
- *Quinqueloculina subimpressa* (Parr) [Loeblich & Tappan, 1994;68(9-15)]
- *Reussella* cf. *hayasakai* Ôki [Loeblich & Tappan, 1994;252(1-4)]
- *Reussella weberi* Hofker [Loeblich & Tappan, 1994;253(8-10)] or *Reussella ?pulchra* Cushman [Loeblich & Tappan, 1994;253(5-7)]

- *Rupertianella rupertiana* (Brady) [Loeblich & Tappan, 1994/Hottinger et al., 1993;106(1-14)]
- *Sagrina jugosa* (Brady) [Loeblich & Tappan, 1994;237(12-17)]
- *Sagrinella convallaria* (Millett) [Loeblich & Tappan, 1994;236(1-8)]
- *Sahulia barkeri* (Hofker) [Loeblich & Tappan, 1994;32(1-8)]
- *Sahulia lutzei* Langer [Loeblich & Tappan, 1994;37(7-8,13-14)]
- *Sigmiliolina carinata* Hofker [Loeblich & Tappan, 1994;100(4-7)]
- *Siphonaperta macbeathi* Vella [Loeblich & Tappan, 1994;74(7-9)]
- *Siphoniferoides siphoniferus* (Brady) [Loeblich & Tappan, 1994;46(1-10)]
- *Siphotextularia mestayerae* Vella [Loeblich & Tappan, 1994;42(11-23)]
- *Siphouvigerina porrecta* (Brady) [Loeblich & Tappan, 1994; 247(6-11)]
- *Sorites marginalis* (Lamarck) [Loeblich & Tappan, 1994; 247(6-11)]
- *Spiroloculina* sp.
- *Spiroplectinella pseudocarinata* (Cushman) [Loeblich & Tappan, 1994;15(1-14)]
- *Spirosigmoilina bradyi* Collins [Loeblich & Tappan, 1994; 102(1-8)]
- *Textularia agglutinans* d'Orbigny [Loeblich & Tappan, 1994;33(8-12)]
- *Textularia candeiana* d'Orbigny
- *Textularia cushmani* Said [Loeblich & Tappan, 1994;35(1-4)]
- *Textularia fistula* Cushman [Loeblich & Tappan, 1994;34(1-5)] or *Textularia stricta* Cushman [Loeblich & Tappan, 1994;38(1-9)]
- *Textularia foliacea* Heron-Allen & Earl [Loeblich & Tappan, 1994;34(6-14)]
- *Textularia kerimbaensis* Said [Hottinger et al., 1993;9(8-12),10(1-10)] or *Siphotextularia rugosa* Cheng & Zheng [Loeblich & Tappan, 1994;43(9-15)]
- *Textularia pseudogramen* Chapman & Parr [Loeblich & Tappan, 1994;37(5, 6)]
- *Textularia truncata* Höglund [Loeblich & Tappan, 1994;35(8-13)]
- *Textularia secasensis* Lalicker & McCulloch [Loeblich & Tappan, 1994;39(8-14)]
- *Triloculina pseudooblonga* (Zheng) [Loeblich & Tappan, 1994;98(1-3, 7-9)]
- *Triloculina tricarinata* d'Orbigny [Loeblich & Tappan, 1994;96(1-7)]
- *Wiesnerella ujiiei* Hatta [Loeblich & Tappan, 1994; 62(4-6)]

Table G1. Systematic count abundances for selected foraminiferal groups. All counts are percentage abundances except the total number of foraminifera counted.

STATION NUMBER	7	11	17	20	32	35	37	40	59	65	67	68
Amphistegina spp.	68	75	68	85	7	27	116	72	47	32	15	42
Assilina ammonoides	63	32	63	44	0	0	38	21	8	2	15	15
Asterotalia gaimardi or Challengerella persica	4	2	7	15	2	1	0	1	0	0	2	1
Elphidium spp.	9	13	15	8	2	6	5	0	2	1	0	3
Fijiella cf. Simplex, ?Ruesella weberi, Ruesella cf. hayasakai	2	6	8	5	3	1	1	3	4	2	1	6
Pseudogaudryina attenuata	0	0	0	0	10	2	4	6	5	2	13	7
Miniacina miniacea	0	0	0	0	0	0	0	5	9	22	1	1
Nubeculina advena	6	2	6	11	2	14	10	20	1	1	20	15
Nummulites venosus	35	31	29	22	0	0	10	5	0	0	1	1
Plotnikovina spp.	0	0	0	0	11	7	1	1	5	1	12	1
Quinqueloculina philippinensis	11	6	8	13	3	5	2	8	1	1	5	1
Spiroplectinella pseudocarinata	0	0	0	0	0	0	0	0	2	0	18	11
Textularia agglutinans	12	12	13	9	4	6	0	3	0	1	0	3
Textularia foliacea	4	15	10	11	2	4	3	4	0	1	1	1
Peneroplids	12	17	3	2	1	0	0	0	0	0	0	0
Planktics	3	3	3	3	69	32	8	32	105	28	72	45
Remaining Species	85	97	113	109	205	229	151	168	145	109	171	223
Total number of foraminifera counted	314	311	346	337	321	334	349	349	334	**201**	**347**	**376**

Appendix H. Core Logs

Core Log Legend

Sedimentary Features

- Shell Hash
- Wood
- Organic Fragments
- Articulated Shell (in-situ)
- Articulated Shell
- Intact Shell Valve(s)
- Laminations
- Burrows
- Unconformity

Fossils

- Gastropods
- Corals
- Bryozoans
- Foraminfers
- Bivalves
- Echnoids
- Halimeda
- Worm Tubes
- Scaphopods
- Crustaceans

Lithology

- Gravel
- Sandy mud
- Silt
- Clay

	Fine	Medium	Coarse
Muddy gravelly sand			
Sand			

Sub-samples

- ◄ Grain-size/$CaCO_3$/XRF
- ■ C-14 age
- x Mineralogy

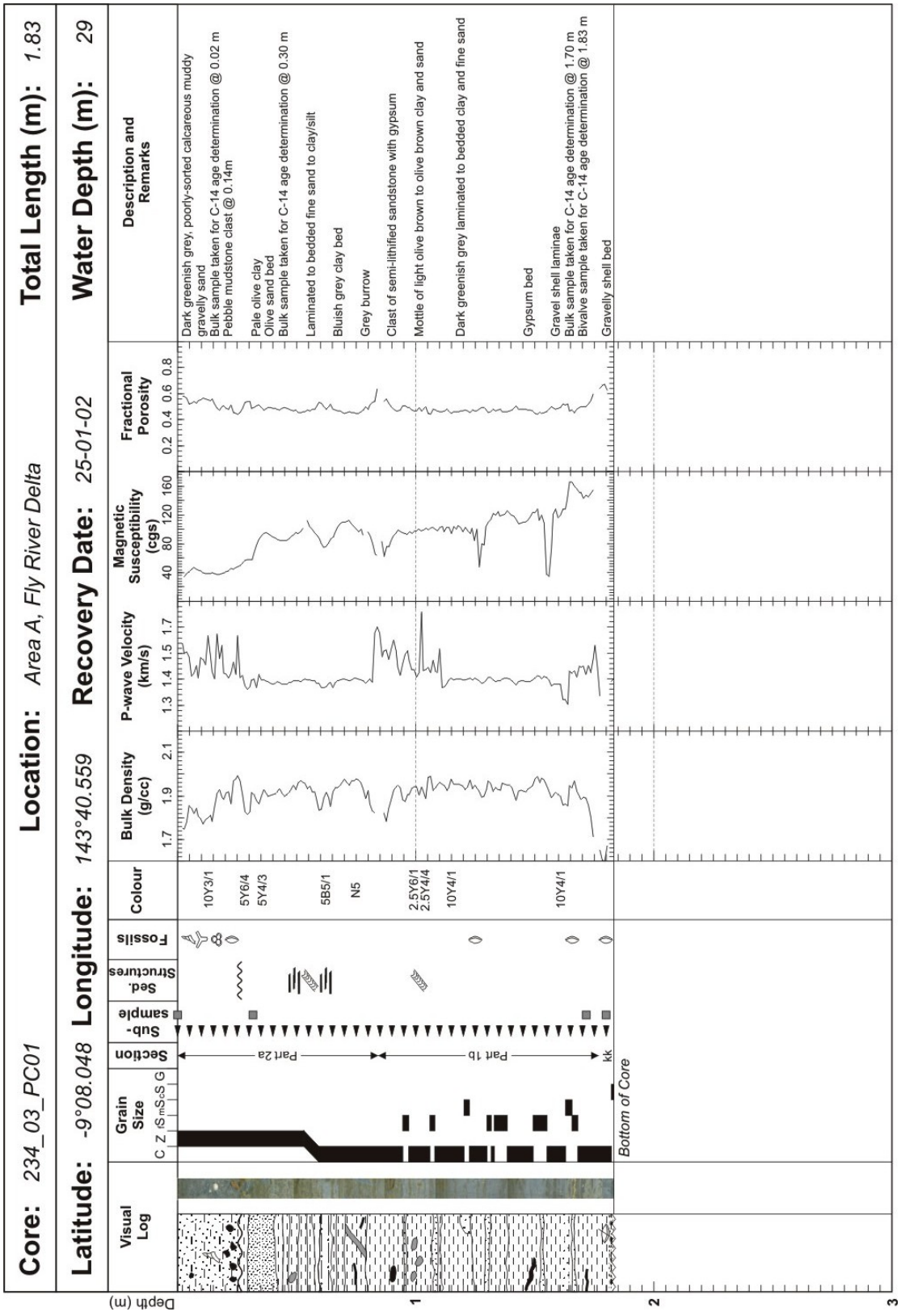
Core: 234_03_PC01
Location: Area A, Fly River Delta
Total Length (m): 1.83
Latitude: -9°08.048
Longitude: 143°40.559
Recovery Date: 25-01-02
Water Depth (m): 29
Visual Log
Grain Size
C Z S mS cS G
Section
Sub-sample
Sed. Structures
Fossils
Colour
Bulk Density (g/cc)
1.7 1.9 2.1
P-wave Velocity (km/s)
1.3 1.4 1.5 1.7
Magnetic Susceptibility (cgs)
40 80 120 160
Fractional Porosity
0.2 0.4 0.6 0.8
Description and Remarks
Part 2a
Part 2b
Part 1b
kk
10Y3/1
5Y6/4
5Y4/3
5B5/1
N5
2.5Y6/1
2.5Y4/4
10Y4/1
10Y4/1
Dark greenish grey, poorly-sorted calcareous muddy gravelly sand
Bulk sample taken for C-14 age determination @ 0.02 m
Pebble mudstone clast @ 0.14m
Pale olive clay
Olive sand bed
Bulk sample taken for C-14 age determination @ 0.30 m
Laminated to bedded fine sand to clay/silt
Bluish grey clay bed
Grey burrow
Clast of semi-lithified sandstone with gypsum
Mottle of light olive brown to olive brown clay and sand
Dark greenish grey laminated to bedded clay and fine sand
Gypsum bed
Gravel shell laminae
Bulk sample taken for C-14 age determination @ 1.70 m
Bivalve sample taken for C-14 age determination @ 1.83 m
Gravelly shell bed
Bottom of Core
Depth (m)
1
2
3

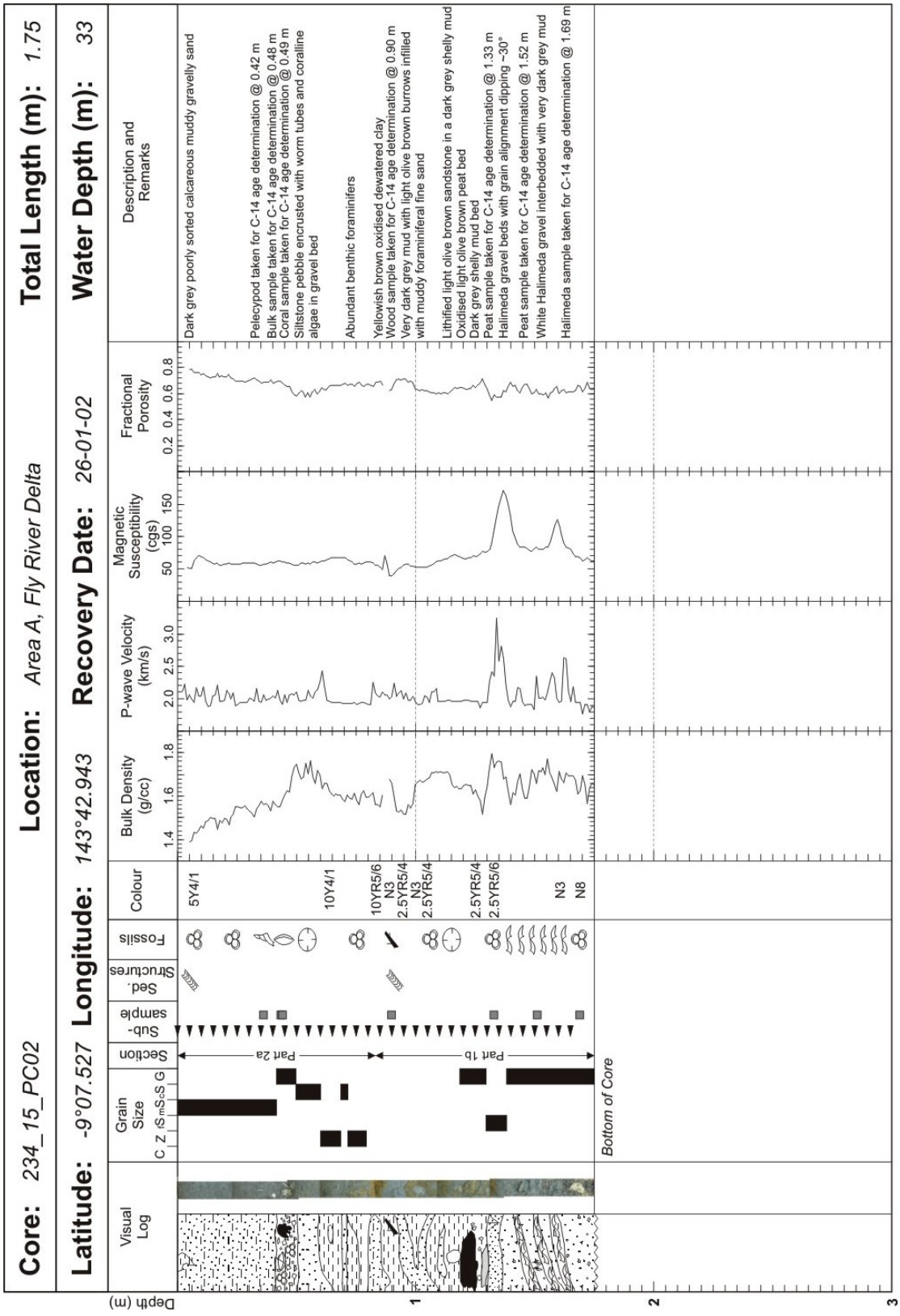
Core: 234_15_PC02
Location: Area A, Fly River Delta
Total Length (m): 1.75
Latitude: -9°07.527 Longitude: 143°42.943
Recovery Date: 26-01-02
Water Depth (m): 33
Visual Log
Grain Size
Section
Sub-sample
Sed. Structures
Fossils
Colour
Bulk Density (g/cc)
P-wave Velocity (km/s)
Magnetic Susceptibility (cgs)
Fractional Porosity
Description and Remarks
Part 2a
Part 1b
Bottom of Core
Depth (m)
Dark grey poorly sorted calcareous muddy gravelly sand
Pelecypod taken for C-14 age determination @ 0.42 m
Bulk sample taken for C-14 age determination @ 0.48 m
Coral sample taken for C-14 age determination @ 0.49 m
Siltstone pebble encrusted with worm tubes and coralline algae in gravel bed
Abundant benthic foraminifers
Yellowish brown oxidised dewatered clay
Wood sample taken for C-14 age determination @ 0.90 m
Very dark grey mud with light olive brown burrows infilled with muddy foraminiferal fine sand
Lithified light olive brown sandstone in a dark grey shelly mud
Oxidised light olive brown peat bed
Dark grey shelly mud bed
Peat sample taken for C-14 age determination @ 1.33 m
Halimeda gravel beds with grain alignment dipping ~30°
Peat sample taken for C-14 age determination @ 1.52 m
White Halimeda gravel interbedded with very dark grey mud
Halimeda sample taken for C-14 age determination @ 1.69 m

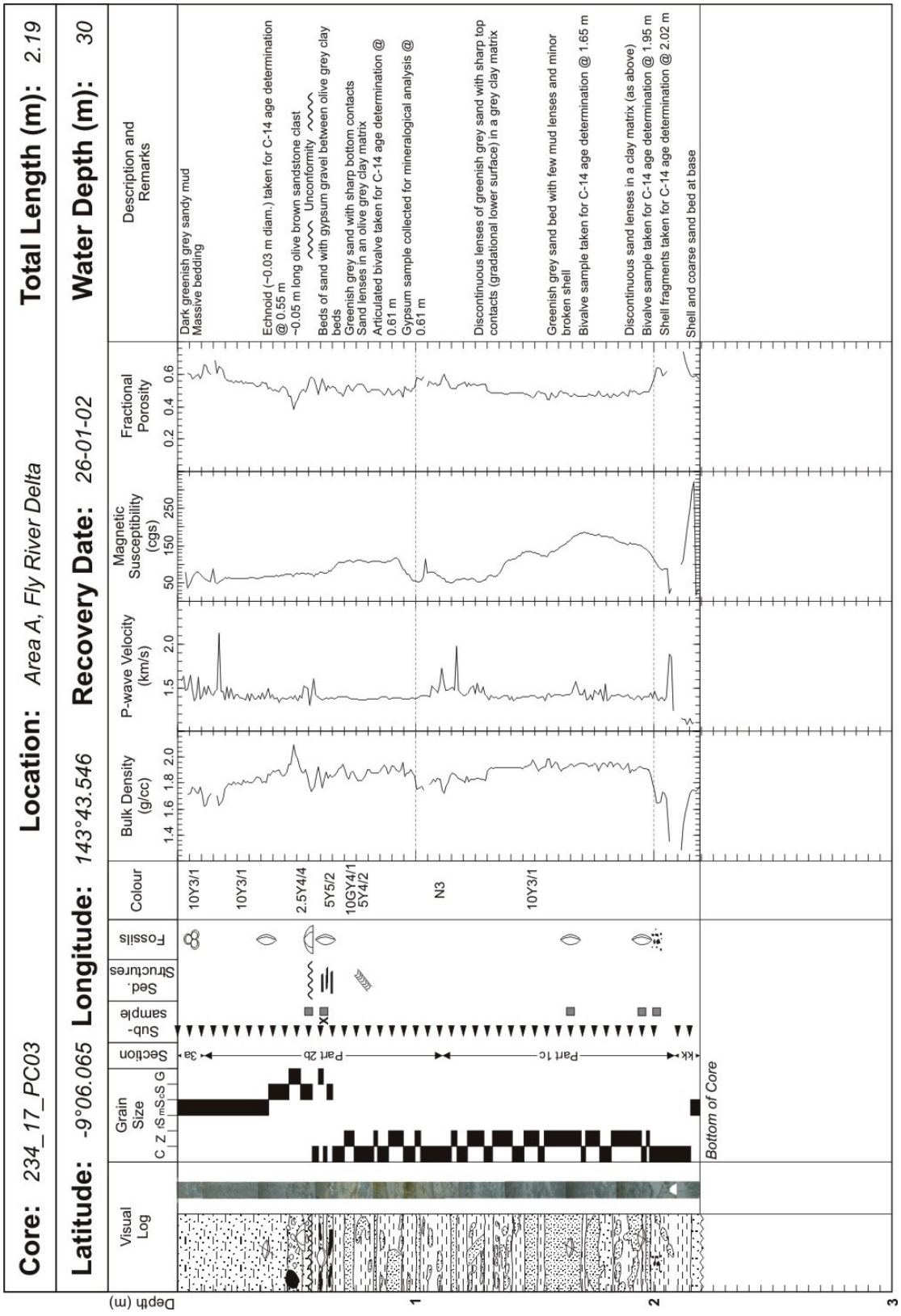
Core: 234_17_PC03
Location: Area A, Fly River Delta
Total Length (m): 2.19
Latitude: -9°06.065 Longitude: 143°43.546
Recovery Date: 26-01-02
Water Depth (m): 30
Visual Log
Grain Size
Section
Sub-sample
Sed. Structures
Fossils
Colour
Bulk Density (g/cc)
P-wave Velocity (km/s)
Magnetic Susceptibility (cgs)
Fractional Porosity
Description and Remarks
Depth (m)
3a
Part 2b
Part 1c
kk
10Y3/1
2.5Y4/4
5Y5/2
10GY4/1
5Y4/2
N3
Dark greenish grey sandy mud
Massive bedding
Echnoid (~0.03 m diam.) taken for C-14 age determination @ 0.55 m
~0.05 m long olive brown sandstone clast
Unconformity
Beds of sand with gypsum gravel between olive grey clay beds
Greenish grey sand with sharp bottom contacts
Sand lenses in an olive grey clay matrix
Articulated bivalve taken for C-14 age determination @ 0.61 m
Gypsum sample collected for mineralogical analysis @ 0.61 m
Discontinuous lenses of greenish grey sand with sharp top contacts (gradational lower surface) in a grey clay matrix
Greenish grey sand bed with few mud lenses and minor broken shell
Bivalve sample taken for C-14 age determination @ 1.65 m
Discontinuous sand lenses in a clay matrix (as above)
Bivalve sample taken for C-14 age determination @ 1.95 m
Shell fragments taken for C-14 age determination @ 2.02 m
Shell and coarse sand bed at base
Bottom of Core

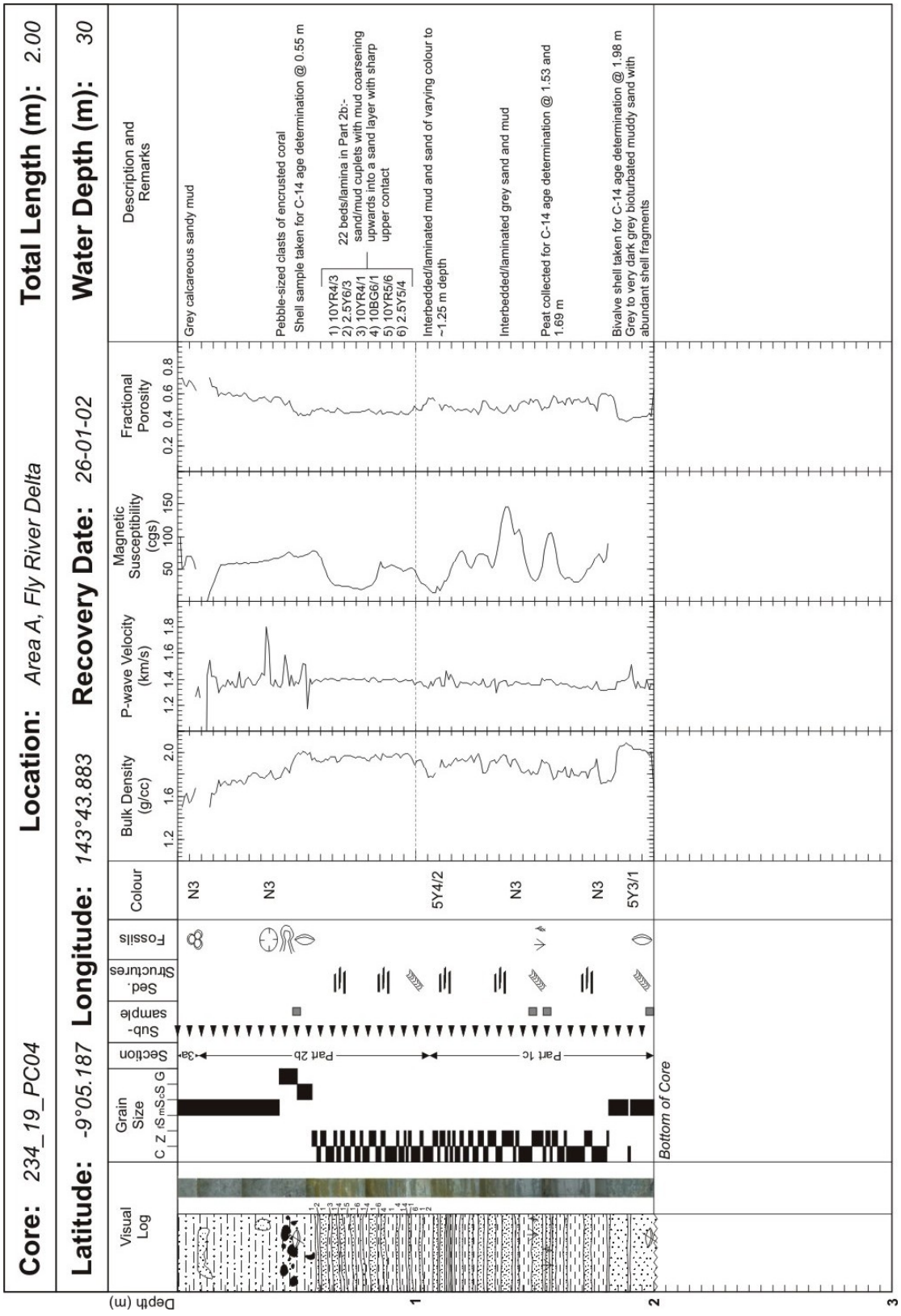
Core: 234_19_PC04
Location: Area A, Fly River Delta
Total Length (m): 2.00
Latitude: -9°05.187 Longitude: 143°43.883
Recovery Date: 26-01-02
Water Depth (m): 30
Visual Log
Grain Size
Section
Sub-sample
Sed. Structures
Fossils
Colour
Bulk Density (g/cc)
P-wave Velocity (km/s)
Magnetic Susceptibility (cgs)
Fractional Porosity
Description and Remarks
Part 2b
Part 1c
Bottom of Core
Grey calcareous sandy mud
Pebble-sized clasts of encrusted coral
Shell sample taken for C-14 age determination @ 0.55 m
1) 10YR4/3
2) 2.5Y6/3
3) 10YR4/1
4) 10BG6/1
5) 10YR5/6
6) 2.5Y5/4
22 beds/lamina in Part 2b:- sand/mud cuplets with mud coarsening upwards into a sand layer with sharp upper contact
Interbedded/laminated mud and sand of varying colour to ~1.25 m depth
Interbedded/laminated grey sand and mud
Peat collected for C-14 age determination @ 1.53 and 1.69 m
Bivalve shell taken for C-14 age determination @ 1.98 m
Grey to very dark grey bioturbated muddy sand with abundant shell fragments
Depth (m)

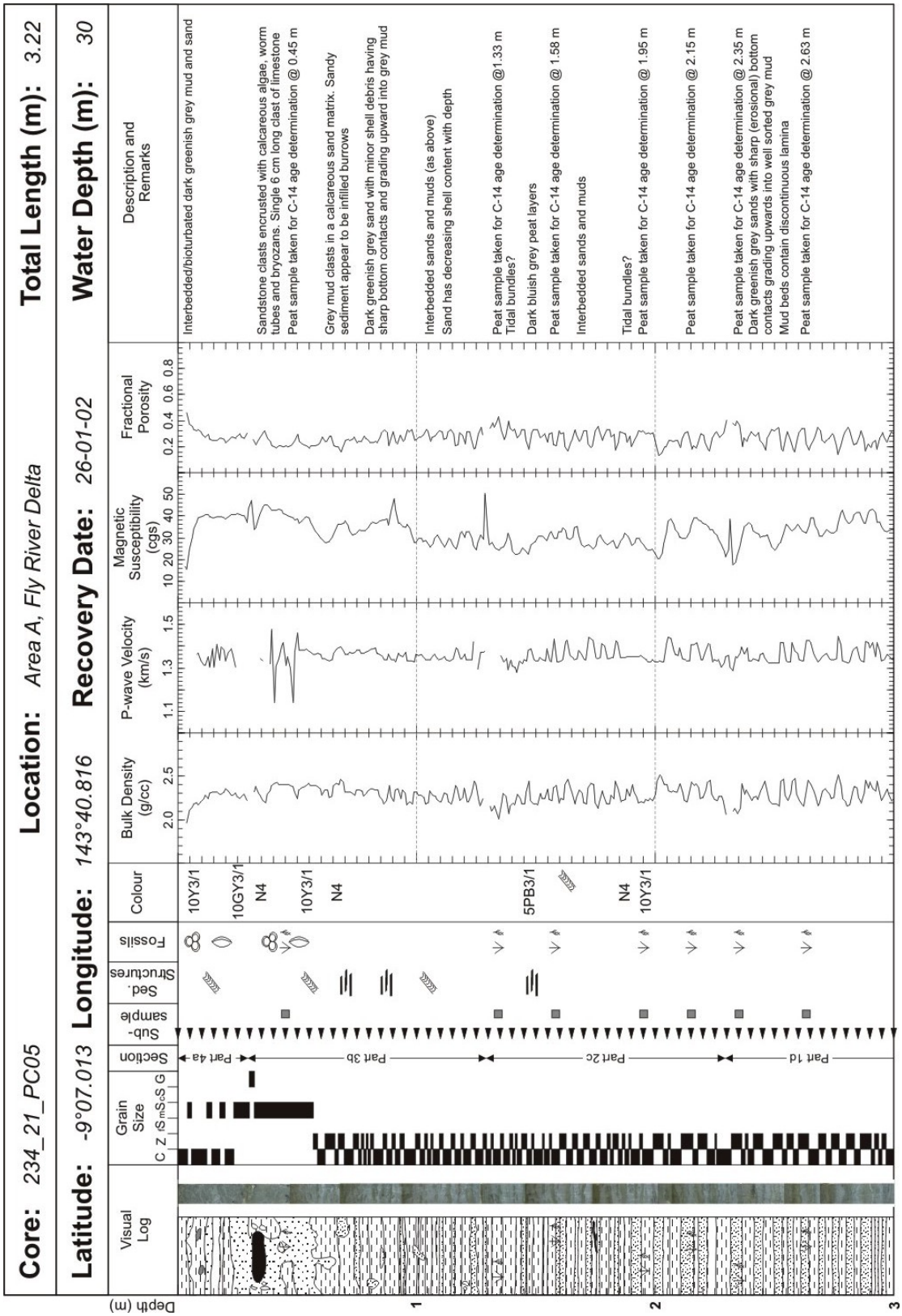
Core: 234_21_PC05
Location: Area A, Fly River Delta
Total Length (m): 3.22
Latitude: -9°07.013 Longitude: 143°40.816
Recovery Date: 26-01-02
Water Depth (m): 30
Visual Log
Grain Size
Section
Sub-sample
Sed. Structures
Fossils
Colour
Bulk Density (g/cc)
P-wave Velocity (km/s)
Magnetic Susceptibility (cgs)
Fractional Porosity
Description and Remarks
Part 4a
Part 3b
Part 2c
Part 1d
10Y3/1
10GY3/1
N4
5PB3/1
Interbedded/bioturbated dark greenish grey mud and sand
Sandstone clasts encrusted with calcareous algae, worm tubes and bryozans. Single 6 cm long clast of limestone
Peat sample taken for C-14 age determination @ 0.45 m
Grey mud clasts in a calcareous sand matrix. Sandy sediment appear to be infilled burrows
Dark greenish grey sand with minor shell debris having sharp bottom contacts and grading upward into grey mud
Interbedded sands and muds (as above)
Sand has decreasing shell content with depth
Peat sample taken for C-14 age determination @1.33 m
Tidal bundles?
Dark bluish grey peat layers
Peat sample taken for C-14 age determination @ 1.58 m
Interbedded sands and muds
Tidal bundles?
Peat sample taken for C-14 age determination @ 1.95 m
Peat sample taken for C-14 age determination @ 2.15 m
Peat sample taken for C-14 age determination @ 2.35 m
Dark greenish grey sands with sharp (erosional) bottom contacts grading upwards into well sorted grey mud
Mud beds contain discontinuous lamina
Peat sample taken for C-14 age determination @ 2.63 m
Depth (m)
1
2
3

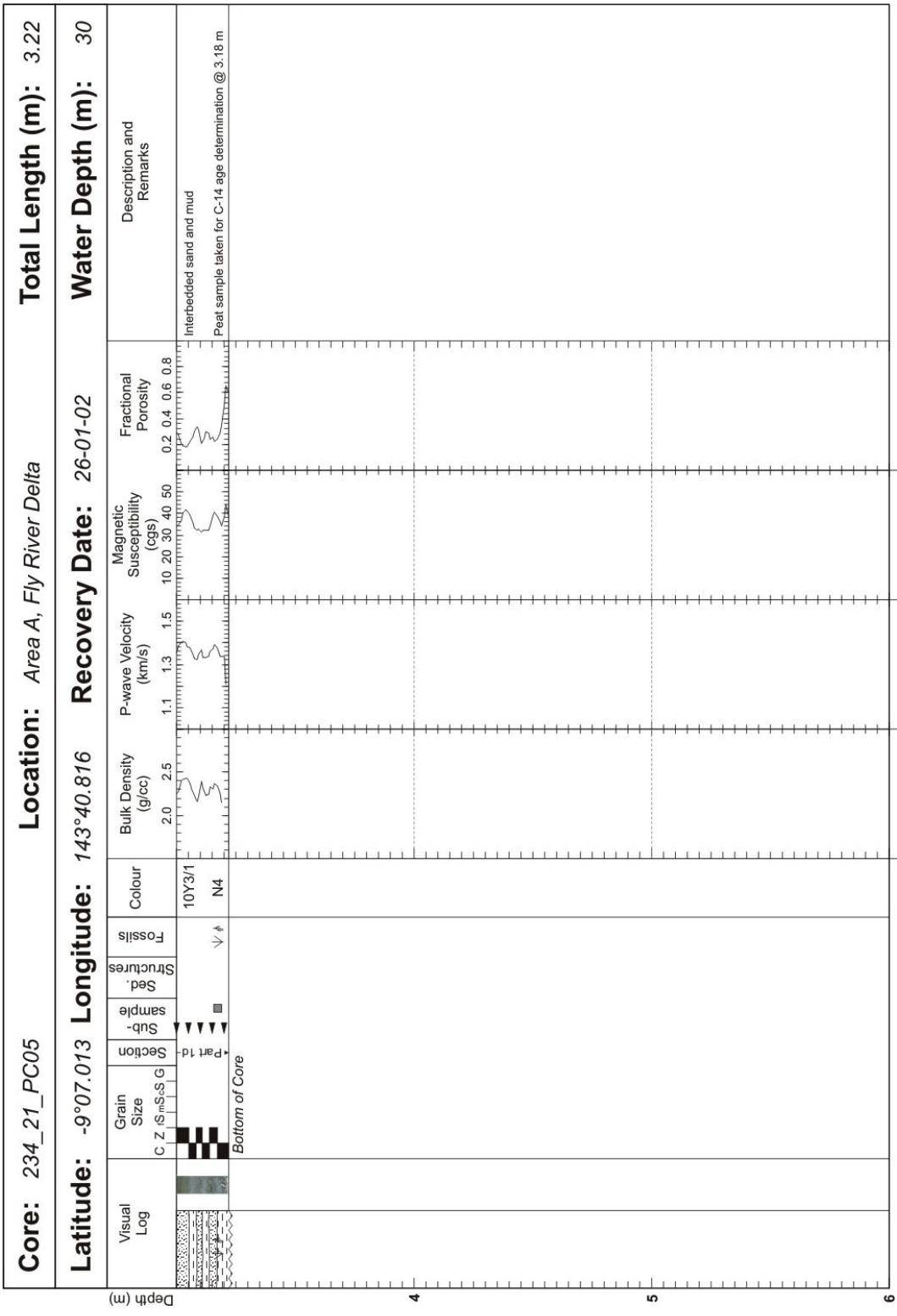
Core: 234_21_PC05
Location: Area A, Fly River Delta
Total Length (m): 3.22
Latitude: -9°07.013 Longitude: 143°40.816
Recovery Date: 26-01-02
Water Depth (m): 30
Visual Log
Grain Size
C Z S mS cS G
Section
Sub-sample
Sed. Structures
Fossils
Colour
10Y3/1
N4
Bulk Density (g/cc)
2.0 2.5
P-wave Velocity (km/s)
1.1 1.3 1.5
Magnetic Susceptibility (cgs)
10 20 30 40 50
Fractional Porosity
0.2 0.4 0.6 0.8
Description and Remarks
Part 1d
Bottom of Core
Interbedded sand and mud
Peat sample taken for C-14 age determination @ 3.18 m
Depth (m)
4
5
6

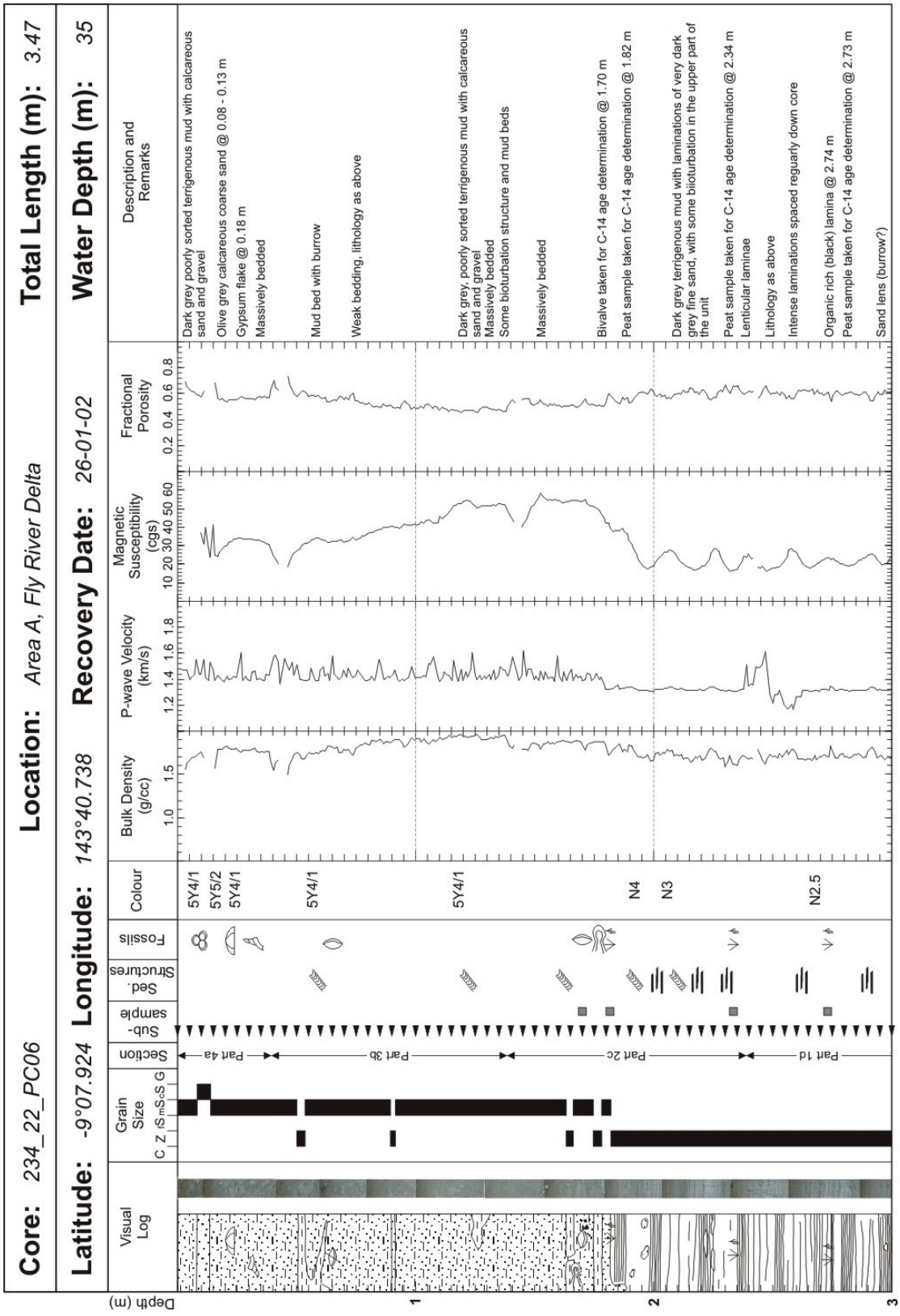
Core: 234_22_PC06
Location: Area A, Fly River Delta
Total Length (m): 3.47
Latitude: -9°07.924 Longitude: 143°40.738 Recovery Date: 26-01-02
Water Depth (m): 35
Visual Log
Grain Size
Section
Sub-sample
Sed. Structures
Fossils
Colour
Bulk Density (g/cc)
P-wave Velocity (km/s)
Magnetic Susceptibility (cgs)
Fractional Porosity
Description and Remarks
Depth (m)
Part 4a
Part 3b
Part 2c
Part 1d
5Y4/1
5Y5/2
N4
N3
N2.5
Dark grey poorly sorted terrigenous mud with calcareous sand and gravel
Olive grey calcareous coarse sand @ 0.08 - 0.13 m
Gypsum flake @ 0.18 m
Massively bedded
Mud bed with burrow
Weak bedding, lithology as above
Dark grey, poorly sorted terrigenous mud with calcareous sand and gravel
Massively bedded
Some bioturbation structure and mud beds
Massively bedded
Bivalve taken for C-14 age determination @ 1.70 m
Peat sample taken for C-14 age determination @ 1.82 m
Dark grey terrigenous mud with laminations of very dark grey fine sand, with some bioturbation in the upper part of the unit
Peat sample taken for C-14 age determination @ 2.34 m
Lenticular laminae
Lithology as above
Intense laminations spaced regularly down core
Organic rich (black) lamina @ 2.74 m
Peat sample taken for C-14 age determination @ 2.73 m
Sand lens (burrow?)

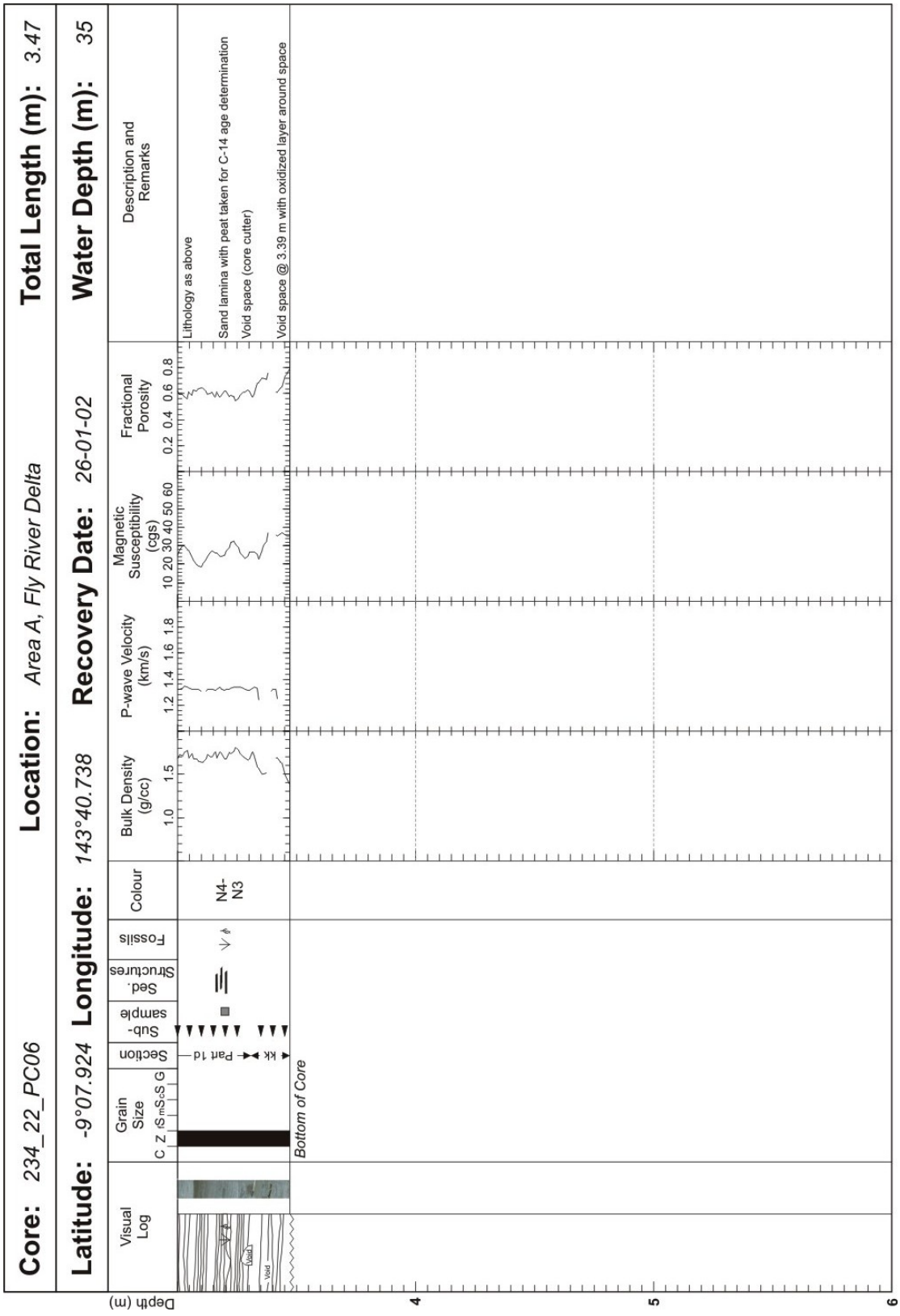
Core: 234_22_PC06
Location: Area A, Fly River Delta
Total Length (m): 3.47
Latitude: -9°07.924 Longitude: 143°40.738
Recovery Date: 26-01-02
Water Depth (m): 35
Visual Log
Grain Size
Section
Sub-sample
Sed. Structures
Fossils
Colour
Bulk Density (g/cc)
P-wave Velocity (km/s)
Magnetic Susceptibility (cgs)
Fractional Porosity
Description and Remarks
Part 1d
KK
N4-N3
Void
Bottom of Core
Lithology as above
Sand lamina with peat taken for C-14 age determination
Void space (core cutter)
Void space @ 3.39 m with oxidized layer around space
Depth (m)
4
5
6

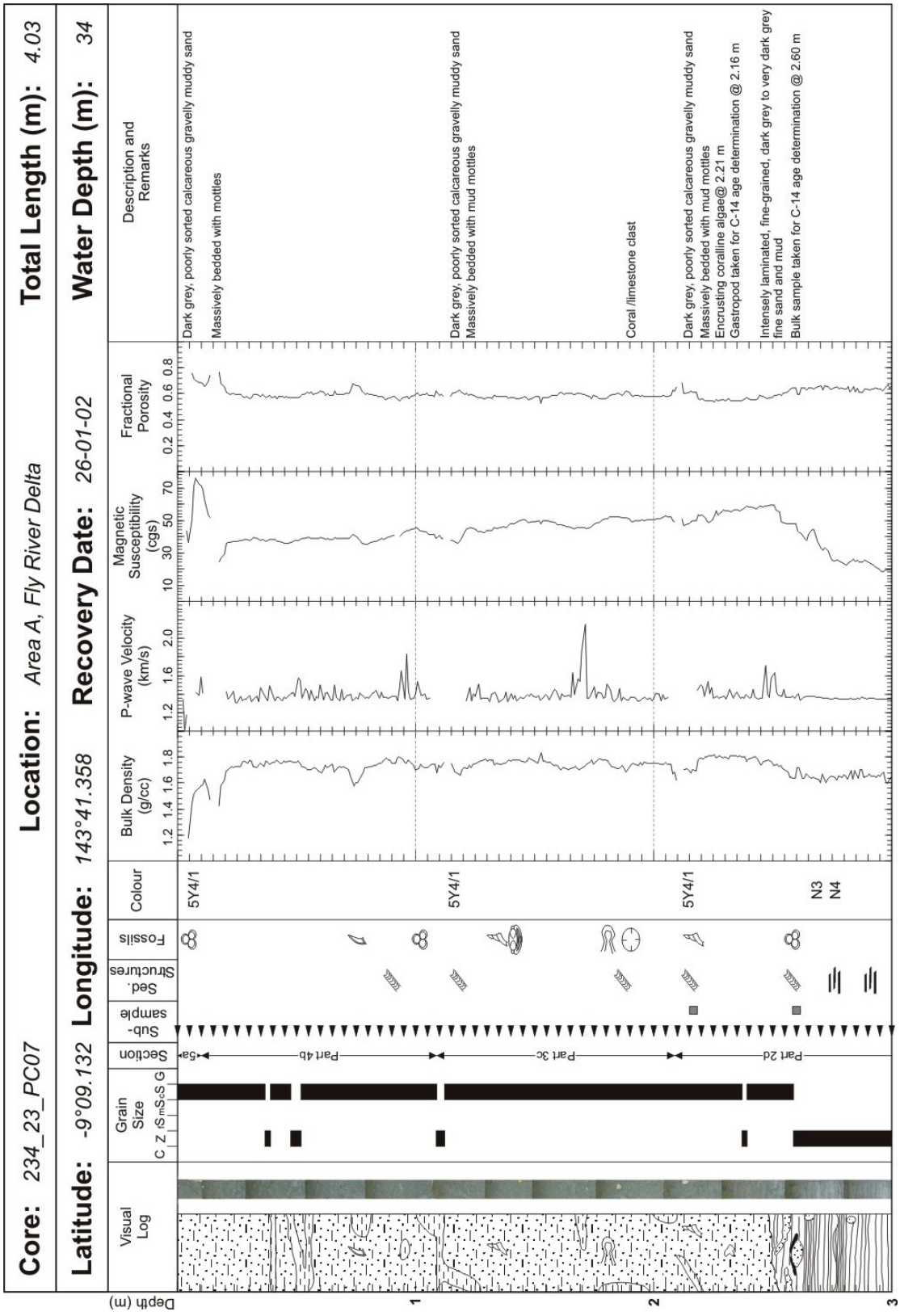
Core: 234_23_PC07
Location: Area A, Fly River Delta
Total Length (m): 4.03
Latitude: -9°09.132 Longitude: 143°41.358
Recovery Date: 26-01-02
Water Depth (m): 34
Visual Log
Grain Size
Section
Sub-sample
Sed. Structures
Fossils
Colour
Bulk Density (g/cc)
P-wave Velocity (km/s)
Magnetic Susceptibility (cgs)
Fractional Porosity
Description and Remarks
Depth (m)
5a
Part 4b
Part 3c
Part 2d
5Y4/1
N3
N4
Dark grey, poorly sorted calcareous gravelly muddy sand
Massively bedded with mottles
Dark grey, poorly sorted calcareous gravelly muddy sand
Massively bedded with mud mottles
Coral /limestone clast
Dark grey, poorly sorted calcareous gravelly muddy sand
Massively bedded with mud mottles
Encrusting coralline algae@ 2.21 m
Gastropod taken for C-14 age determination @ 2.16 m
Intensely laminated, fine-grained, dark grey to very dark grey fine sand and mud
Bulk sample taken for C-14 age determination @ 2.60 m

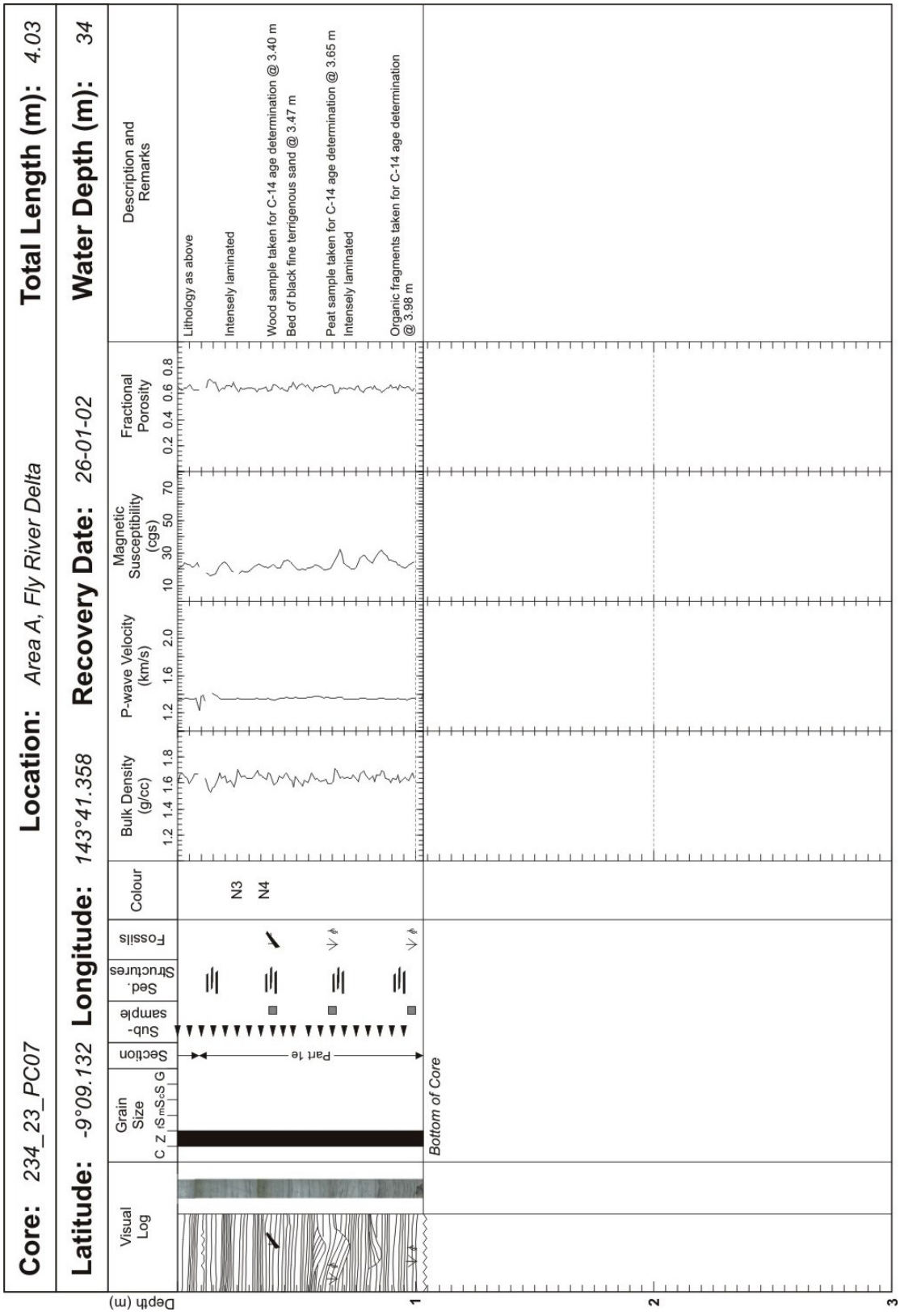
Core: 234_23_PC07
Location: Area A, Fly River Delta
Total Length (m): 4.03
Latitude: -9°09.132 Longitude: 143°41.358
Recovery Date: 26-01-02
Water Depth (m): 34
Visual Log
Grain Size
Section
Sub-sample
Sed. Structures
Fossils
Colour
Bulk Density (g/cc)
P-wave Velocity (km/s)
Magnetic Susceptibility (cgs)
Fractional Porosity
Description and Remarks
Part 1e
N3
N4
Lithology as above
Intensely laminated
Wood sample taken for C-14 age determination @ 3.40 m
Bed of black fine terrigenous sand @ 3.47 m
Peat sample taken for C-14 age determination @ 3.65 m
Intensely laminated
Organic fragments taken for C-14 age determination @ 3.98 m
Bottom of Core
Depth (m)

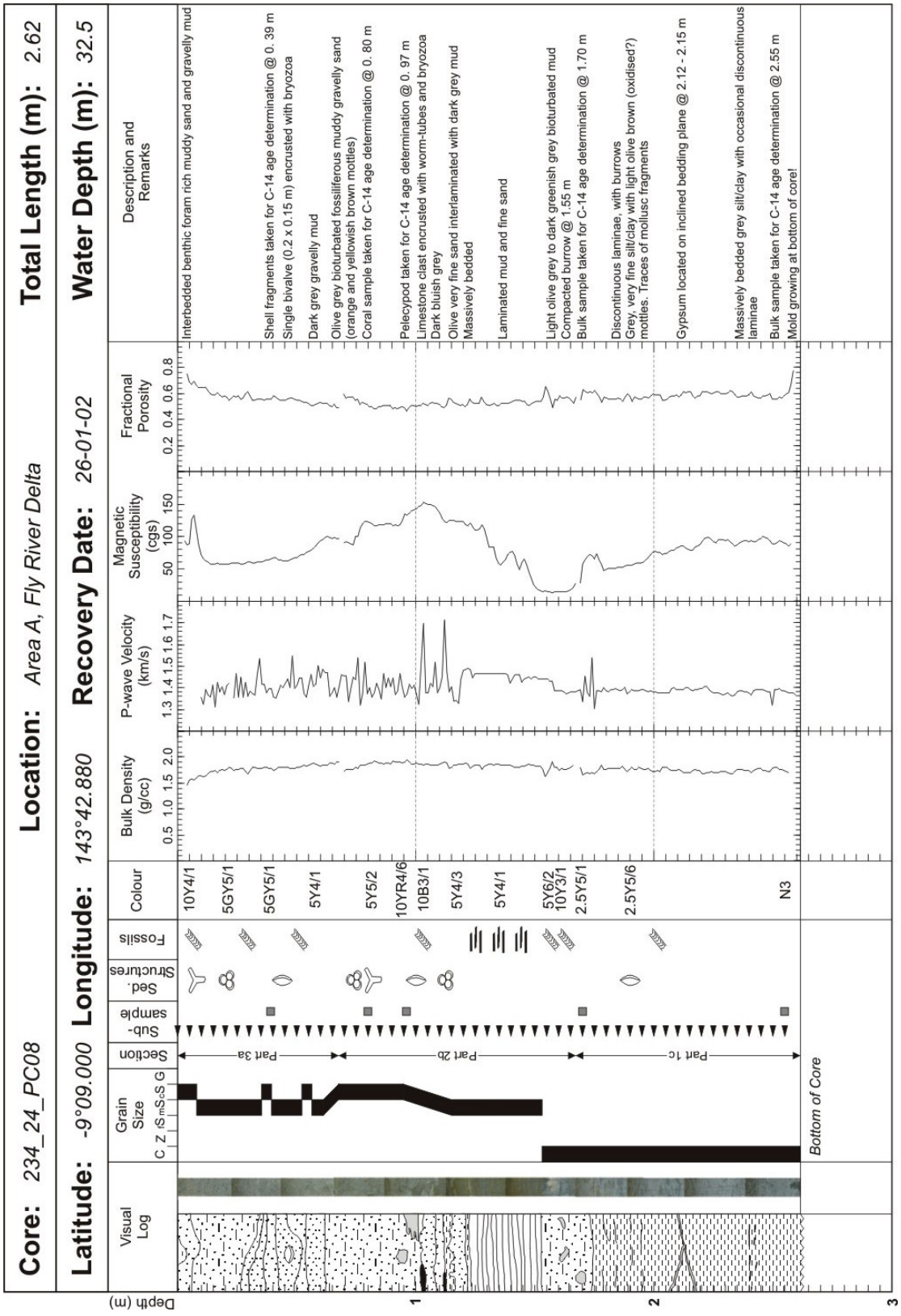
Core: 234_24_PC08
Location: Area A, Fly River Delta
Total Length (m): 2.62
Latitude: -9°09.000 Longitude: 143°42.880
Recovery Date: 26-01-02
Water Depth (m): 32.5
Visual Log
Grain Size
Section
Sub-sample
Sed. Structures
Fossils
Colour
Bulk Density (g/cc)
P-wave Velocity (km/s)
Magnetic Susceptibility (cgs)
Fractional Porosity
Description and Remarks
Part 3a
Part 2b
Part 1c
Bottom of Core
Depth (m)
Interbedded benthic foram rich muddy sand and gravelly mud
Shell fragments taken for C-14 age determination @ 0. 39 m
Single bivalve (0.2 x 0.15 m) encrusted with bryozoa
Dark grey gravelly mud
Olive grey bioturbated fossiliferous muddy gravelly sand (orange and yellowish brown mottles)
Coral sample taken for C-14 age determination @ 0. 80 m
Pelecypod taken for C-14 age determination @ 0. 97 m
Limestone clast encrusted with worm-tubes and bryozoa
Dark bluish grey
Olive very fine sand interlaminated with dark grey mud
Massively bedded
Laminated mud and fine sand
Light olive grey to dark greenish grey bioturbated mud
Compacted burrow @ 1.55 m
Bulk sample taken for C-14 age determination @ 1.70 m
Discontinuous laminae, with burrows
Grey, very fine silt/clay with light olive brown (oxidised?) mottles. Traces of mollusc fragments
Gypsum located on inclined bedding plane @ 2.12 - 2.15 m
Massively bedded grey silt/clay with occasional discontinuous laminae
Bulk sample taken for C-14 age determination @ 2.55 m
Mold growing at bottom of core!

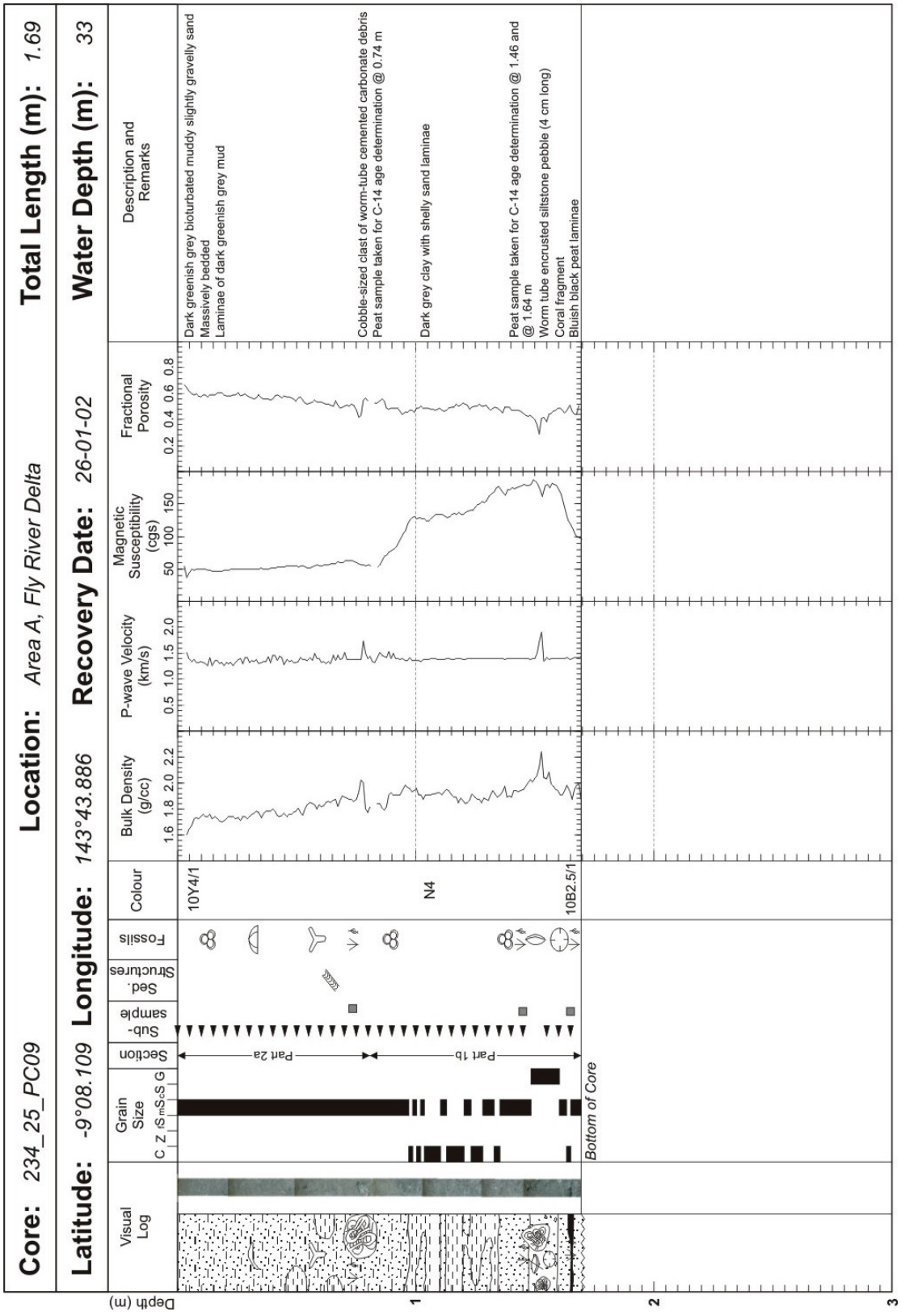
Core: 234_25_PC09
Location: Area A, Fly River Delta
Total Length (m): 1.69
Latitude: -9°08.109 Longitude: 143°43.886
Recovery Date: 26-01-02
Water Depth (m): 33
Visual Log
Grain Size
Section
Sub-sample
Sed. Structures
Fossils
Colour
Bulk Density (g/cc)
P-wave Velocity (km/s)
Magnetic Susceptibility (cgs)
Fractional Porosity
Description and Remarks
Part 2a
Part 1b
10Y4/1
N4
10B2.5/1
Bottom of Core
Dark greenish grey bioturbated muddy slightly gravelly sand
Massively bedded
Laminae of dark greenish grey mud
Cobble-sized clast of worm-tube cemented carbonate debris
Peat sample taken for C-14 age determination @ 0.74 m
Dark grey clay with shelly sand laminae
Peat sample taken for C-14 age determination @ 1.46 and @ 1.64 m
Worm tube encrusted siltstone pebble (4 cm long)
Coral fragment
Bluish black peat laminae
Depth (m)

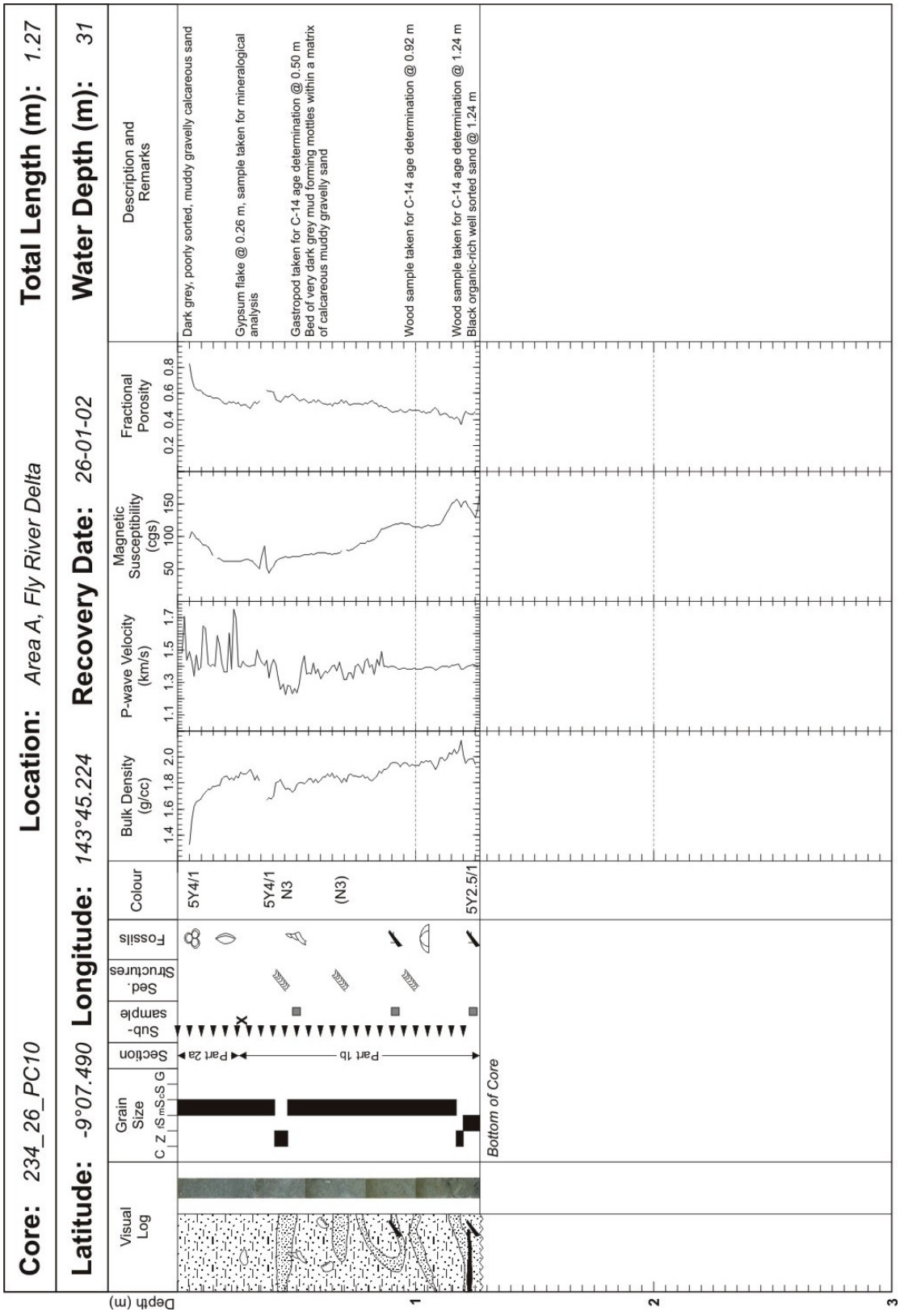
Core: 234_26_PC10
Location: Area A, Fly River Delta
Total Length (m): 1.27
Latitude: -9°07.490 Longitude: 143°45.224
Recovery Date: 26-01-02
Water Depth (m): 31
Visual Log
Grain Size
Section
Sub-sample
Sed. Structures
Fossils
Colour
Bulk Density (g/cc)
P-wave Velocity (km/s)
Magnetic Susceptibility (cgs)
Fractional Porosity
Description and Remarks
Part 1b
Part 2a
5Y4/1
5Y4/1 N3
(N3)
5Y2.5/1
Dark grey, poorly sorted, muddy gravelly calcareous sand
Gypsum flake @ 0.26 m, sample taken for mineralogical analysis
Gastropod taken for C-14 age determination @ 0.50 m
Bed of very dark grey mud forming mottles within a matrix of calcareous muddy gravelly sand
Wood sample taken for C-14 age determination @ 0.92 m
Wood sample taken for C-14 age determination @ 1.24 m
Black organic-rich well sorted sand @ 1.24 m
Bottom of Core
Depth (m)
1
2
3

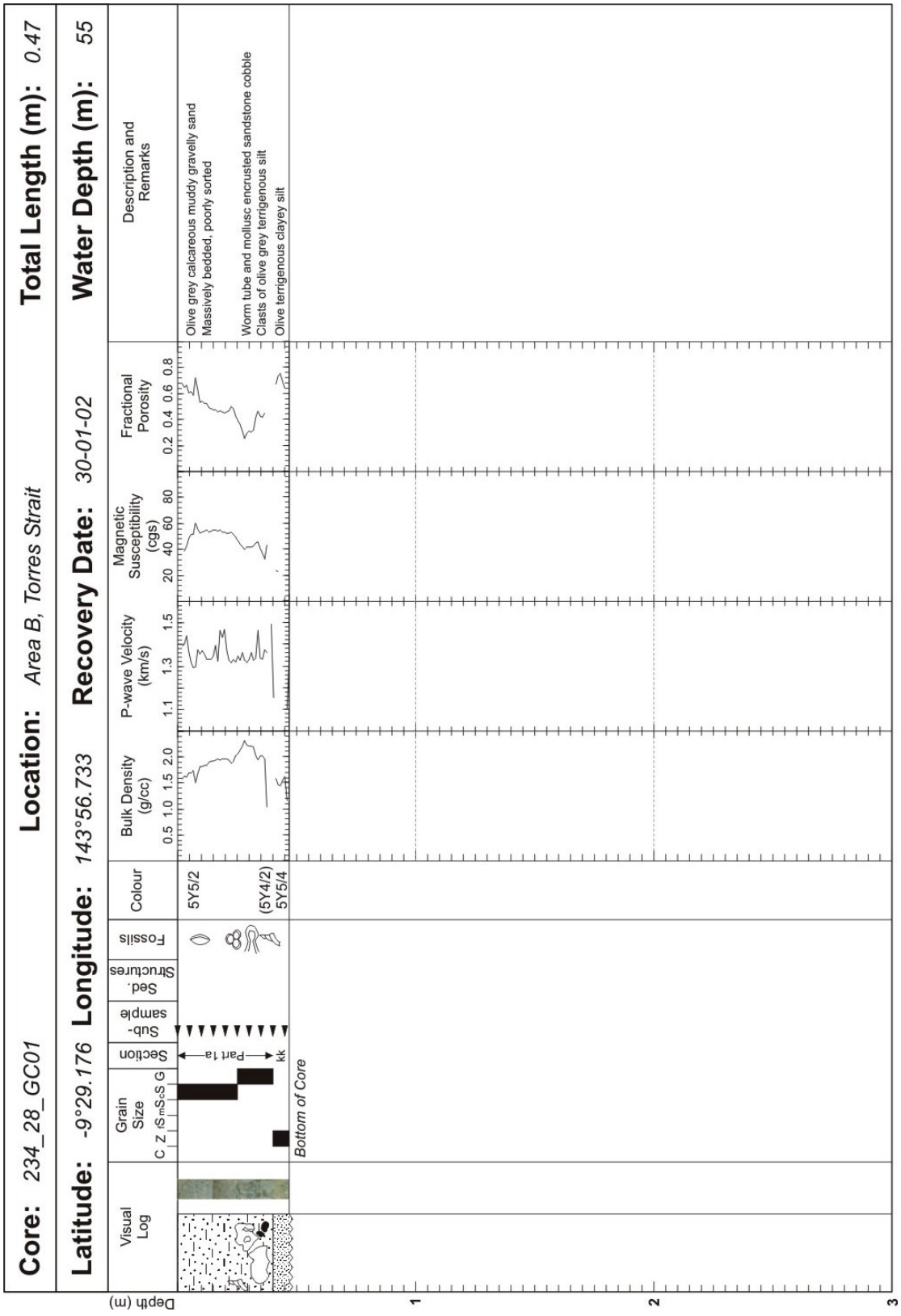
Core: 234_28_GC01
Location: Area B, Torres Strait
Total Length (m): 0.47
Latitude: -9°29.176 Longitude: 143°56.733
Recovery Date: 30-01-02
Water Depth (m): 55
Visual Log
Grain Size
C Z S mS cS G
Section
Part 1a
kk
Sub-sample
Sed. Structures
Fossils
Colour
5Y5/2
(5Y4/2) 5Y5/4
Bulk Density (g/cc)
0.5 1.0 1.5 2.0
P-wave Velocity (km/s)
1.1 1.3 1.5
Magnetic Susceptibility (cgs)
20 40 60 80
Fractional Porosity
0.2 0.4 0.6 0.8
Description and Remarks
Olive grey calcareous muddy gravelly sand
Massively bedded, poorly sorted
Worm tube and mollusc encrusted sandstone cobble
Clasts of olive grey terrigenous silt
Olive terrigenous clayey silt
Bottom of Core
Depth (m)
1
2
3

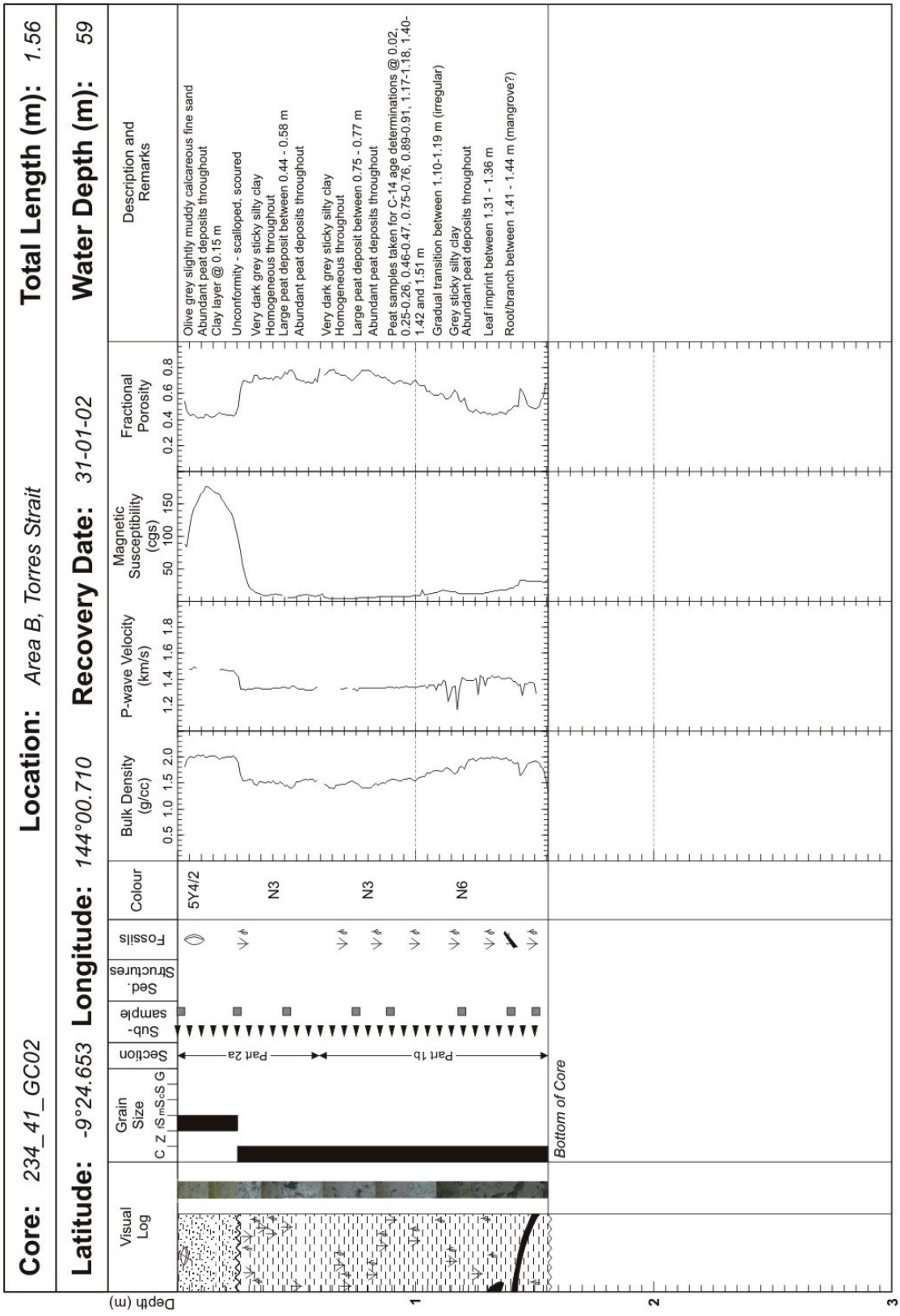
Core: 234_41_GC02
Location: Area B, Torres Strait
Total Length (m): 1.56
Latitude: -9°24.653
Longitude: 144°00.710
Recovery Date: 31-01-02
Water Depth (m): 59
Visual Log
Grain Size
Section
Sub-sample
Sed. Structures
Fossils
Colour
Bulk Density (g/cc)
P-wave Velocity (km/s)
Magnetic Susceptibility (cgs)
Fractional Porosity
Description and Remarks
Part 2a
Part 1b
5Y4/2
N3
N3
N6
Olive grey slightly muddy calcareous fine sand
Abundant peat deposits throughout
Clay layer @ 0.15 m
Unconformity - scalloped, scoured
Very dark grey sticky silty clay
Homogeneous throughout
Large peat deposit between 0.44 - 0.58 m
Abundant peat deposits throughout
Very dark grey sticky silty clay
Homogeneous throughout
Large peat deposit between 0.75 - 0.77 m
Abundant peat deposits throughout
Peat samples taken for C-14 age determinations @ 0.02, 0.25-0.26, 0.46-0.47, 0.75-0.76, 0.89-0.91, 1.17-1.18, 1.40-1.42 and 1.51 m
Gradual transition between 1.10-1.19 m (irregular)
Grey sticky silty clay
Abundant peat deposits throughout
Leaf imprint between 1.31 - 1.36 m
Root/branch between 1.41 - 1.44 m (mangrove?)
Bottom of Core
Depth (m)

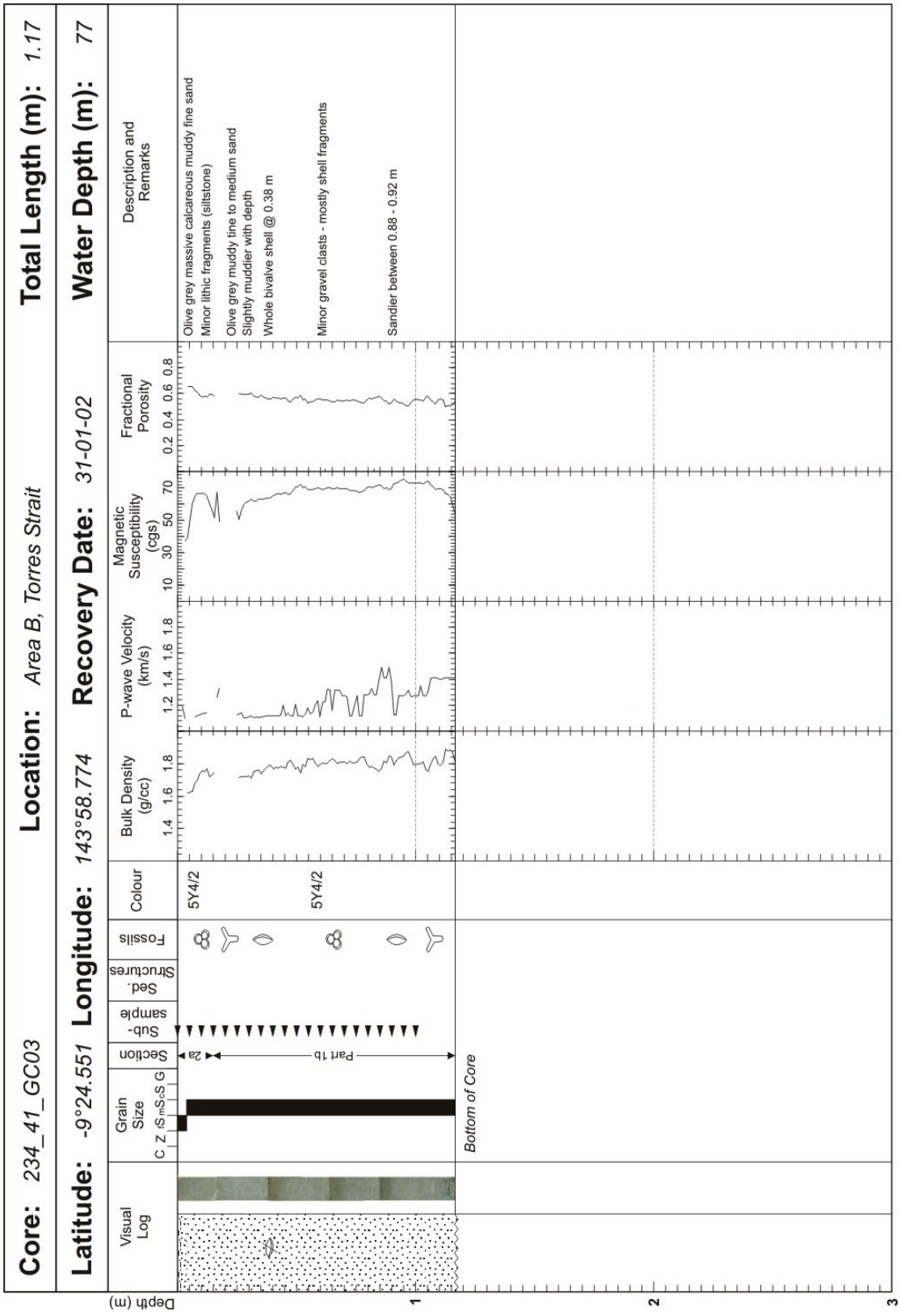
Core: 234_41_GC03
Location: Area B, Torres Strait
Total Length (m): 1.17
Latitude: -9°24.551 Longitude: 143°58.774 Recovery Date: 31-01-02
Water Depth (m): 77
Visual Log
Grain Size
C Z S mS cS G
Section
2a
Part 1b
Sub-sample
Sed. Structures
Fossils
Colour
5Y4/2
5Y4/2
Bulk Density (g/cc)
1.4 1.6 1.8
P-wave Velocity (km/s)
1.2 1.4 1.6 1.8
Magnetic Susceptibility (cgs)
10 30 50 70
Fractional Porosity
0.2 0.4 0.6 0.8
Description and Remarks
Olive grey massive calcareous muddy fine sand
Minor lithic fragments (siltstone)
Olive grey muddy tine to medium sand
Slightly muddier with depth
Whole bivalve shell @ 0.38 m
Minor gravel clasts - mostly shell fragments
Sandier between 0.88 - 0.92 m
Bottom of Core
Depth (m)
1
2
3

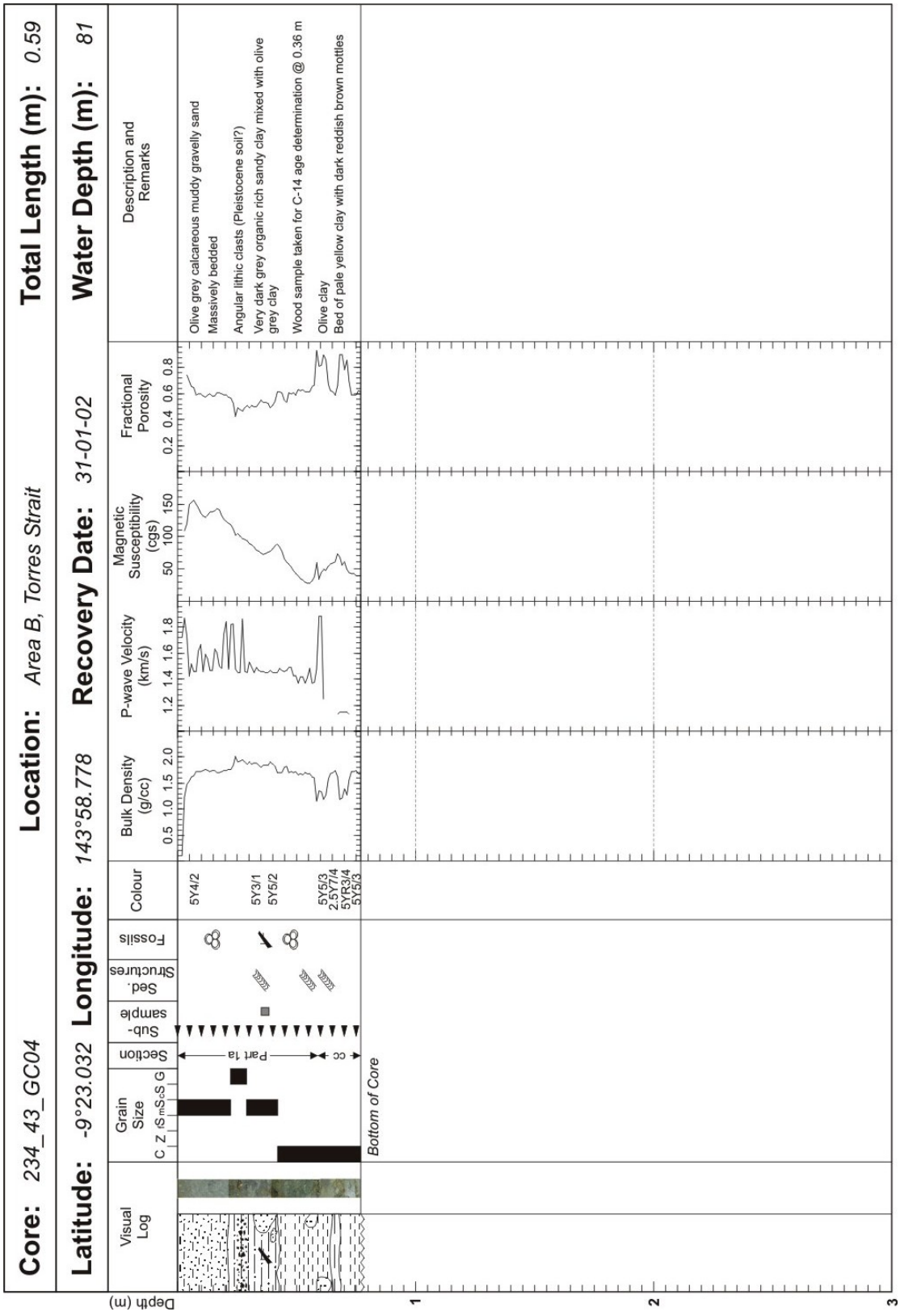
Core: 234_43_GC04
Location: Area B, Torres Strait
Total Length (m): 0.59
Latitude: -9°23.032 Longitude: 143°58.778
Recovery Date: 31-01-02
Water Depth (m): 81
Visual Log
Grain Size
C Z S mS cS G
Section
Sub-sample
Sed. Structures
Fossils
Colour
Bulk Density (g/cc)
0.5 1.0 1.5 2.0
P-wave Velocity (km/s)
1.2 1.4 1.6 1.8
Magnetic Susceptibility (cgs)
50 100 150
Fractional Porosity
0.2 0.4 0.6 0.8
Description and Remarks
Part 1a
cc
5Y4/2
5Y3/1
5Y5/2
5Y5/3
2.5Y7/4
5YR3/4
5Y5/3
Olive grey calcareous muddy gravelly sand
Massively bedded
Angular lithic clasts (Pleistocene soil?)
Very dark grey organic rich sandy clay mixed with olive grey clay
Wood sample taken for C-14 age determination @ 0.36 m
Olive clay
Bed of pale yellow clay with dark reddish brown mottles
Bottom of Core
Depth (m)
1
2
3

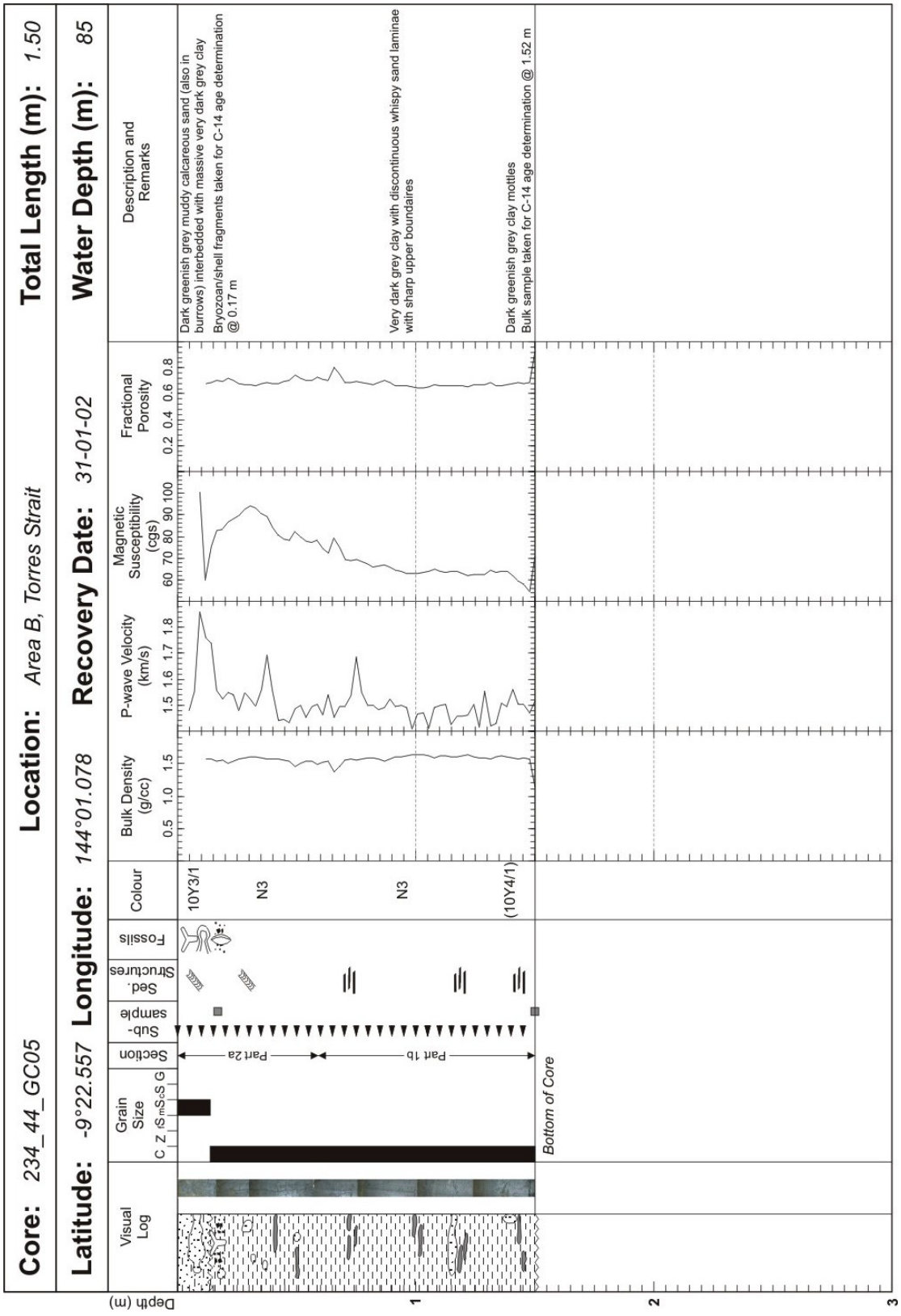
Core: 234_44_GC05
Location: Area B, Torres Strait
Total Length (m): 1.50
Latitude: -9°22.557 Longitude: 144°01.078
Recovery Date: 31-01-02
Water Depth (m): 85
Visual Log
Grain Size
Section
Sub-sample
Sed. Structures
Fossils
Colour
Bulk Density (g/cc)
P-wave Velocity (km/s)
Magnetic Susceptibility (cgs)
Fractional Porosity
Description and Remarks
Part 2a
Part 1b
10Y3/1
N3
N3
(10Y4/1)
Dark greenish grey muddy calcareous sand (also in burrows) interbedded with massive very dark grey clay
Bryozoan/shell fragments taken for C-14 age determination @ 0.17 m
Very dark grey clay with discontinuous whispy sand laminae with sharp upper boundaires
Dark greenish grey clay mottles
Bulk sample taken for C-14 age determination @ 1.52 m
Bottom of Core
Depth (m)

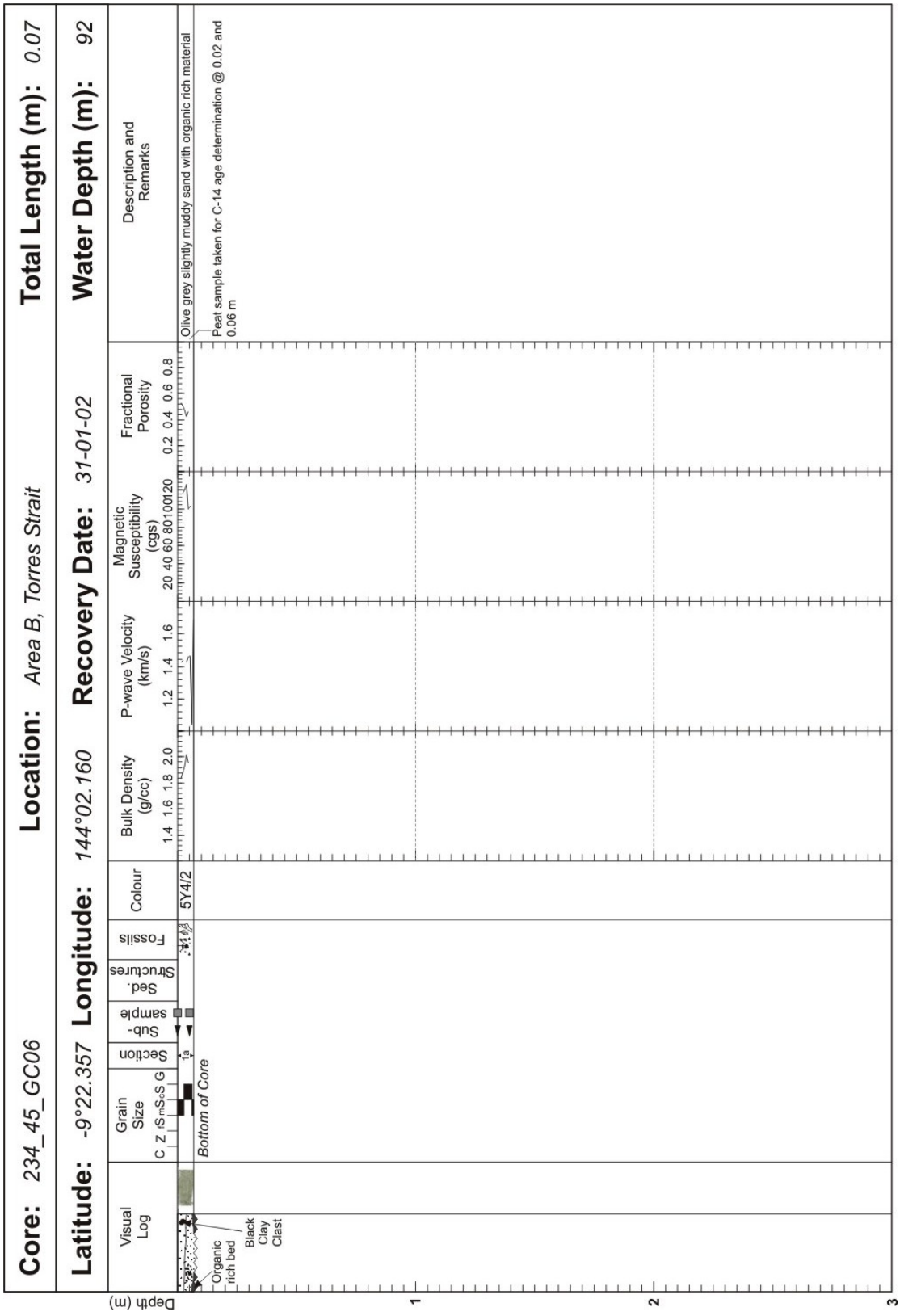
Core: 234_45_GC06
Location: Area B, Torres Strait
Total Length (m): 0.07
Latitude: -9°22.357 Longitude: 144°02.160 Recovery Date: 31-01-02
Water Depth (m): 92
Visual Log
Grain Size
C Z fS mS cS G
Section
Sub-sample
Sed. Structures
Fossils
Colour
Bulk Density (g/cc)
1.4 1.6 1.8 2.0
P-wave Velocity (km/s)
1.2 1.4 1.6
Magnetic Susceptibility (cgs)
20 40 60 80 100 120
Fractional Porosity
0.2 0.4 0.6 0.8
Description and Remarks
Depth (m)
Organic rich bed
Black Clay Clast
Bottom of Core
5Y4/2
Olive grey slightly muddy sand with organic rich material
Peat sample taken for C-14 age determination @ 0.02 and 0.06 m
1
2
3

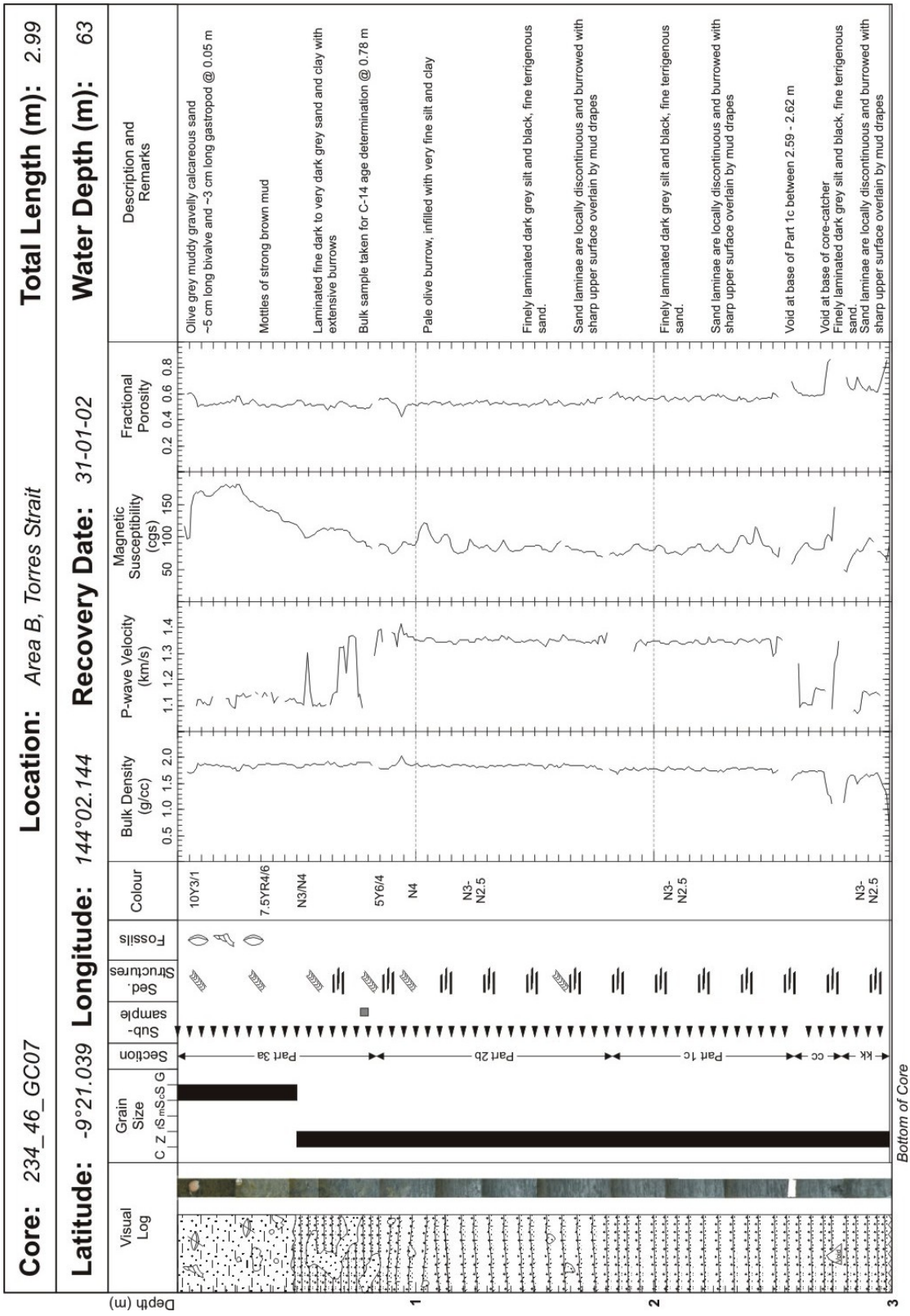
Core: 234_46_GC07
Location: Area B, Torres Strait
Total Length (m): 2.99
Latitude: -9°21.039 Longitude: 144°02.144
Recovery Date: 31-01-02
Water Depth (m): 63
Visual Log
Grain Size
Section
Sub-sample
Sed. Structures
Fossils
Colour
Bulk Density (g/cc)
P-wave Velocity (km/s)
Magnetic Susceptibility (cgs)
Fractional Porosity
Description and Remarks
Depth (m)
Part 3a
Part 2b
Part 1c
cc
kk
10Y3/1
7.5YR4/6
N3/N4
5Y6/4
N4
N3-N2.5
Olive grey muddy gravelly calcareous sand ~5 cm long bivalve and ~3 cm long gastropod @ 0.05 m
Mottles of strong brown mud
Laminated fine dark to very dark grey sand and clay with extensive burrows
Bulk sample taken for C-14 age determination @ 0.78 m
Pale olive burrow, infilled with very fine silt and clay
Finely laminated dark grey silt and black, fine terrigenous sand.
Sand laminae are locally discontinuous and burrowed with sharp upper surface overlain by mud drapes
Void at base of Part 1c between 2.59 - 2.62 m
Void at base of core-catcher
Bottom of Core

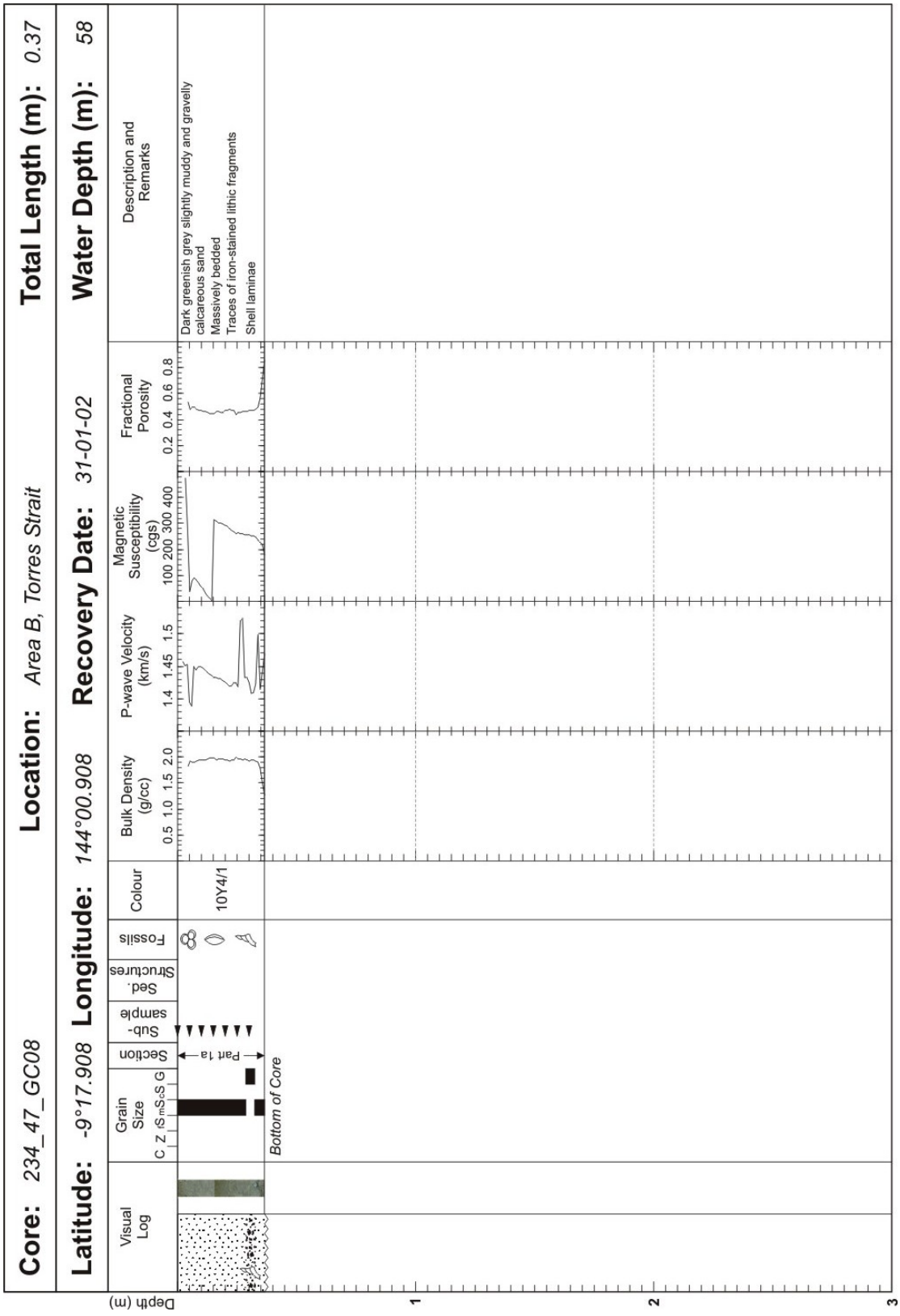
Core: 234_47_GC08
Location: Area B, Torres Strait
Total Length (m): 0.37
Latitude: -9°17.908 Longitude: 144°00.908
Recovery Date: 31-01-02
Water Depth (m): 58
Visual Log
Grain Size
C Z S mS cS G
Section
Sub-sample
Sed. Structures
Fossils
Colour
Bulk Density (g/cc)
0.5 1.0 1.5 2.0
P-wave Velocity (km/s)
1.4 1.45 1.5
Magnetic Susceptibility (cgs)
100 200 300 400
Fractional Porosity
0.2 0.4 0.6 0.8
Description and Remarks
Part 1a
10Y4/1
Dark greenish grey slightly muddy and gravelly calcareous sand
Massively bedded
Traces of iron-stained lithic fragments
Shell laminae
Bottom of Core
Depth (m)
1
2
3

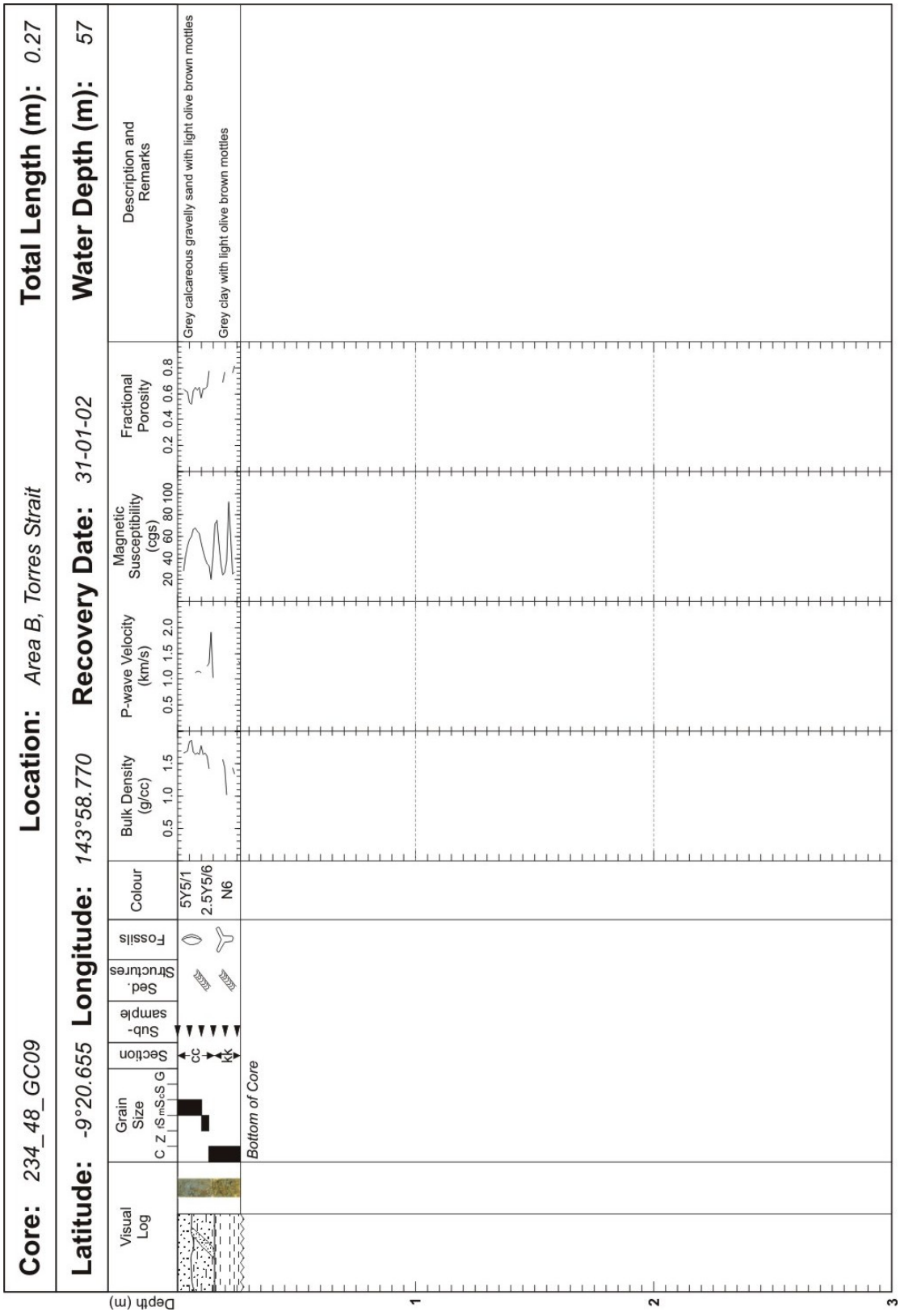
Core: 234_48_GC09
Location: Area B, Torres Strait
Total Length (m): 0.27
Latitude: -9°20.655 Longitude: 143°58.770
Recovery Date: 31-01-02
Water Depth (m): 57
Visual Log
Grain Size
C Z fS mS cS G
Section
Sub-sample
Sed. Structures
Fossils
Colour
Bulk Density (g/cc)
0.5 1.0 1.5
P-wave Velocity (km/s)
0.5 1.0 1.5 2.0
Magnetic Susceptibility (cgs)
20 40 60 80 100
Fractional Porosity
0.2 0.4 0.6 0.8
Description and Remarks
cc
kk
5Y5/1
2.5Y5/6
N6
Grey calcareous gravelly sand with light olive brown mottles
Grey clay with light olive brown mottles
Bottom of Core
Depth (m)
1
2
3

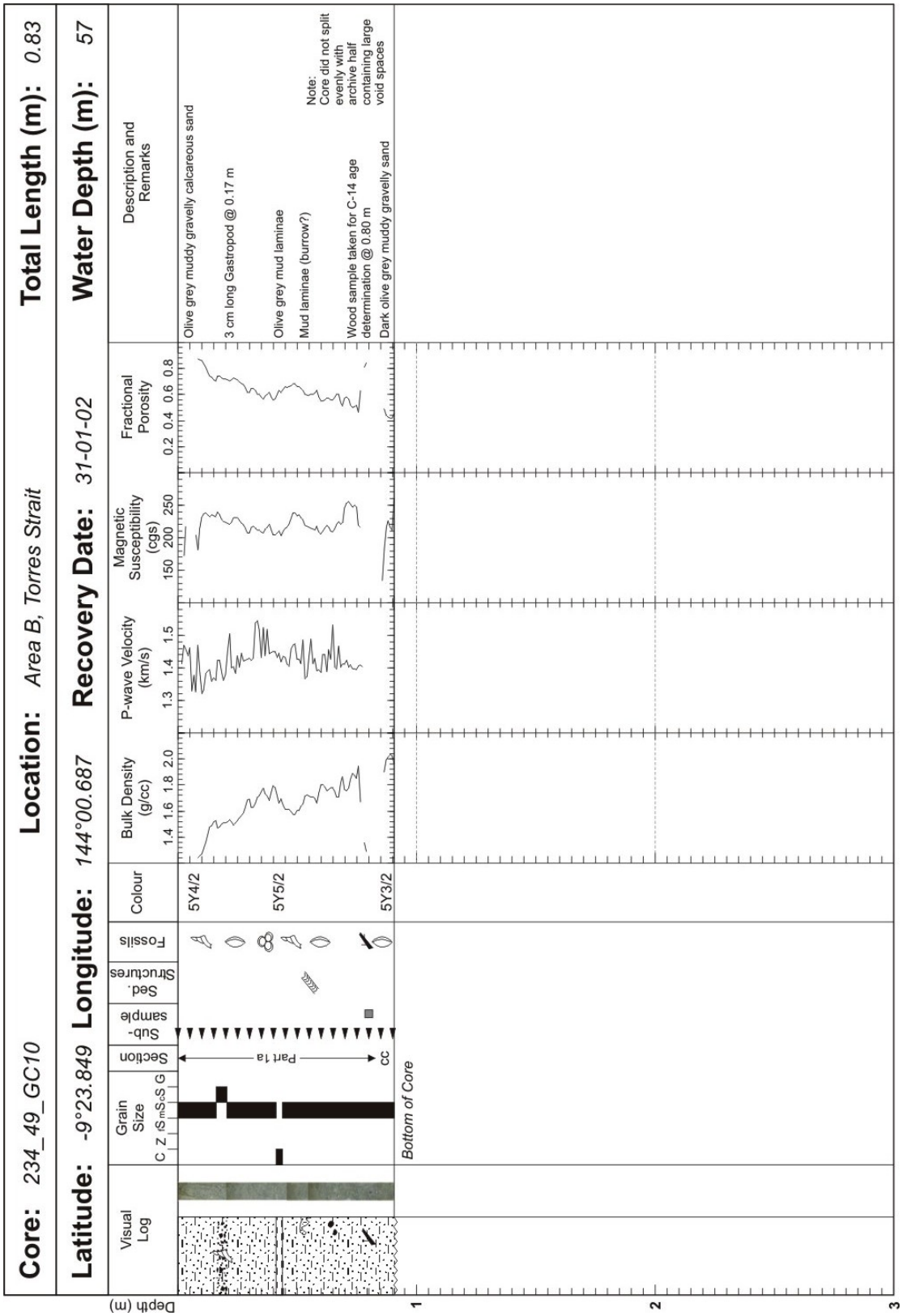
Core: 234_49_GC10
Location: Area B, Torres Strait
Total Length (m): 0.83
Latitude: -9°23.849 Longitude: 144°00.687
Recovery Date: 31-01-02
Water Depth (m): 57
Visual Log
Grain Size
C Z S mS cS G
Section
Sub-sample
Sed. Structures
Fossils
Colour
Bulk Density (g/cc)
1.4 1.6 1.8 2.0
P-wave Velocity (km/s)
1.3 1.4 1.5
Magnetic Susceptibility (cgs)
150 200 250
Fractional Porosity
0.2 0.4 0.6 0.8
Description and Remarks
Part 1a
cc
5Y4/2
5Y5/2
5Y3/2
Olive grey muddy gravelly calcareous sand
3 cm long Gastropod @ 0.17 m
Olive grey mud laminae
Mud laminae (burrow?)
Wood sample taken for C-14 age determination @ 0.80 m
Dark olive grey muddy gravelly sand
Note: Core did not split evenly with archive half containing large void spaces
Bottom of Core
Depth (m)
1
2
3

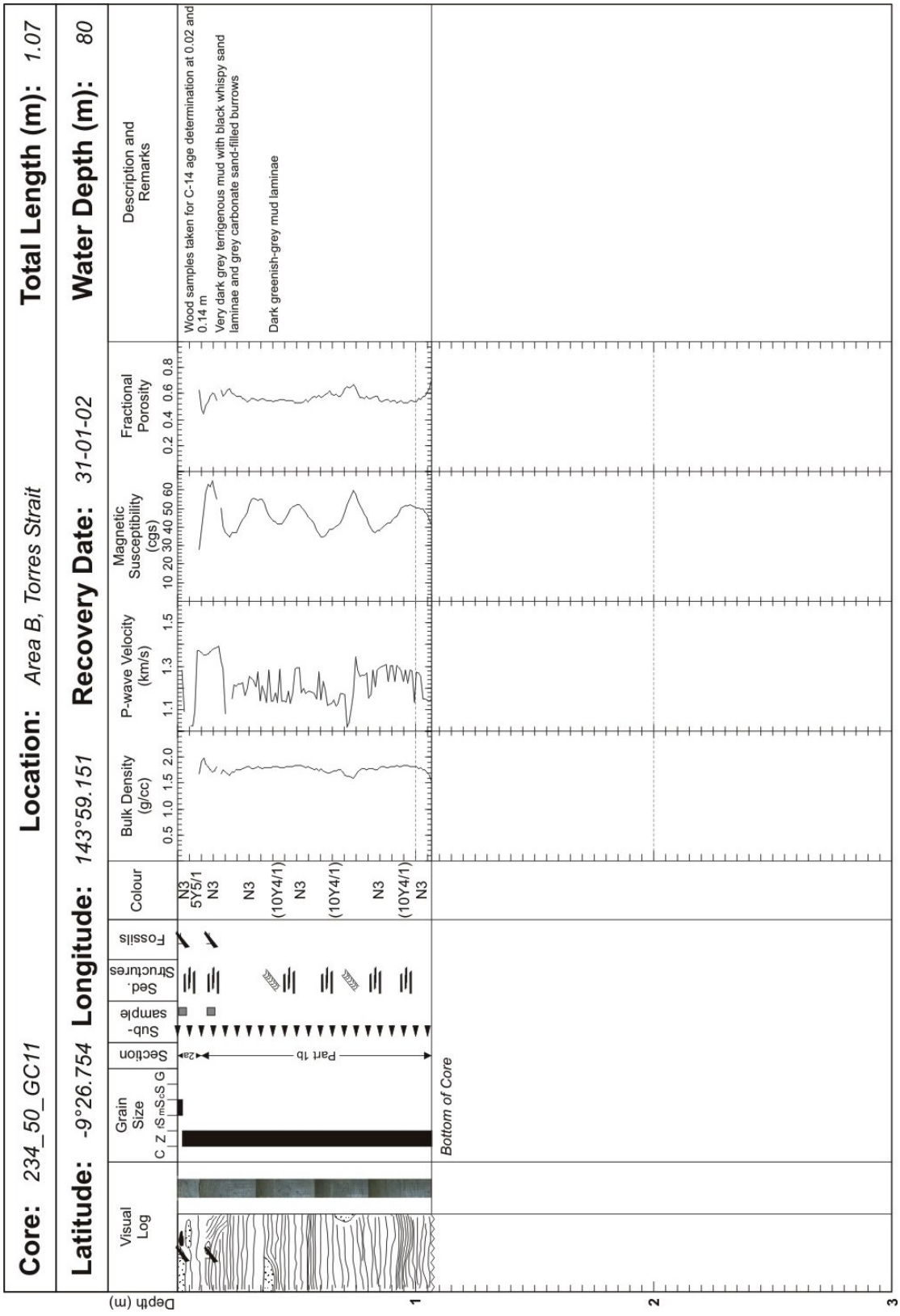
Core: 234_50_GC11
Location: Area B, Torres Strait
Total Length (m): 1.07
Latitude: -9°26.754 Longitude: 143°59.151 Recovery Date: 31-01-02
Water Depth (m): 80
Visual Log
Grain Size
Section
Sub-sample
Sed. Structures
Fossils
Colour
Bulk Density (g/cc)
P-wave Velocity (km/s)
Magnetic Susceptibility (cgs)
Fractional Porosity
Description and Remarks
Wood samples taken for C-14 age determination at 0.02 and 0.14 m
Very dark grey terrigenous mud with black whispy sand laminae and grey carbonate sand-filled burrows
Dark greenish-grey mud laminae
Part 1b
Bottom of Core
Depth (m)

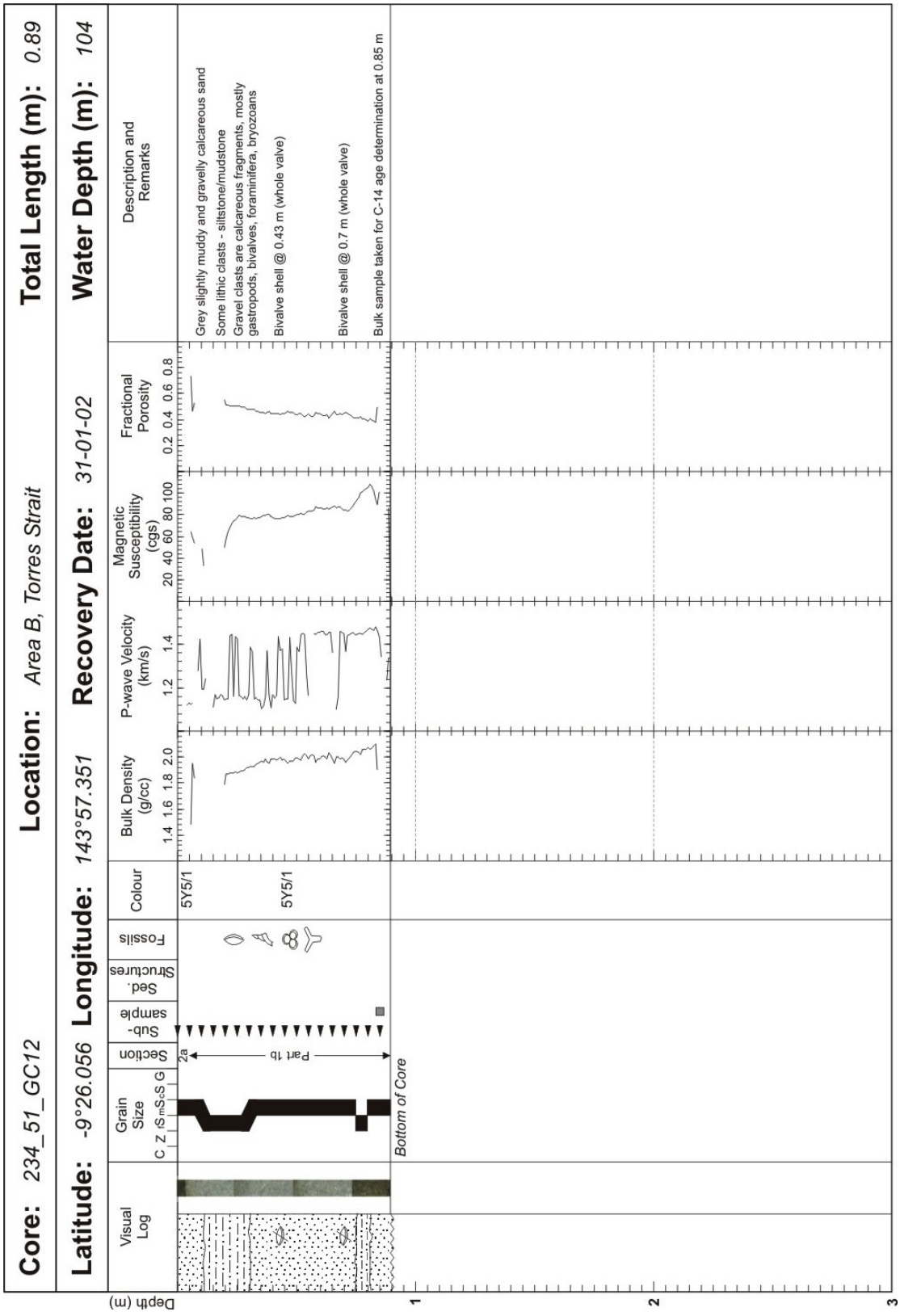
Core: 234_51_GC12
Location: Area B, Torres Strait
Total Length (m): 0.89
Latitude: -9°26.056 Longitude: 143°57.351
Recovery Date: 31-01-02
Water Depth (m): 104
Visual Log
Grain Size
C Z S mS cS G
Section
Sub-sample
Sed. Structures
Fossils
Colour
Bulk Density (g/cc)
1.4 1.6 1.8 2.0
P-wave Velocity (km/s)
1.2 1.4
Magnetic Susceptibility (cgs)
20 40 60 80 100
Fractional Porosity
0.2 0.4 0.6 0.8
Description and Remarks
2a
Part 1b
5Y5/1
5Y5/1
Grey slightly muddy and gravelly calcareous sand
Some lithic clasts - siltstone/mudstone
Gravel clasts are calcareous fragments, mostly gastropods, bivalves, foraminifera, bryozoans
Bivalve shell @ 0.43 m (whole valve)
Bivalve shell @ 0.7 m (whole valve)
Bulk sample taken for C-14 age determination at 0.85 m
Bottom of Core
Depth (m)
1
2
3

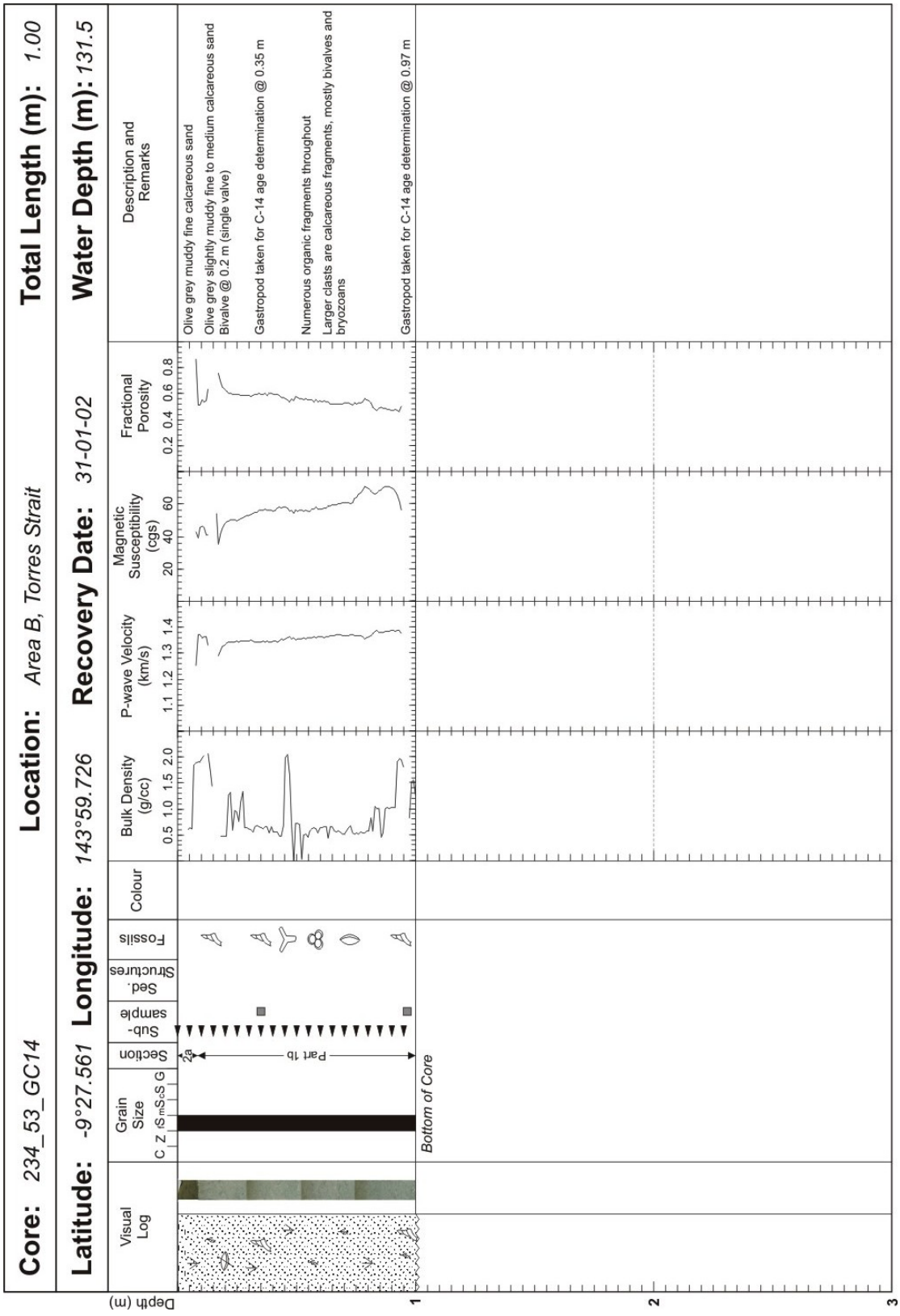
Core: 234_53_GC14
Location: Area B, Torres Strait
Total Length (m): 1.00
Latitude: -9°27.561 Longitude: 143°59.726 Recovery Date: 31-01-02
Water Depth (m): 131.5
Visual Log
Grain Size
Section
Sub-sample
Sed. Structures
Fossils
Colour
Bulk Density (g/cc)
P-wave Velocity (km/s)
Magnetic Susceptibility (cgs)
Fractional Porosity
Description and Remarks
Olive grey muddy fine calcareous sand
Olive grey slightly muddy fine to medium calcareous sand
Bivalve @ 0.2 m (single valve)
Gastropod taken for C-14 age determination @ 0.35 m
Numerous organic fragments throughout
Larger clasts are calcareous fragments, mostly bivalves and bryozoans
Gastropod taken for C-14 age determination @ 0.97 m
Part 1b
Bottom of Core
Depth (m)

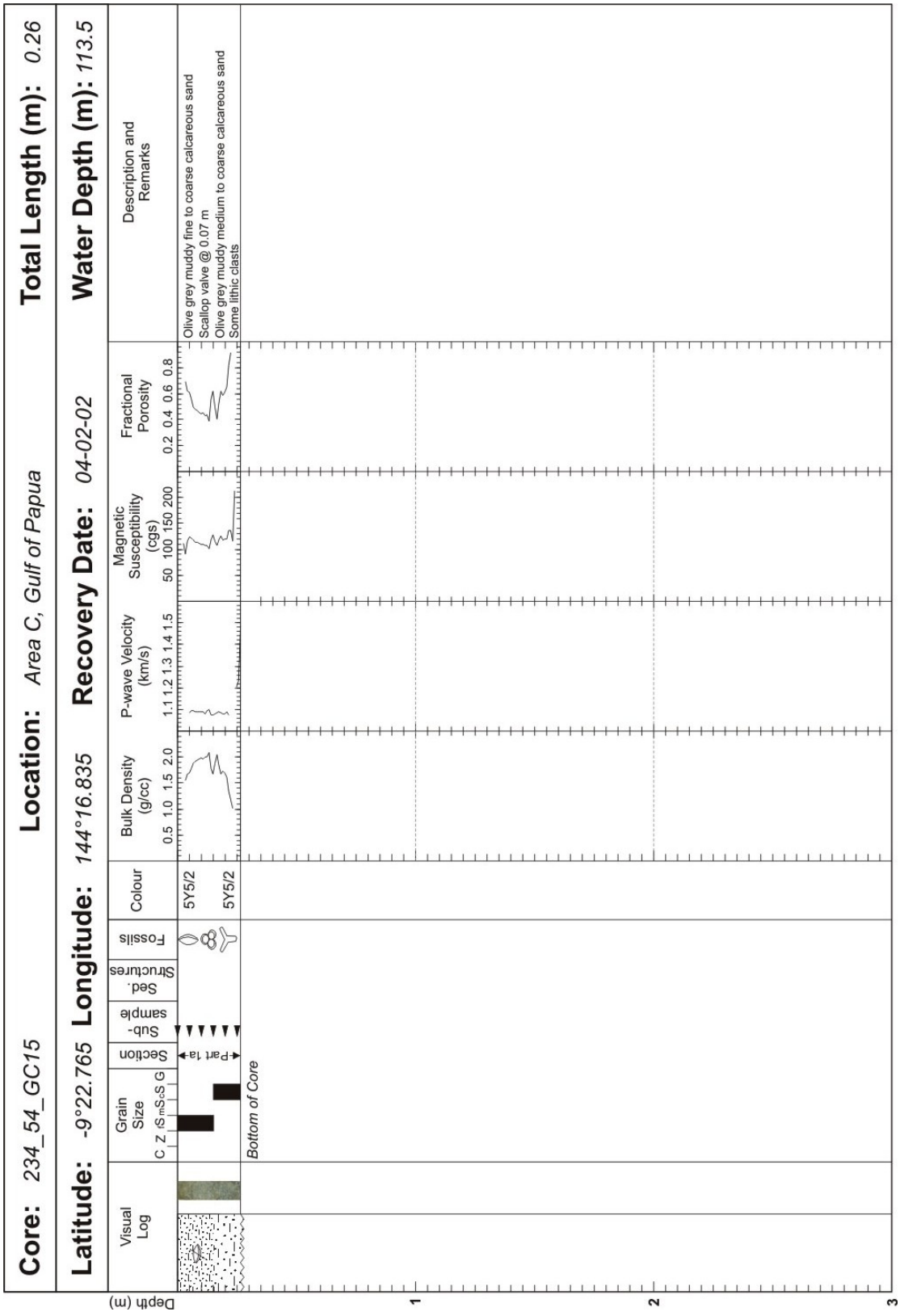
Core: 234_54_GC15
Location: Area C, Gulf of Papua
Total Length (m): 0.26
Latitude: -9°22.765 Longitude: 144°16.835
Recovery Date: 04-02-02
Water Depth (m): 113.5
Visual Log
Grain Size
C Z S mS cS G
Section
Sub-sample
Sed. Structures
Fossils
Colour
Bulk Density (g/cc)
0.5 1.0 1.5 2.0
P-wave Velocity (km/s)
1.1 1.2 1.3 1.4 1.5
Magnetic Susceptibility (cgs)
50 100 150 200
Fractional Porosity
0.2 0.4 0.6 0.8
Description and Remarks
Part 1a
5Y5/2
5Y5/2
Olive grey muddy fine to coarse calcareous sand
Scallop valve @ 0.07 m
Olive grey muddy medium to coarse calcareous sand
Some lithic clasts
Bottom of Core
Depth (m)
1
2
3

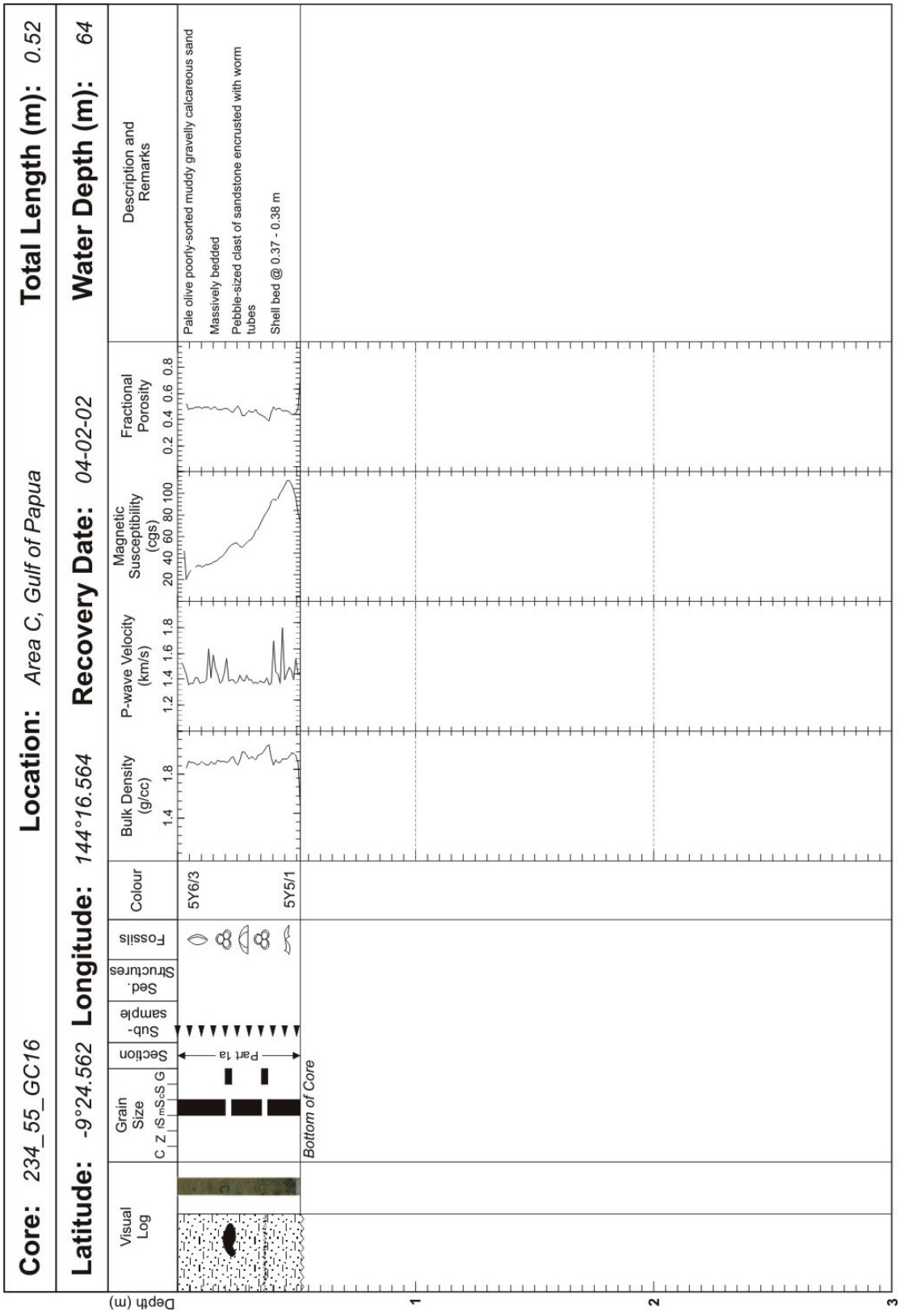
Core: 234_55_GC16
Location: Area C, Gulf of Papua
Total Length (m): 0.52
Latitude: -9°24.562 Longitude: 144°16.564
Recovery Date: 04-02-02
Water Depth (m): 64
Visual Log
Grain Size
C Z S mS S G
Section
Sub-sample
Sed. Structures
Fossils
Colour
Bulk Density (g/cc)
1.4 1.8
P-wave Velocity (km/s)
1.2 1.4 1.6 1.8
Magnetic Susceptibility (cgs)
20 40 60 80 100
Fractional Porosity
0.2 0.4 0.6 0.8
Description and Remarks
Part 1a
5Y6/3
5Y5/1
Pale olive poorly-sorted muddy gravelly calcareous sand
Massively bedded
Pebble-sized clast of sandstone encrusted with worm tubes
Shell bed @ 0.37 - 0.38 m
Bottom of Core
Depth (m)
1
2
3

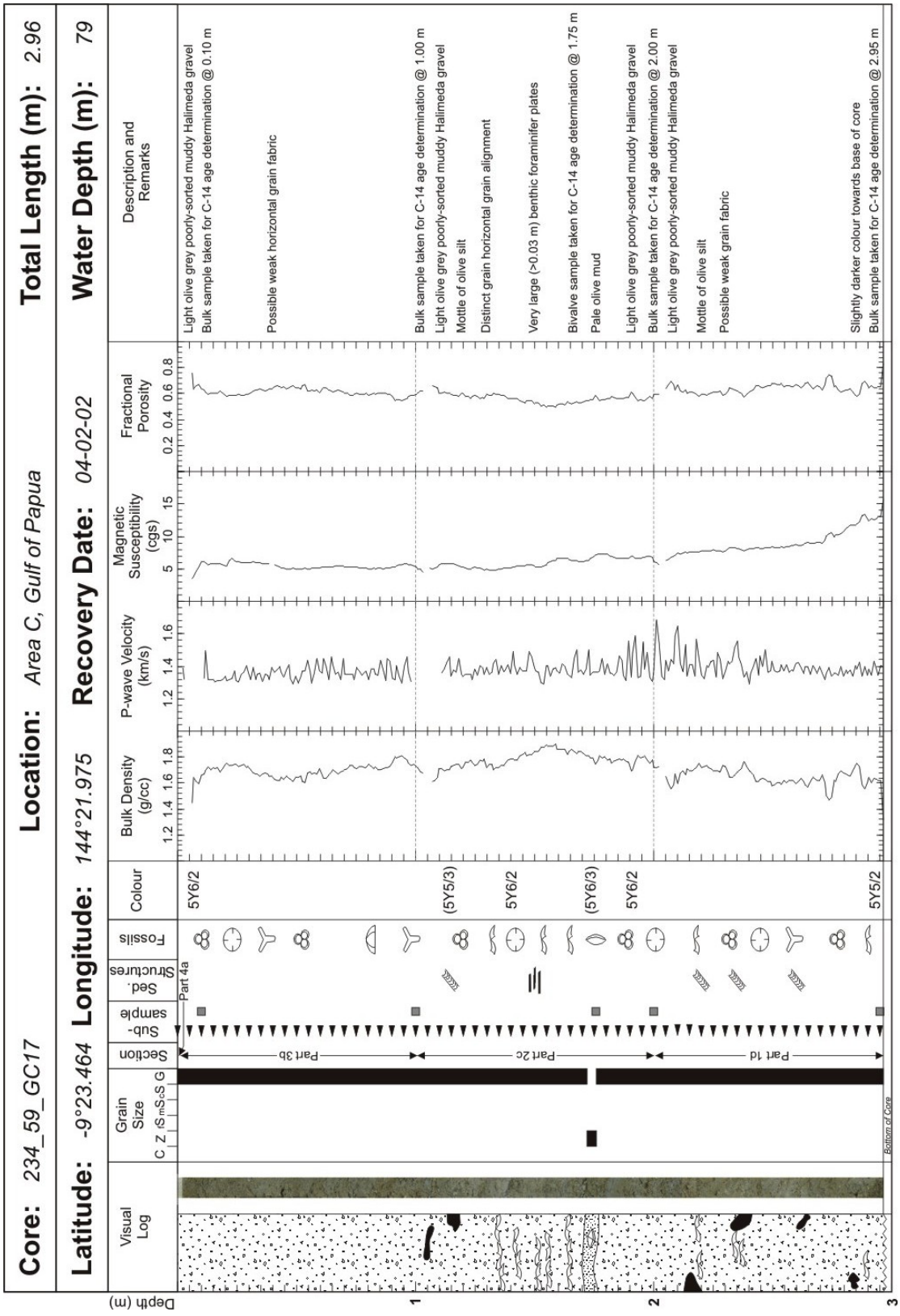
Core: 234_59_GC17
Location: Area C, Gulf of Papua
Total Length (m): 2.96
Latitude: -9°23.464 Longitude: 144°21.975
Recovery Date: 04-02-02
Water Depth (m): 79
Visual Log
Grain Size
Section
Sub-sample
Sed. Structures
Fossils
Colour
Bulk Density (g/cc)
P-wave Velocity (km/s)
Magnetic Susceptibility (cgs)
Fractional Porosity
Description and Remarks
Part 4a
Part 3b
Part 2c
Part 1d
5Y6/2
(5Y5/3)
5Y6/2
(5Y6/3)
5Y6/2
5Y5/2
Light olive grey poorly-sorted muddy Halimeda gravel
Bulk sample taken for C-14 age determination @ 0.10 m
Possible weak horizontal grain fabric
Bulk sample taken for C-14 age determination @ 1.00 m
Light olive grey poorly-sorted muddy Halimeda gravel
Mottle of olive silt
Distinct grain horizontal grain alignment
Very large (>0.03 m) benthic foraminifer plates
Bivalve sample taken for C-14 age determination @ 1.75 m
Pale olive mud
Light olive grey poorly-sorted muddy Halimeda gravel
Bulk sample taken for C-14 age determination @ 2.00 m
Light olive grey poorly-sorted muddy Halimeda gravel
Mottle of olive silt
Possible weak grain fabric
Slightly darker colour towards base of core
Bulk sample taken for C-14 age determination @ 2.95 m
Bottom of Core
Depth (m)
1
2
3

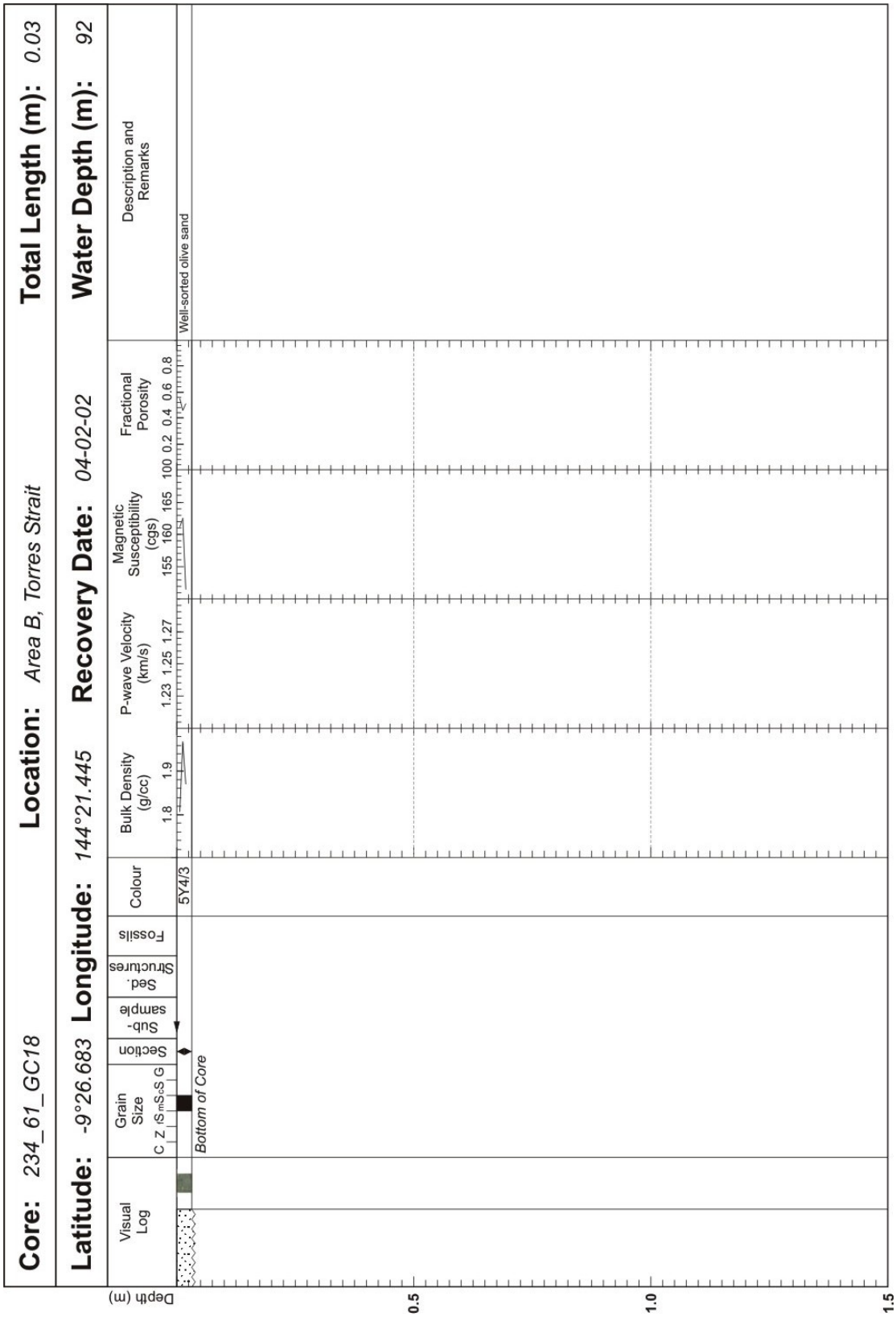
Core: 234_61_GC18
Location: Area B, Torres Strait
Total Length (m): 0.03
Latitude: -9°26.683 Longitude: 144°21.445
Recovery Date: 04-02-02
Water Depth (m): 92
Visual Log
Grain Size
C Z fS mS cS G
Section
Sub-sample
Sed. Structures
Fossils
Colour
Bulk Density (g/cc)
1.8 1.9
P-wave Velocity (km/s)
1.23 1.25 1.27
Magnetic Susceptibility (cgs)
155 160 165
Fractional Porosity
100 0.2 0.4 0.6 0.8
Description and Remarks
5Y4/3
Well-sorted olive sand
Bottom of Core
Depth (m)
0.5
1.0
1.5

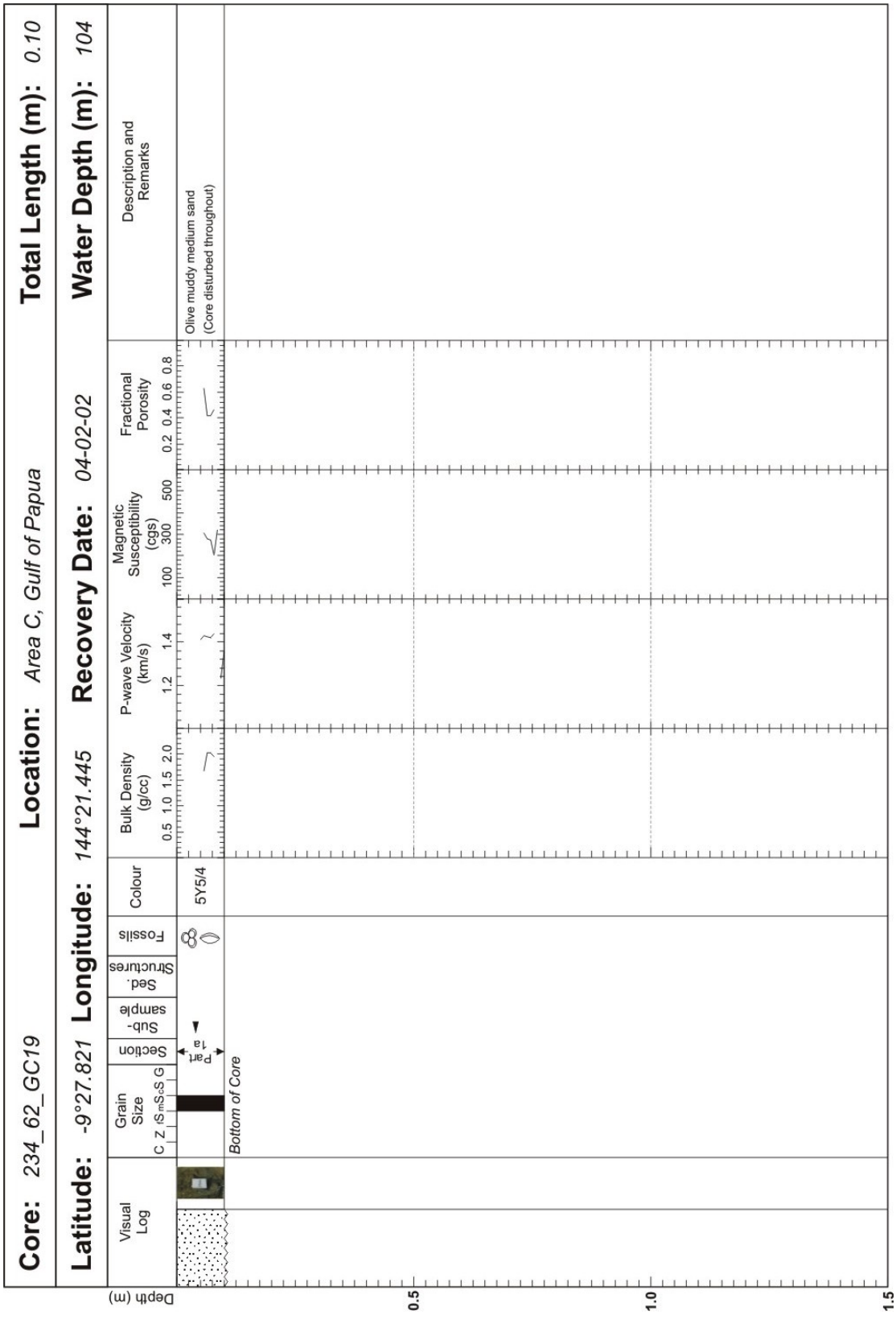
Core: 234_62_GC19
Location: Area C, Gulf of Papua
Total Length (m): 0.10
Latitude: -9°27.821 Longitude: 144°21.445
Recovery Date: 04-02-02
Water Depth (m): 104
Visual Log
Grain Size
C Z S mS cS G
Section
Part 1a
Sub-sample
Sed. Structures
Fossils
Colour
Bulk Density (g/cc)
0.5 1.0 1.5 2.0
P-wave Velocity (km/s)
1.2 1.4
Magnetic Susceptibility (cgs)
100 300 500
Fractional Porosity
0.2 0.4 0.6 0.8
Description and Remarks
5Y5/4
Olive muddy medium sand
(Core disturbed throughout)
Bottom of Core
Depth (m)
0.5
1.0
1.5

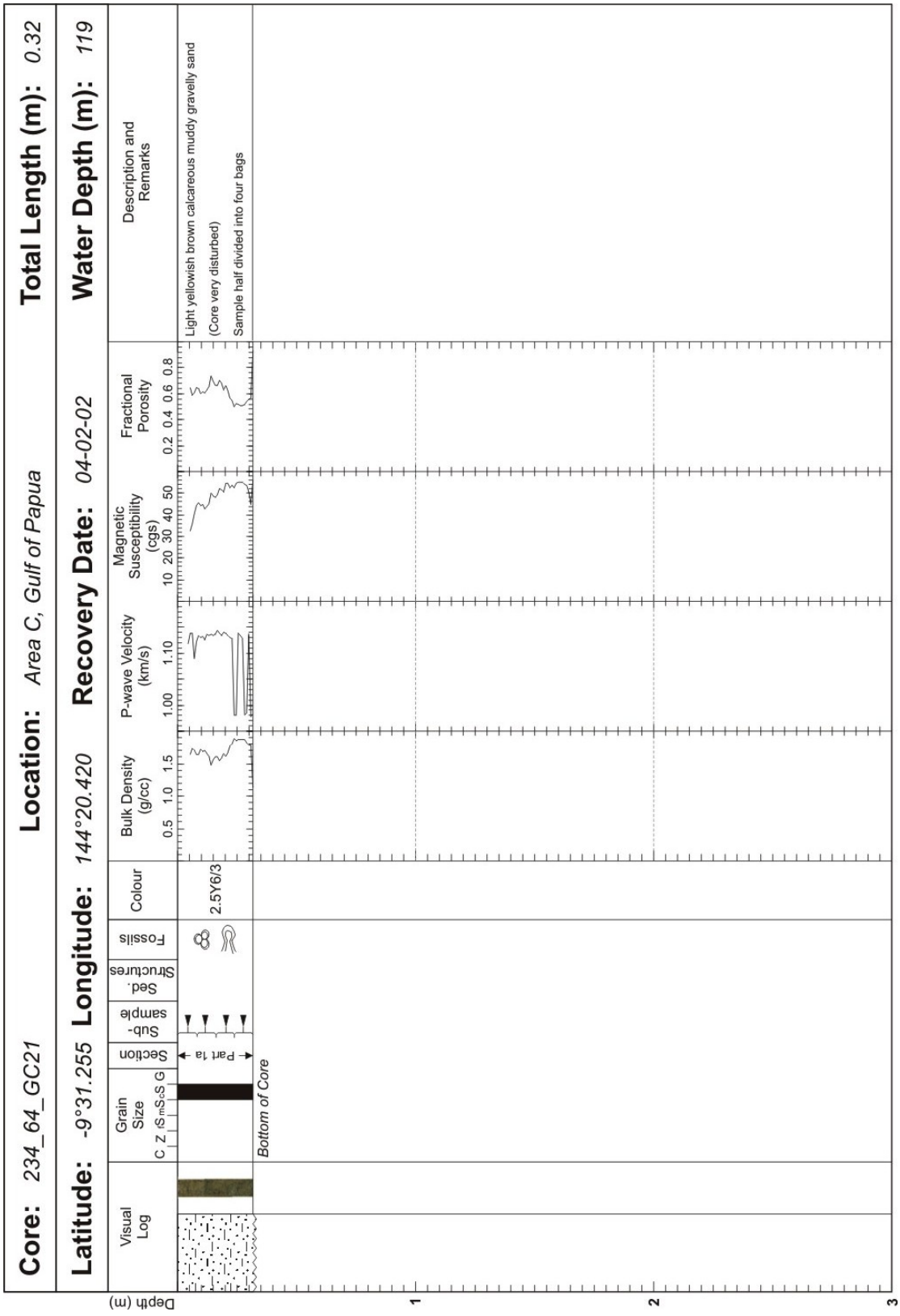
Core: 234_64_GC21
Location: Area C, Gulf of Papua
Total Length (m): 0.32
Latitude: -9°31.255 Longitude: 144°20.420
Recovery Date: 04-02-02
Water Depth (m): 119
Visual Log
Grain Size
C Z S mS cS G
Section
Sub-sample
Sed. Structures
Fossils
Colour
Bulk Density (g/cc)
0.5 1.0 1.5
P-wave Velocity (km/s)
1.00 1.10
Magnetic Susceptibility (cgs)
10 20 30 40 50
Fractional Porosity
0.2 0.4 0.6 0.8
Description and Remarks
Part 1a
2.5Y6/3
Bottom of Core
Light yellowish brown calcareous muddy gravelly sand
(Core very disturbed)
Sample half divided into four bags
Depth (m)
1
2
3

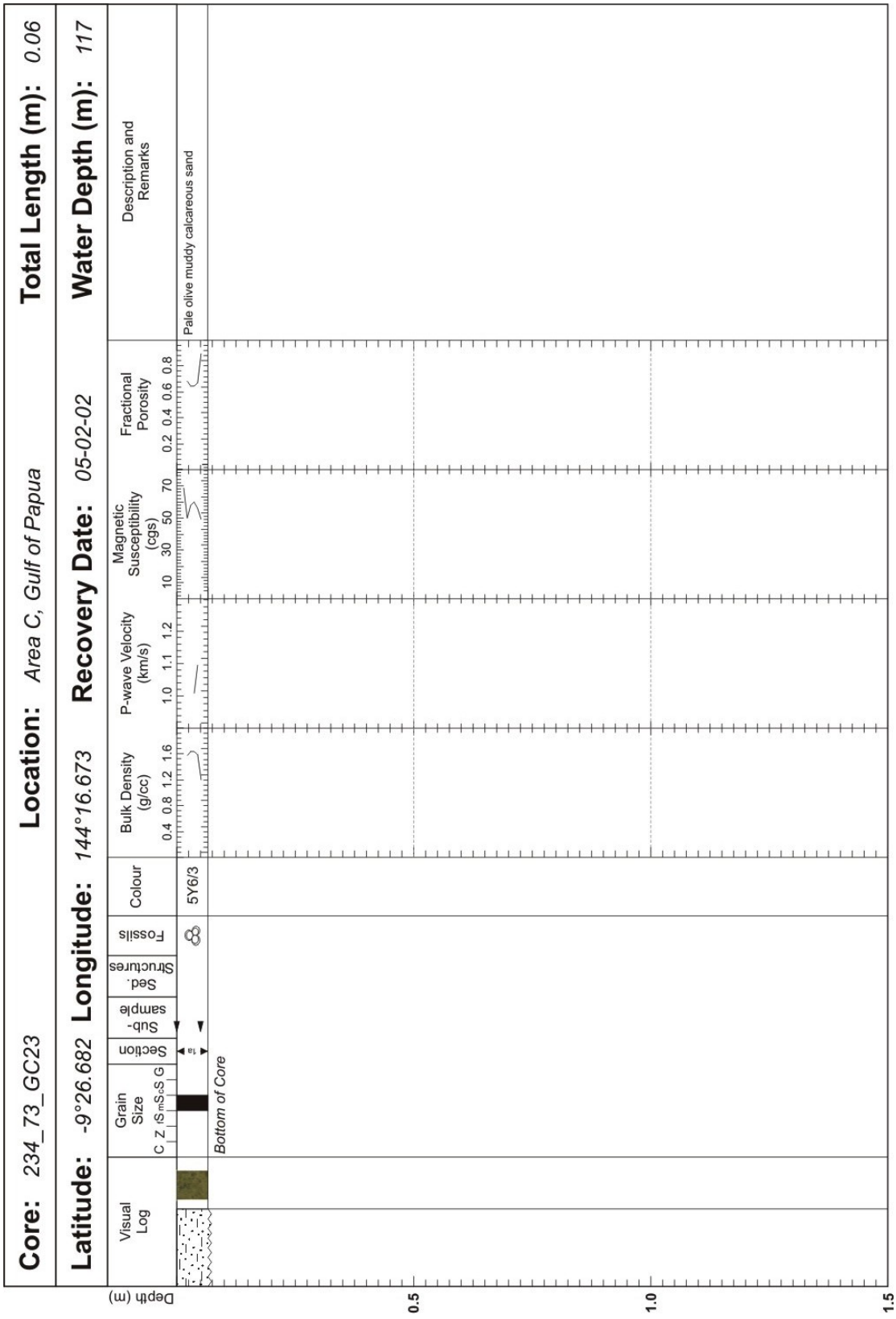
Core: 234_73_GC23
Location: Area C, Gulf of Papua
Total Length (m): 0.06
Latitude: -9°26.682 Longitude: 144°16.673
Recovery Date: 05-02-02
Water Depth (m): 117
Visual Log
Grain Size
C Z S mS cS G
Section
Sub-sample
Sed. Structures
Fossils
Colour
Bulk Density (g/cc)
0.4 0.8 1.2 1.6
P-wave Velocity (km/s)
1.0 1.1 1.2
Magnetic Susceptibility (cgs)
10 30 50 70
Fractional Porosity
0.2 0.4 0.6 0.8
Description and Remarks
5Y6/3
Pale olive muddy calcareous sand
Bottom of Core
Depth (m)
0.5
1.0
1.5

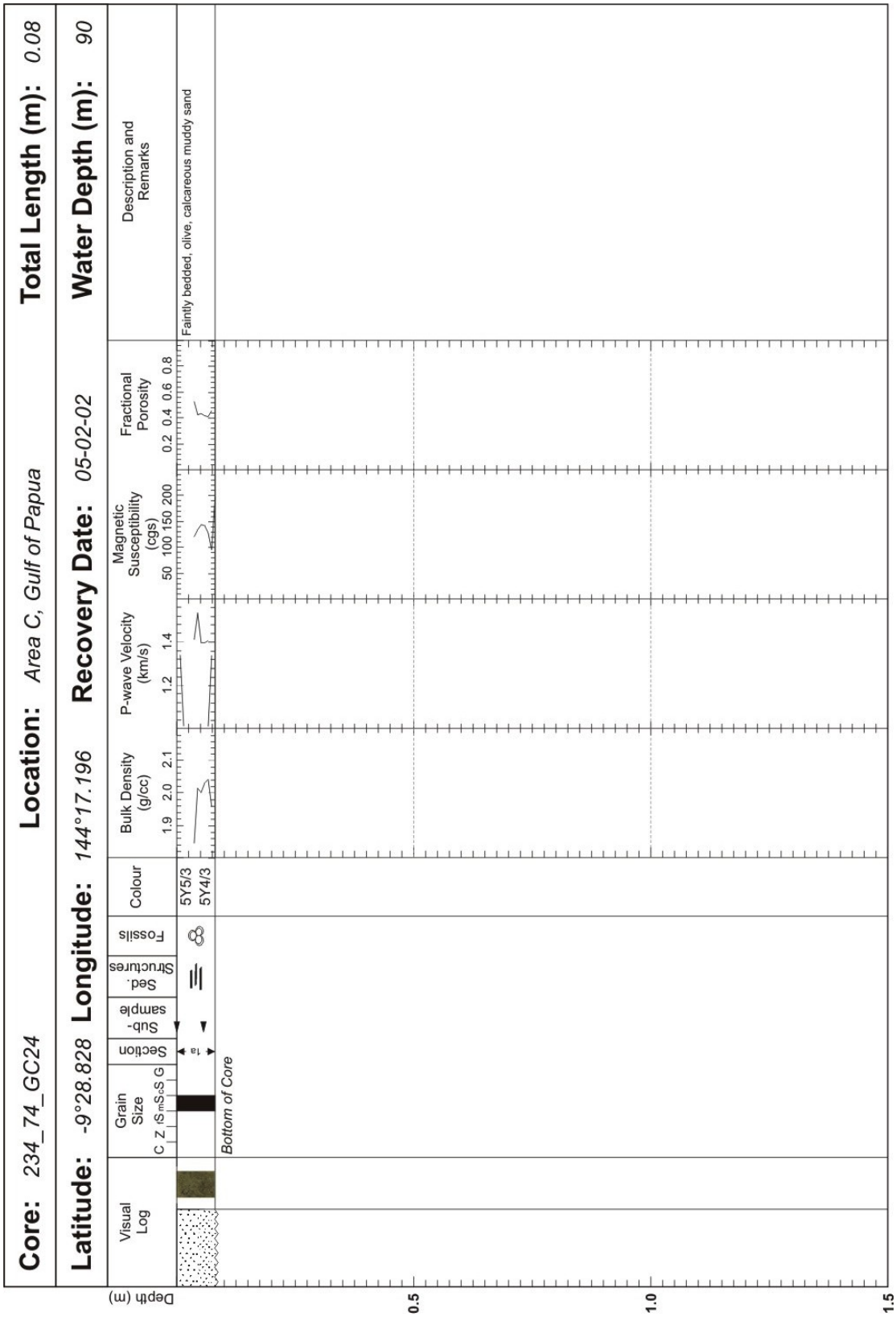
Core: 234_74_GC24
Location: Area C, Gulf of Papua
Total Length (m): 0.08
Latitude: -9°28.828 Longitude: 144°17.196
Recovery Date: 05-02-02
Water Depth (m): 90
Visual Log
Grain Size
C Z S mS cS G
Section
Sub-sample
Sed. Structures
Fossils
Colour
Bulk Density (g/cc)
1.9 2.0 2.1
P-wave Velocity (km/s)
1.2 1.4
Magnetic Susceptibility (cgs)
50 100 150 200
Fractional Porosity
0.2 0.4 0.6 0.8
Description and Remarks
1a
5Y5/3
5Y4/3
Faintly bedded, olive, calcareous muddy sand
Bottom of Core
Depth (m)
0.5
1.0
1.5

Appendix I. Core X-Rays

See attached CD-ROM 2.

Appendix I contains X-radiograph images of the cores. The files are jpeg images. The filenames are of following convention: GA Cruise number_Station number_Operation type_Operation number (e.g., 234_02_gr02.jpg). The following codes are used for the operation types, GR (grab), GC (gravity core) and PC (piston core).

Appendix J. Seabed Video Footage

See attached CD-ROM 2.

Select seabed video footage is stored on the CD for Appendix J in mpeg format. The filenames reflect the following naming convention, GA Survey Number - Station Number, Operation Type (CAM = camera tow) and Operation Number (e.g., 234-10CAM10).